RESERVOIR CHARACTERIZATION RESEARCH LABORATORY

Noel Tyler, Project Director

1986-1987 ANNUAL REPORT

GEOLOGICAL CHARACTERIZATION AND RESERVE GROWTH POTENTIAL OF SPRABERRY RESERVOIRS IN THE MIDLAND BASIN, WEST TEXAS

by

Noel Tyler, E. H. Guevara, and G. R. Coates

with contributions by

Martin Wolff, P. K. Mukhopadhyay, and M. P. Roberts

assisted by

J. C. Gholston, J. J. Farrely, R. L. Graham
Timothy Walter, and J. R. Reistroffer

Bureau of Economic Geology
W. L. Fisher, Director
The University of Texas at Austin
University Station, Box X
Austin, Texas 78713

October 1987

CONTENTS

Figures

Tables

Work Maps and Cross Sections (in pocket)

EXECUTIVE SUMMARY

Major reservoirs in the Spraberry-Dean play of the Midland Basin, West Texas, contained at discovery 10.6 billion barrels of oil. Current projections suggest that only 7 percent of this huge resource will be recovered. Because vast amounts of mobile oil remain trapped in place by reservoir heterogeneities at abandonment, these reservoirs are prime candidates for reserve growth through extended conventional recovery. Spraberry reservoirs were targeted for detailed reinvestigation because of the huge resource (more than 4 billion barrels of movable, nonresidual oil) potentially available for extended conventional recovery by strategic infield exploration. Recognizing that the Spraberry reservoirs display pronounced heterogeneity, we decided that the principal objective of the project was to determine how an understanding of the genetic stratigraphy of these reservoirs may be utilized to maximize recovery. Spraberry reservoirs have long been considered to be homogeneous "layer cake" oil pools fully capable of being efficiently drained at 160-acre well spacing. Historically, development emphasized natural fractures but ignored the depositional sedimentary architecture of the productive sandstones and siltstones.

Studies were conducted at several levels. Regional studies focused on determining basinwide stratigraphy, lithofacies composition and distribution trends, and the relationship between regional stratigraphy and oil recovery. Field studies aimed to delineate prospective, high-porosity sandstone belts in an ununitized area of the Spraberry Trend. Well studies were conducted to identify and evaluate a suite of well logs appropriate for the determination of porous and permeable intervals and their corresponding fluid saturations as a means of detecting bypassed or unproduced oil-bearing reservoir compartments. Additionally, the influence of mineralogy and diagenesis on well log response and reservoir quality was evaluated. Results obtained from these

studies are directly applicable to deeper reservoirs of the same genesis in the Midland Basin, such as the reservoirs of the Wolfcamp and of the Dean Sandstone.

The Spraberry Formation is broadly subdivided into siltstone- and sandstone-rich upper and lower intervals (the upper and lower Spraberry), separated by an interval of interbedded calcareous terrigenous mudstones, argillaceous limestones, and lesser siltstones and sandstones (the middle Spraberry). Terrigenous clastics of the upper and lower Spraberry are the submarine fan deposits of saline density underflows and turbidity currents. Three submarine fans were recognized basinwide: the Jo Mill fan, composing the lower Spraberry, and the Driver and the overlying Floyd fans, composing the upper Spraberry.

Spraberry submarine fans, extending for 200 mi down the axis of the Midland Basin, form a mud-rich system characterized by high sediment transport efficiency through leveed channels. Neither large rivers nor mountain-building processes, which are the two principal tectonosedimentary sources of modern submarine fans, were active in the Permian Basin or its hinterland during Leonardian time; thus the processes responsible for deposition and the resulting sedimentary facies of Spraberry submarine fans differ from those of more typical submarine fan settings. The deep-water fan-shaped deposits of the Spraberry are considered to be somewhat unusual submarine fans that formed as a response to the unique architectural and climatic setting of the Permian Basin.

Approximately 1,200 well logs were utilized in the regional study. In addition to the tripartite division of the Spraberry Formation, the sand-rich upper and lower Spraberry intervals were further divided into a number of thinner units (operational units) that are correlatable across the entire basin. Six units are recognized in the upper Spraberry (1U to 6U), and two in the lower Spraberry (1L and 2L). Principal

oil-producing units in the central Spraberry Trend are units 1U, 5U, and 1L. In the more proximal parts of the system, particularly in the Jo Mill field, unit 2L is an important producer.

Unit 2L composes the first pulse of lower Spraberry submarine fan progradation and aggradation in the Midland Basin. Maximum deposition occurred near the sediment source in the north half of the basin. The shape of the basin and the bathymetry of the paleosurface upon which unit 2L was deposited influenced sedimentation trends. The thick, sand-rich northern third of the fan north of the Horseshoe Atoll was dominated by channel sedimentation on the inner fan. Farther basinward, south of the Atoll and north of the Glasscock County narrows, midfan sediments of considerable internal and lateral variability were deposited, grading basinward into outer-fan sediments. Constriction of unit 2L channels through a bathymetric low between subjacent pinnacles of the Horseshoe Atoll produced the sand thick productive in the Jo Mill field. Unit 1L, a far more sand-rich system than unit 2L, records maximum progradation of the Jo Mill fan.

Units 5U and 1U contain the principal reservoirs of the upper Spraberry in the central Midland Basin. Unit 5U comprises the most proximal deposits of the Driver fan. Thick aggradational inner-fan facies are confined to the northernmost parts of the basin, and midfan facies extend basinward to the Glasscock County narrows, south of which outer-fan facies predominate. Both the inner and outer fan were channelized, yet channel deposits were not a dominant constructional element. Sediments entered the basin mostly from the north, but there were also contributions from the Central Basin Platform and the Eastern Shelf. Unit 1U, capping the Floyd fan, resulted from more vigorous sediment supply and depositional processes than unit 5U. The distribution of facies of unit 1U in the proximal parts of the basin results in an asymmetric arrangement of submarine fan divisions. The boundary separating the inner fan from

the midfan extends from southwest Terry to north-central Glasscock Counties. Midfan facies extend from this area to the map limits.

There is a strong bimodal basinwide distribution of oil in the Spraberry Formation. Accumulations are small and erratically distributed in the inner fan; they are much more widespread in midfan to outer-fan facies south of the Horseshoe Atoll. The most proximal of the major oil fields is the Jo Mill, which produces from an inner-fan channel sequence, the location of which was constrained by paleobathymetry resulting from differential compaction over the Horseshoe Atoll. Petrophysical characteristics of Spraberry reservoirs of the Jo Mill field are superior to those of the more distal fields such as the Spraberry Trend and the Benedum field. As a consequence, recovery of mobile oil is excellent in the Jo Mill field. Porosities and permeabilities are lower in midfan to outer-fan reservoirs, in which reservoir stratification, decreasing bed thickness, and pronounced internal variability at the between-well scale are equally important to reservoir behavior. Poor internal continuity and stratification result in low recovery efficiencies (6 percent in the Spraberry Trend) and low mobile oil recoveries in midfan and outer-fan reservoirs.

Many small-field discovery opportunities still exist in Spraberry fans. Pinch-out of sands against the carbonate shelf slope may provide small, en echelon stratigraphic traps that are elongate parallel to the basin margin and narrow normal to the basin edge. With the exception of the north half of the basin, sand quality would be poor. Wedge-out of sand-rich canyon-fill sediments against overlying bounding surfaces also may provide stratigraphic traps. Pay would be elongate normal to the basin edge and narrow parallel to the shelf. Seismic investigations would be invaluable in detecting this class of trap. If Spraberry fans are lowstand deposits, sand-filled channels could provide linear shoestring stratigraphic or structurally modified stratigraphic traps.

Slump fans resulting from failure of an unstable shelf and slope may locally be sealed in basinal deposits, particularly in the muds of the middle Spraberry. Structural tilt with updip porosity pinch-out would create a combined structural/stratigraphic trap.

The greatest potential for additional recovery from the Spraberry, however, lies in reexploration of existing fields. The complex internal architecture of Spraberry reservoirs presents opportunities for the drilling of geologically targeted infill wells in depositional axes and for recompletion of existing wells in previously untapped zones. Areas where midfan facies are stacked in multiple zones maximize opportunities for extended conventional development. In the midfan to distal fan, facies variability reaches a zenith, allowing for maximum between-well variability. In addition, in this part of the fan the stacking of channel axes defines production sweet spots.

To locally assess the potential for reserve growth, studies were conducted on a 60-mi^2, ununitized area of the Spraberry Trend north of the Driver and east of the Preston/Shackelford waterflood units. Operational units of this area form part of a gently northwest-dipping monocline having local, northwest-plunging anticlinal undulations or noses. Midfan (units 1U and 1L) and outer-fan (unit 5U) reservoir sandstones and siltstones were deposited mainly in NNW-SSE- to NNE-SSW-trending belts that are generally 0.5 to 1 mi wide and locally 3 mi wide. These belts, which transect predominantly progradational fan facies, are composed primarily of channelized, aggrading facies.

Lithofacies architecture in the ununitized area, characterized by laterally discontinuous sandstones and siltstones encased by poor-quality reservoirs and nonreservoir rocks, results in stratigraphically complex reservoirs. Lateral variability of total thickness of sandstone and siltstone and the corresponding variation in matrix

porosity result in intrareservoir traps. The occurrence of separate accumulations in the upper and lower Spraberry has been known since early field development. Furthermore, sand-poor areas separating units 1U and 5U suggest stratified oil pools within the upper Spraberry.

Effective porosities ranging from less than 1 percent to approximately 18 percent were determined in the ununitized area using gamma-ray/neutron logs (GNT). Areas having the best effective porosities do not always coincide with the belts of isolith maxima, mainly because of porosity reduction predominantly by carbonate cementation. Thus, porosity maps allow high grading of prospective locations for infill drilling. Sectors having more than 12 percent effective porosity usually occur locally in the south-central, northeast, and northwest parts of the area.

Upper and lower Spraberry reservoirs are each capable of locally producing more than 100,000 barrels of oil in the ununitized area, and primary recovery per well in this area appears to be higher than in the Preston/Shackelford waterflood units. Relatively high recoveries locally in the south part of the ununitized area may be in part a response to effects of waterfloods in the adjacent Driver and Preston units. However, relatively high recoveries in the ununitized area and in the northeast sector of the Driver waterflood unit probably reflect local superior reservoir quality in the eastern depositional axis of the Spraberry and, furthermore, a thicker oil column near the eastern updip seal of the Spraberry Trend. Continuations of sand-rich belts of the ununitized area contain the sweet spots of the Preston/Shackelford and Driver waterflood units, suggesting comparable superior recoveries and high grading prospects, especially in the depositional axes of the east-central part of the study area.

Detailed petrophysical information on Spraberry reservoirs, essential to the detection of bypassed oil zones, is scarce. To obtain new reservoir data, state-of-the-art suites of open-hole and cased-hole logs were run, cores were cut, and formation pressures were measured in two newly drilled wells in the Spraberry Trend: the Mobil Preston-37 and the Mobil Judkins A No. 5 wells.

Data from sidewall cores from the Preston-37 well suggest that no major compositional or textural differences exist between upper and lower Spraberry sandstones and siltstones, which consist mainly of quartz (70 to 90 percent), feldspars (up to 10 percent), and clay minerals (less than 10 percent). Cement is mainly dolomite distributed irregularly in patches, and some quartz overgrowths. Intergranular primary porosity is locally preserved in these reservoirs but most was lost during early compactional diagenesis. Dissolution of unstable minerals, followed by carbonate cementation, occurred after compactional diagenesis and resulted in the development of secondary porosity that may be locally important in the Spraberry Trend. Calcite and expanding clays are either not present in the samples studied or occur in very low proportions. However, well logs suggest the occurrence of expanding clays. Organic geochemistry data from Spraberry shales indicate the occurrence of mature source rocks (within the early phase of principal oil generation) in the upper Spraberry, and mature, depleted source rocks (within the final phase of principal oil generation) in the lower Spraberry.

Core data from the Preston-37 well indicate that matrix porosities range from 8.1 to 14.3 percent, air permeabilities are less than 1 md, and water saturations range from 27.6 to 80.6 percent (per volume). Comparison of results of core and log analysis indicates that the main petrophysical characteristics of Spraberry reservoirs can be adequately described using well logs. Data from natural gamma-ray, density, compensated neutron, and sonic logs were used to determine porosity, and data from logs that record the deep resistivity (to determine Rt) were used to assess fluid saturations.

The open-hole suite run in the Preston-37 well consisted of the natural gamma-ray spectroscopy (NGT), dual induction (DIL/SFL), electromagnetic propagation (EPT), lithodensity (LDT), compensated neutron (CNL), log spacing sonic (LSS/WFM), and formation microscanner (FMS) logs. VOLAN and GLOBAL evaluations and CFIL and dual dip logs were computed by the logging company using these open-hole logs. The VOLAN and GLOBAL evaluations show porosities ranging from approximately 5 to 15 percent and hydrocarbon zones having 50 to 70 percent water saturation in the sandstone zones of operational units 1U, 5U, and 1L.

Natural fracture detection remains problematic. The NGT, LSS, and well logs, and the FMS, CFIL, and VOLAN synergetic logs were used to assess the occurrence of natural fractures. Fracture detection using these data was inconclusive because each method presented a different result. Similarly, the distinction between natural and induced fractures using well logs remains unresolved because no agreement was found between several commonly used fracture indices.

Determinations of formation pressures were attempted using Schlumberger's Repeat Formation Tester at 13 depth locations in the Preston-37 well and at 14 depth locations in the Judkins A No. 5 well. Two pressure tests were successful, both in lower Spraberry sandstones of the Preston-37 well. Results of these tests suggest pristine reservoir pressures, clearly indicating that the Preston-37 well penetrated an untapped reservoir compartment in the lower Spraberry.

Current completion practices leave mobile, potentially producible oil in Spraberry reservoirs because, as indicated by this investigation and by low recovery efficiencies and as confirmed by RFT data, not all compartmentalized oil accumulations have been systematically tapped. Well spacing may locally be too wide for adequate drainage of some reservoir compartments, especially if the stratigraphic distribution of intervals open to production is considered. Conventional reserves can be added in the Spraberry

Trend by well recompletions that would open to production bypassed oil-bearing intervals, deepening of wells to produce from units 5U and 1L, and programs of strategic infill drilling and secondary recovery in sectors having superior effective porosity in the depositional axes. The unrecovered mobile oil resource base in submarine fans of the Spraberry exceeds four billion barrels; additional recovery of just 2 percent of this resource using strategies outlined in this report would more than double existing Spraberry reserves.

INTRODUCTION

Modern and ancient deep-sea fans are excellent targets for the exploration and exploitation of oil and gas because these deposits are composed of reservoir sandstones interbedded with organic-rich, hemipelagic source mudstones. The muds encase the reservoir rocks, provide a source of hydrocarbons, and seal the reservoirs (Wilde and others, 1978; Nelson and Nilsen, 1984). As a result, modern and ancient deep-sea fan deposits, as a class, contain vast volumes of oil. Southern California and the North Sea, two world-class petroleum provinces, are examples. In Southern California, 90 percent of the hydrocarbons (Nelson and Nilsen, 1984) are produced from multistoried oil sands of coalesced deep-sea fans that, per unit volume of sediment, are the richest in the world (Redin, 1984) In the North Sea Province, almost one-quarter (22 percent) of the proved recoverable reserves of 23 billion barrels of oil and 50 trillion cubic feet of gas lies trapped in deep-sea fan deposits (Watson, 1984).

Deep-water sandstones are also important reservoirs in Texas. The Spraberry-Dean sandstone play in the Midland Basin, West Texas, the subject of this contract report, is the largest deep-sea fan play in the state (fig. I-1). Major reservoirs in the Spraberry-Dean contained at discovery 10.6 billion barrels of oil (Galloway and others, 1983). Other important deep-sea fan plays in Texas include the Delaware sandstone play (0.48 billion barrels of original oil in place) and the Upper Pennsylvanian slope sandstone play (0.5 billion barrels of original oil in place). All together, 11.6 billion barrels of oil, or 26 percent of the original oil in place, in sandstones has been discovered in major deep-sea fan reservoirs in the State (fig. I-2; Galloway and others, 1983; Tyler and others, 1984); all of this resource lies in the Permian Basin in West

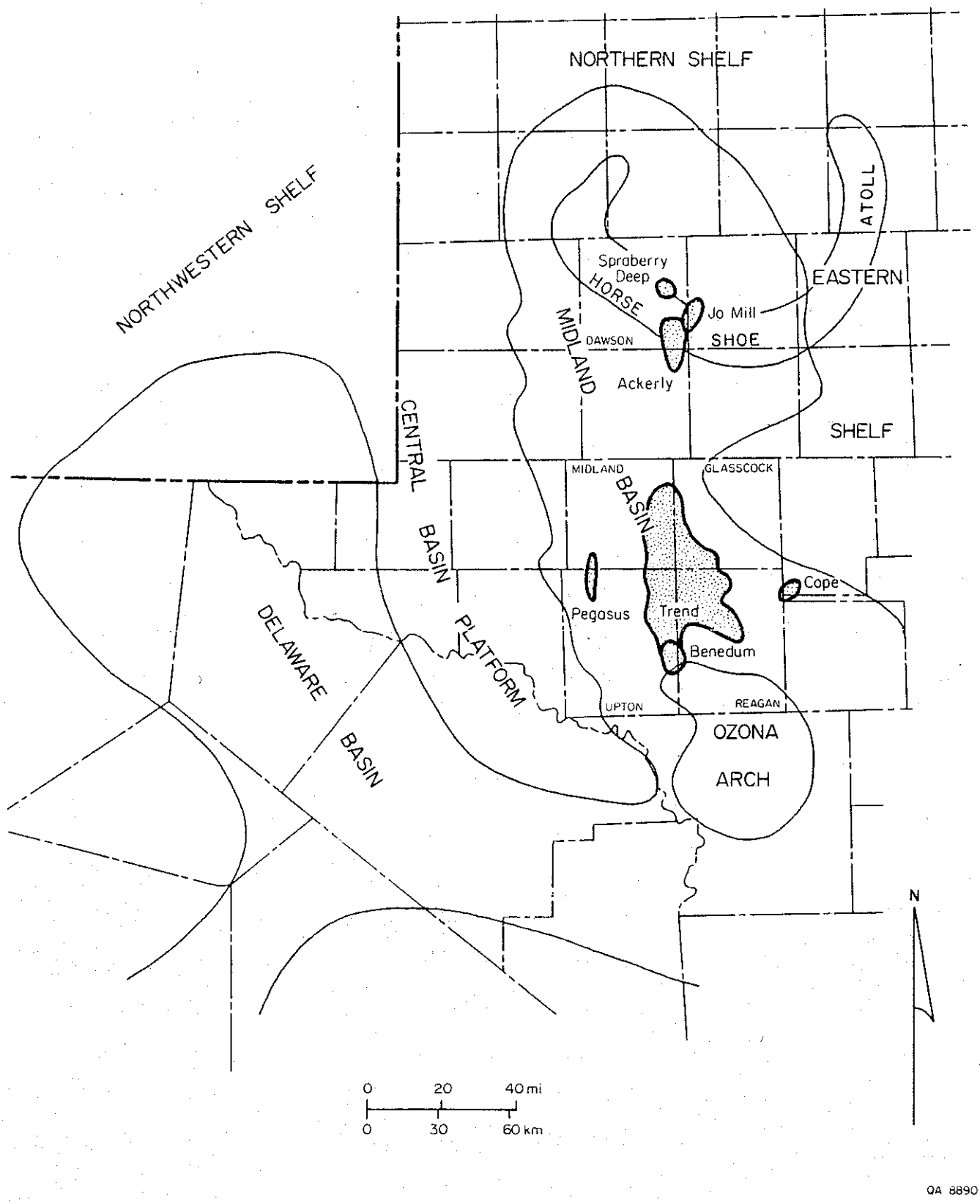

Figure I-1. Simplified structure of the Permian Basin and location of major Spraberry/Dean oil fields in the Midland Basin.

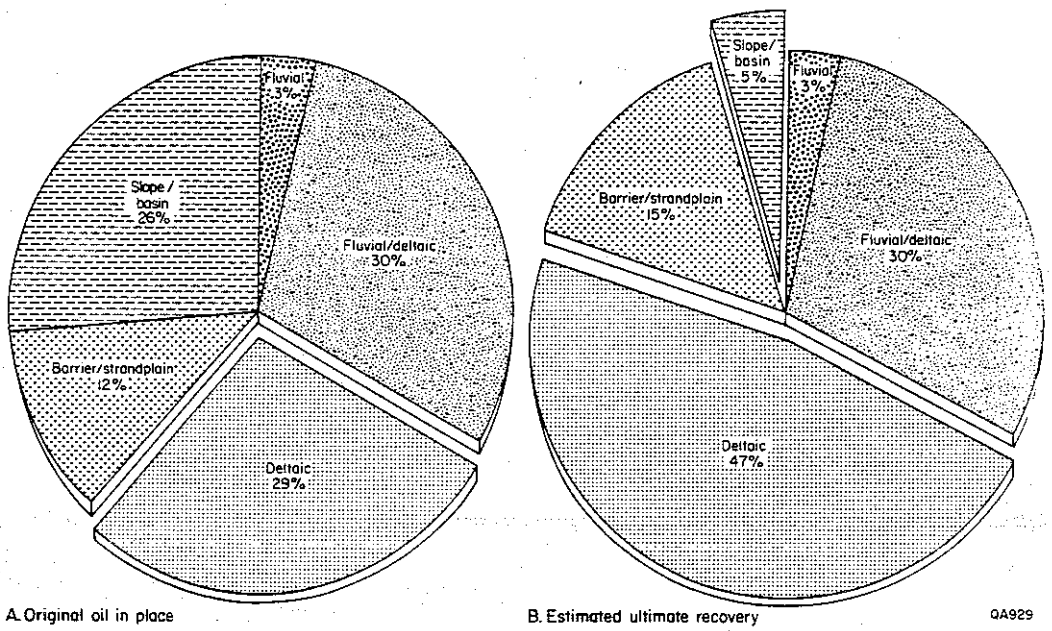

Figure I-2. Exploded pie diagrams illustrating the relation between reservoir genesis and the patterns of (A) oil accumulation in and (B) subsequent recovery from sandstone reservoirs. Production from deltaic deposits accounts for almost half of all production from sandstones; deep-water reservoirs, which contain one-quarter of the total resource, will produce only five percent of the estimated ultimate recovery. From Tyler and others (1984).

Texas (fig. I-1). A number of smaller deep-water sandstone plays have been located in the Gulf coastal province since exploration shifted seaward of paleoshelf deposits of Early and Late Cretaceous and Tertiary age. These lesser plays include, among others, the slope and continental-rise deposits of the Late Cretaceous Olmos Formation in South Texas (Tyler and Ambrose, 1986), submarine fan deposits of the Woodbine-Eagle Ford interval in East Texas (Siemers, 1978), and canyon and fan deposits of the Hackberry Sandstone in southeast Texas (Ewing and Reed, 1984). It is probable that better understanding of shelf break, slope, and deep-sea fan depositional systems, coupled with advanced seismic exploration, drilling, well logging, and well stimulation technology, will lead to the discovery of additional deep-water sandstone reservoirs both onshore and offshore Texas.

As a class, particularly in Texas, submarine fan reservoirs are characterized by very poor recovery efficiencies. In Texas, the average recovery efficiency of slope and deep-basin reservoirs at current technological levels is only 15 percent of the original oil in place. The weighted recovery efficiency for Texas deep-water sandstone reservoirs, determined by dividing the estimated total ultimate recovery of all the plays in the system by the total oil in place in the system, is only 8 percent (Tyler and others, 1984). In the Spraberry-Dean sandstone play, which contained 10.6 billion barrels of oil at discovery, current projections suggest that only 7 percent of this huge resource will be recovered. Deep-water sediments clearly fall at the low end of the sandstone-reservoir recovery-efficiency spectrum (fig. I-3). Although these sediments contained more than one-quarter of the in-place oil resource, they will yield only one-twentieth of the total production from sandstones in Texas (fig. I-2). Conversely, because vast volumes of movable oil remain trapped in place by reservoir

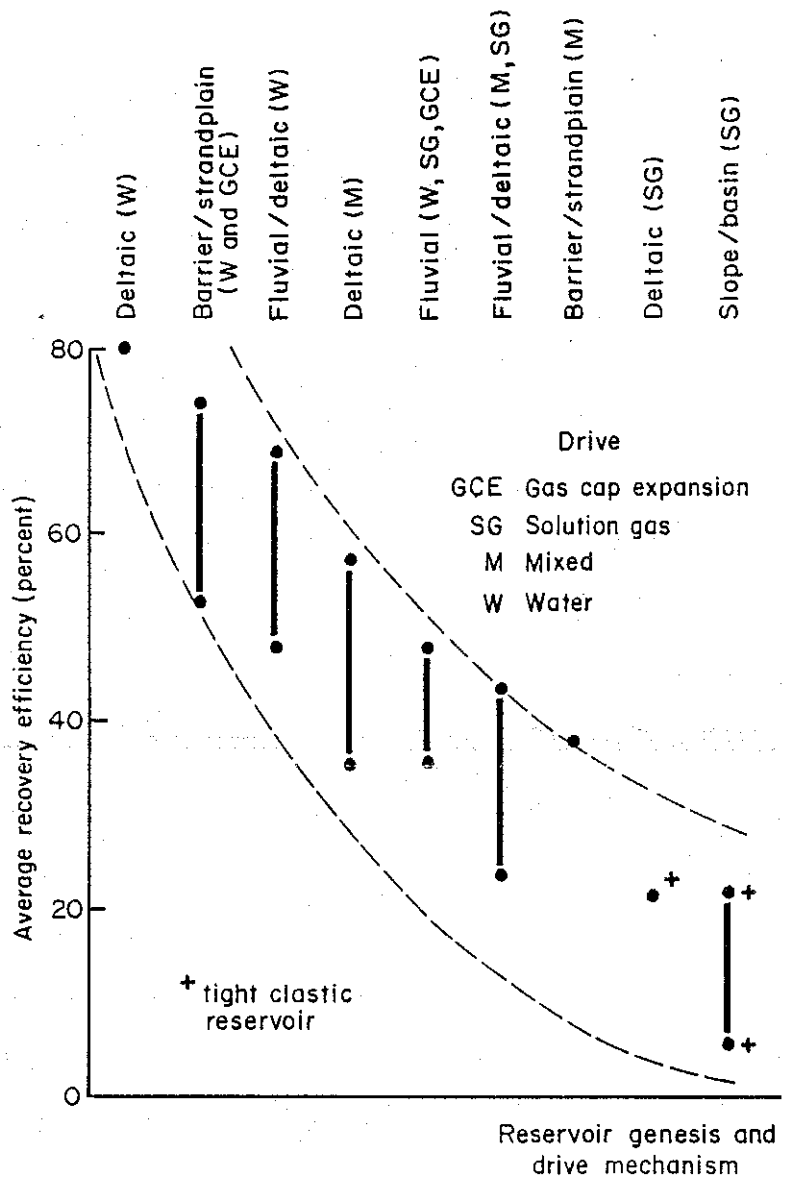

Figure I-3. The spectrum of recovery efficiencies in typical Texas reservoirs. Deep-water sandstone reservoirs display the lowest recoveries. From Tyler and others (1984).

heterogeneities at abandonment (fig. I-4), submarine fan reservoirs are prime candidates for reserve growth through extended conventional recovery.

Reservoir Characterization for Improved Recovery

The Spraberry Formation has long been notorious for its low-permeability, low-recovery reservoirs. The largest pool in the sandstone, known as the Spraberry Trend, covers one-half million acres (2,500 mi^2). It was once known as the world's largest uneconomic oil field (Handford, 1981a). Historically, development of the Spraberry Trend emphasized the natural fracturing in these stacked reservoirs (Bristol and Helm, 1951; Gibson, 1951; Elkins, 1953; Wilkinson, 1953; Barfield and others, 1959; Elkins and Skov, 1960) but ignored the depositional sedimentary architecture of the productive siltstones and sandstones.

Because of very poor recovery and the huge resource (more than 4 billion barrels of movable, nonresidual oil) potentially available in the Spraberry (exclusive of the Dean Formation) for extended conventional recovery by strategic infield exploration, the Spraberry was targeted for detailed reinvestigation by an integrated, multidisciplinary research team that included geologists, well log analysts, and engineers. Recognizing that the Spraberry displays pronounced heterogeneity, we decided that the principal objective of the project was to determine how an understanding of the genetic stratigraphy of Spraberry reservoirs may be utilized to maximize recovery. Previous studies (Galloway and Cheng, 1985; Tyler and Ambrose, 1985; Tyler and others, 1986) show that sedimentary facies and the boundaries separating facies create discrete compartments in reservoirs, influence saturations, determine paths of fluid (oil, gas, and water) movement, and ultimately result in segments of the reservoir remaining

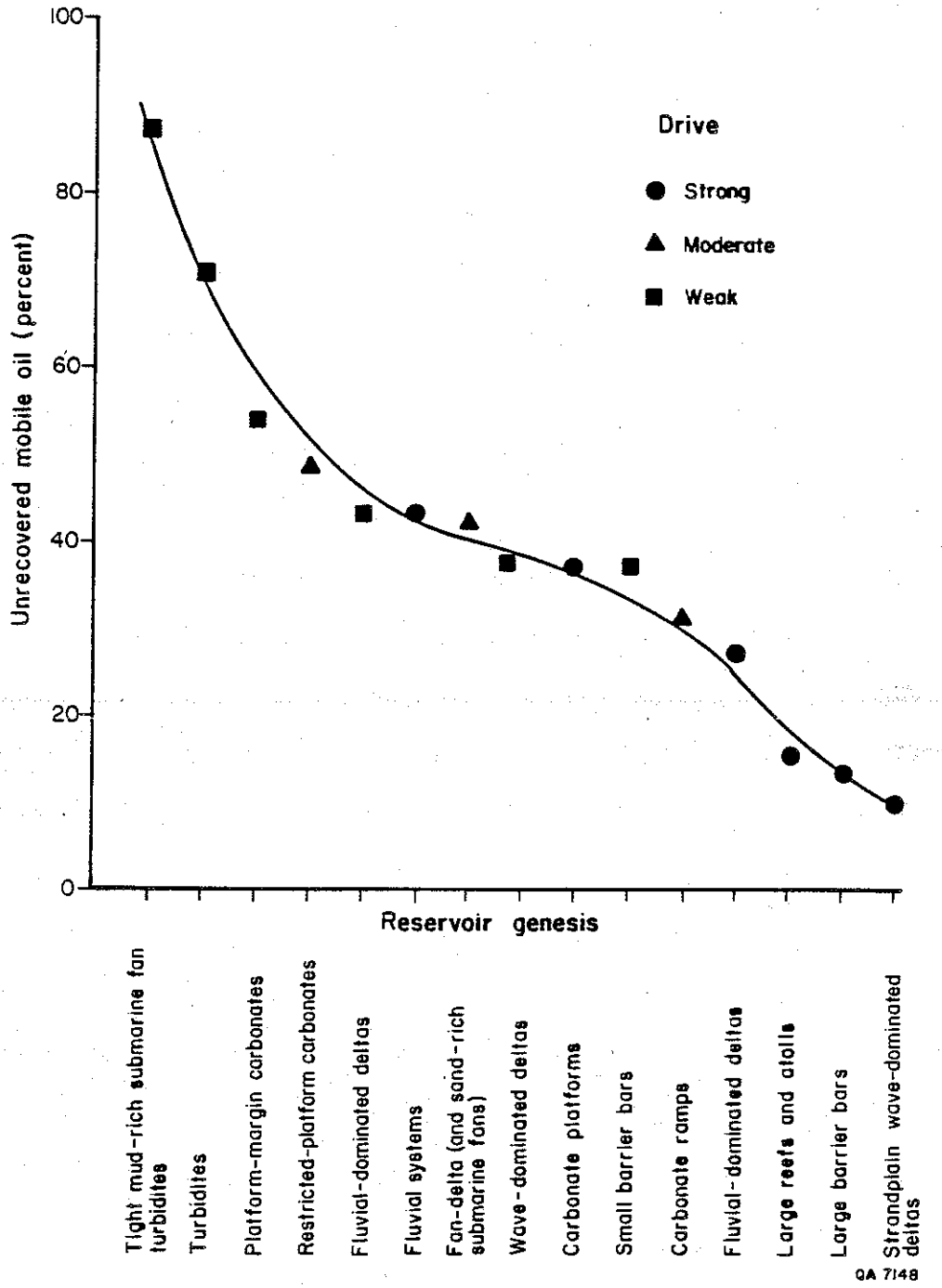

Figure I-4. Cross plot of unrecovered mobile oil against reservoir genesis based on a sample of 450 Texas reservoirs. Because of poor recovery, deep-water sediments are excellent candidates for reexploration for the high percentage of unproduced movable oil remaining in the pool at abandonment. In collaboration with W. L. Fisher.

undrained at abandonment. Intuitively submarine fan reservoirs such as the Spraberry (Handford, 1981a) would be predicted to be highly heterogeneous, yet the Spraberry has long been considered to be a classic, laterally homogeneous, "layer cake" oil pool fully capable of being efficiently drained at 160-acre well spacing (Elkins, 1953).

Research Approach

Studies were initiated at several levels. They included regional studies, field studies, and well studies. The entire project was based on recently completed work on waterflood units in the central Spraberry Trend (Guevara, in press; Tyler and Gholston, in press).

Regional studies: This part of the project included determining the basinwide stratigraphy of the formation, mapping sand distribution trends, determining from well logs the extent and composition of facies that compose the principal reservoir units, and examining the basinwide relationship between the geology of the formation and oil recovery. Objectives were twofold; the first was to develop a stratigraphic framework that would assist in the exploration process in undeveloped areas of the Spraberry, and the second was to establish the basinwide architecture of producing intervals for incorporation into field-specific studies.

Field studies: This part of the project aimed to extend conventional mapping of sand distribution into adjacent, nonunitized areas of the Spraberry Trend and to develop methodologies for the delineation of prospective, high-porosity sand belts.

Well studies: Objectives of well studies were twofold: the first was to identify and evaluate a suite of well logs appropriate for the determination of porous and permeable intervals and of their corresponding fluid saturations as a means of detecting bypassed or unproduced oil-bearing reservoir compartments; and the second was to evaluate the influence of mineralogy and diagenesis on well log response and reservoir quality by means of petrographic studies.

Stratigraphic Setting of the Spraberry Formation

The Paleozoic stratigraphic section in West Texas records a fascinating history of structural deformation, episodic basin formation, and basin infilling. During early Paleozoic time, Ordovician, Silurian, and Devonian shelf and ramp carbonates and minor terrigenous clastics were deposited on a southward-sloping shelf that formed part of an ancestral Permian Basin--the Tobosa Basin (Galley, 1958). The dominance of carbonate deposition began to wane during the Mississippian as a ring of uplifts encircled the intracratonic depression that was the incipient Permian Basin. Early sedimentation of Mississippian limestone gave way to deposition of terrigeneous mud that continued through the early Pennsylvanian.

In the center of the basin a fault-bounded horst began to rise in the late Mississippian. This north-south elongate, positive structural element, the Central Basin Platform, subdivided the Permian Basin into two subbasins. To the east lay the Midland Basin, and subsidence west of the platform resulted in the formation of the larger and deeper Delaware Basin (fig. I-1). Sedimentary fill in both basins consisted of interbedded terrigenous mud, carbonate mud, and lesser deep-water silts and sands. Together with middle to late Pennsylvanian (Strawn through Cisco age) reef builders of the Horseshoe Atoll, these coarser grained terrigenous clastics compose the principal producing intervals of the Midland Basin.

Reservoirs in the Leonardian Spraberry Formation provide most of the oil produced from siltstones and sandstones in the Midland Basin. Other deep-water sandstones in the Wolfcamp and in the Dean that overlies the Wolfcamp also are productive. Thus results obtained from the detailed study of the Spraberry are directly applicable to deeper reservoir units of the same genesis in the Midland Basin.

The Spraberry Formation is broadly subdivided into siltstone- and sandstone-rich upper and lower intervals separated by a middle interval of interbedded calcareous terrigenous mudstones, argillaceous limestones, and lesser siltstones and sandstones. Although this threefold division is relatively simple and reflects the depositional history of the formation, there has been considerable variation in how previous authors divided the Spraberry since McLennan and Bradley (1951) first proposed a tripartite characterization of the interval (table I-1).

Basinwide maps of sand distribution in the broadly defined lower and upper Spraberry clastic members (Handford, 1981a) show that the principal sediment sources lay to the northwest, north, and northeast. Sand and silt, which were transported down the long axis of the basin, gradually decrease from north to south. Handford (1981a) interpreted the large-scale genetic cyclic sequences of the Spraberry as submarine fans deposited by turbidity currents and saline density underflows.

Submarine Fan Depositional Systems

Modern and ancient submarine fans have been the focus of tremendous interest during the last 20 years. As a result, literature describing aspects of this last great conventional-exploration frontier is voluminous. Modern fans have been examined

Table I-1. Subdivisions of the Spraberry Formation.

McLennan & Bradley (1951)	Senning (1951)	Bartley (1951)	Mardock and Myers (1951)	Warn and others (1952)	Wilkinson (1953)	Handford (1981 a,b)	Matchus and Jonas (1984)	This Report *	This Report **	
FIRST SAND ZONE	UPPER SPRABERRY	UPPER SPRABERRY 1 (SAND)	UPPER SPRABERRY	UPPER SPRABERRY	UPPER SPRABERRY	UPPER SPRABERRY	FIRST SPRABERRY	UPPER SPRABERRY 1U	c	FLOYD SUBMARINE FAN
	FLOYD	2						2U		
		3						3U		
								4U		
								5U	f	DRIVER SUBMARINE FAN
								6U		
	INTERMEDIATE ZONE	MIDDLE SPRABERRY FLOYD SAND	MIDDLE SPRABERRY	MIDDLE SPRABERRY	MIDDLE SPRABERRY	MIDDLE SPRABERRY 4		MIDDLE SPRABERRY 1M		
SECOND SAND ZONE		LOWER SPRABERRY 1	LOWER SPRABERRY	LOWER SPRABERRY	MIDDLE SPRABERRY	MIDDLE SPRABERRY 5	SECOND SPRABERRY	2M		
		2			LOWER SPRABERRY	LOWER SPRABERRY		3M		
								4M		
		3						5M		
	LOWER SPRABERRY	4						6M		
								LOWER SPRABERRY 1L	r	JO MILL SUBMARINE FAN
									s	
								2L	v	

* Operational unit

** Sandstone zone

QA 8903

mostly by North American geoscientists using acoustic techniques such as echo sounding and high-resolution to long-range side-scan sonar systems, deep-sea video and still cameras, continuous seismic profiling using a wide range of frequencies, and sampling techniques such as piston cores and Deep Sea Drilling Project (DSDP) drill holes (Nelson and Nilsen, 1984; Bouma and others, 1985). Ancient fans have been studied in even greater detail. The work of Mutti and Ricci Lucchi and associates has received considerable attention (Mutti and Ricci Lucchi, 1972, 1975; Mutti, 1974, 1977; Ricci Lucchi, 1975; Mutti and others, 1978; Ricci Lucchi and Valmori, 1980; Mutti and Sonnino, 1981).

The scales of the two types of investigations differ widely. Outcrop studies of ancient fans such as those of Mutti and Ricci Lucchi have largely concentrated on the description of the vertical profiles of individual sandstone bodies or cyclical sandstone accumulations. In contrast, analysis of modern fans is primarily limited to determining the external dimensions, morphology, and large-scale seismic character of the fan system. More detailed sampling of the system is limited to grab samples, piston cores, which sample only the upper veneer of the fan, and, at best, widely spaced DSDP cores. With each scale of study, a terminology particularly suited to the problems addressed has evolved. Furthermore, modern fans are highly variable in composition, extent, and form. The result is considerable terminological confusion in the literature and a variety of models that describe either modern deep-water fans or their ancient counterparts.

Two models describe modern (Normark, 1970, 1978) and ancient (Mutti and Ricci Lucchi, 1972; subsequent modifications by Ricci Lucchi, 1975; Mutti, 1977) submarine fan facies associations. Walker (1978) synthesized the terminology and morphological data of modern fans with the vertical facies associations of ancient fans into a single model or norm that initially received criticism but now appears to be gaining acceptance.

Submarine fans can be subdivided into four facies associations (Walker, 1978). The slope, canyon, and feeder-channel assemblages grade basinward into the inner (or upper) fan having a single active leveed channel (fig. I-5). In the midfan the channels are shallower and bifurcate, ultimately depositing a depositional lobe (the suprafan lobe in Normark [1978]). Basinward and adjacent to the suprafan lobes, laterally persistent outer-fan turbidites are deposited on a topographically smooth outer (or lower) fan that merges with the basin plain (Walker, 1984). Progradation of the submarine fan over a stationary, distal point would result in a composite, upward-thickening, upward-coarsening sequence.

The Spraberry submarine fan complex has many characteristics in common with modern elongate fan systems as defined by Stow and others (1985). These fan systems are found on the open basin floor and are mud rich. Sediment transport efficiency is high, and consequently much of the sand is deposited in the distal parts of the system. Channels are leveed, and channel formation is extensive (Nelson and Nilsen, 1984). The Spraberry extends for 200 mi (330 km) down the axis of the Midland Basin, is a mud-rich system, and is characterized by high sediment transport efficiency through leveed channels.

Two fundamental aspects differentiate modern fans from the Leonardian submarine fans of the Midland Basin. Modern fans form in two principal tectonosedimentary settings: at the terminuses of continental-scale rivers such as the Mississippi and the Amazon of the Americas and the Orange, Congo, and Niger of Africa and on the flanks of major mountain-building belts such as along the west coast of the United States and the Alps. Neither large rivers nor mountains were present in the Permian Basin or its hinterland during Leonardian time; thus the processes responsible for deposition and the resulting sedimentary facies of the Spraberry fan system differ from those described from more typical submarine fan settings. Nonetheless, regional

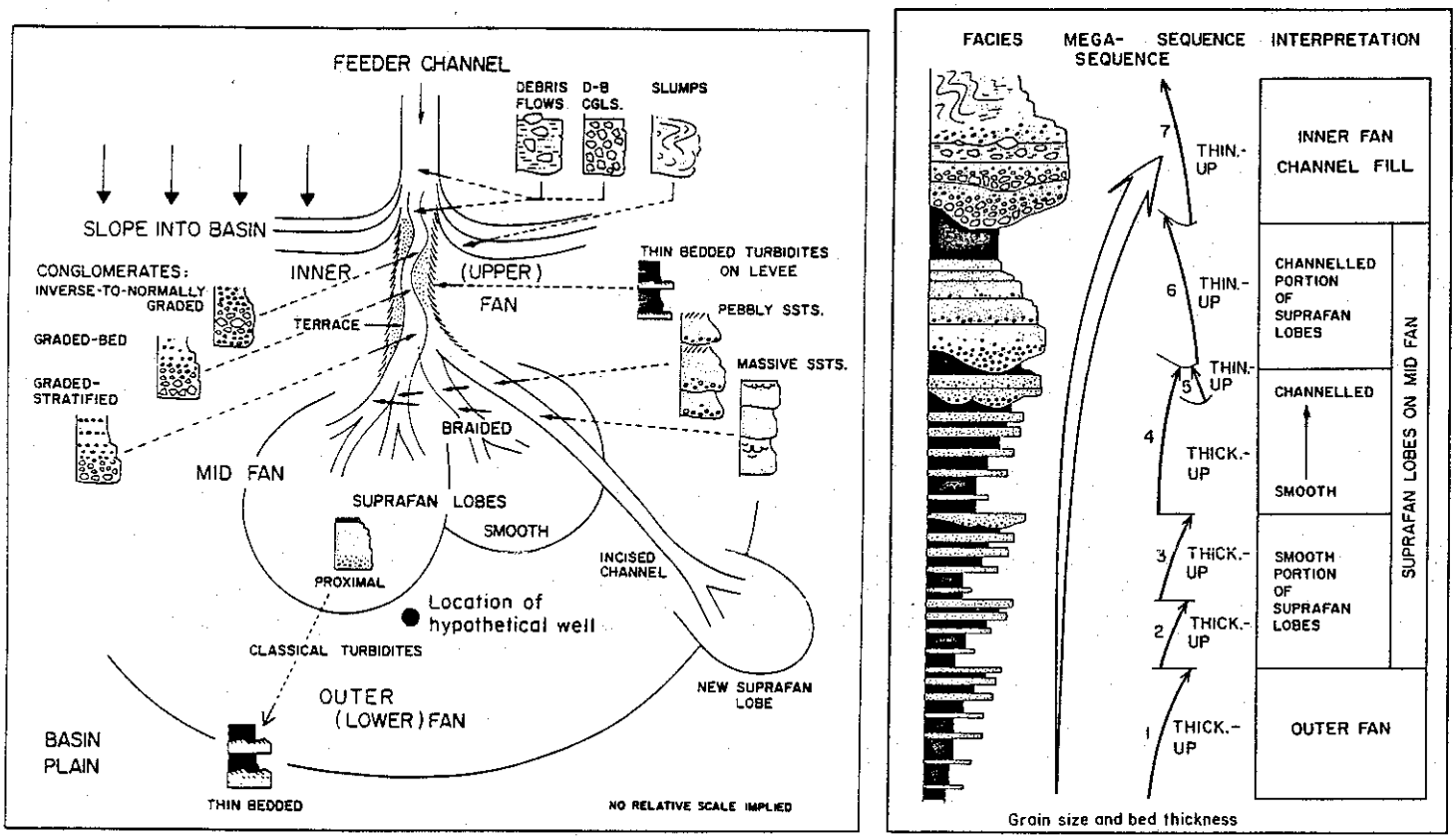

Figure I-5. Submarine fan environmental model and hypothetical vertical profile of a prograded fan system. After Walker (1978).

mapping has documented the fan-shaped geometry of sand-rich intervals in the Spraberry and established water depths to be 600 to 1,000 ft (Handford, 1981a; Sarg, in press). Thus the deep-water fan-shaped deposits of the Spraberry are considered to be somewhat unusual submarine fans that formed as a response to the unique architectural and climatic setting of the Permian Basin.

I. BASINWIDE ARCHITECTURE OF THE SPRABERRY FORMATION

Approximately 1,200 well logs were utilized in the regional study. These were selected on the basis of log quality, resolution, and depth of penetration. A correlation network of six depositional strike sections and three depositional dip sections (fig. I-6) was constructed to establish the regional framework of the Spraberry.

In addition to the tripartite division of the Spraberry, the upper and lower sand-rich intervals are further divisible into a number of thinner units termed operational units in this report. Operational units are correlatable across the entire basin. Six operational units are recognized in the upper Spraberry and two in the lower Spraberry in the central part of the Midland Basin (fig. I-7). Principal oil-producing units in the central Spraberry trend are units 1U and 5U of the upper Spraberry and 1L of the lower Spraberry. In the more proximal parts of the system, particularly in the Jo Mill field, unit 2L is an important producer. Drafted maps of these four intervals are included in the report (figs. I-8, I-9, and II-21); copies of work maps of the less important intervals accompany the report in a separate folder.

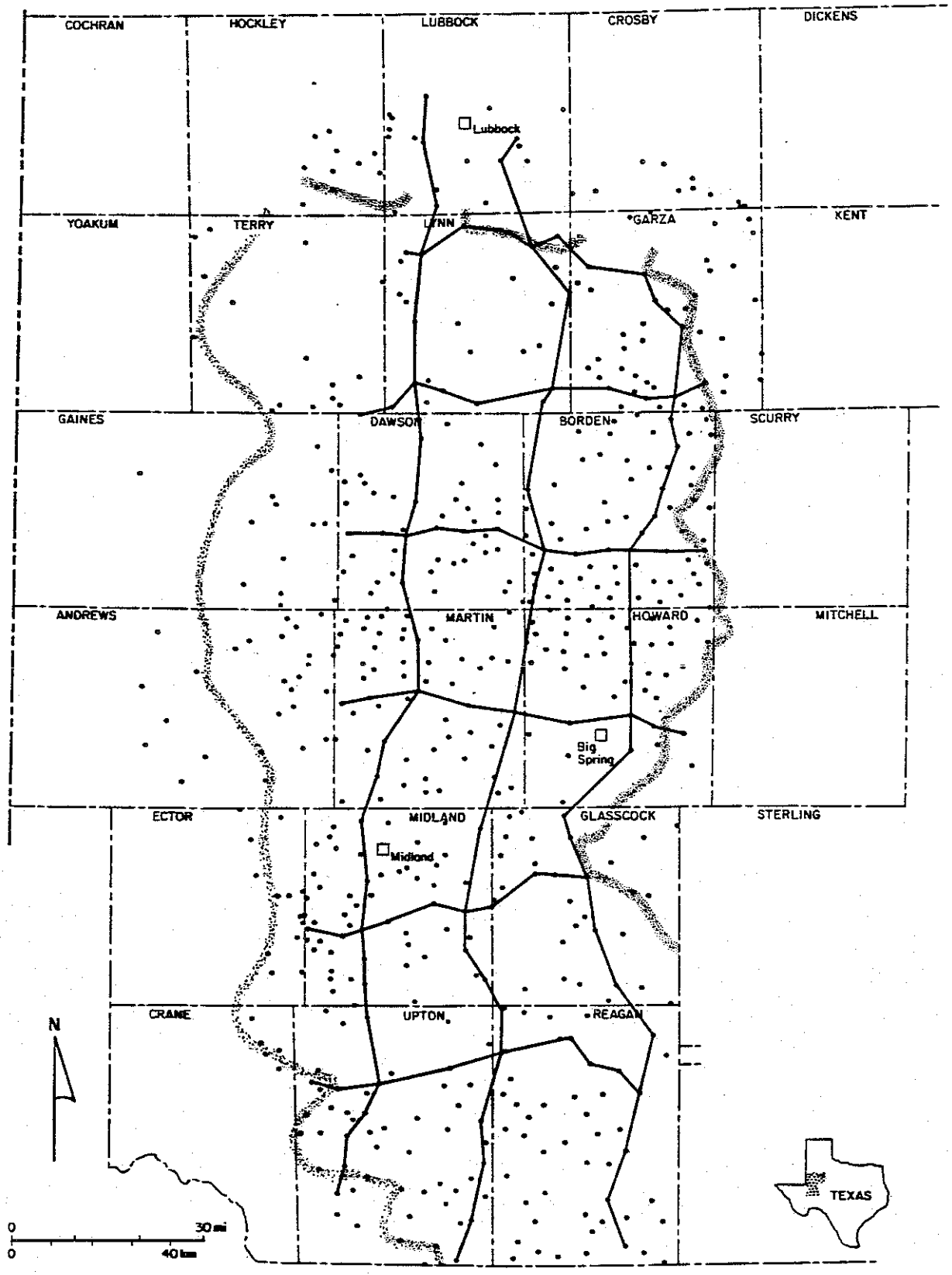

Figure I-6. Well log data base and cross section grid used in this study.

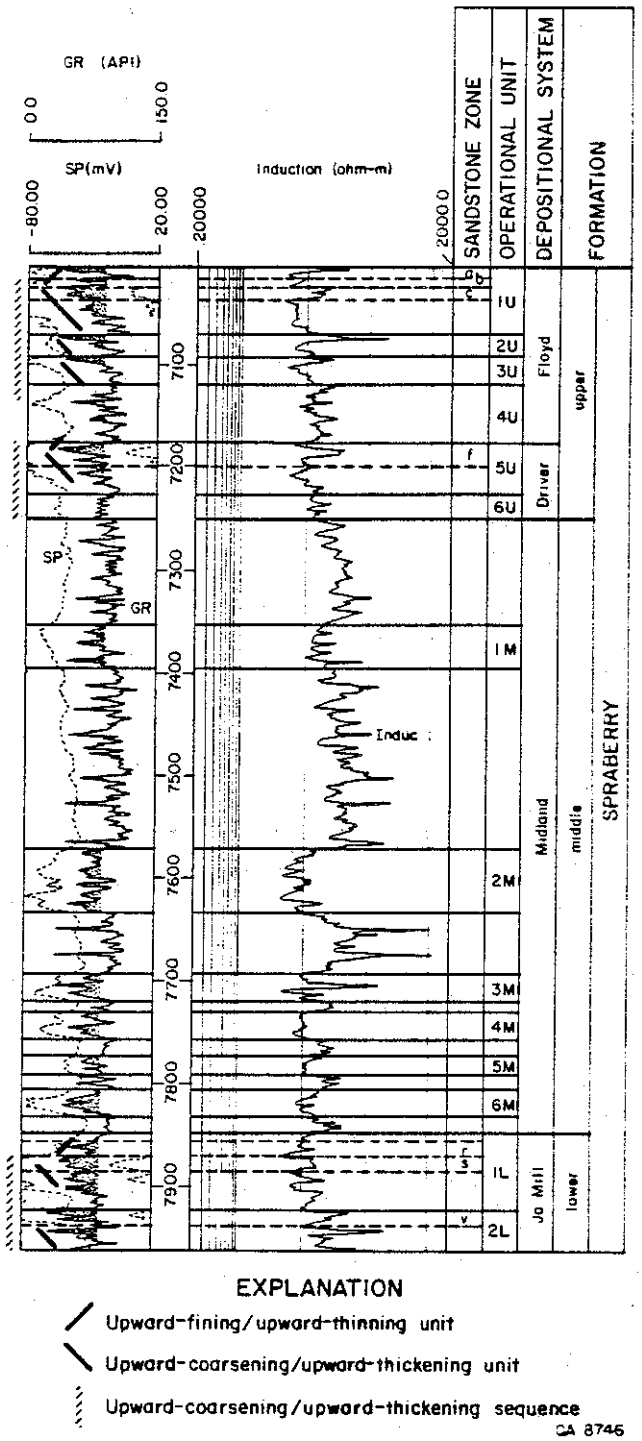

Figure I-7. Type log of the Spraberry Formation in the central Spraberry Trend, Mobil Judkins A No. 5, Midland County, showing several scales of division of the formation and principal vertical sequence trends.

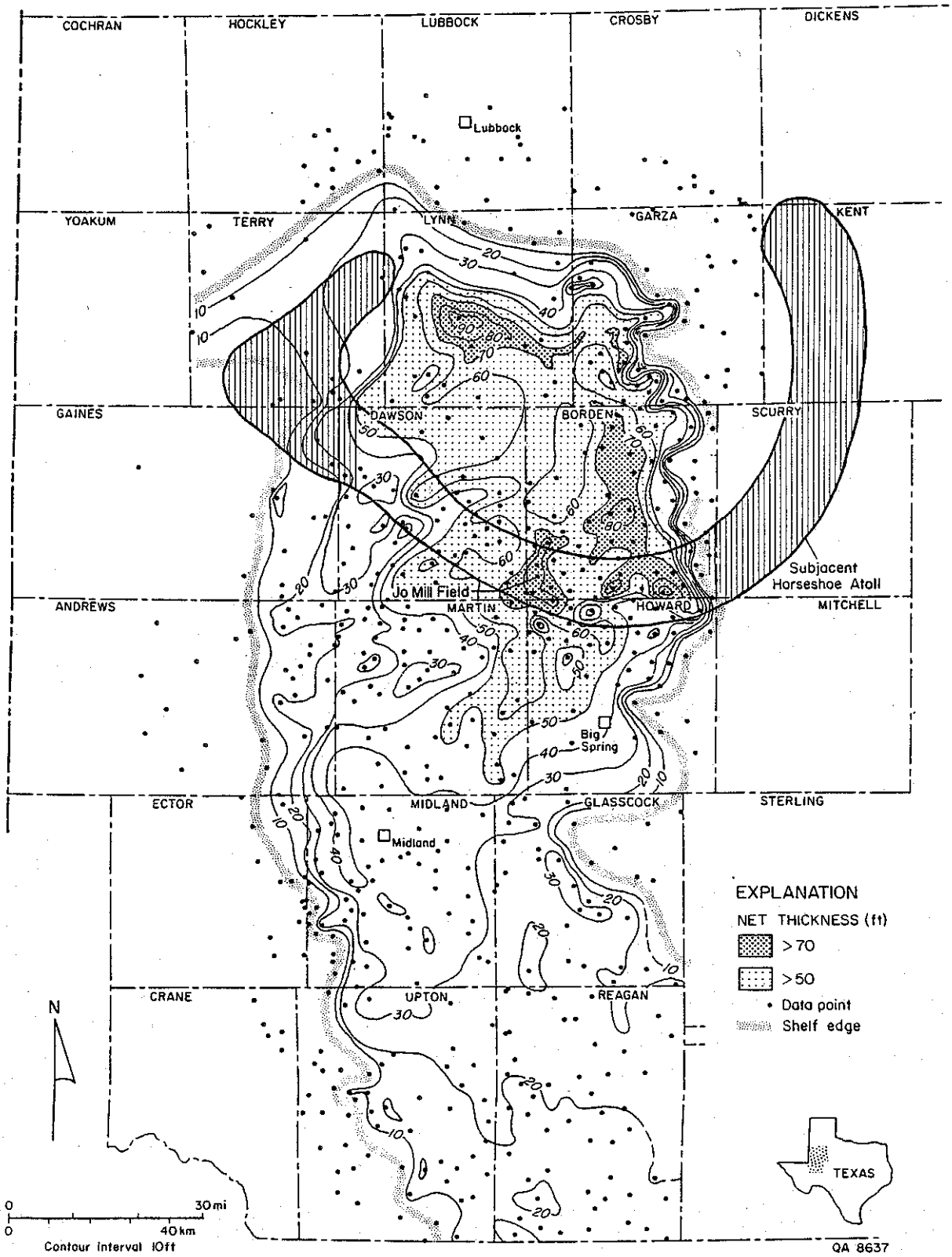

Figure I-8. Isopach map of lower Spraberry unit 2L. The principal zone of sediment accumulation lies north of the Horseshoe Atoll.

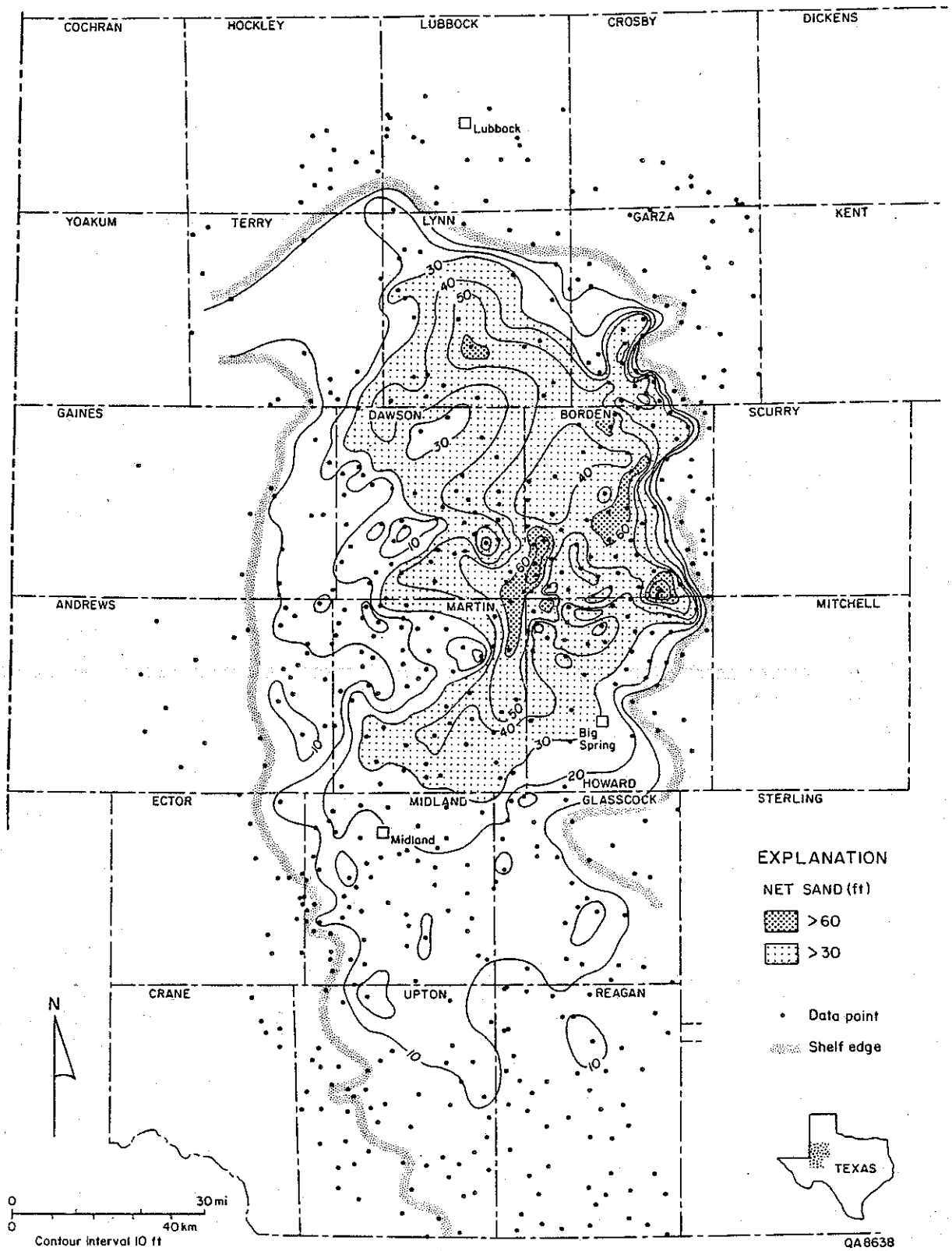

Figure I-9. Net-sand map of unit 2L. Note the pronounced thick in the Jo Mill field area in southwestern Borden County.

Lower Spraberry Unit 2

Thickness Trends

The principal depocenter of unit 2L is in the north quarter of the basin. Maximum isopach thicknesses of more than 70 ft form linear trends in central Lynn and central Borden counties (fig. I-8). A third belt of anomalously high thicknesses lies in southwest Borden County directly above the subjacent Horseshoe Atoll. Thicknesses of intermediate to high values (greater than 50 ft.) are mostly confined to the area updip of the Atoll; south of this feature, unit 2L thins gradually to less than 20 ft, with the exception of a tongue of higher values associated with the southwest Borden County thick.

Sand-Distribution Patterns

Net-Sand Trends

Net-sand patterns also show that the focus of sedimentation lies primarily north of the Horseshoe Atoll (fig. I-9). The source of sediment influx into the basin is not well defined for this unit. Possible entrants may have been from the north in central Garza County and from the northwest in Terry County.

Coincident with the isopach thick centered over the Horseshoe Atoll in southwest Borden County is a north-south trending linear sand thick. Comparison of the location of this sand axis with the paleobathymetry of the underlying Horseshoe Atoll shows the sand thick to be lying in a saddle between two carbonate buildups (fig. I-10). This sand thick, deposition of which was a response to differential compaction over the underlying carbonate mounds and the resulting focusing of channels through a paleobathymetric low, is the principal reservoir in the Jo Mill field. Futher, similar conditions must have prevailed during deposition of the Dean Formation because this bathymetric low is the location of the Ackerly (Dean) field.

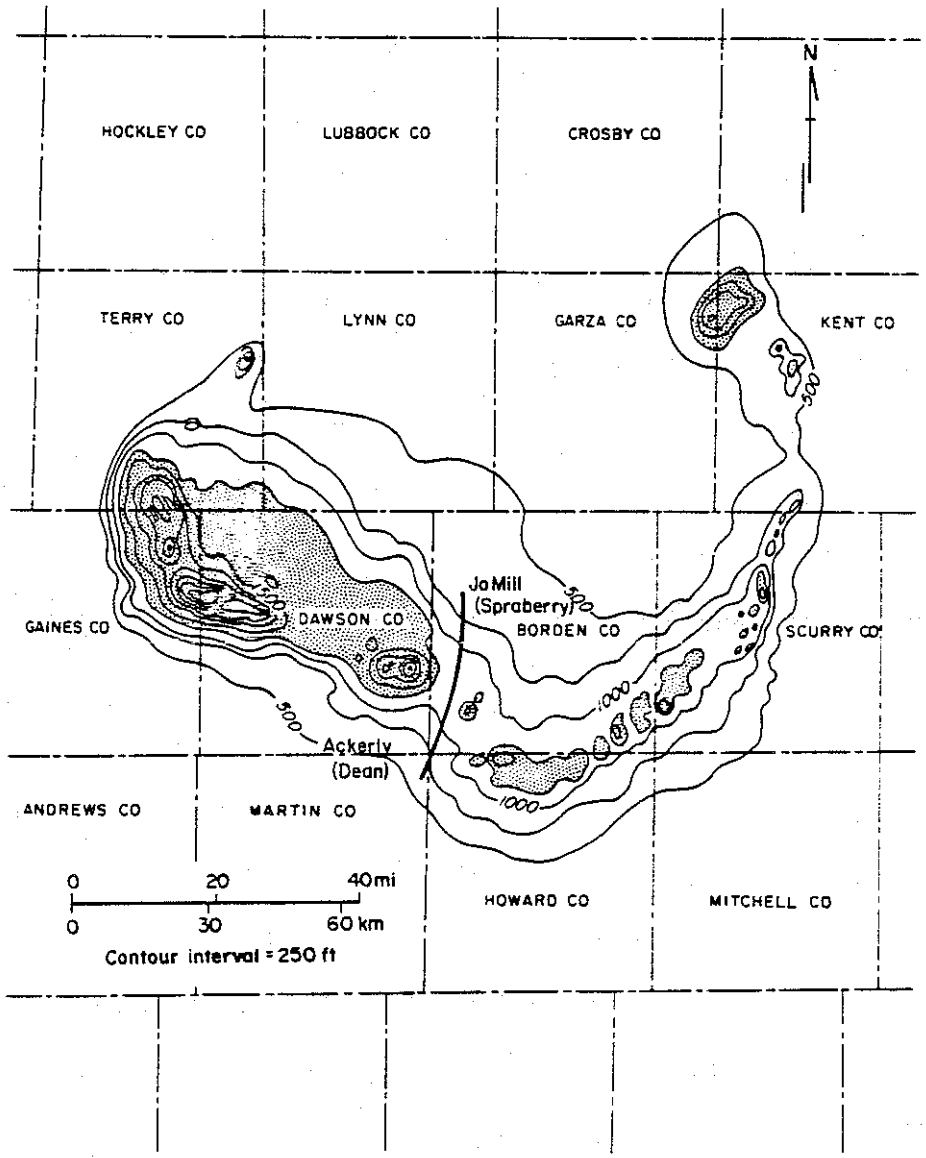

Figure I-10. Isopach map of the Horseshoe Atoll (modified from Vest, 1970) and location of major submarine fan fields in paleobathymetric lows between the subjacent carbonate buildups.

Much of the sand fed through this feeder system was deposited immediately south of the subjacent Atoll (see fig. I-8). Further south, sand content decreases systematically to less than 10 ft of net sand in the distal parts of the Midland Basin (fig. I-9).

Percent-Sand Trends

Percent-sand maps suggest that most of the sand entered into the basin from the northwest through Terry County, perhaps with a minor contribution from the north through Garza County (fig. I-11). Two high-percent-sand axes are present; one hugs the east flank of the Central Basin Platform (CBP), the other sweeps in from Terry County toward the east through Lynn County, then turns due south through Borden County and into Martin County. Sand lows with erratically distributed minima separate these two axes. Farther basinward sand percent decreases in a nonsystematic manner, with isolated pods of high sand percent occurring as far south as southern Reagan County.

The east shelf edge of the CBP shows evidence of instability and failure. Anomalously low sand percentages along the shelf slope in Andrews County extend eastward into adjacent Martin County. Well logs in this area show that much of the interval is composed of carbonate, which accounts for the low-percent-sand values. These mixed sediments are interpreted as carbonate slump deposits that moved as much as 15 to 20 mi into the basin. These deposits may be responsible for the abrupt termination of the west high-percent-sand axis (fig. I-11).

Facies Composition

Gamma-ray logs record naturally occurring gamma rays emitted from shales and clays in the formations adjacent to the borehole. These logs are thus used to indicate the shale content of the formation. Shaliness increases with decreasing grain

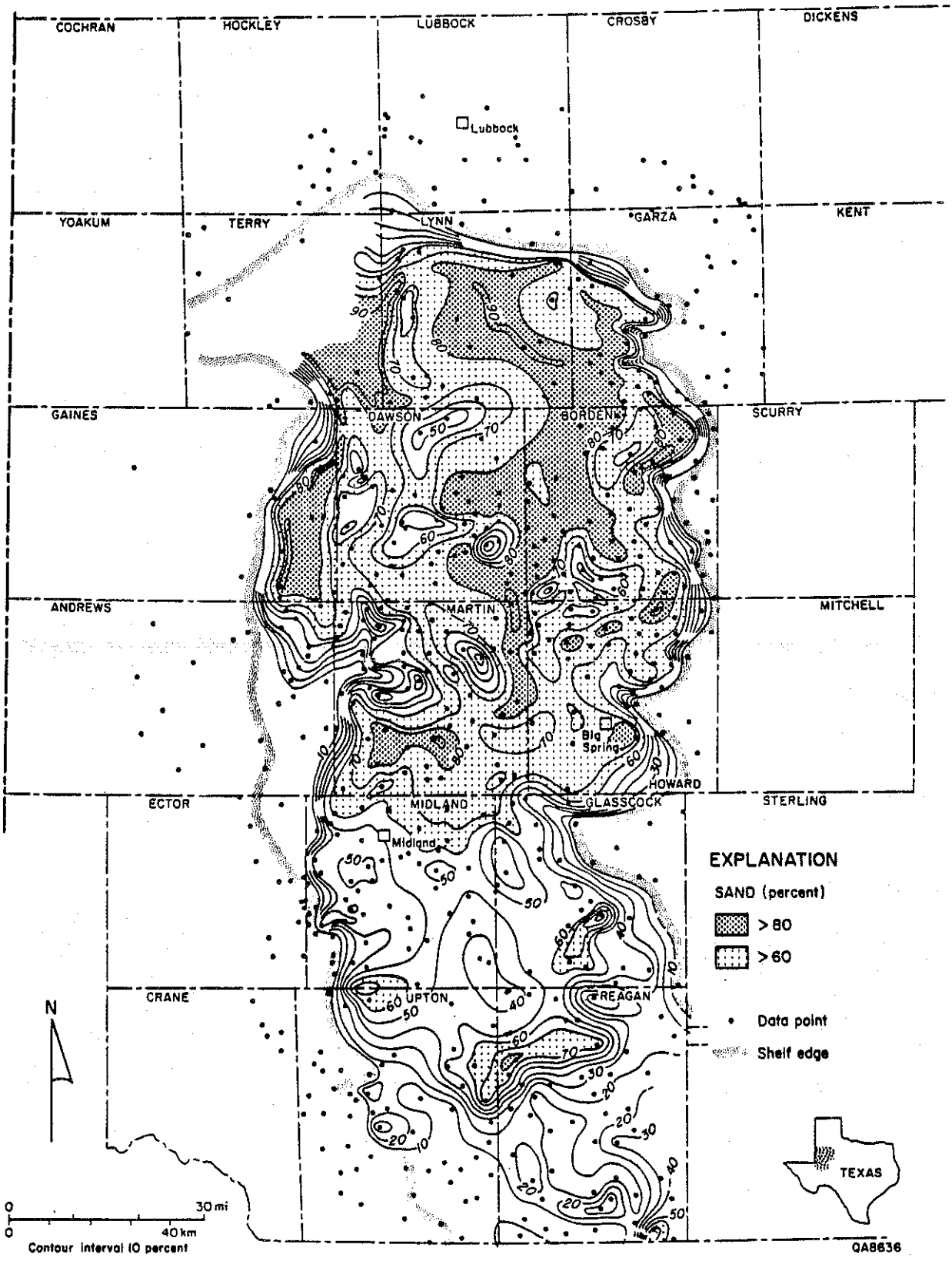

Figure I-11. Percent-sand map of unit 2L showing highs of net percent sand extending only as far as the Glasscock County narrows.

size, so the gamma-ray log can be used as a first approximation of grain size. The logs selected for the regional study all had resisivity curves to differentiate between terrigenous clastics and carbonates. The combination of these two log types allowed the mapping of lateral variation in vertical grain size trends throughout the basin. These maps are called log facies maps.

Log facies are grouped into three main categories: aggradational facies with upward-fining or massive sand, progradational facies consisting of upward-coarsening sand, and mixed facies, which are a combination of aggradational and progradational elements. Aggradational sand-rich facies dominated the north half of the basin during deposition of unit 2L (fig. I-12). South of central Midland County progradational facies dominate. This transition from dominantly aggradational to dominantly progradational facies coincides with a pronounced narrowing of the basin resulting from a carbonate-shelf-edge promontory that extends 15 mi westward into the basin in northeast Glasscock County (termed the Glasscock County narrows in this report). Between these two end members is an area of considerable facies variability in which upward-coarsening sands overlain by upward-fining sands that impart a "spiked" log response are common.

Interpretation

Unit 2L composes the first pulse of lower Spraberry submarine fan progradation and aggradation in the Midland Basin. Maximum deposition occurred near the sediment source in the northern half of the basin. Narrow, elongate depositional patterns were clearly influenced by the shape of the basin. Furthermore the bathymetry of the paleosurface upon which unit 2L was deposited also influenced sedimentation trends, as is well illustrated in the Jo Mill field area.

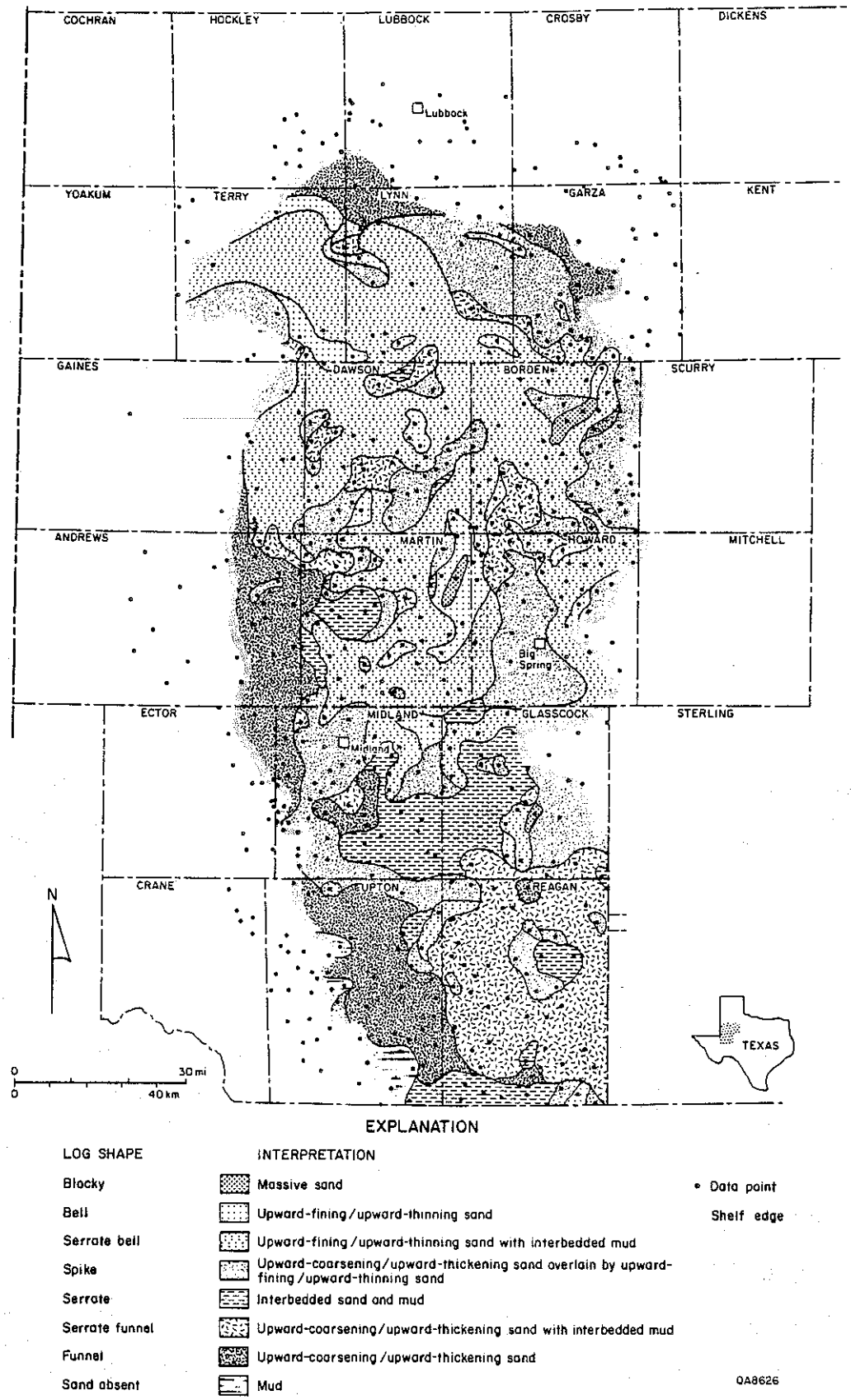

Figure I-12. Log facies map of unit 2L. Aggradational facies of innerfan and midfan origin extend as far south as the Glasscock County narrows.

As indicated by log facies mapping, the thick, sand-rich northern third of the fan that lies north of the Horseshoe Atoll was dominated by channel sedimentation. These sediments were deposited on the inner fan. Further basinward, south of the Atoll and north of the Glasscock County narrows, midfan sediments of considerable internal and lateral variability (as shown by log facies maps) were deposited. These sediments grade basinward into outer-fan sediments where the sands display upward-coarsening trends. Higher-resolution maps of smaller study areas have shown that channels traversed the outer fan; however, the dominant vertical succession is one of increasing grain size and bed thickness as successively more proximal deposits of channel or interchannel origin were vertically superposed during progradation of the fan system.

Lower Spraberry Unit 1

Thickness Trends

As with lower Spraberry unit 2, lower Spraberry unit 1 was strongly influenced by the paleobathymetry of the subjacent Atoll. However, in contrast to unit 2L, unit 1L has two distinct depocenters: one north of the Atoll, and the other basinward of the Atoll (fig. I-13). The proximal depocenter is centered in Lynn County and extends southward into Borden County, where it terminates immediately superjacent to the Atoll. The second depocenter lies in southern Martin and in Midland Counties.

Sand-Distribution Patterns

Net-Sand Trends

Unit 1L was a far more vigorous system than the underlying unit 2L. Net-sand thicknesses of greater than 30 ft extend as far south as central Reagan County 60 mi

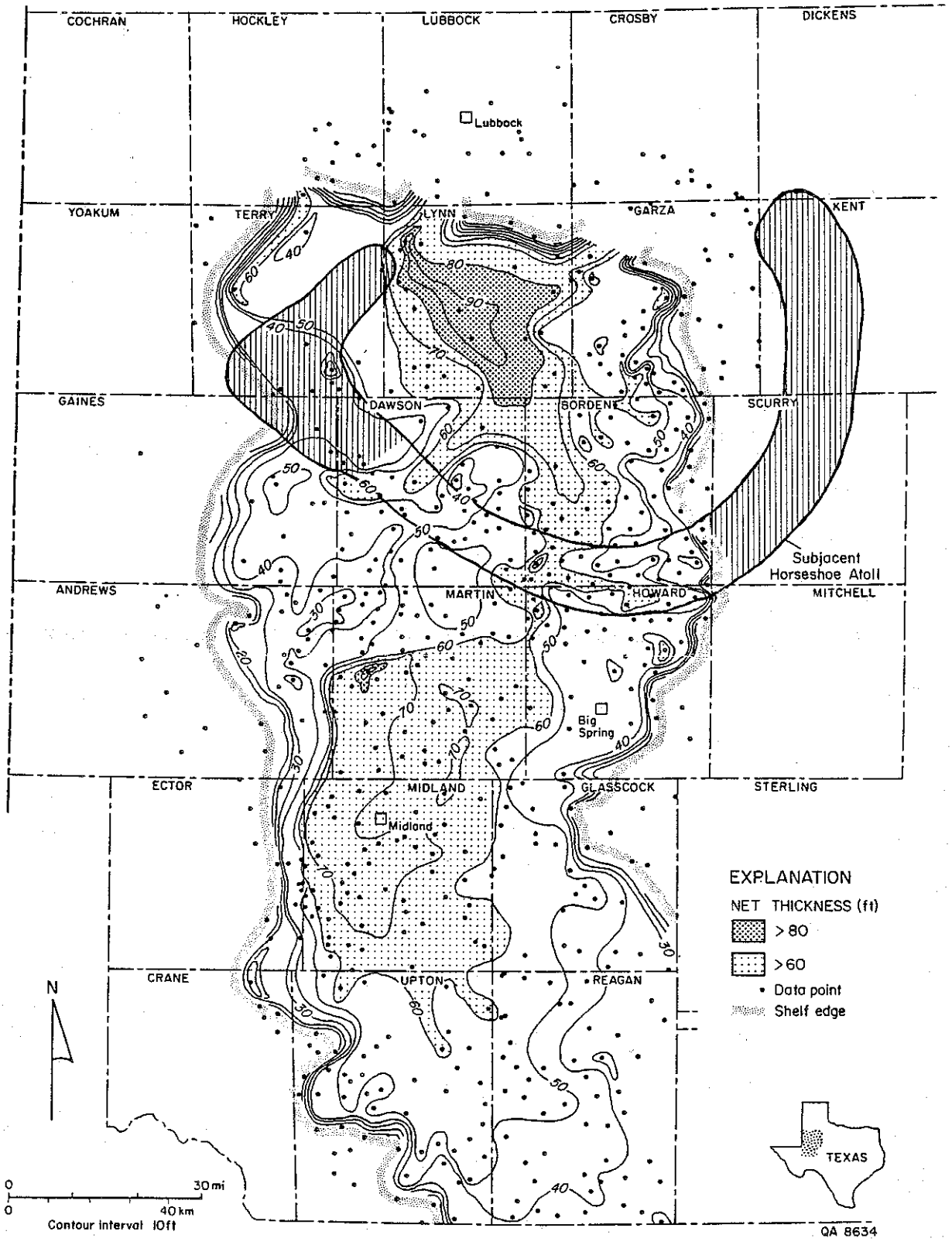

Figure I-13. Isopach map of unit 1L showing two principal depocenters: one north of the subjacent Atoll and the other in Martin and Midland Counties.

farther south than the equivalent net-sand thickness in the underlying unit. Sand supply was from the north primarily through Lubbock County and perhaps to a lesser extent through Hockley County (fig. I-14). The Lynn County depocenter received more than 60 to more than 90 ft of net sand, and the Martin County depocenter was only slightly less active. The two depocenters were linked through the Jo Mill bathymetric low in the Horseshoe Atoll; this area also contains high-net-sand values. Away from the two depocenters, sand distribution shows minor variations in thickness. Greater than 30 ft of net sand extends over much of the basin floor.

Percent-Sand Trends

High-percent-sand values (greater than 80 percent) extend as far south into the basin as central Midland County, 100 mi from the north shelf edge and sediment supply source. Greater than 60 percent sand extends beyond southern Reagan County (fig. I-15). Much of the north half of the basin north of the Glasscock County narrows contained more than 80 percent sand. The gradation from sand-rich deposits of the fan to the sand-poor shelf slope is rapid along much of both the east and west margins of the basin. Subtle sand-thickness variations in this area are magnified by percent-sand contours, which outline linearly oriented but irregularly shaped sand-percent lows.

Interpretation

Lower Spraberry unit 1 is a record of maximum progradation of the lower Spraberry submarine fan (termed the Jo Mill fan by Guevara [in press] and Tyler and Gholston [in press]) into the Midland Basin. Maximum accumulation of sediments occurred in the Lynn County depocenter immediately above the principal depocenter of unit 2L (see figs. I-8 and I-13). Away from this depocenter, in Borden County for example, depositional trends followed the principal of compensation cycles (Mutti and

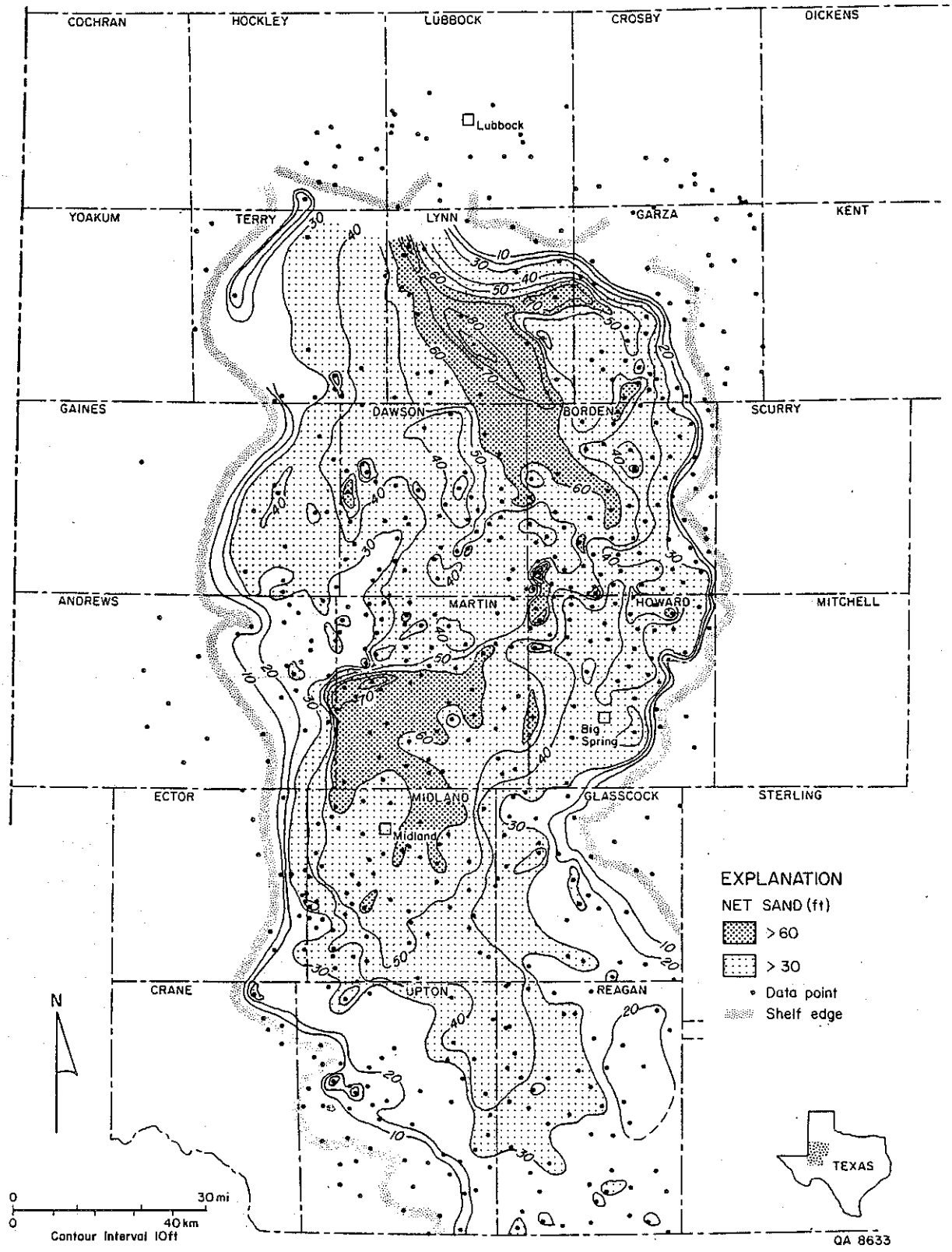

Figure I-14. Net-sand map of unit 1L showing sand maxima in the two depocenters.

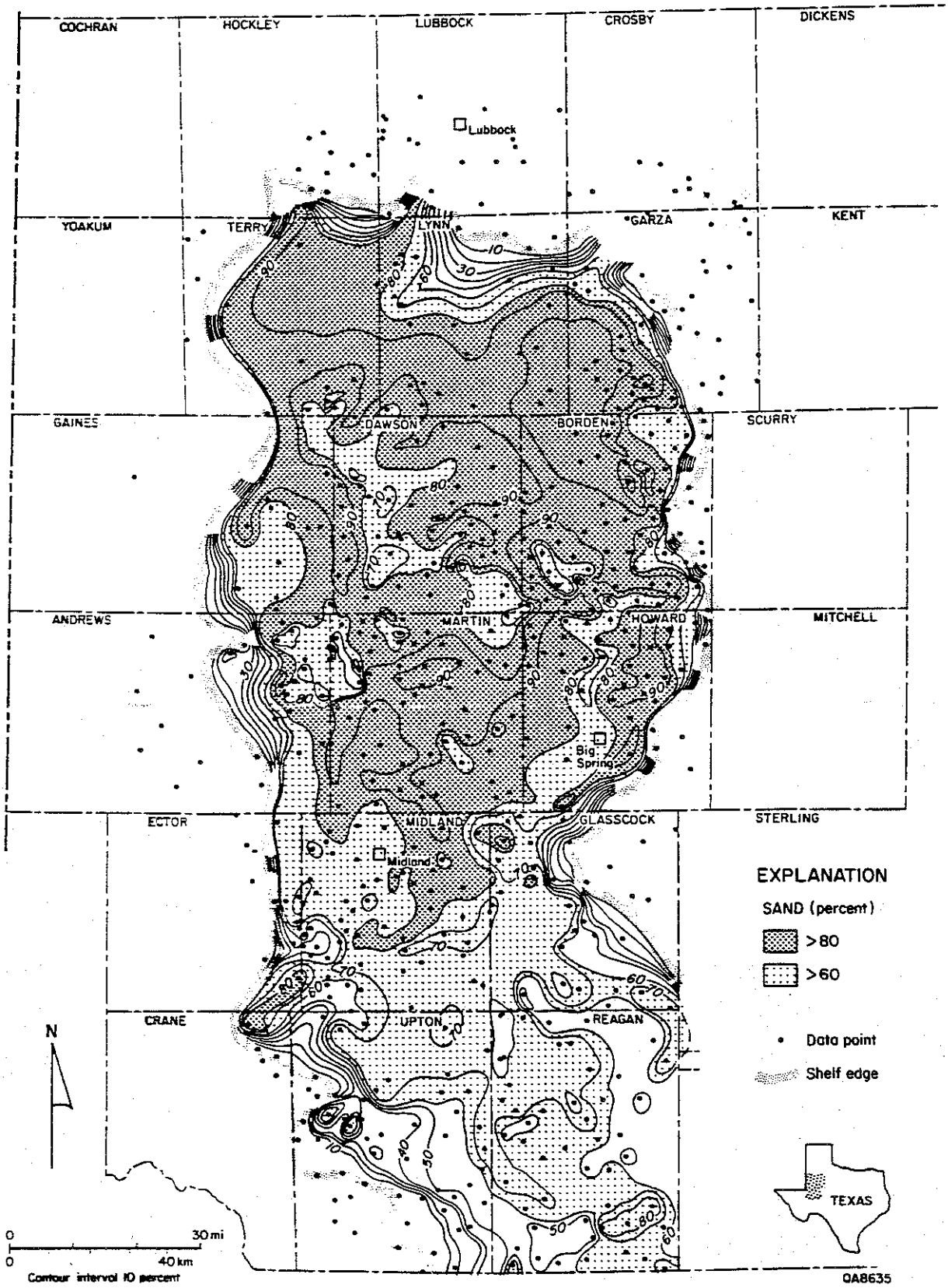

Figure I-15. Percent-sand map of unit 1L showing high values across the entire basin. This unit, which composes the uppermost operational unit of the Jo Mill fan, advanced vigorously across the basin floor and is productive in the most distal Spraberry fields.

Sonnino, 1981) as thicks in unit 1L are displaced relative to thicks in unit 2L.

Unit 1L is a far more sand-rich system than the underlying unit. Inner-fan facies composed of more than 80 percent sand extended to the Glasscock county narrows and midfan facies and beyond to the basinward limit of mapping.

The Jo Mill fan was thus a highly active, vigorous system that extended at least 120 mi from the principal sediment source into the basin. Basin-floor bathymetry shaped patterns of sedimentation, as did the elongate morphology of the basin.

Upper Spraberry Unit 5

Spraberry units 5U and 1U are the principal reservoirs in the upper Spraberry in the central Midland Basin. These two sand-rich intervals cap upward-coarsening and upward-thickening sequences (fig. I-7) and have been interpreted as the most proximal deposits of two stacked submarine fan assemblages in the upper Spraberry (Guevara, in press; Tyler and Gholston, in press).

Thickness Trends

During sedimentation of unit 5U, two discrete depocenters actively received sediment. The principal center, where maximum thicknesses of 120 ft are attained, is in the most proximal part of the basin, north of the Horseshoe Atoll (see map in folder). Immediately south of the Atoll thicknesses are low but again increase into the second depocenter in Midland and Upton Counties, where thicknesses of between 60 and 70 ft are present.

Sand-Distribution Patterns

Net-Sand Trends

Three point sources supplied sediment into the basin during deposition of unit 5U. Sand influx was from the north through Lubbock County, from the northwest through Hockley County, and from the west through Terry County via Yoakum County (fig. I-16). Anomalously low net-sand values in the core of the Hockley and Terry point sources are interpreted as mud-filled inner-fan channels. Immediately basinward of these three input sources is a linear belt of more than 60 ft net sand. Vector movement of sediment was from the northwest toward the east shelf in southern Garza and eastern Borden Counties, where a second sand thick was formed, then swept southwest parallel to the Glasscock County narrows into Martin and Howard Counties. Here sand trends tend to bifurcate into southwestward-oriented axial/interaxial elements and then merge into a single, broad, high-sand axis that extends over most of Midland County. A second high-sand axis hugs the east shelf slope of the CBP (fig. I-16).

Percent-Sand Trends

The Terry County depocenter is well illustrated by the percent-sand map. The very proximal fan contains 90 percent sand (fig. I-17). Intermediate sand contents of 60 percent and greater display similar orientations as the net-sand trends and extends basinward to the Glasscock County narrows. Axial/interaxial elements are well defined in the central basin. Basinward decrease in sand percentage south of this area is irregular, with erratically distributed areas of less than 30 percent sand interspersed with sand-rich belts containing more than 50 percent sand.

Two prominent sand-rich areas lie in far western Midland County and in northeastern Reagan County (fig. I-17). The Midland County anomaly is characterized

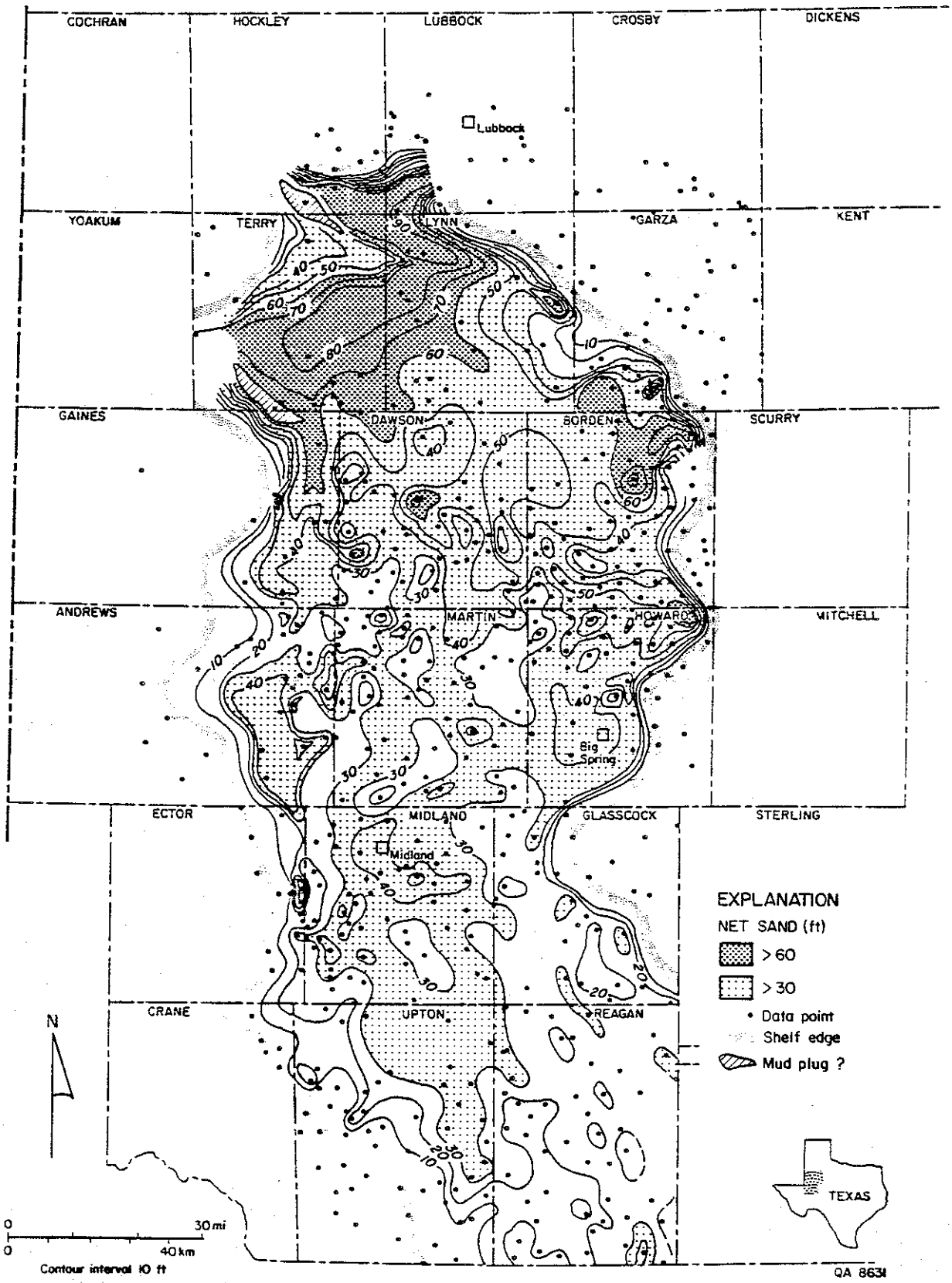

Figure I-16. Net-sand map of unit 5U.

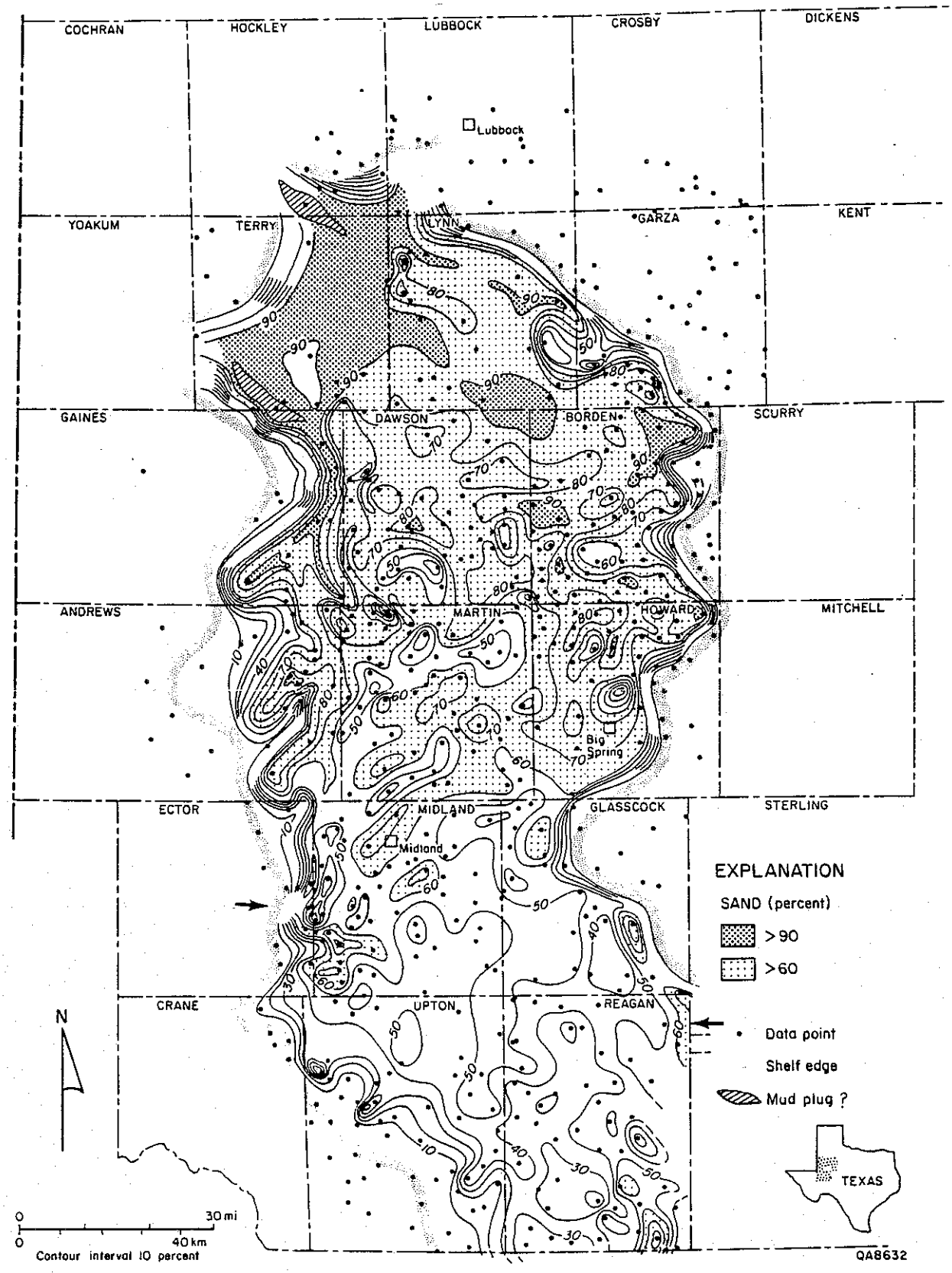

Figure I-17. Percent-sand map of unit 5U showing linear depositional axes of high and low values. Results of possible failure of the shelf edge are shown in Reagan and Ector Counties.

by a lobate character; the Reagan County sand thick is, as a result of widely separated data points, less well defined.

Facies Composition

Spraberry unit 5U is dominated by progradational facies (fig. I-18). Aggradational facies are best developed in the most proximal parts of the fan in Terry and Lynn Counties. Farther south, to the Glasscock County narrows, aggradational facies form discrete linear belts or isolated pods and are less abundant than upward-coarsening facies. South of the narrows, aggradational facies are almost entirely absent, and the fan is composed almost entirely of upward-thickening and upward-coarsening sediments.

Interpretation

Unit 5L comprises the most proximal deposits of the Driver fan. However, this fan was not highly active. Thick aggradational facies that compose the inner fan are confined to the northernmost parts of the basin in Terry and Lynn Counties. Midfan facies extend basinward to the Glasscock County narrows, south of which outer-fan facies predominated. Both the inner and outer fan was channelized, yet channel deposits were not a dominant constructional element.

Sediments entered the basin almost exclusively from the north. However, there was a contribution from the CBP and from the eastern shelf. High-percent-sand belts flanking the shelf may be the products of slope failure and gravity sliding into the basin. Alternatively, the sand-percent high adjacent to the eastern shelf in Reagan County may be the product of deltation during sea-level lowstand. The east shelf had historically been the site of active deltaic and submarine fan sedimentation, which was possibly reactivated during the Leonardian.

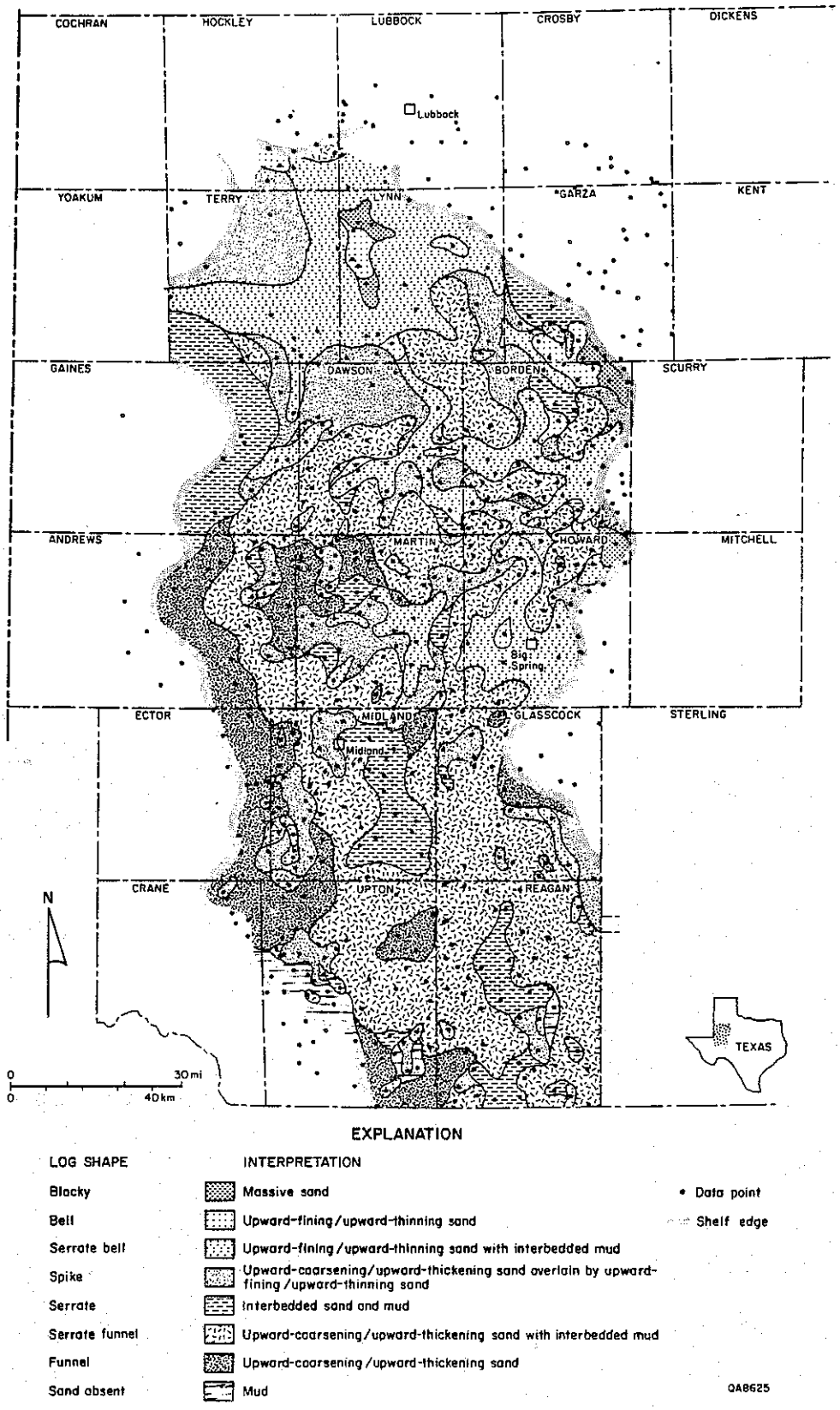

Figure I-18. Log facies map of unit 5U showing aggradational inner-fan facies confined to the northern third of the basin; the remaining basin floor is covered by progradational facies. Unit 5U is the uppermost operational unit of the Driver fan.

Upper Spraberry Unit 1

Thickness Trends

Sedimentation patterns in upper Spraberry unit 1 are similar to those displayed in unit 5U. Two depocenters actively received sediment in unit 1U: a proximal depocenter between the shelf edge and the Atoll and a second depocenter south of the Atoll in Midland and Upton Counties (see map in folder). Sediment accumulation in the proximal depocenter was less than that of unit 5L; only a maximum thickness of 100 ft was attained. In the southern depocenter, thicknesses of 60 to 70 ft are comparable with those of unit 5U.

Sand-Distribution Patterns

Net-Sand Trends

As with unit 5U, sand influx into the basin was dominantly from the northwest through Terry County (fig. I-19). Sand swept southeastward toward the east shelf, then veered toward the southwest. South of the Glasscock County narrows in the second of the two-unit 1U depocenters, the area containing greater sand thicknesses of 40 ft or more expands over parts of Midland, Glasscock, Reagan, and Upton Counties.

Percent-Sand Trends

In unit 1U the proximal Spraberry in Terry and adjacent counties contains more than 90 percent sand (fig. I-20). Sand-distribution orientations shown in net-sand maps are repeated in percent-sand maps with high-sand axes sweeping toward the east shelf then being deflected toward the southwest. In the six-county area of intermediate sand values north of the Glasscock County narrows, southwest-oriented axial/interaxial sand trends are present. Sand-rich axes are even better defined south of the narrows. These axes are strongly evident in the detailed maps presented later

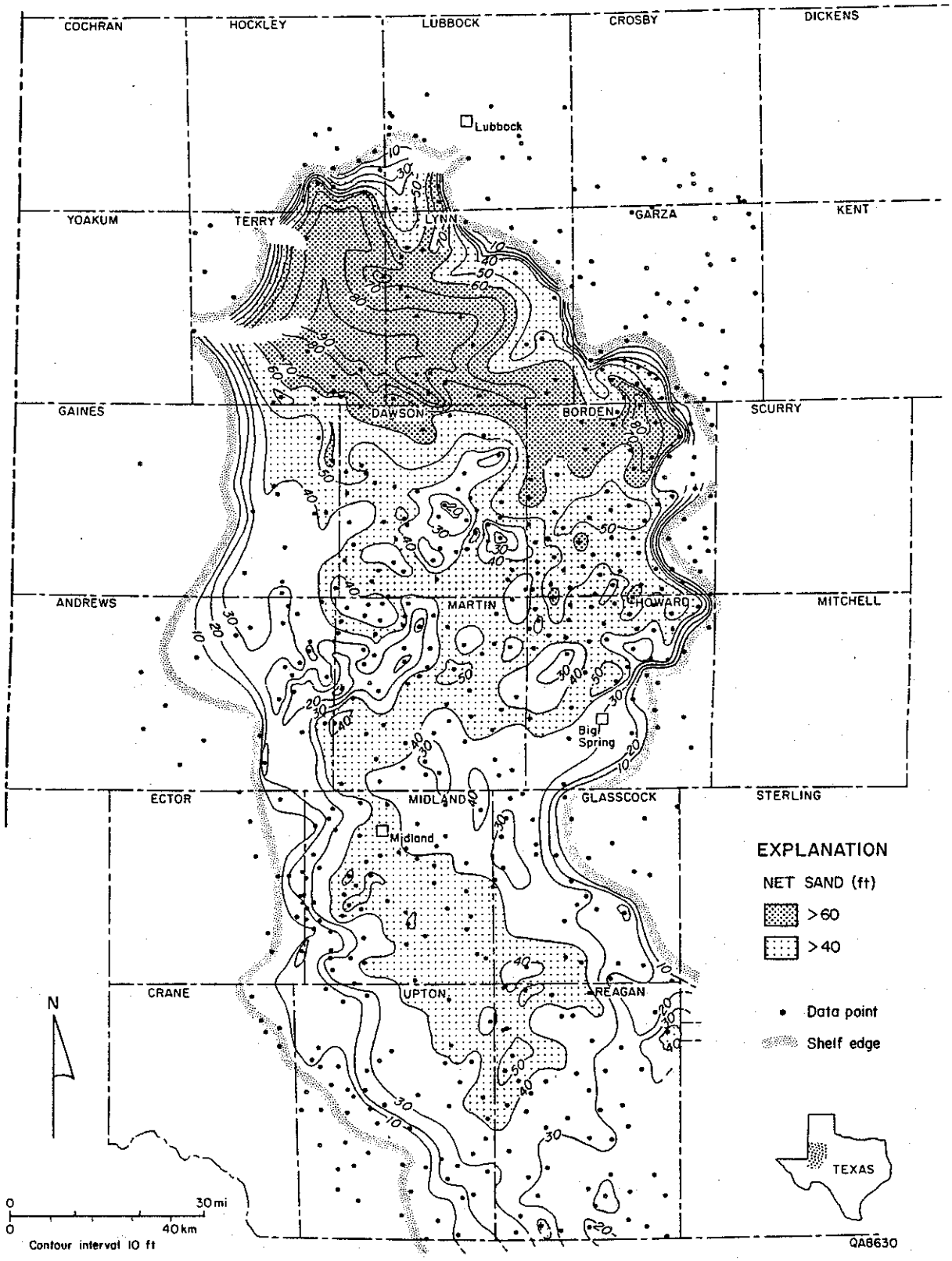

Figure I-19. Net-sand map of unit 1U showing high sand values extending as far south as Reagan County. Sand trends were strongly influenced by the shape of the basin.

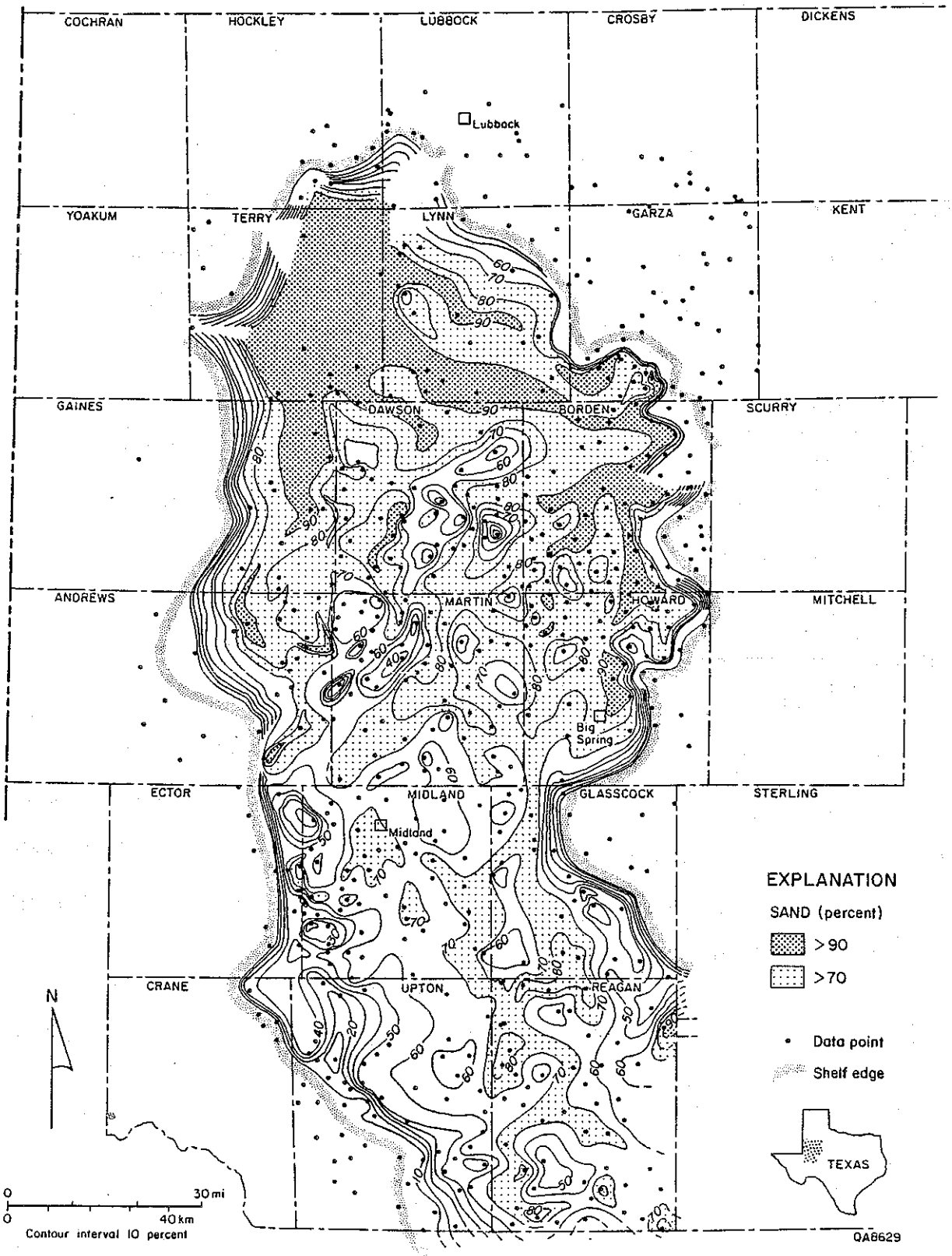

Figure I-20. Percent-sand map of unit 1U illustrating well-defined depositional axes throughout the basin.

in this report and furthermore have been shown to control production trends in the Shackelford and Preston waterflood units in the central Spraberry Trend (Tyler and Gholston, in press).

Facies Composition

Sand-rich aggradational facies dominate the north and northeast parts of the basin (fig. I-21), reflecting sediment dispersal patterns in the basin. The west flank of the north half of the basin contains mostly progradational or mixed facies. Aggradational facies extend through the map area, but their dominance is subsumed at the Glasscock County narrows, where progradational and mixed facies assume a dominant role. Nonetheless, aggradational facies are still an important element of these basinward deposits.

Interpretation

The distribution of facies in the proximal parts of the basin result in an asymmetric arrangement of submarine fan divisions. The boundary separating the inner fan from the midfan extends from southwestern Terry to north-central Glasscock Counties. Midfan facies extend to the map limits. Upper Spraberry unit 1, which caps the Floyd fan sequence (fig. I-7), resulted from more vigorous sediment supply and depositional processes than unit 5U at the top of the Driver fan.

HYDROCARBON DISTRIBUTION AND RELATION TO BASIN ARCHITECTURE

Current Spraberry producing areas are shown in figure I-22. There is a strongly bimodal distribution of oil in the formation. In the inner fan, accumulations of oil are

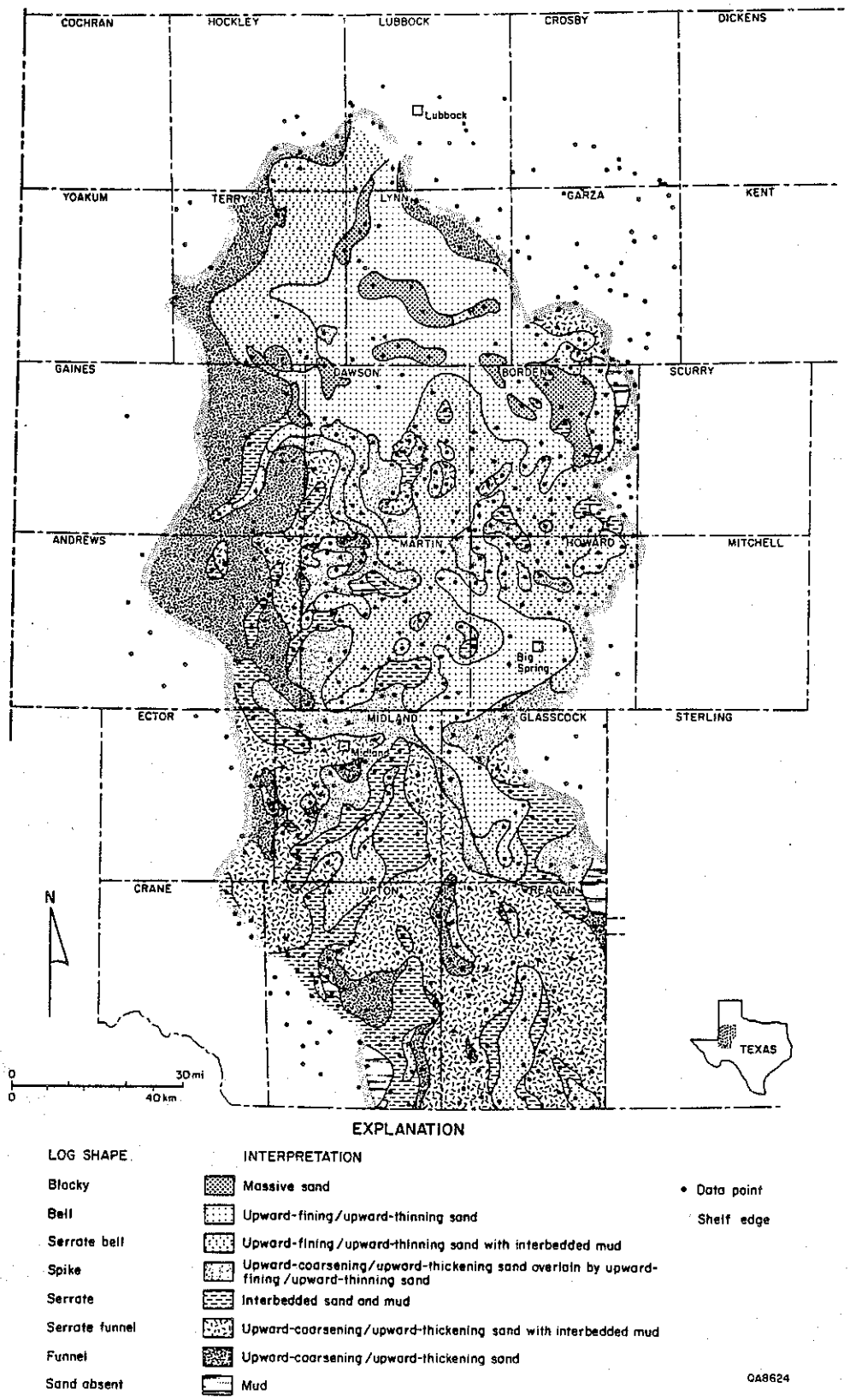

Figure I-21. Log facies map of unit 1U. Facies trends, which are are asymmetrically arranged in the basin, are explained in the text.

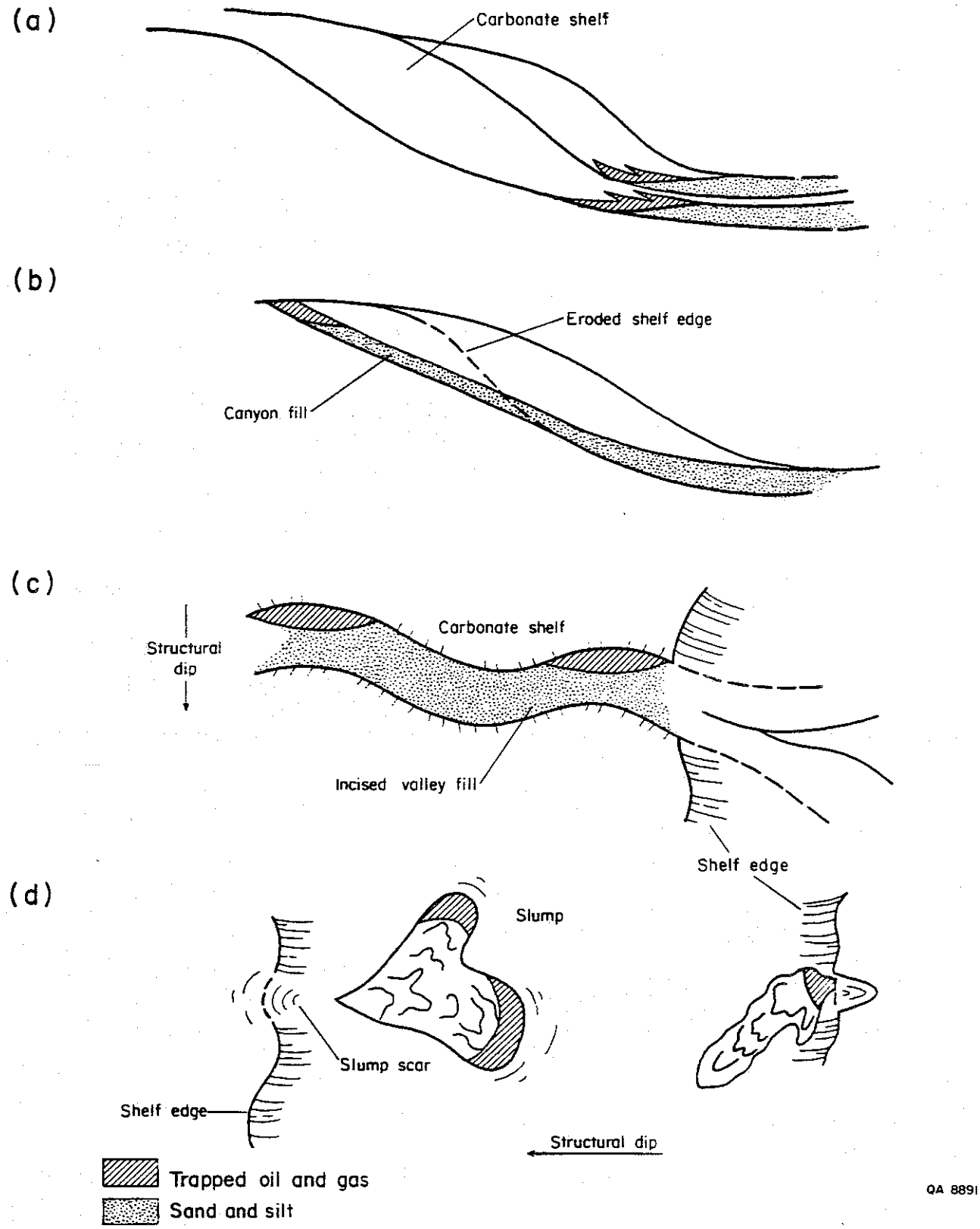

Figure I-23. Potential small field stratigraphic traps in the basin and basin margin. (A) Pinch-out of sand against the advancing toe of the shelf slope. (B) Truncated and sealed sand-rich canyon fill. (C) Possible lowstand incised river valleys on the shelf. (D) Carbonate or sand slumps onto the basin floor.

class of trap would be arranged en echelon coincident with the shelf-slope/basin-floor transition. With the exception of the north half of the basin, sand quality would be poor.

Influx into the basin was through a limited number of canyons along the north and northwest shelf edge. Wedge-out of sand-rich canyon-fill sediments against overlying bounding surfaces (fig. I-23b) also may provide a stratigraphic trap. Pay would be elongate normal to the basin edge and narrow parallel to the shelf. Seismic investigations would be invaluable in detecting this class of trap.

Although the prevailing model for the origin of the Spraberry holds that the sands were originally eolian in origin, deposited subaqueously on the shelf, and subsequently flushed into the basin by density currents, a yet-to-be-tested alternative hypothesis is that the Spraberry fans are lowstand deposits. In this event, sand entering the basin would pass through incised channels on the shelf. Sand-filled channels would provide linear shoestring stratigraphic or structurally modified stratigraphic traps (fig. I-23c) in the subsurface.

Instability of the prograding shelf and resultant slope failure have been demonstrated in units 2L and 5U (figs. I-11 and I-17). The deposits arising from these events are of local extent and trend normal to obliquely to the shelf edge (fig. I-23d). These slump fans are predominantly composed of lithic carbonate fragments that may be locally sealed in basinal deposits, particularly if they occur in the muds of the middle Spraberry. Structural tilt coupled with updip porosity pinch-out would create a combined structural/stratigraphic trap.

Additional Recovery from Existing Fields

It remains our conviction that the greatest potential for additional recovery from the Spraberry lies in reexploration of existing fields. As has been demonstrated by

Guevara (in press) and Tyler and Gholston (in press) and as documented later in this report, the complex internal architecture of Spraberry reservoirs presents opportunities for the drilling of geologically targeted infill wells in depositional axes and for recompletion of wells in previously untapped zones. From a regional perspective, and with particular reference to property acquisition, areas where midfan facies are stacked in multiple zones maximize opportunities for extended conventional development of this highly stratified pool. It is in the midfan to distal fan that facies variability reaches a zenith, allowing for maximum between-well variability. Additionally it is in this part of the fan that stacking of channel axes defines production sweet spots. For these reasons the studies described in the following sections of this report have focused primarily on midfan to distal-fan facies at and south of the Glasscock County narrows.

II. FIELD STUDIES

Studies on the stratigraphy of Spraberry oil reservoirs were conducted on a 60-mi^2 ununitized area north of the Driver and east of the Preston/Shackelford waterflood units in parts of blocks 36 and 37 of the T&P RR survey in east-central Midland and west-central Glasscock Counties (fig. II-1). During the last quarter of the RCRL's first project year, Mobil Producing Texas and New Mexico drilled the Judkins A No. 5 well in the northwest part of the study area in Midland County (fig. II-1); cores and logs from this well will be available to the RCRL for study during the second project year.

Objectives of the field studies were (1) to extend mapping of genetic intervals of the Spraberry Formation previously delineated by Guevara (in press) and Tyler and Gholston (in press) in the adjacent unitized areas; (2) to map porosity distribution of the principal Spraberry oil reservoirs using the available log data; and (3) to assess recovery from Spraberry reservoirs that have not been subjected to waterflooding.

More than 200 wireline logs were used (fig. II-2), mostly gamma-ray/neutron (GNT) and logs consisting of a gamma-ray curve only or combinations of gamma-ray and resistivity curves. Production data from 18 wells (provided by RCRL sponsors), logs, and scout cards were the main sources of data.

Stratigraphic sections were constructed, three approximately east-west, or strike-oriented and two approximately north-south or parallel to the paleodip. Two sections are included in this report (fig. II-2). Structure, isopach, isolith, log facies, sandstone shaliness, and porosity maps were constructed, as well as percent-sand cross sections using percent-sand maps. All basic data and drafts of maps and sections constructed are on file at the Bureau of Economic Geology and are available to RCRL sponsors.

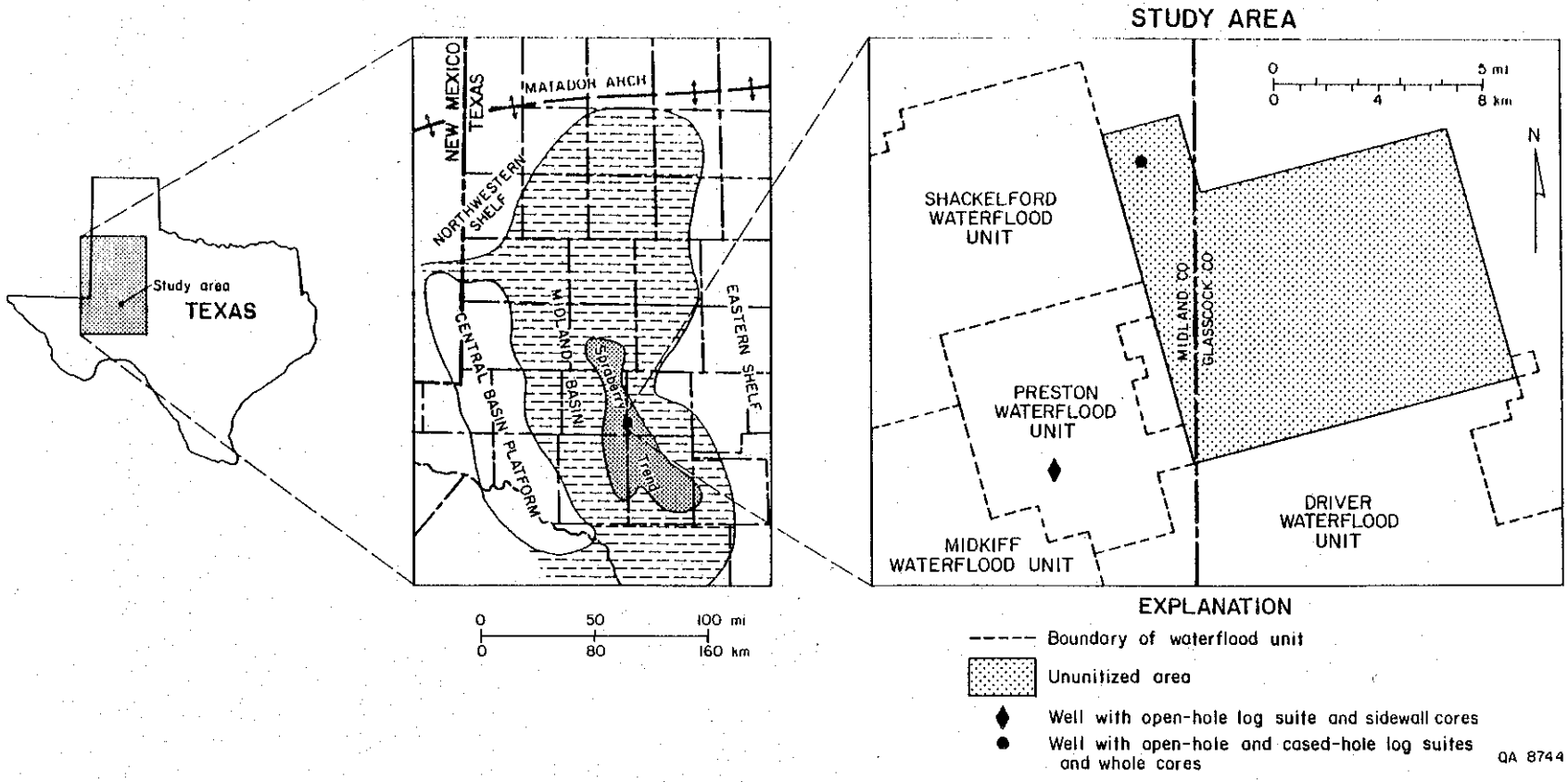

Figure II-1. Locations of the ununitized area studied and of the wells cored and logged in the Spraberry Trend.

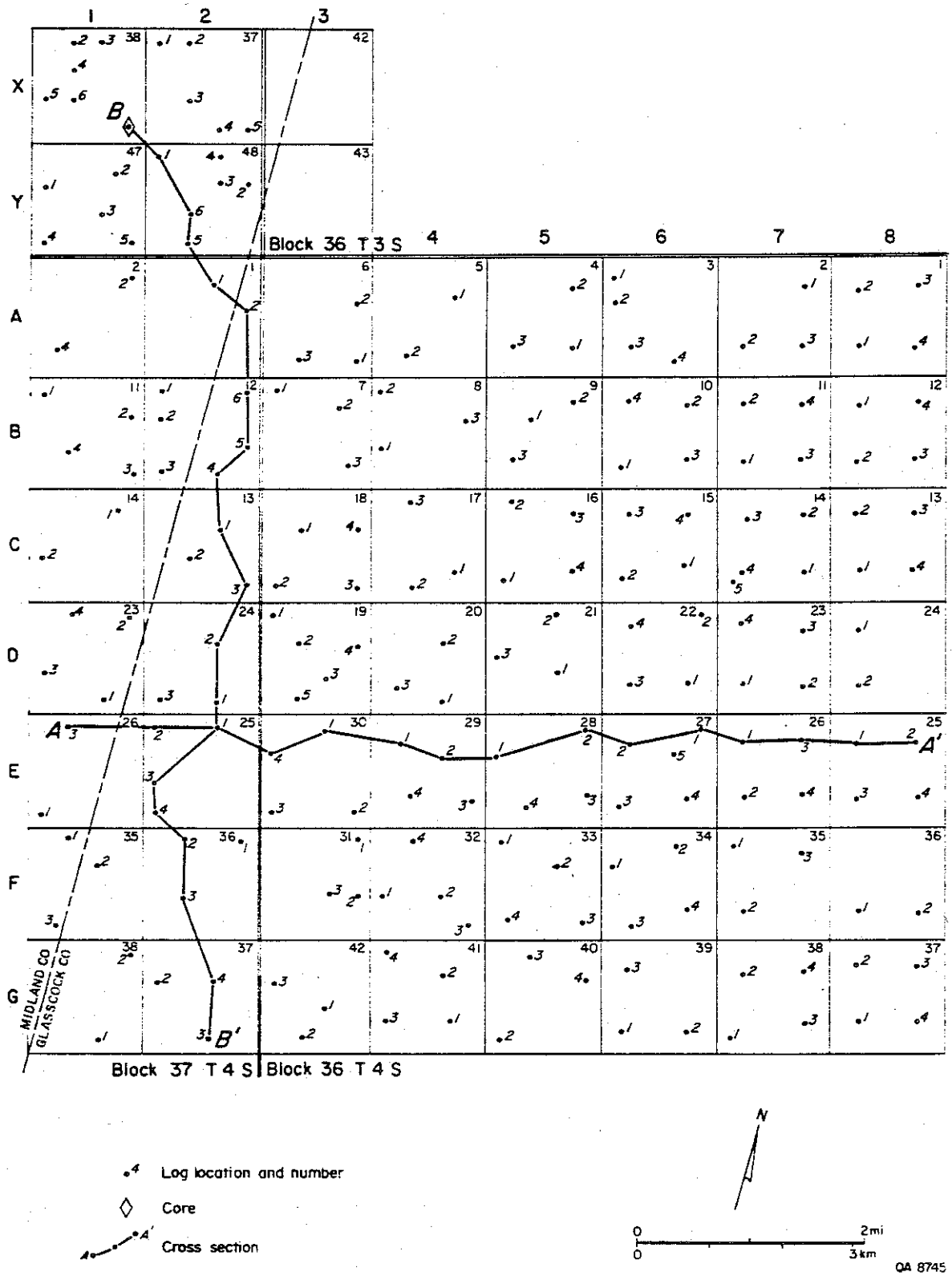

Figure II-2. Subsurface control and cross sections, ununitized area, Spraberry Trend.

Subdivisions of the Spraberry Formation

Stratigraphic distribution and log signature of operational units composed mainly of sandstone and siltstone (fig. I-7) permitted a threefold subdivision of the Spraberry Formation in the study area. The upper six units, named 1U through 6U (figs. I-7, II-3, and II-4), compose the upper Spraberry. They generally show funnel log shapes in the study area and are stacked, forming two successive upward-coarsening and upward-thickening sequences (1U through 4U and 5U through 6U). The thickest beds of sandstone and siltstone occur in sandstone zones c and f (fig. I-7) in the upper parts of the upward-thickening sequences. The intermediate six units, named 1M through 6M (figs. I-7, II-3, and II-4), occur in the middle Spraberry and are vertically separated by shales and carbonates. They generally display bell log motifs, except unit 1M, which shows funnel log shapes. The lower 2 units, named 1L and 2L and composing the lower Spraberry (figs. I-7, II-3, and II-4), usually display funnel log motifs and are stacked, forming an upward-coarsening and upward-thickening sequence. The thickest beds of sandstone and siltstone occur in sandstone zones s and v (fig. I-7). Operational unit 1L was subdivided in the study area into a lower part having funnel log shapes and capped by sandstone zone s and an upper part that displays bell log motifs and includes sandstone zone r in its lower part (fig. I-7). All the operational units extend throughout the study area. They show only minor thickness variations, which give rise to an apparent layer-cake stratigraphic framework (figs. II-3 and II-4).

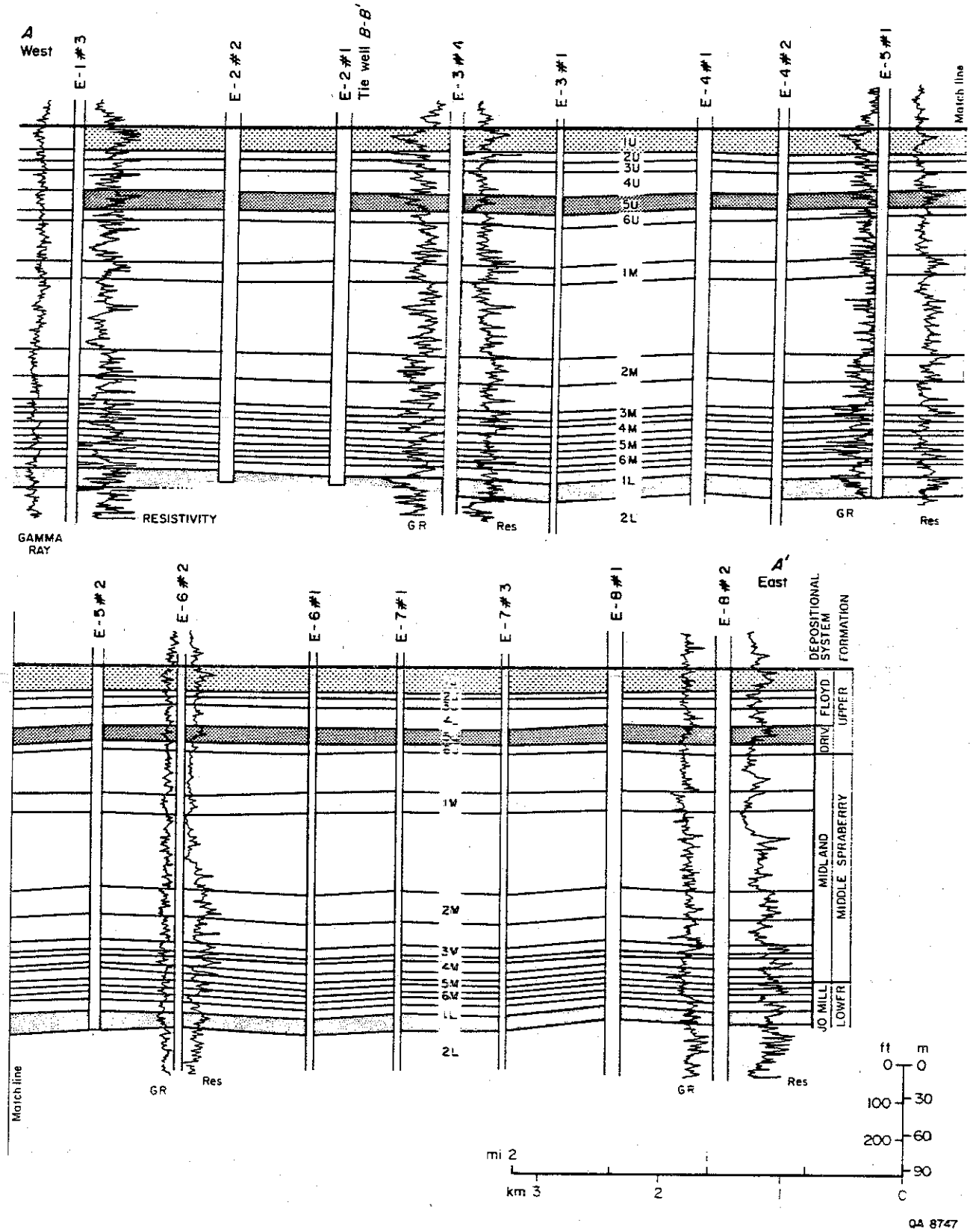

Figure II-3. West-east stratigraphic section, ununitized area, Spraberry Trend. Location in figure II-2.

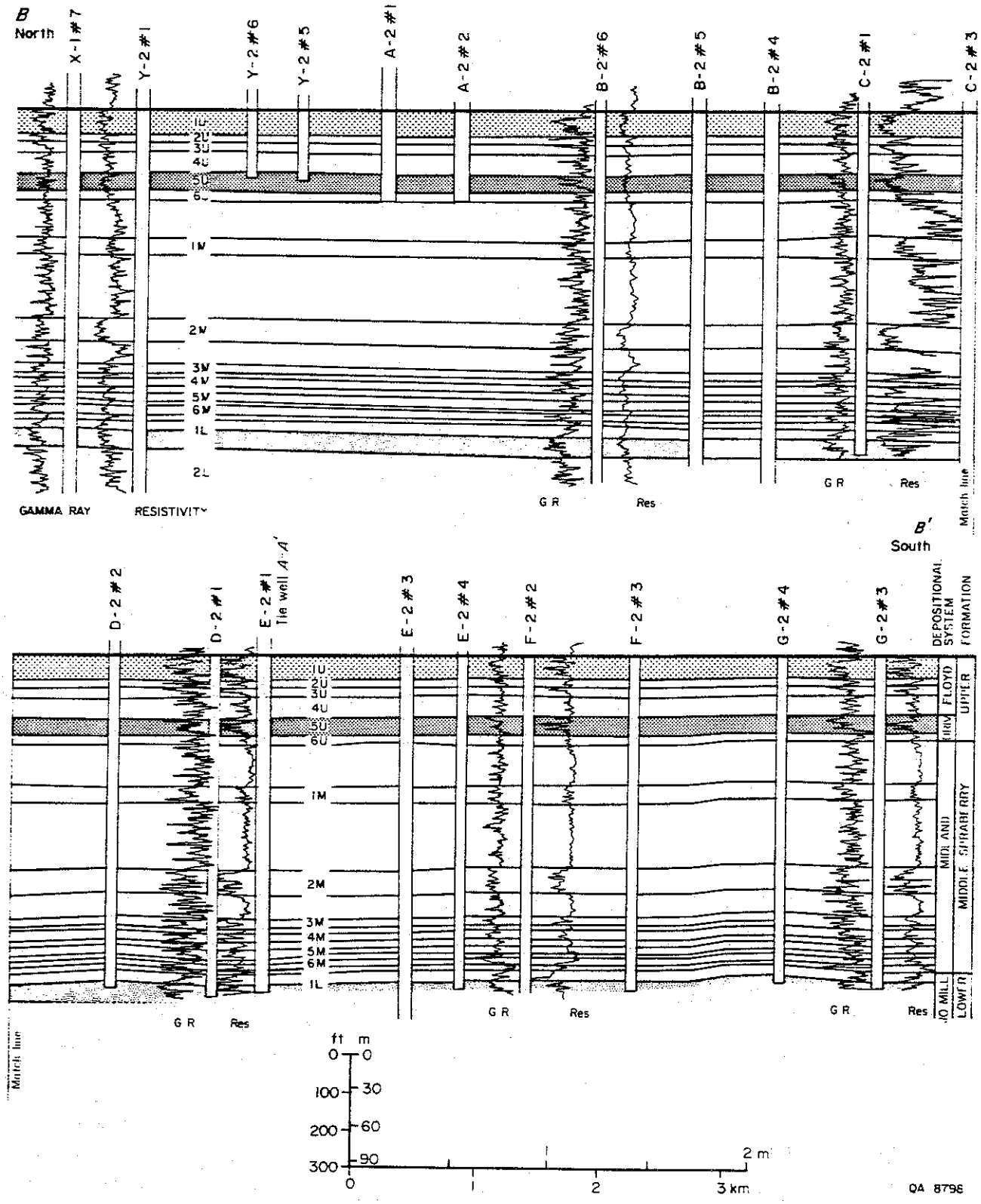

Figure II-4. North-south stratigraphic section, ununitized area, Spraberry Trend. Location in figure II-2.

Distribution of Spraberry Reservoir Rocks

Structure maps show that the operational units in the study area form part of a gently northwest-dipping monocline having local anticlinal noses or wrinkles (figs. II-5 to II-7). Isolith maps were constructed for each operational unit of the upper Spraberry, for the lower and upper parts of unit 1L of the lower Spraberry, and for sandstone zones c (of unit 1U), f (of 5U), and s (of 1L). Studies of waterflood units adjacent to the study area indicate that the best oil reservoirs occur in units 1U (sandstone zone c), 5U (zone f), and 1L (zone s) (Guevara, in press; Tyler and Gholston, in press). Thus, isolith maps of these operational units are presented in this report. Isolith maps were constructed using values of net thicknesses of sandstone and siltstone determined on each gamma-ray log. These maps indicate that although sandstones and siltstones are widespread in the study area, they were deposited mainly in dip-oriented belts (approximately parallel to the basin axis) (figs. II-8 to II-11). These belts trend NNW-SSE to NNE-SSW and are generally 0.5 to 1 mi wide, locally up to approximately 3 mi in width.

The 45-ft isolith of unit 1U (upper Spraberry) depicts mostly meandering and locally braided belts in the northeast, south-central, and west parts of the study area, forming a distributary network (fig. II-8, app. II-A). Total thickness of sandstone and siltstone averages 44 ft and ranges from 56 to 26 ft, both extreme figures occurring in the south-central part of the study area. The 15-ft isolith of sandstone zone c, containing the thickest beds of sandstone and siltstone, shows similar, mainly dip-elongate belts occurring in the west, central, and east (fig. II-9). Total thickness of sandstone and siltstone of this sandstone zone averages 14 ft and ranges from 6 ft in the northeast to 22 ft in the southeast.

The 25-ft isolith of unit 5U of the upper Spraberry defines locally discontinuous, predominantly braided belts in the central and east parts of the study area and a

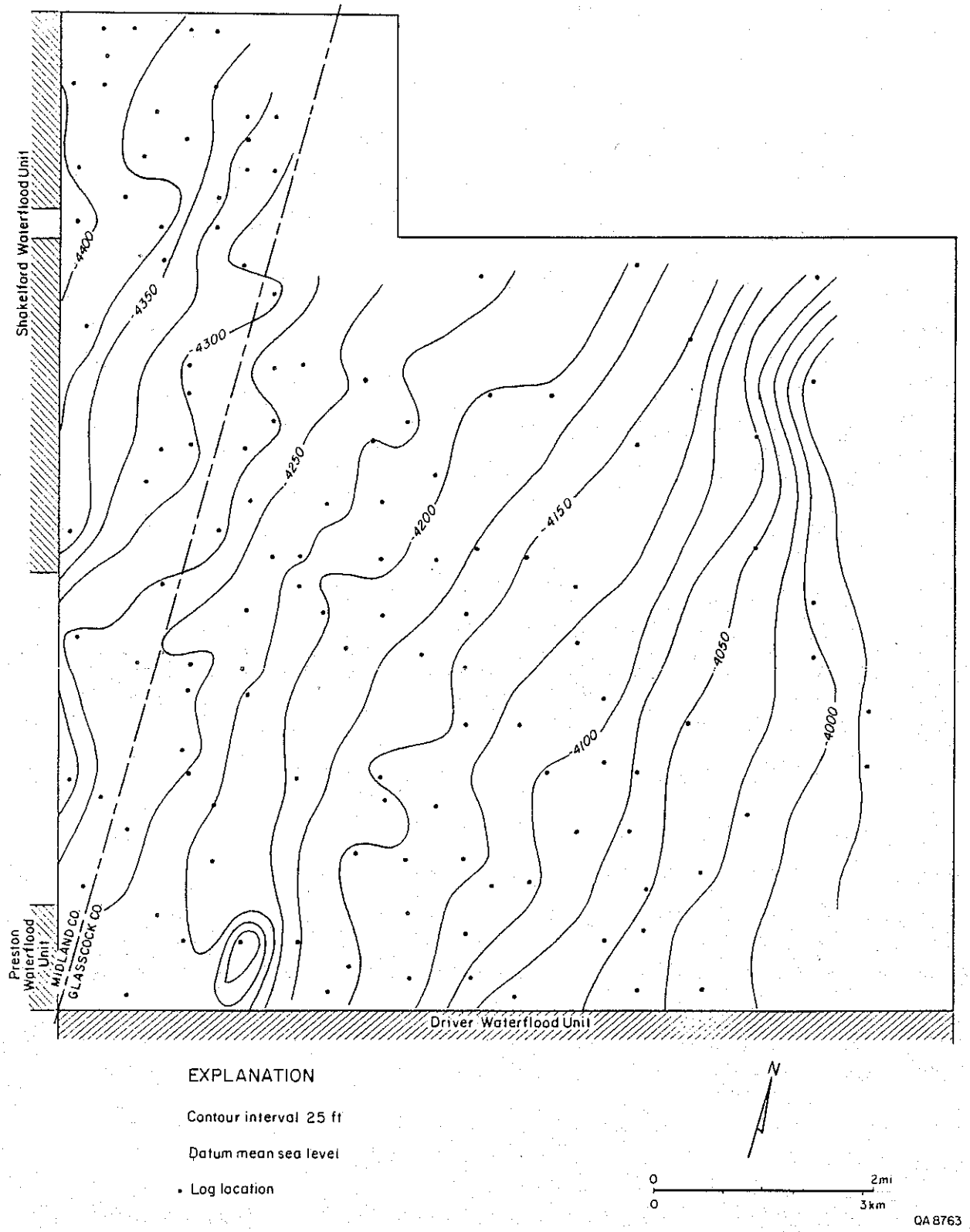

Figure II-5. Structure map of the top of the Spraberry Formation (operational unit 1U, upper Spraberry), ununitized area, Spraberry Trend.

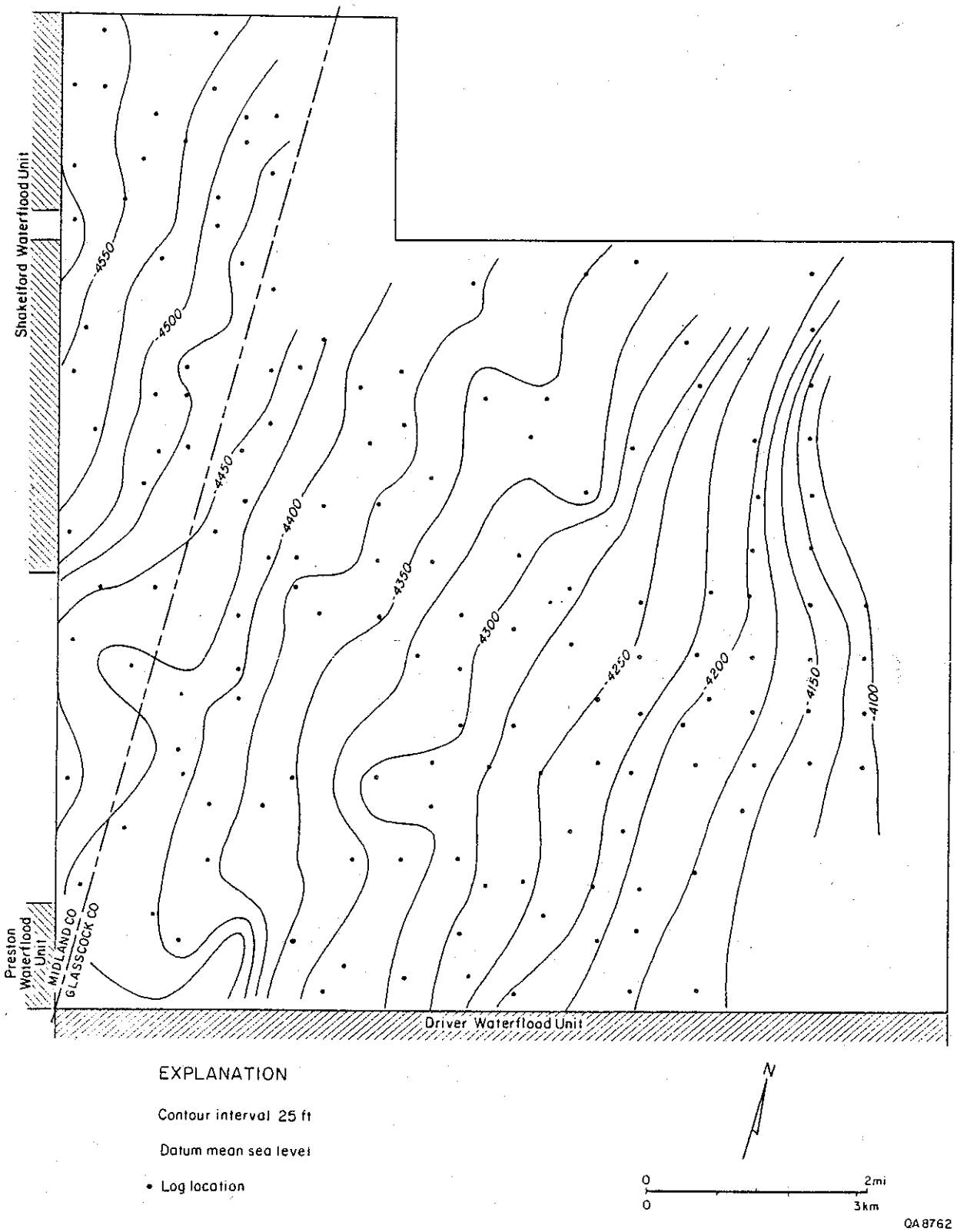

Figure II-6. Structure map of the top of operational unit 5U (upper Spraberry), ununitized area, Spraberry Trend.

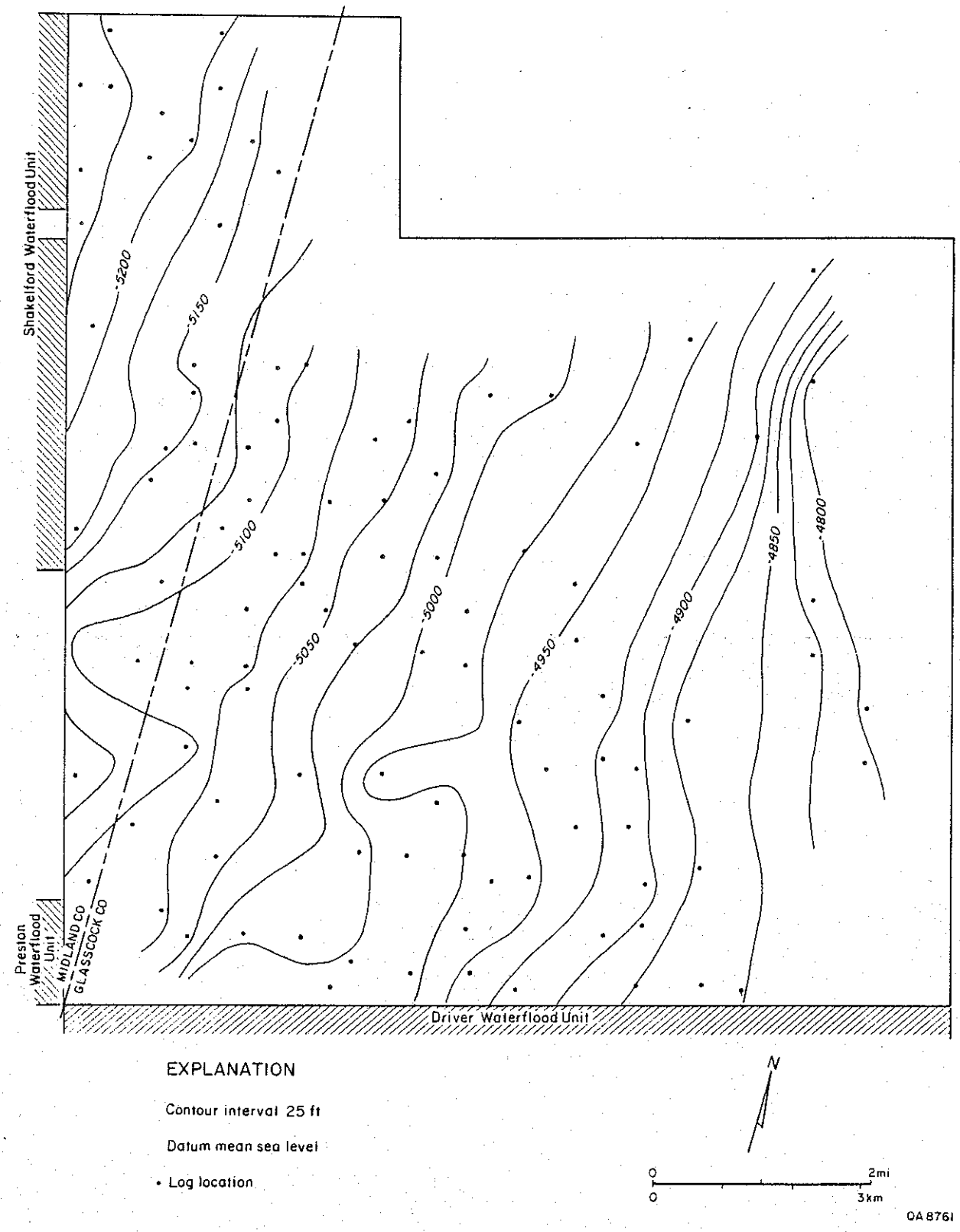

Figure II-7. Structure map of the top of sandstone zone s, operational unit 1L (lower Spraberry), ununitized area, Spraberry Trend.

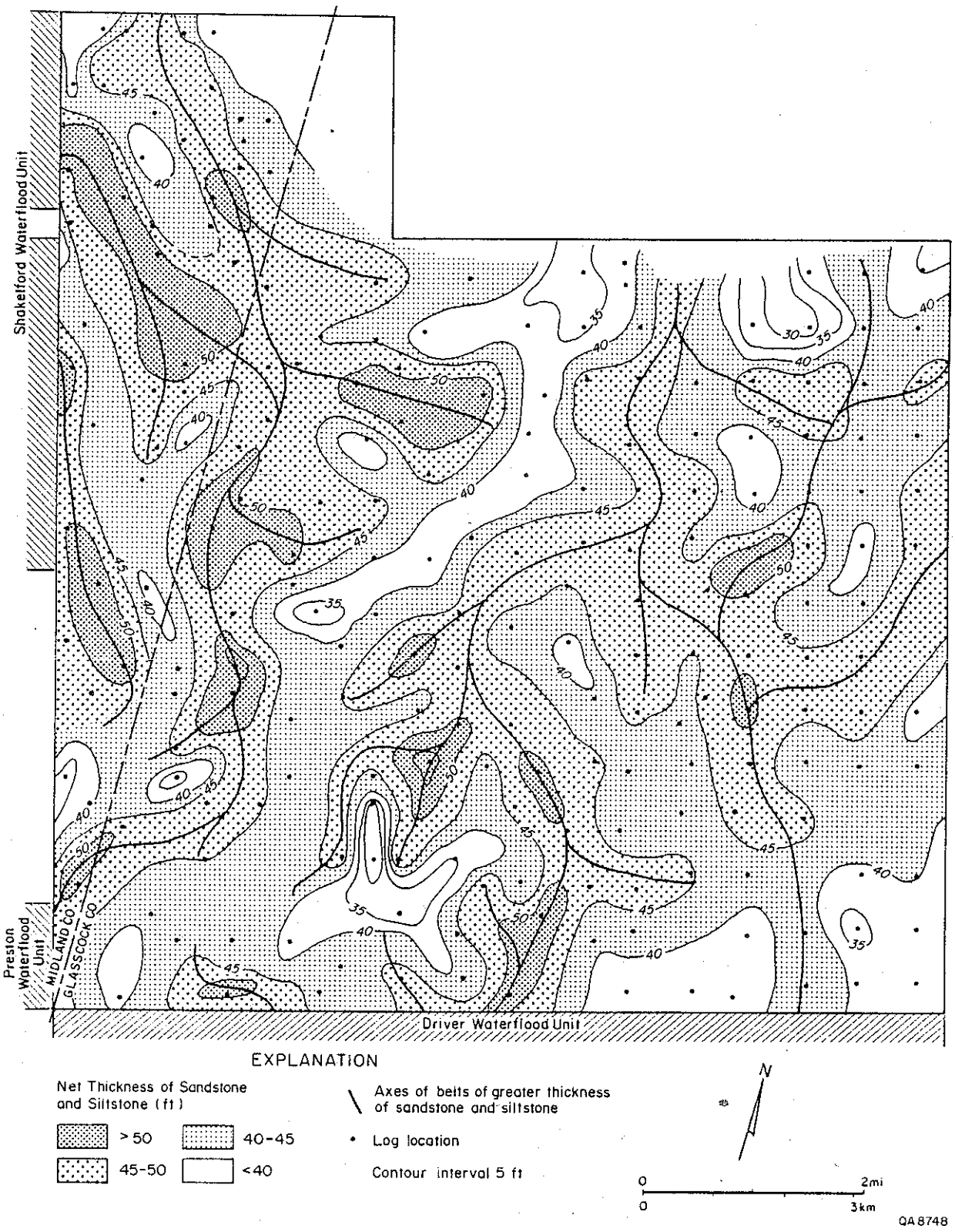

Figure II-8. Map of total thickness of sandstone and siltstone, operational unit 1U (upper Spraberry), ununitized area, Spraberry Trend.

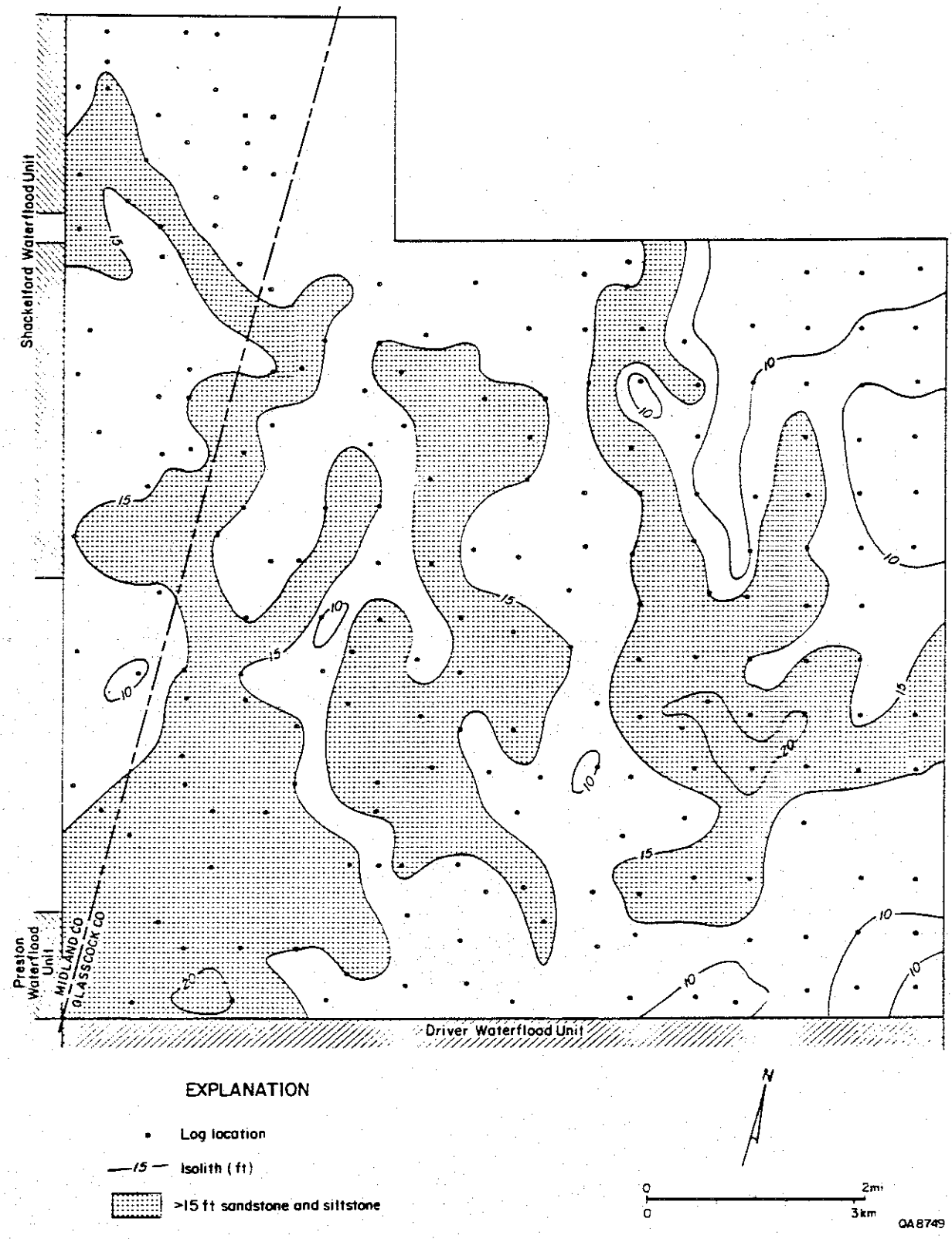

Figure II-9. Map of total thickness of sandstone and siltstone, sandstone zone c, operational unit 1U (upper Spraberry), ununitized area, Spraberry Trend.

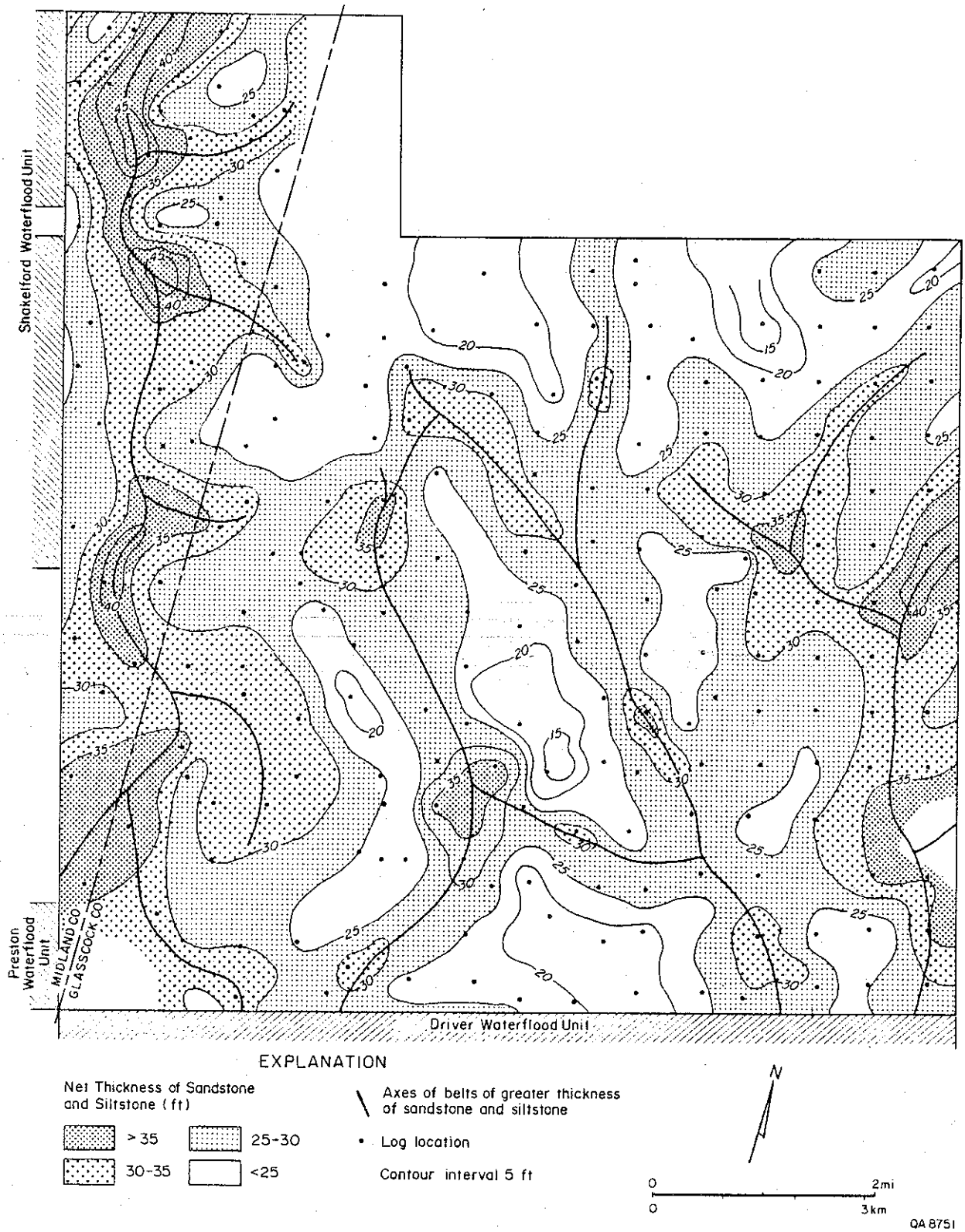

Figure II-10. Map of total thickness of sandstone and siltstone, operational unit 5U (upper Spraberry), ununitized area, Spraberry Trend.

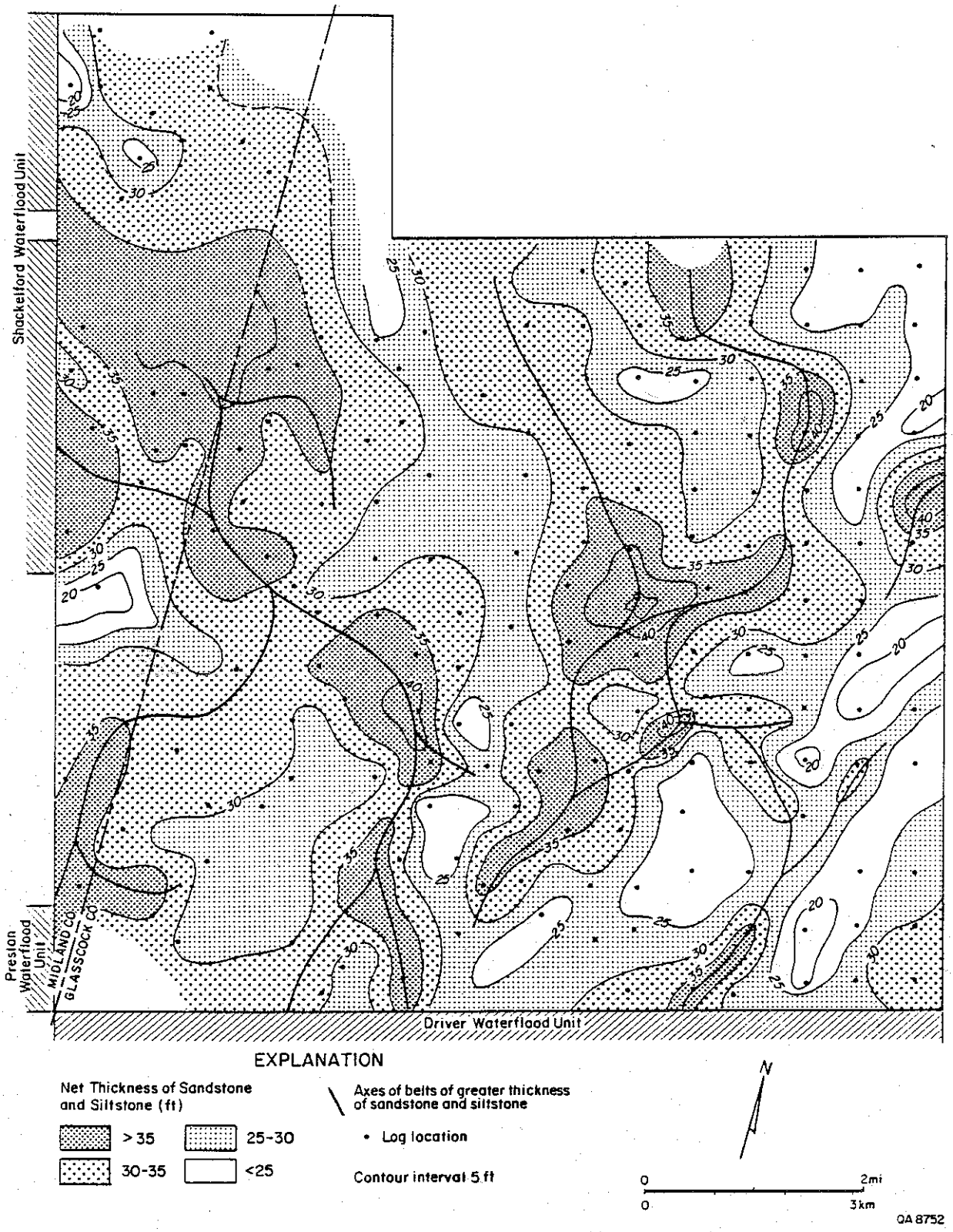

Figure II-11. Map of total thickness of sandstone and siltstone, operational unit 1L (lower part) (lower Spraberry), ununitized area, Spraberry Trend.

continuous, predominantly meandering belt near the west boundary (fig. II-10). Total thickness of sandstone and siltstone averages 28 ft and ranges from 45 ft in the northwest to 11 ft in the northeast.

The 30-ft isolith of the lower part of unit 1L (from the top of unit 2L to the top of sandstone zone s) defines meandering, locally braided belts in the west and east parts of the study area (fig. II-11). Total thickness of sandstone and siltstone averages 31 ft and ranges from 45 ft in the east-central part of the study area to 16 ft in the southeast.

Belts defined by isolith maxima of units 1U, 5U, and 1L occur mainly in the west and east-central parts of the study area (fig. II-12). These belts usually lie adjacent to the thicks of the underlying deposits, resembling compensation cycles of turbidites (Mutti and Sonino, 1981). Locally persistent belts of greater total thickness sandstone and siltstone result in stacked reservoir rocks and multipay oil accumulations.

Paleogeographic Setting and Depositional Systems

Regional studies (Silver and Todd, 1969; Handford, 1981a, 1981b; Section I, this report) indicate that terrigenous clastics of the Spraberry Formation were deposited in a relatively deep basin. Handford (1981a, 1981b) estimated a relief of approximately 1,700 to 2,000 ft between the floor of the Midland Basin and the Northwest Shelf during deposition of the Dean and Spraberry Formations. The basin lay close to the equator according to paleogeographic reconstructions by van Hilten (1962) and Habitch (1979).

Submarine fan deposits compose the upper and lower Spraberry (figs. I-7, II-3, and II-4). Subsurface data analyzed in the RCRL (Section I, this report) permitted recognition of a threefold segmentation of Spraberry submarine fans, the inner, mid, and outer fan. In the study area, located south of the Glasscock County narrows,

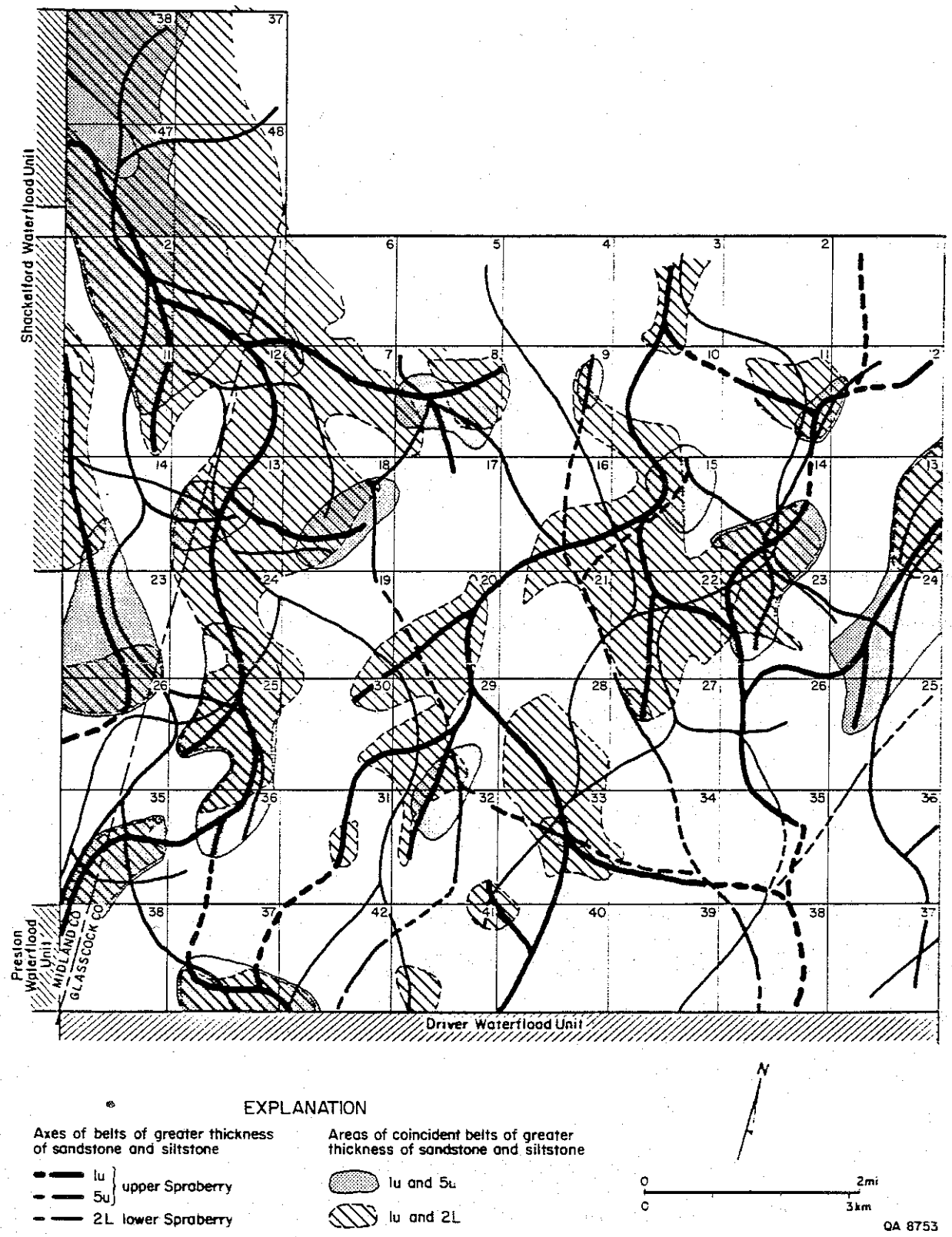

Figure II-12. Geographic distribution of belts of isolith maxima, ununitized area, Spraberry Trend.

operational units 1U and 1L are composed of midfan deposits. Belts defined by isolith maxima of these units (figs. II-8, II-9, and II-11) thus comprise midfan channel fills. Operational unit 5U comprises outer-fan facies and was thus deposited in a more distal setting (with respect to a sediment source located north of the study area) than that of units 1U and 1L. Patterns on isolith maps of unit 5U (fig. II-10) represent belts of peripheral outer-fan channels.

Facies Architecture

Log facies maps indicate that midfan and outer-fan facies of the Spraberry Formation in the study area consist of (1) upward-coarsening and upward-thickening, laterally extensive, predominantly mud deposits of unconfined flow and (2) laterally discontinuous channel fills composed of sandstone and siltstone. Log facies maps depict the areal distribution of shapes or motifs of the gamma-ray logs. Most of the logs in the study area display blocky, funnel, bell, or serrate motifs. Blocky shapes, having relatively sharp base and top, are interpreted as the log response to relatively thick, massive beds of sandstone and siltstone. Because the range in grain size of the Spraberry Formation is small (Handford, 1981a, 1981b), log shapes other than blocky result mainly from variations in the proportion of interbedded shale beds (Guevara, in press; Tyler and Gholston, in press). Bell log shapes, having relatively sharp lower boundaries and gamma-ray values that increase upward, reflect upward-fining and upward-thinning intervals. Funnel motifs, which display upward-diminishing gamma-ray values, result from upward-coarsening and upward-thickening intervals or from "upward-cleaning" beds of sandstone and siltstone having less clay in their upper parts. Serrate log shapes, which show relatively thin, alternating intervals having successively low and high gamma-ray values, reflect interbedded shales, sandstones, and siltstones. Spike, or symmetrical, log motifs probably result from the inability of

the logging tool to discriminate between thin beds in intervals (which are very common in the Spraberry Formation) comprising interbedded shales, sandstones, and siltstones.

The log facies map of sandstone zone c (unit 1U) shows that funnel log motifs occur in most of the study area, except in locally discontinuous, dip-elongate belts in the west and east parts (fig. II-13). Belts having log shapes other than funnel are approximately 0.5 to 1.5 mi wide. Usually the central parts of these belts display bell, bell over funnel, or blocky log motifs that are locally flanked by areas having serrate log shapes. Belts of bell, bell over funnel, and blocky log motifs are interpreted as principal channel axes or sandstone and siltstone depocenters, and areas of serrate logs as comprising overbank, interchannel deposits. Log motifs related to aggradational facies seem to dissect fan-progradational deposits of unconfined flow (having funnel log motifs) occurring in more laterally extensive areas.

Stratigraphically Controlled Reservoir Heterogeneity

Facies architecture of operational units of the upper and lower Spraberry, characterized by laterally discontinuous sandstones and siltstones that are encased by predominantly nonreservoir rocks, results in stratigraphically complex oil reservoirs (Guevara and Tyler, 1986; Tyler and Guevara, 1987). Oil accumulations are multilayered or stratified because they are separated vertically by shales and carbonates. Oil accumulations are also laterally compartmentalized because of facies changes across the submarine fan paleosurface.

The Spraberry Trend is a multipay field. Increased oil production in wells deepened to the lower Spraberry (wells that had been producing from almost depleted

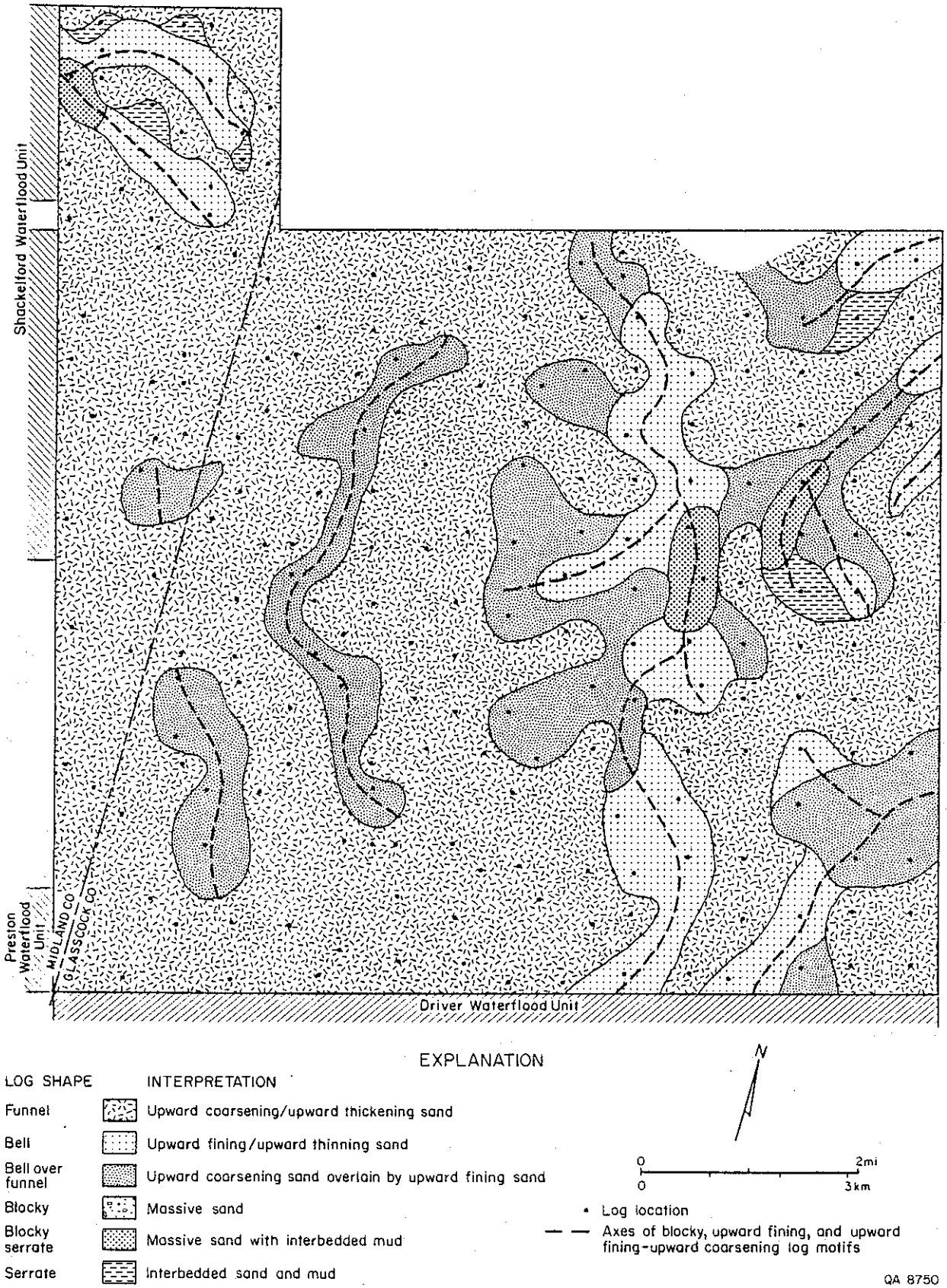

Figure II-13. Log facies map, sandstone zone c, operational unit 1U (upper Spraberry), ununitized area, Spraberry Trend.

upper Spraberry reservoirs) documented during early field development the occurrence of separate accumulations in the upper and lower Spraberry (Elkins, 1953; Elkins and others, 1968).

The layer-cake stratigraphy depicted by the areal distribution of operational units (figs. II-3 and II-4) has been traditionally interpreted as reflecting laterally continuous and homogeneous reservoirs. However, Spraberry reservoirs are highly heterogeneous. Lateral and vertical stratigraphic heterogeneity in the study area is depicted on cross sections displaying percent-sand values of unit 1L (upper and lower parts) and of each of the upper Spraberry units. Sandstone-rich areas (those areas having more than 70 percent sandstone and siltstone) occur mainly in units 1U, 5U, and 1L (lower part) (fig. II-14). Most of the sandstone-poor areas (those areas having less than 50 percent sandstone and siltstone) occur in units 4U and 6U. Sandstone-rich areas correspond to belts of greater total thickness of sandstone and siltstone (figs. II-8 to II-11). Sand-rich areas of units 1U, 5U, and 1L reflect at least partly the distribution of relatively thick beds of sandstone zones c, f, and s (fig. I-7). The lateral variability of facies-controlled total thickness of sandstone and siltstone and the corresponding variation in matrix porosity result in reservoir compartments and intrareservoir traps. Furthermore, sandstone-poor areas locally separate reservoir rocks of units 1U and 5U (for example, in the west-central part of the study area [fig. II-14]), suggesting stratified oil pools (if not linked by fractures) within the upper Spraberry, in addition to the well-known occurrence of separate, upper and lower Spraberry accumulations.

Areal Distribution of Porosity

No data on core porosities and permeabilities were available from the study area. Analysis of cores from the newly drilled Mobil Judkins A No. 5 well (figs. II-1 and II-

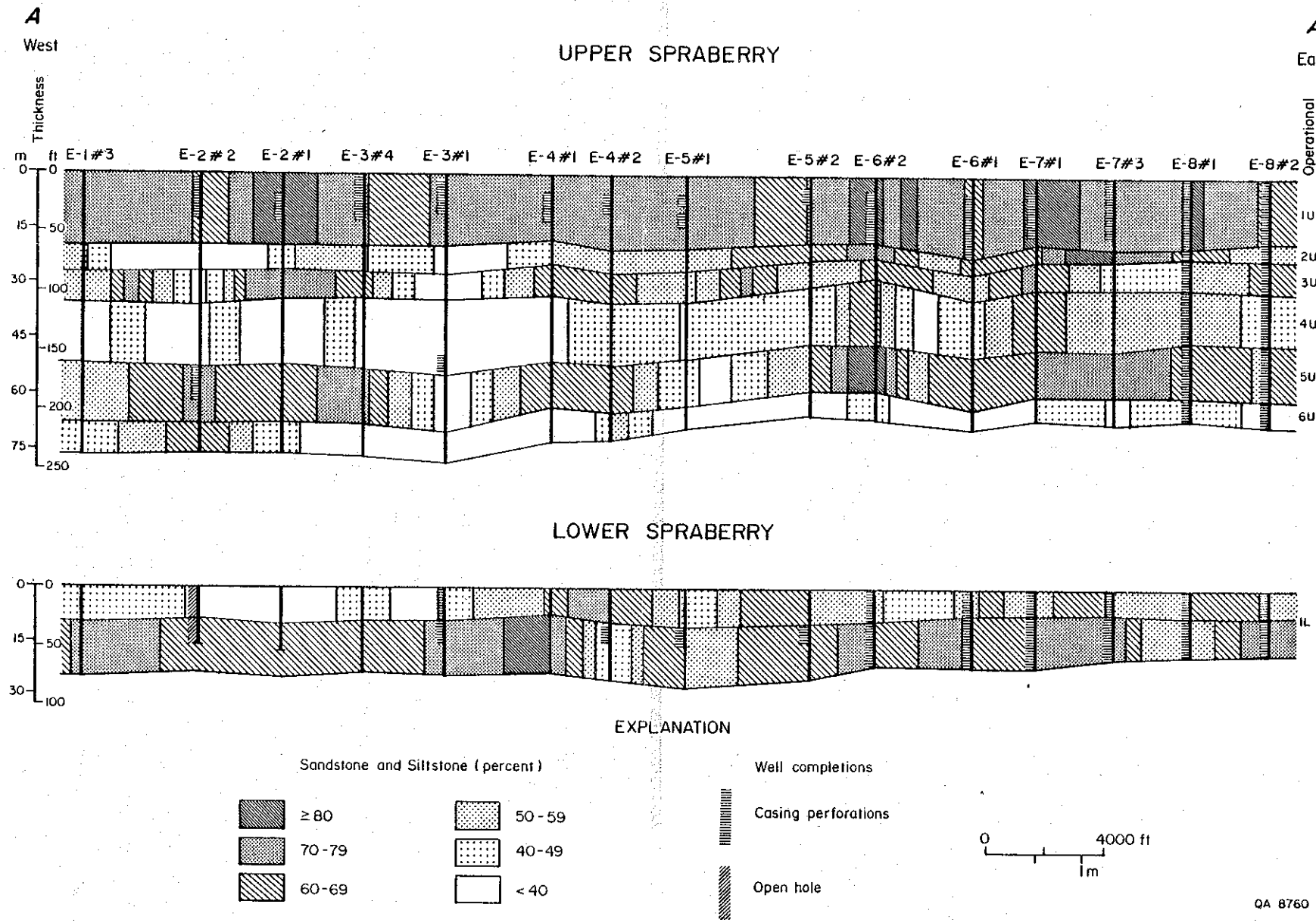

Figure II-14. Stacked percent-sand cross section, ununitized area, Spraberry Trend. Location in figure II-2.

2) is in progress at Core Laboratories, Midland. Core data from other areas of the Spraberry Trend (Gibson, 1951; Elkins, 1953; Wilkinson, 1953; Guevara, in press; Tyler and Gholston, in press) indicate that matrix porosities of Spraberry reservoirs range from less than 8 to approximately 15 percent, and that permeabilitites can be as much as 20 md but are mostly less than 1 md. Comparable values were determined during RCRL studies of drilled sidewall cores from the Mobil Preston-37 well (Section III, this report).

Maps of effective porosity and sandstone shaliness of operational units 1U, 5U, and 1L (lower part) and of sandstone zones c, f, and s were prepared using gamma-ray - neutron (GNT) logs. These logs, which are mainly correlation tools, are not normally used for quantitative porosity determinations. In this study, only those GNT logs displaying scaled values either in counts per second or in API units were selected for porosity determinations. Approximately 90 GNT logs, or less than 50 percent of the total number of logs used for stratigraphic studies, fulfilled these criteria.

The readings of the logs selected required normalization because significant differences exist among the logs used, and simple, fixed cut-off values on the gamma-ray and neutron curves could result in significant errors in the determinations of porosity and reservoir thickness. These differences are due, among other factors, to variations in tool performace and wellbore environment and in the technologies and calibration procedures used by the logging companies. Normalization of GNT data is particuarly important because these logs are more sensitive to the mentioned variables than are acoustic or resistivity logs.

A data normalization procedure was implemented by which all logs were standardized to the tool response and borehole environment characteristic of an arbitrarily selected base or standard log. The log from the B-7#1 well (figs. II-2 and II-15) was chosen as the standard among the selected logs because it displays easily

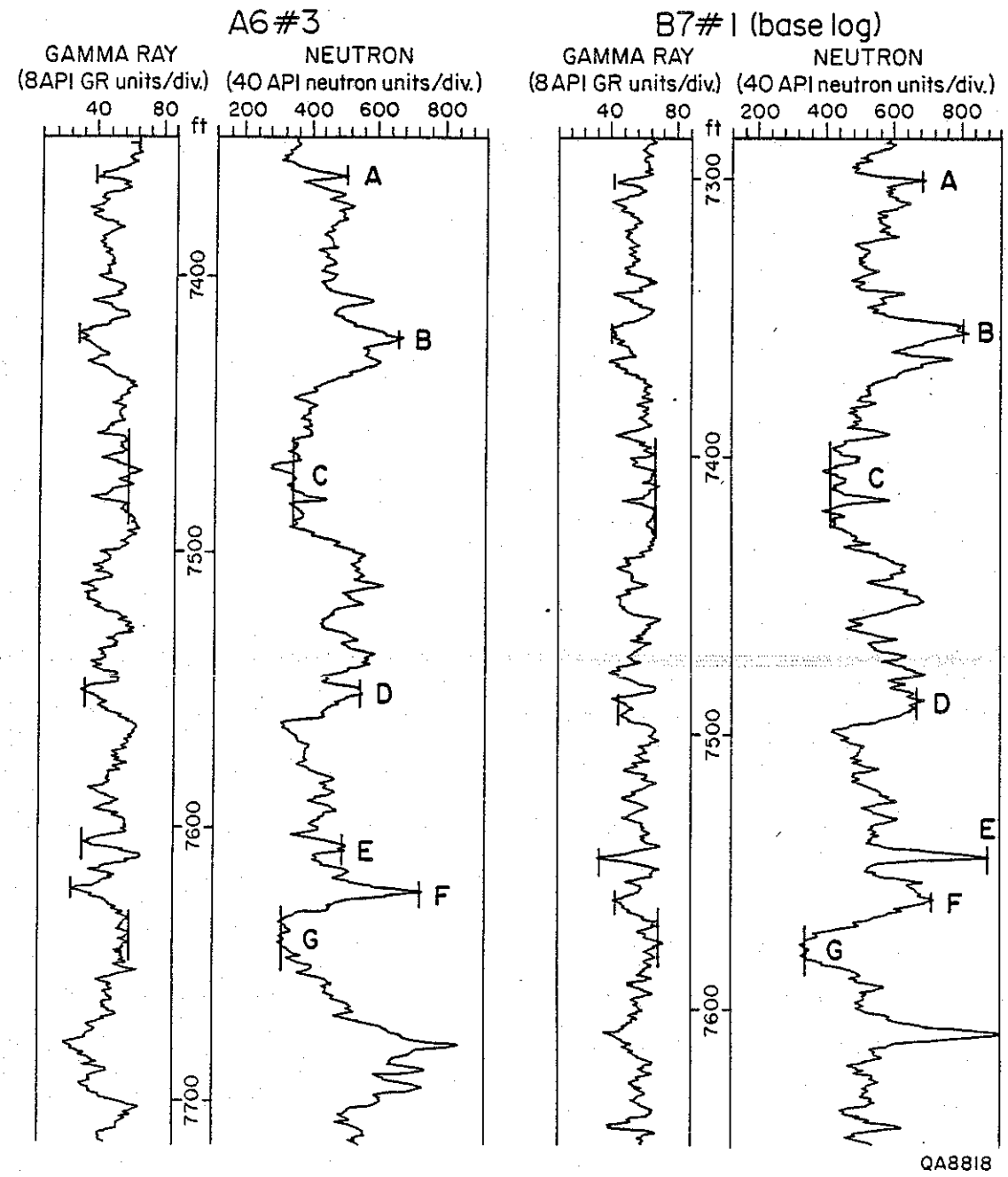

Figure II-15. Example of correlation of markers selected on the base gamma-ray-neutron log. Vertical bars indicate log markers used in the transform (see figs. II-16 and II-17).

identifiable correlation units (log markers), was recorded in constant borehole environment, and is a representative, average log response for the study area. Selected well log markers covering the full spectrum of log responses in the entire Spraberry Formation were correlated from the base log to each log used in the study (fig. II-15). Gamma-ray and neutron readings of these correlation intervals were recorded on each log, noting all sensitivity changes and scale shifts. These data were plotted using cartesian coordinates, and a best-fit line determined by visual inspection established a transform equation that permitted normalization of every log to the standard response (figs. II-16 and II-17). Figure II-18 illustrates the effects of data normalization on log response.

Porosity calibration was done using normalized logs. Total porosity, including the apparent porosity due to log response to formation shaliness, was determined using the neutron curve. Effective formation porosity was determined by removing the effects of shaliness by means of the gamma-ray curve. Calibrations of total porosity and determination of shaliness corrections were accomplished using a Schlumberger technique. This technique involves using an empirical log-linear relation to convert the neutron curve to total porosity (fig. II-19). At least two points are necessary to establish the calibration, a shale value (N_{sh}, Φ_{Nsh}) and a tight-sand value (approximately 1 to 2 percent porosity).

Clay content was ascertained from the normalized gamma-ray log using an empirical log-linear relation that is a direct transform from API units to porosity (fig. II-20), similar to the transformation made of neutron logs. A minimum of 1 percent porosity due to clay was assigned to the cleanest sandstones and siltstones, and shales were considered to have 30 percent neutron porosity. One percent porosity was used for the clean-sand point because 0 percent porosity cannot be represented on a

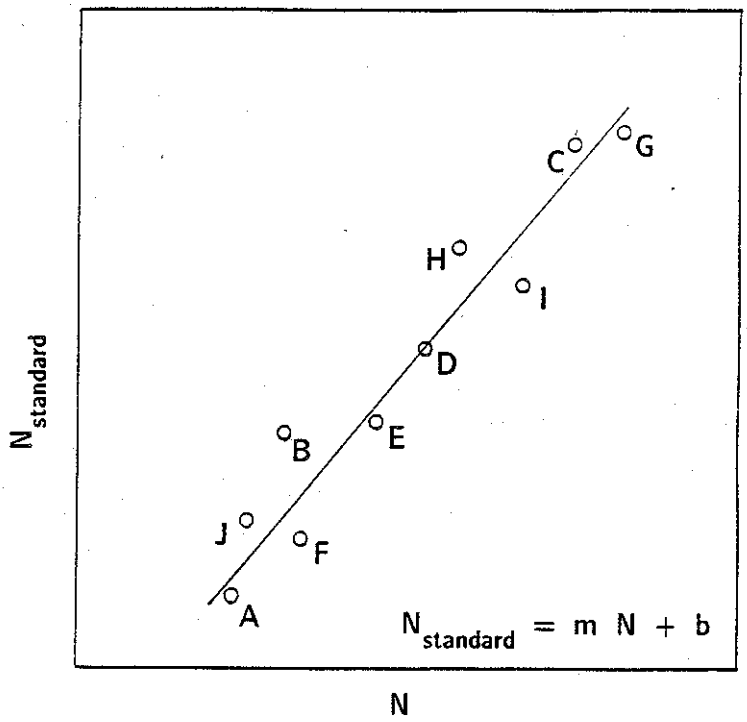

Figure II-16. Use of well log markers to establish the linear relationship for neutron logs between each log and the base or standard log.

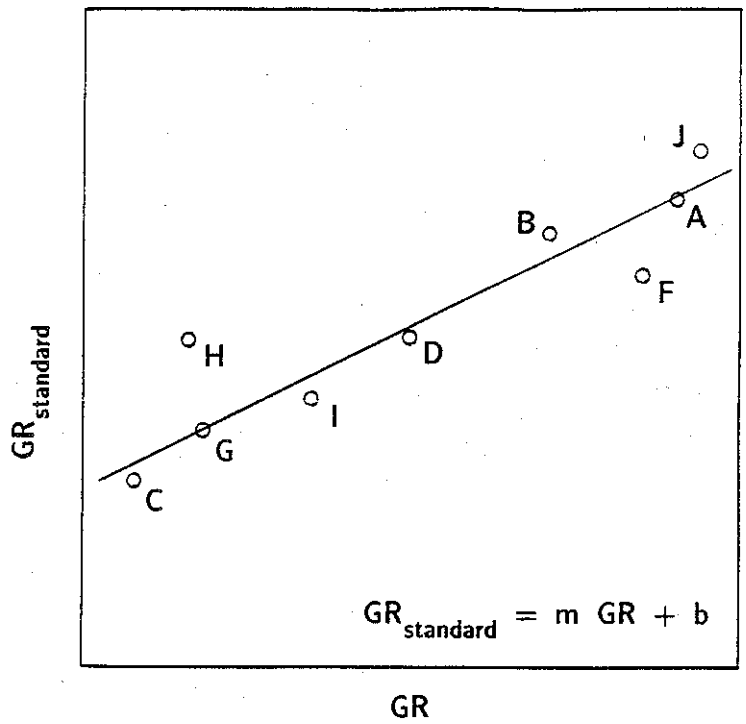

Figure II-17. Use of well log markers to establish the linear relationship for gamma-ray logs between each log and the base or standard log.

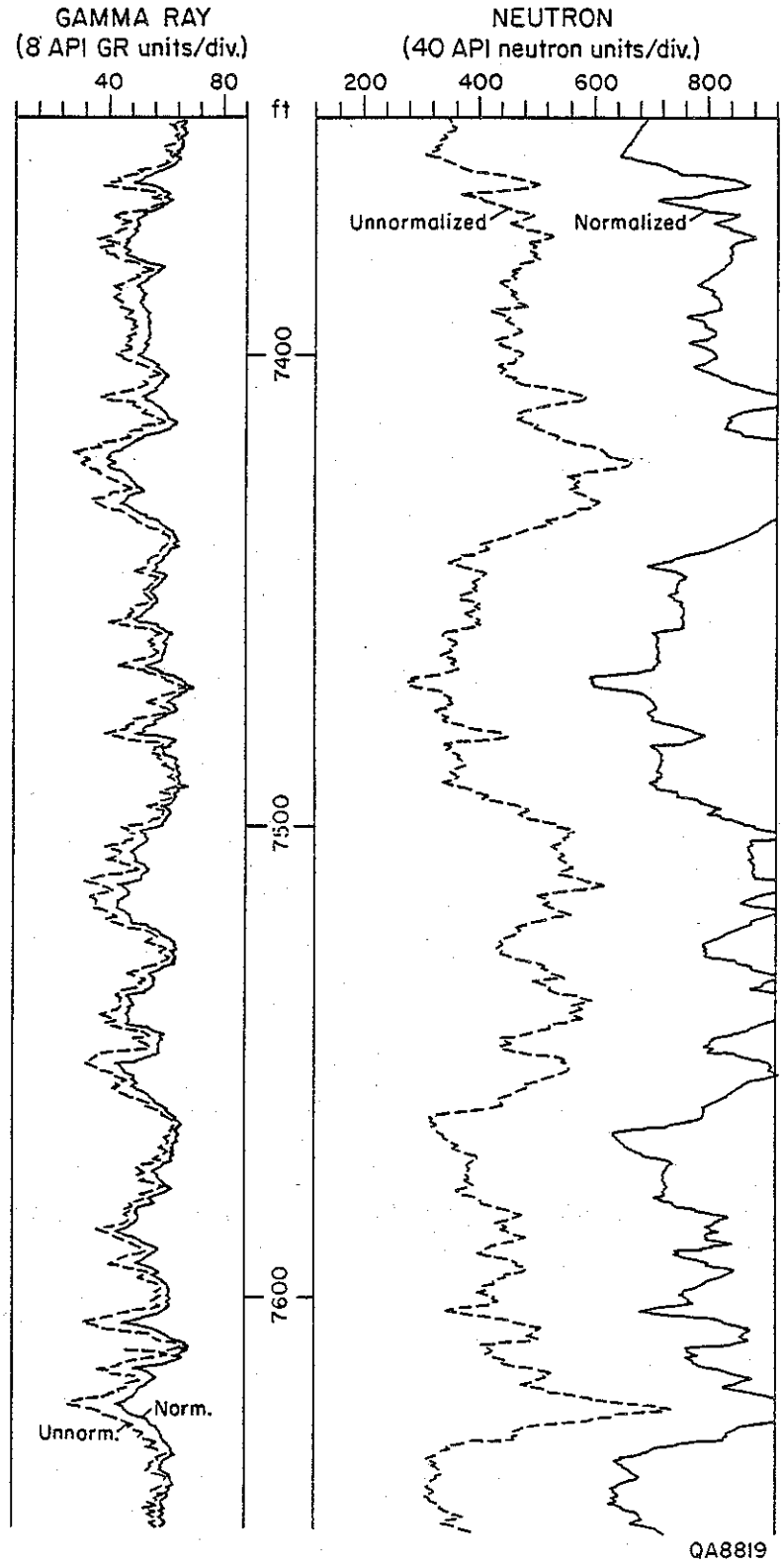

Figure II-18. Comparison of normalized and unnormalized gamma-ray and neutron curves.

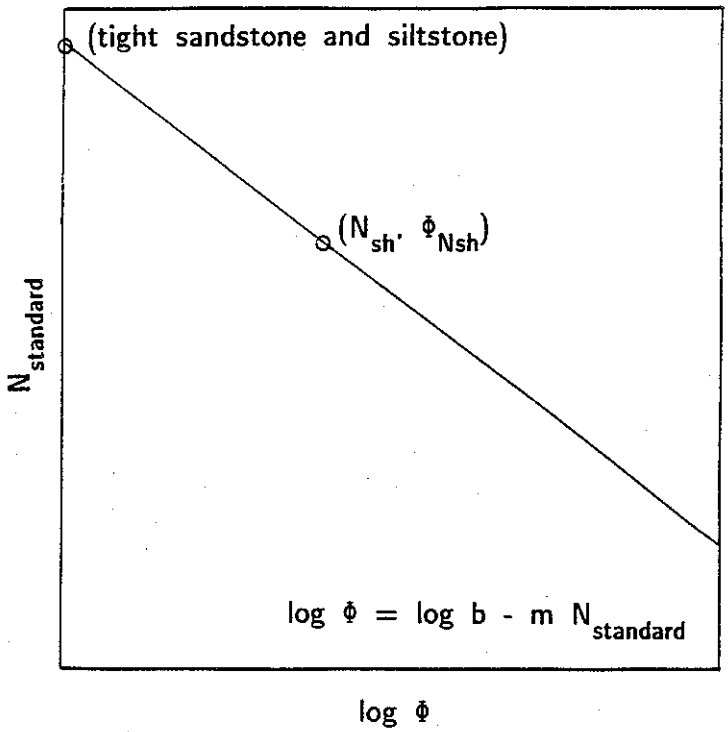

Figure II-19. Calibration of the standard log to porosity using a log-linear regression of log porosity to linear neutron API count rates.

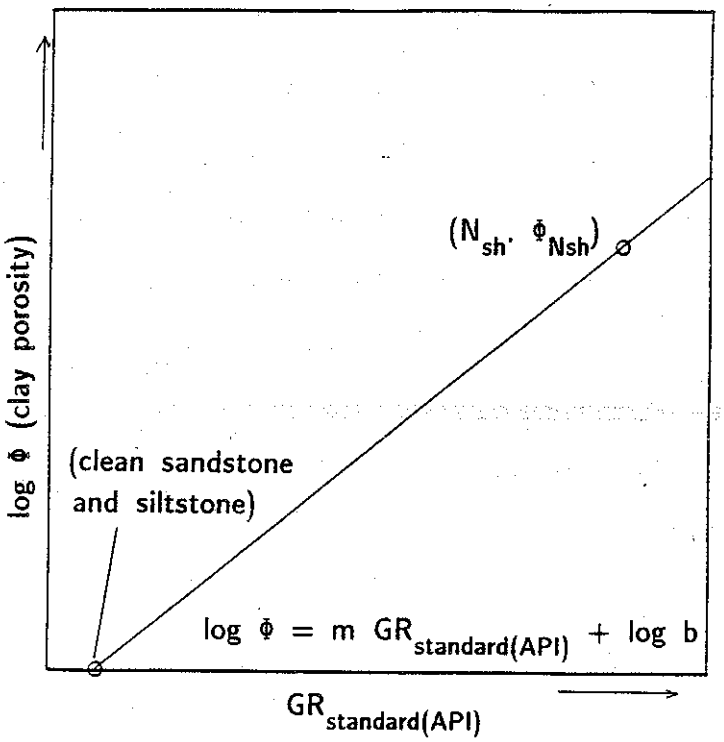

Figure II-20. Gamma-ray calibration to porosity, used to determine the component of porosity due to clay.

logarithmic scale. To account for this, the correction was reduced by 1 percent before being applied to the total porosity.

The effective formation porosity was obtained by subtracting the shale porosity (determined using the gamma-ray curve) from the total, neutron porosity. The impact of such a correction on the apparent porosities is shown on figure II-21. Several of the thicker, cleaner beds of sandstone and siltstone actually have low porosity, and the best porosities appear to be related to intermediate clay contents shown by the gamma-ray values.

Shaliness is an index of reservoir quality that can be used to further qualify isolith maps (figs. II-8 to II-11) that were constructed using gamma-ray cut-off values (V_{sh} approximately 67 percent) on unnormalized curves. Volumetric shaliness of sandstones and siltstones was determined establishing the linear relation

$$V_{sh} = (GR - GR_{cs}) / (GR_{sh} - GR_{cs})$$

between the gamma-ray readings of clean (GR_{cs}) and shaly (GR_{sh}) sandstones and siltstones on the normalized gamma-ray curve. Figure II-22 contrasts the methodologies used to determine shaliness and total thickness of sandstone and siltstone. It indicates that values of total thickness of sandstones and siltstones determined using a cut-off value of 67 percent shaliness are higher than those that consider shaliness on normalized gamma-ray curves.

Values of sandstone shaliness and effective porosity (neutron porosity minus porosity due to shaliness) were determined on each of the selected logs for operational units 1U, 5U, and 1L (lower part) and for sandstone zones a, b, c, f, and s. Maps were constructed for units 1U, 5U, and 1L (lower part) and for sandstone zones c, f, and s.

Shaliness of unit 1U averages 46 percent and ranges from 32 percent in the northeast to 73 percent in the southwest parts of the study area (fig. II-23). Values lower than 40 percent (in the cleanest sandstones and siltstones) occur in the

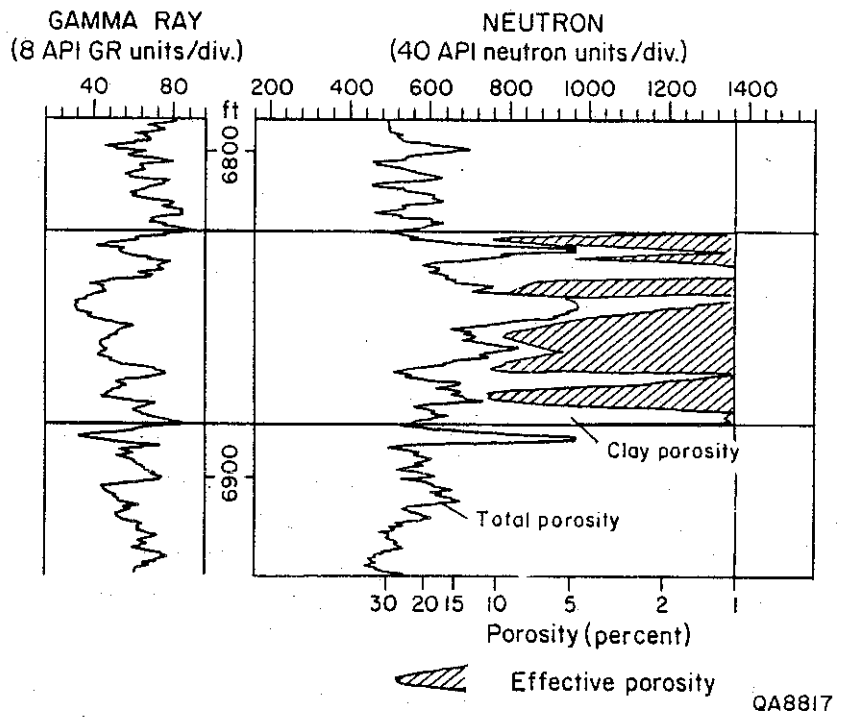

Figure II-21. Comparison between total (neutron) porosity and effective (neutron-gamma ray) porosity.

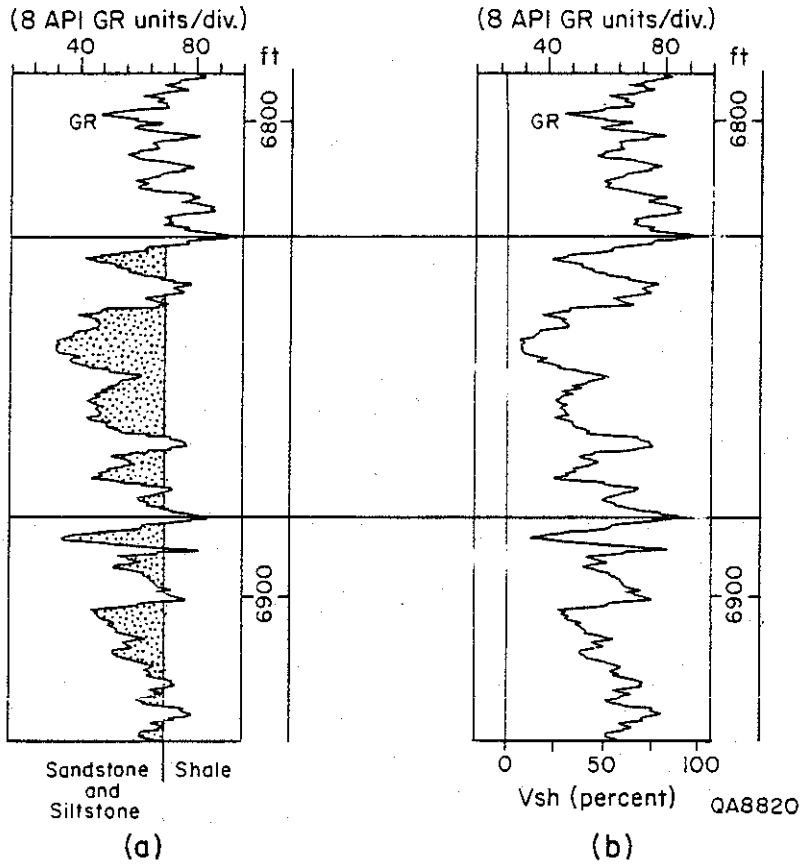

Figure II-22. Comparison of methodologies used to determine total thickness of sandstone and siltstone (a) and shaliness (b). A cut-off line is used to determine the thickness of intervals having 100 percent sandstone and siltstone (a). The values thus determined disregard the thickness of shales thinly interbedded in these intervals. Shaliness, ranging from almost 0 (clean sandstones and siltstones) to 100 percent (shales), includes these interbedded shales (b). Therefore, total thickness of sandstone and siltstone determined using the cut-off line (a) is greater than that determined using shaliness values (b).

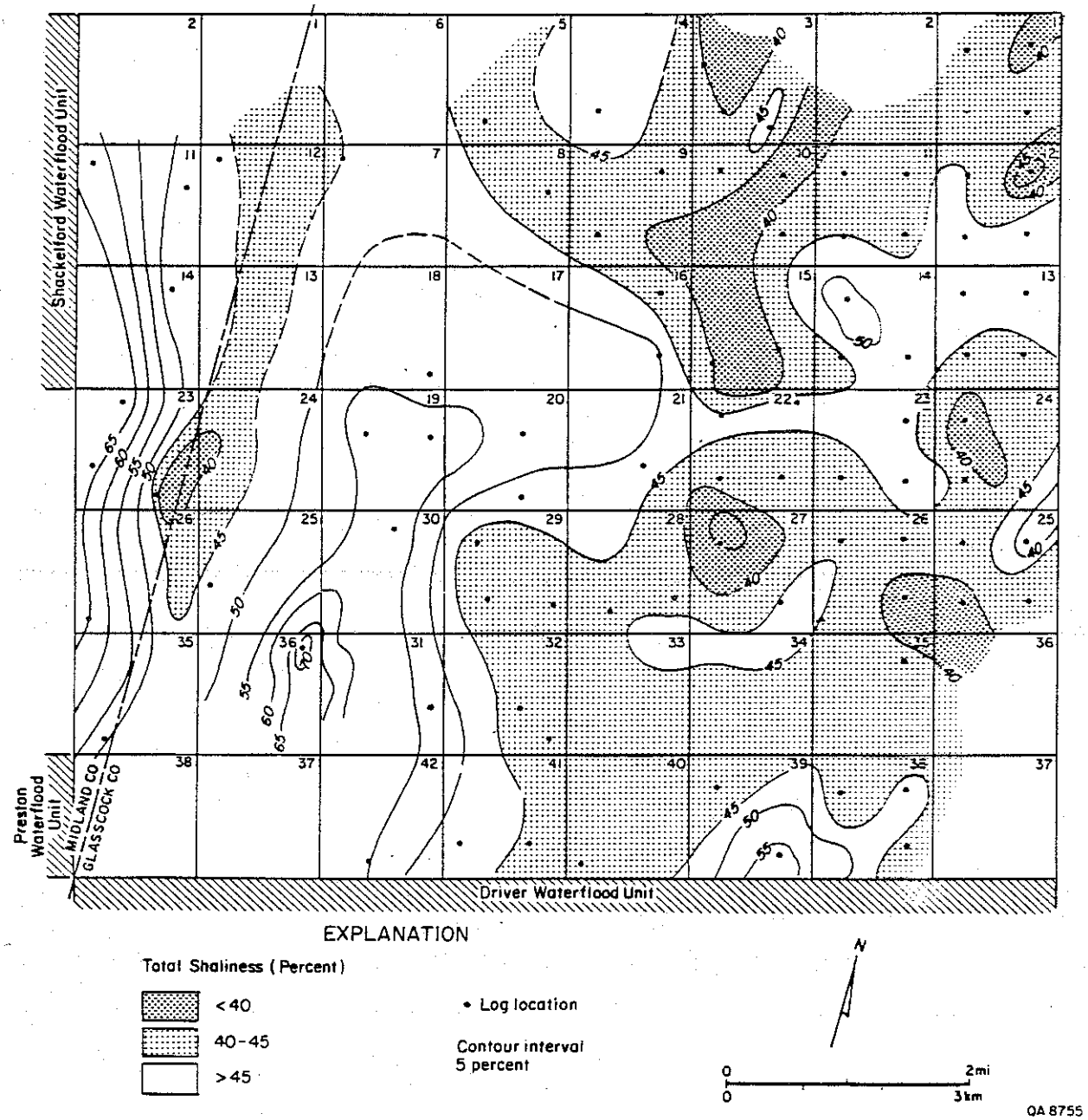

Figure II-23. Map of shaliness, operational unit 1U (upper Spraberry), ununitized area, Spraberry Trend.

northeastern and east-central parts. Effective porosities average 8.1 percent and range from less than 1 percent in the east-central part to 16 percent in the south-central part (fig. II-24). Values greater than 12 percent (the best porosities) are more frequent in the northeast and south-central parts. Effective porosities of sandstone zone c average 7.7 percent and range from less than 1 percent in the east-central, central, and southwest parts to 14 percent in the south-central part (fig. II-25). The best porosities of this sandstone zone (greater than 12 percent) occur in the northwest, northeast, and south-central parts.

Effective porosities of operational unit 5U average 9.3 percent and range from less than 1 percent in the east-central part of the study area to 19 percent in the north-central part (fig. II-26). Porosities greater than 12 percent occur in the northwest, northeast, south-central, and southeastern parts of the study area.

Effective porosities of the lower part of unit 1L average 9.4 percent, ranging from 1 percent in the eastern part of the study area to 18 percent in the west-central part (fig. II-27). Porosities greater than 12 percent occur in the northwest, northeast, west-central, and south-central parts.

Relationship between Isoliths and Maps of Shaliness and Porosity

Areas having the best effective porosities (figs. II-24 to II-27) do not always coincide with the belts of isolith maxima (figs. II-8 to II-11). Therefore, porosity maps constructed using normalized data allow high grading of prospective locations for infill drilling. Discrepancies between isolith and porosity maps result mainly from porosity reduction by predominantly carbonate cementation and to a lesser extent from differences in methodology (fig. II-22) and from fewer control points on porosity and shaliness maps than on isolith maps. Secondary porosity and carbonate cementation, probably having great importance for reservoir quality locally in the study area, were

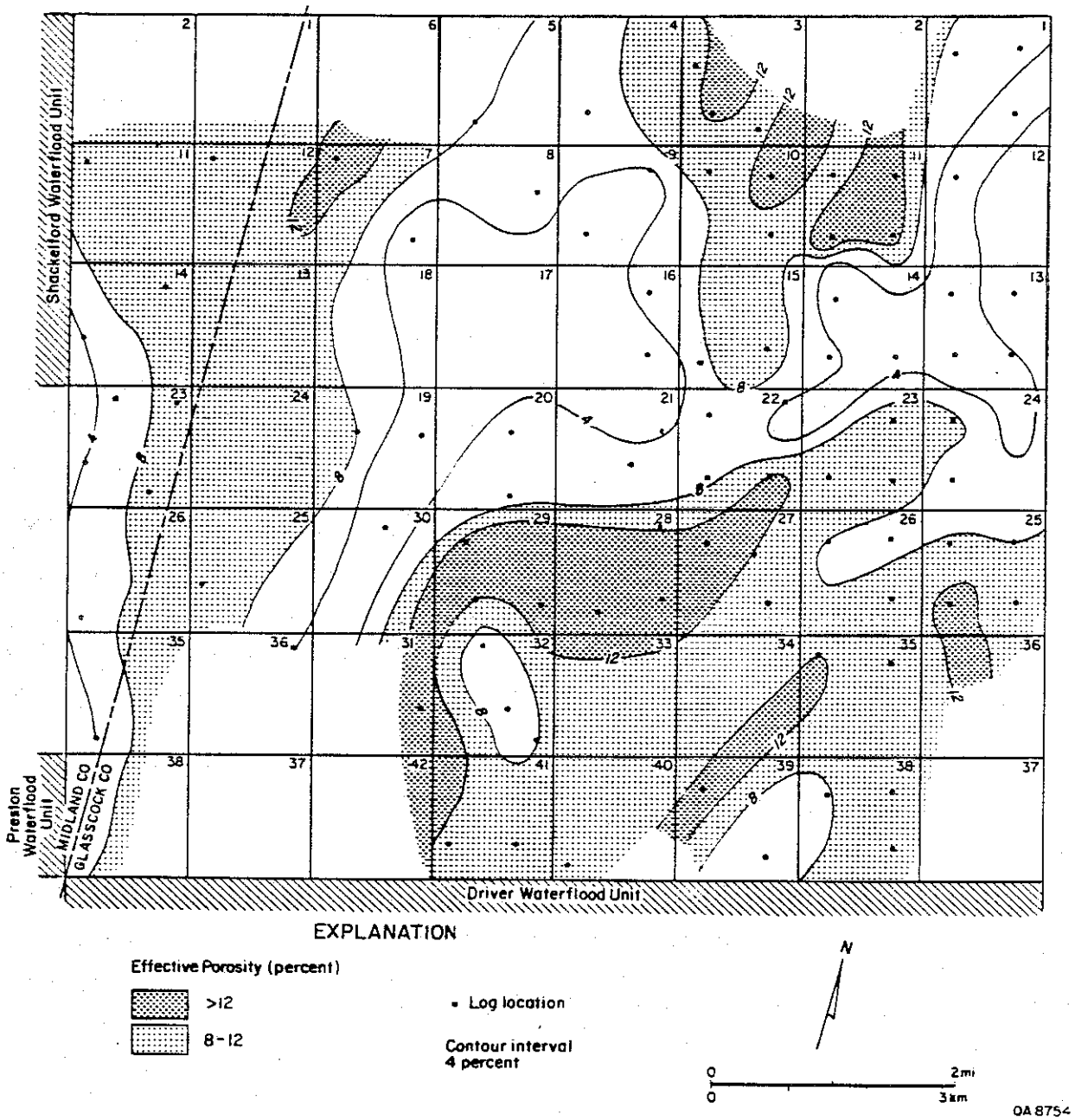

Figure II-24. Areal distribution of effective porosity, operational unit 1U (upper Spraberry), ununitized area, Spraberry Trend.

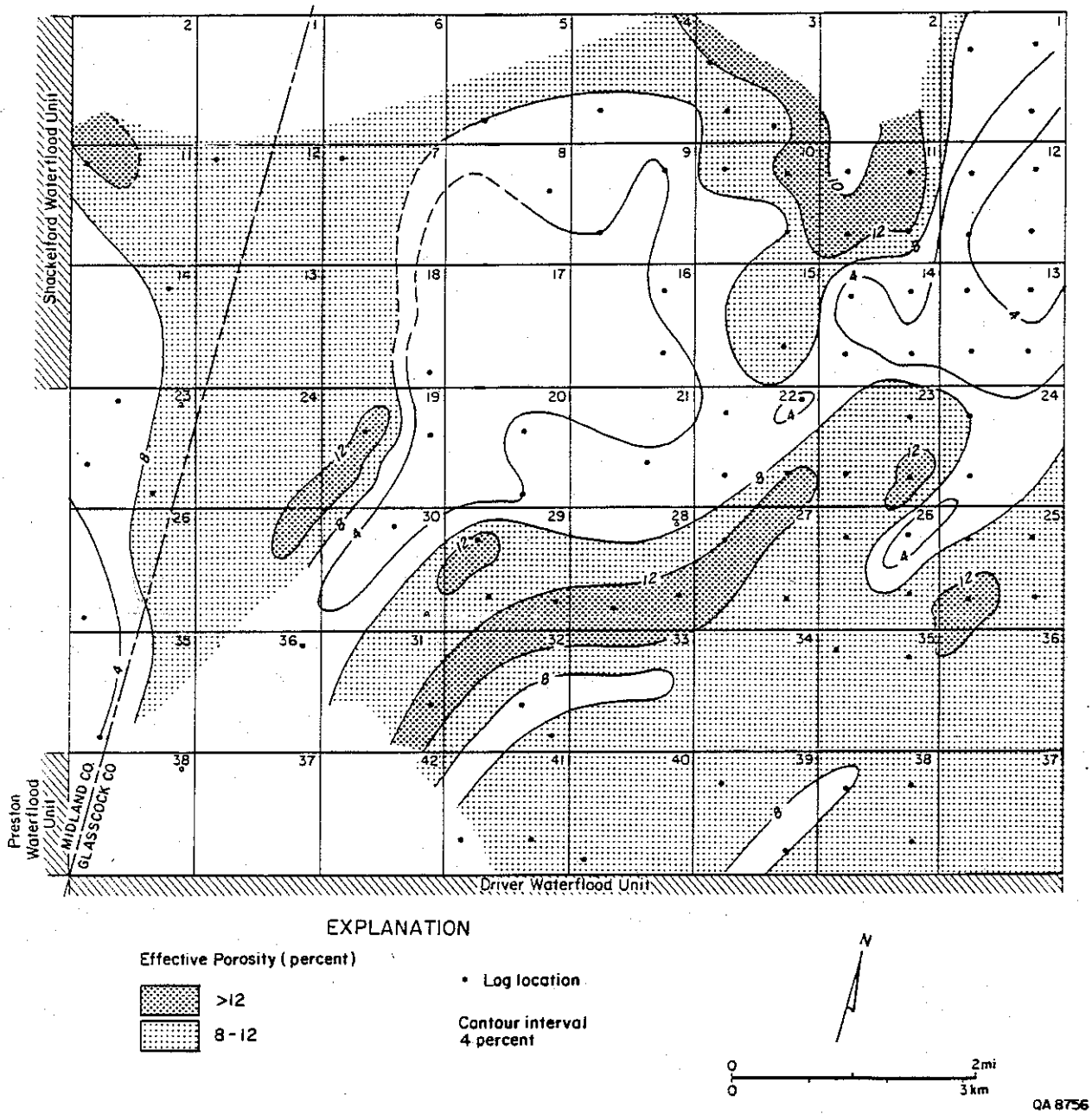

Figure II-25. Areal distribution of effective porosity, sandstone zone c, operational unit 1U (upper Spraberry), ununitized area, Spraberry Trend.

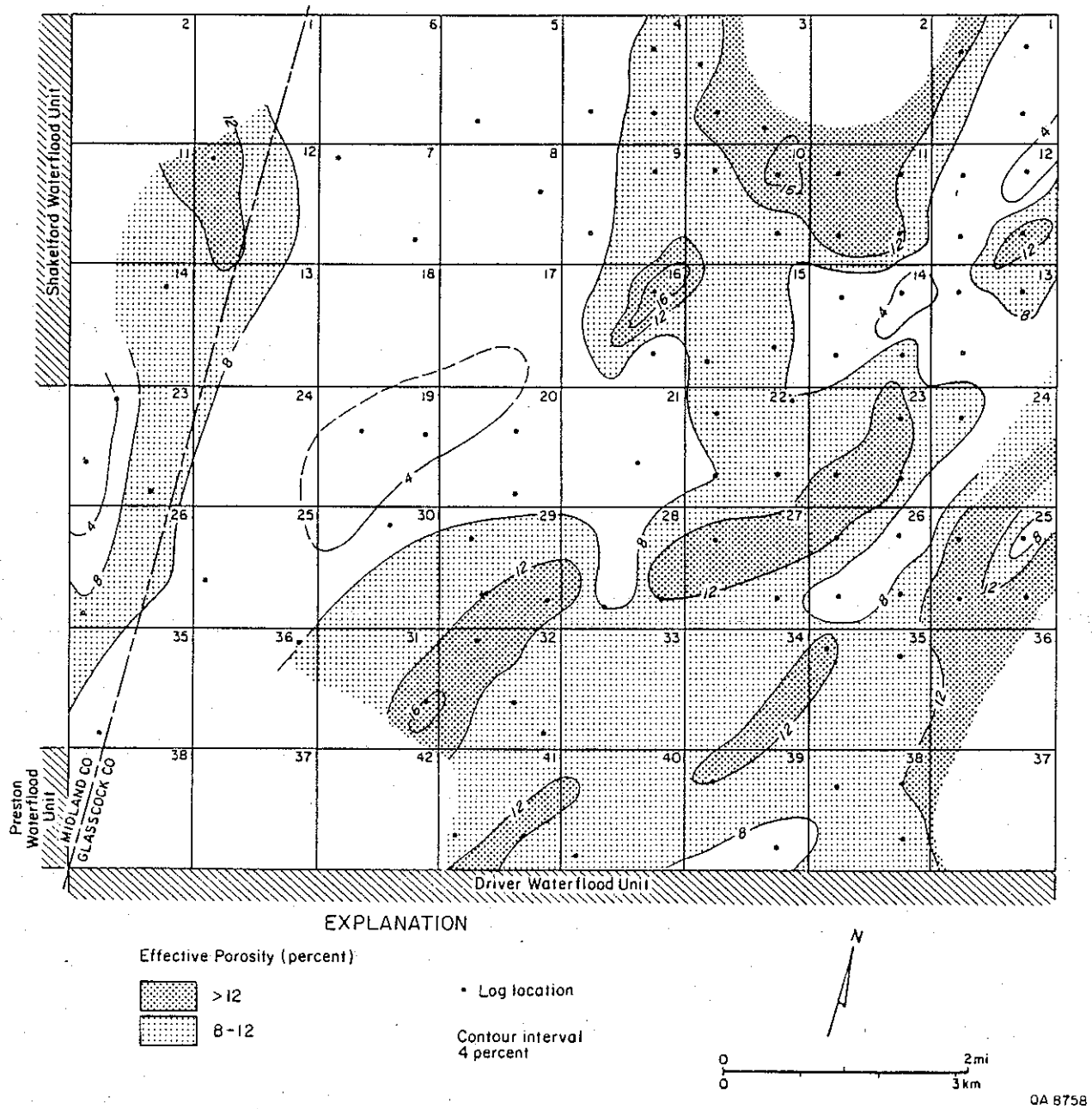

Figure II-26. Areal distribution of effective porosity, operational unit 5U (upper Spraberry), ununitized area, Spraberry Trend.

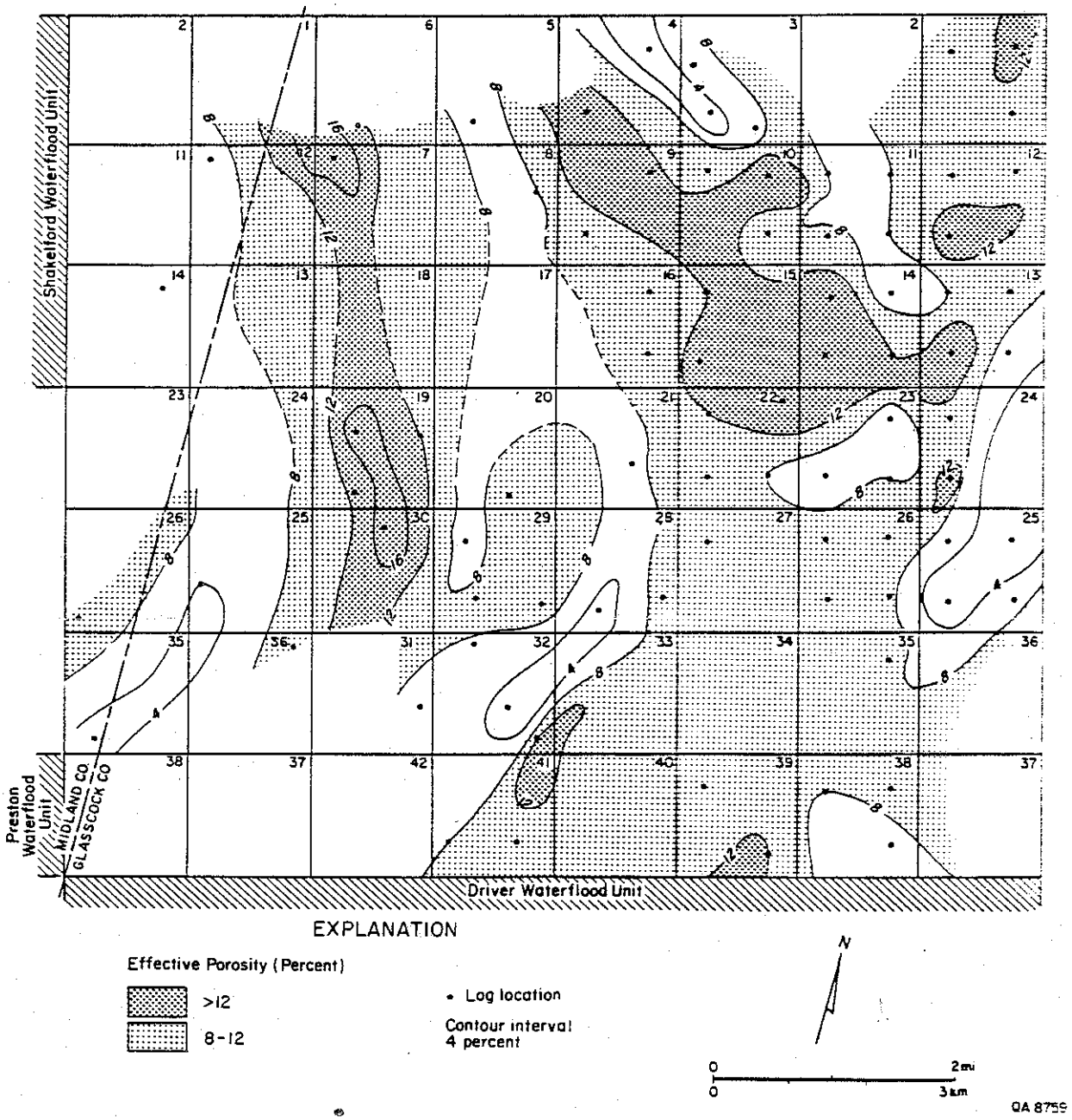

Figure II-27. Areal distribution of effective porosity, operational unit 1L (lower part) (lower Spraberry), ununitized area, Spraberry Trend.

observed in sidewall cores of the Preston-37 well (Section III, this report).

There is no direct relation between shaliness and isoliths in the study area, as indicated by corresponding plots (fig. II-28). These data would plot along a straight line if the operational units are relatively constant in thickness, if the cut-off values were properly selected, and if shaliness is the only variable in determining total thickness of sandstone and siltstone. A conceptual line (A-A') representing this expected trend was drawn using the thickness value zero (representing 100 percent shale) and the average thickness of the respective operational unit or sandstone zone (representing 100 percent sandstone and siltstone). The graph prepared for unit 1U shows most of the data plot above this trend line, indicating that the basic condition necessary for a linear correlation is not met (fig. II-28). Because fieldwide cross sections (figs. II-3 and II-4) show only minor thickness variations, this discrepancy is attributed mainly to lithological changes (for example, lithofacies, diagenesis) that affect the absolute values of the gamma-ray curve. It is also possible that the calculated shaliness values are too high. Lack of core precludes further evaluation of this possibility.

Graphs of effective porosity and isolith data also indicate that other factors in addition to shaliness influence porosity in the study area. Effective porosity and net thickness of sandstone and siltstone should conceptually plot along a straight line (A-A,' fig. II-29) if sand thicknesses and porosities are uniquely related, that is, if shaliness is the main factor controlling porosity. The tendency of the data to show a porosity lower than that which thickness of sandstone and siltstone would have predicted (fig. II-21) indicates, however, that other factors are influencing porosity. Cleaner rocks usually having effective porosities much lower than predicted (fig. II-29) strongly suggest diagenetic reduction of porosity (cementation).

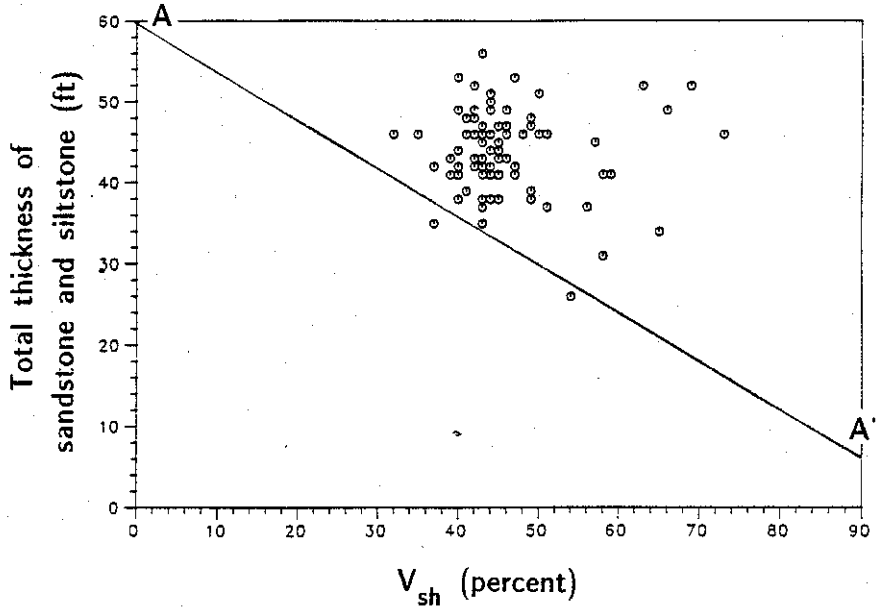

Figure II-28. Relation between shaliness and total thickness of sandstone and siltstone, operational unit 1U (upper Spraberry), ununitized area, Spraberry Trend.

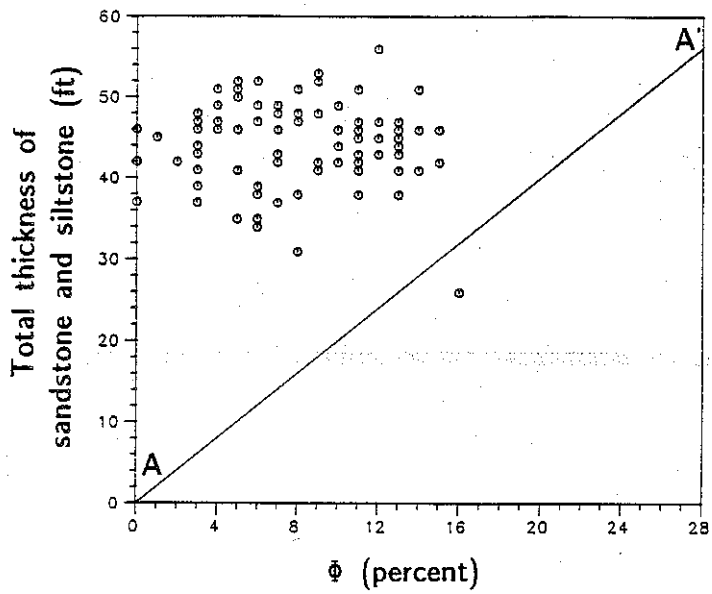

Figure II-29. Relation between effective porosity and total thickness of sandstone and siltstone, operational unit 1U (upper Spraberry), ununitized area, Spraberry Trend.

Graphs of shaliness and effective porosity would also be expected to show a linear correlation from the average porosity of clean sandstone and siltstone to zero porosity at 100 percent shaliness if shaliness were the principal influence, because these graphs were constructed using only normalized data (as opposed to graphs that display thicknesses of sandstone and siltstone determined using unnormalized logs). However, the plot constructed for unit 1U does not show such a relation (fig. II-30), again suggesting that cementation is influencing porosity in the study area.

Completion Intervals and Production Data

The geographic distribution of intervals open to production in operational units of the Spraberry Formation (fig. II-31) was determined using data from scout cards that show mostly original well completions. Current completion intervals may differ locally from those of the scout cards because no additional data on well recompletions were available to update this information. Data at hand indicate that the majority of the oil-producing intervals are selective casing perforations (few wells have open-hole completions) and that few wells are completed only in either upper, middle, or lower Spraberry reservoirs. Upper Spraberry reservoirs are open to production in most of the wells of the study area. Most of these completions are in operational unit 1U, but some (especially in the north-central and northeast parts) also include unit 5U. Most wells are open to production from unit 1L (lower Spraberry), usually in multiple completions for production commingled with that from upper Spraberry and locally (especially in the east and north-central parts) middle Spraberry reservoirs. Three wells in the north-central part of the study area were completed only in middle Spraberry reservoirs (fig. II-31).

Production data were available from 18 wells that, except for one, are located in the west half of the study area (fig. II-31). Twelve wells (or two-thirds of the total

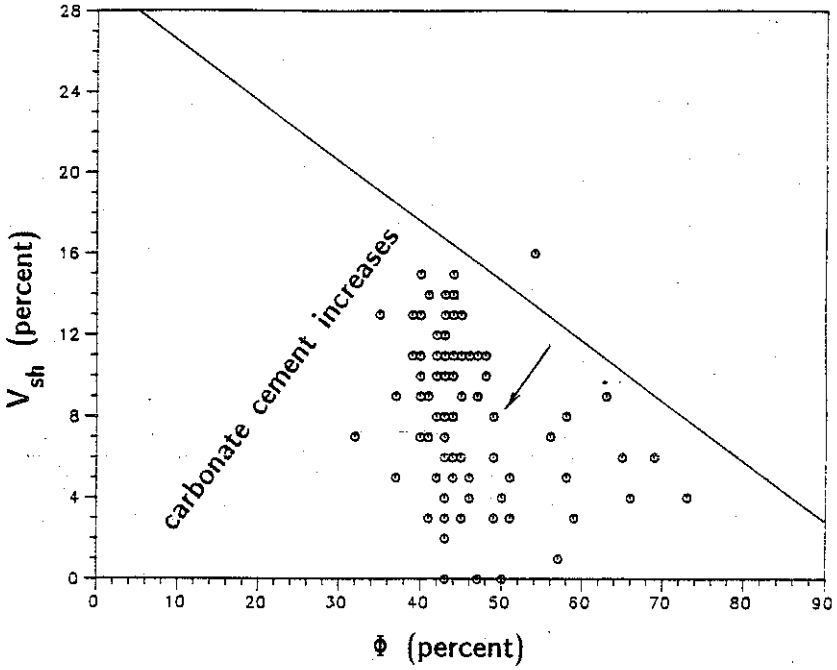

Figure II-30. Relation between shaliness and effective porosity, operational unit 1U (upper Spraberry), ununitized area, Spraberry Trend.

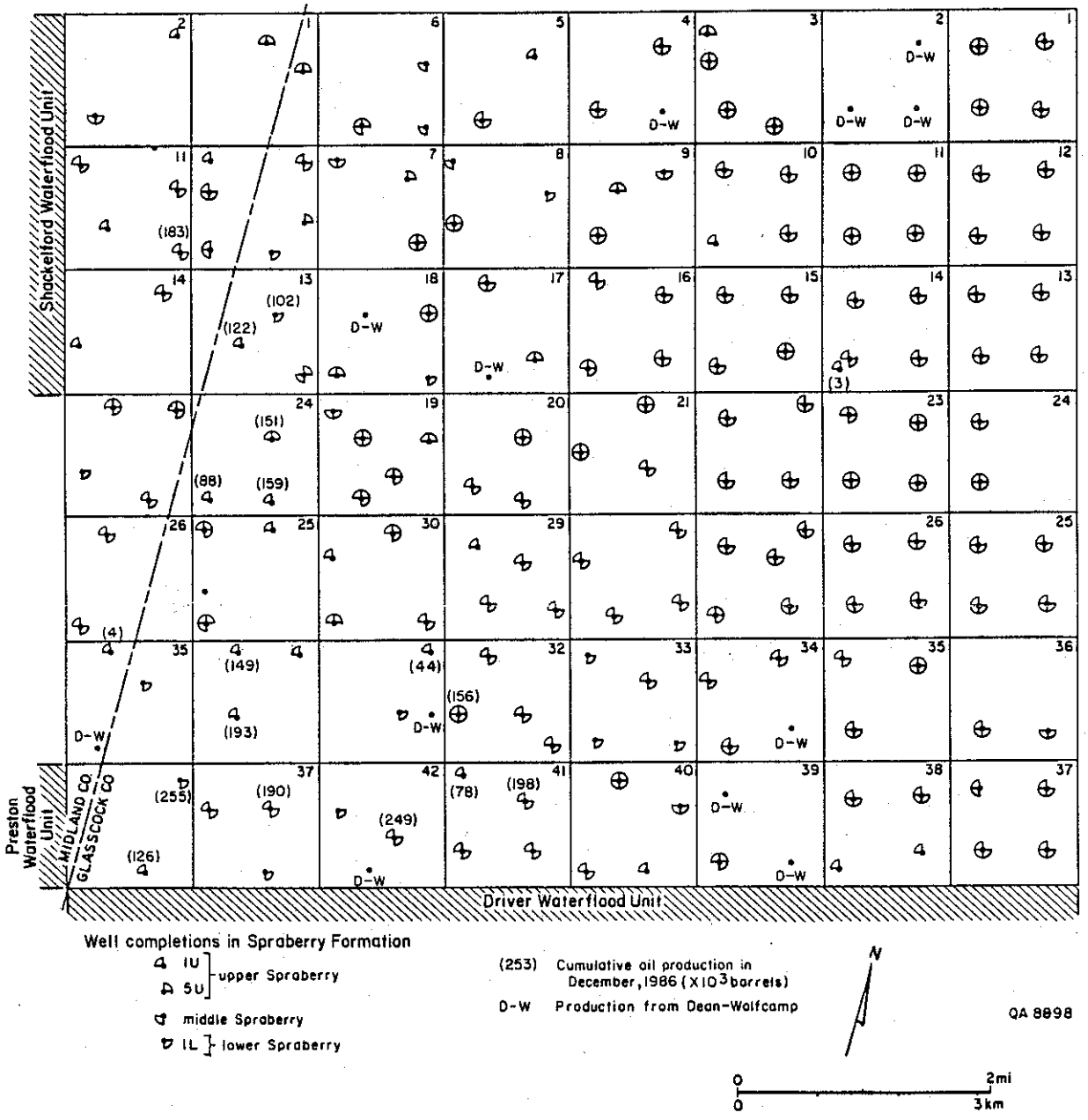

Figure II-31. Geographic distribution of producing intervals, ununitized area, Spraberry Trend.

sample) had cumulative productions of more than 100,000 barrels of oil in December 1986. Maximum cumulative production is 249,000 barrels in a well in the southwest part of the area having upper and lower Spraberry reservoirs open to commingled production. Four wells (22 percent of the total sample), all completed only in the upper Spraberry, have produced less than 80,000 barrels. Two of the sample wells were completed only in lower Spraberry reservoirs and have produced 102,000 and 255,000 barrels. Cumulative productions of 11 sample wells completed only in the upper Spraberry range from 193,000 barrels (in a well in the southwest part of the area) to 3,000 barrels (in a well in the east-central part). Four wells having commingled production from upper and lower Spraberry reservoirs have each yielded more than 180,000 barrels, and one well having commingled production from upper and middle Spraberry reservoirs has produced 156,000 barrels.

The available production data indicate that cumulative primary recovery per well in the study area is, as expected, lower than the cumulative production of the Driver unit after waterflooding (post-1963, thus including secondary recovery) (table II-1). Maximum cumulative well production in this unit is approximately 450,000 barrels (in a well in the northeast part of the unit) (Guevara, in press). Production data also suggest that primary recovery per well in the study area is relatively higher than in the Preston/Shackelford waterflood units (table II-1), where the highest total (primary and secondary) cumulative well production is approximately 350,000 barrels (in a well in the east-central part of the Shackelford unit) (Tyler and Gholston, in press).

Table II-1. Comparison of cumulative oil production per well in the ununitized area and adjacent waterflood units.

Area	Production per well ($x10^3$ bbl)			
	>400	300-400	200-300	100-200
	Number of wells			
Driver	1	3	3	33
Ununitized	0	0	2	11
Preston/Shackelford	0	1	1	31

Although production information from only 18 wells of the study area is a very small sample (fig. II-31), comparison with production data from adjacent waterflood units (table II-1) suggests that these values are representative of primary well production in this part of the Spraberry Trend. The data suggest that upper and lower Spraberry reservoirs are each capable of locally producing more than 100,000 barrels of oil per well. The locations of the areas of higher oil production ("sweet spots") in the adjacent waterflood units generally correspond to the axes of belts of greater total thickness of sandstone and siltstone (Guevara, in press; Tyler and Gholston, in press). Isolith, porosity, and production data suggest that sweet spots of the study area (fig. II-31) also occur mainly in the belts of isolith maxima (figs. II-8 to II-11). Paucity of production data from the study area precludes further evaluation of this relation.

Relatively high recoveries in wells in the south part of the study area (fig. II-31) may be the response to waterfloods south and west of this area (the Driver and Preston units, respectively) (fig. II-1). Recoveries in the ununitized area and in the Driver waterflood unit higher than in the Preston/Shackelford units (table II-1) probably reflect both local better reservoir quality in the eastern depositional axes of sandstone and siltstone (fig. II-32) and a thicker oil column near the eastern updip seal (stratigraphic and possibly also partly diagenetic) of the Spraberry Trend.

Production data indicate that recoveries of wells producing from either upper or lower Spraberry reservoirs are generally comparable to those of wells having

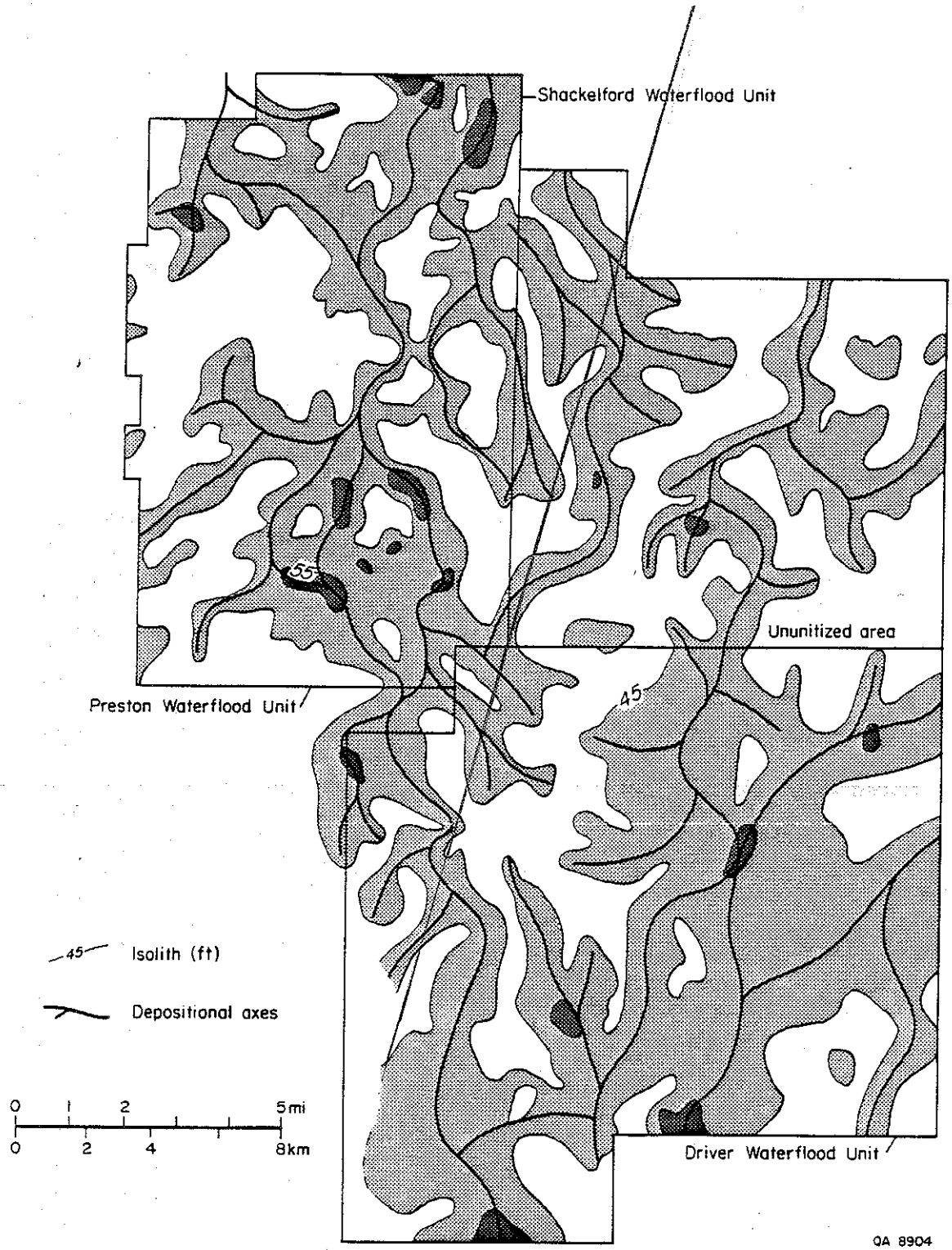

Figure II-32. Belts of midfan channel fills of operational unit 1U (upper Spraberry) in the ununitized area and adjacent waterflood units. Isoliths define two main sectors having channel fills. One of these sectors is located in the east-central part of the Preston/Shackelford units, extending to the west parts of the ununitized area and the Driver unit. The other one occurs in the east-central parts of the ununitized area and the Driver unit. Areas of superior oil production ("sweet spots") of the waterflood units usually occur in these belts. Therefore, areas having relatively high effective porosities in these sand-rich belts, and in those of operational unit 1L (lower Spraberry), are prime candidates for extended development and secondary recovery in the ununitized area and in the adjacent waterflood units.

commingled upper and lower Spraberry production. This similarity may be partly due to local loss of potential production into low-pressure reservoir compartments acting as "thief zones" in dually completed wells. Detailed pressure data and production logs are needed to evaluate this hypothesis.

Opportunities for Additional Oil Recovery

Handford (1981a, 1981b) called attention to Spraberry and Dean reservoirs as prime candidates for reexploration and Galloway (1983) emphasized the possibilities for additional oil recovery from these highly heterogeneous submarine fan reservoirs. Geological characterization of oil reservoirs in unitized areas of the central Spraberry Trend (Guevara and Tyler, 1986; Tyler and Guevara, 1987; Guevara, in press; Tyler and Gholston, in press) indicate that additional recovery using nontertiary techniques can be obtained from reservoir compartments that have been partly drained or that remain untapped.

Reserves can be added in the study area (and in the Spraberry Trend in general) by considering the implications of facies architecture on oil distribution and recovery. This reserve growth can be achieved by (1) well recompletions that would open to production bypassed oil-bearing intervals currently behind casing; (2) deepening of wells to produce from units 5U and 1L (figs. II-6 and II-7); and (3) programs of strategic infill drilling and secondary recovery.

The distribution (stratigraphic and geographic) of intervals open to oil production and its relation to reservoir stratigraphy and actual well spacing need special consideration in programs of reserve growth. Traditionally, well completions in the study area have been based on the concepts of laterally extensive and homogeneous reservoirs that are completely linked by natural fractures. Consequently, 80-acre well spacing predominates, in which well locations are approximately 2,650 ft apart.

However, current well spacing may locally be too wide for adequate drainage of some reservoir compartments, especially if the stratigraphic distribution of the intervals open to production is considered (fig. II-31).

Current completion practices leave mobile, potentially producible oil in Spraberry reservoirs because not all accumulations nor the stratigraphically controlled compartments within those accumulations have been systematically tapped. For example, although most wells in the study area produce from unit 1U (which includes the shallowest and probably the most prolific Spraberry reservoirs in this part of the Spraberry Trend), few tap or have even tested the also potentially productive reservoir rocks of unit 5U (figs. II-14 and II-31). Testing the production potential of unit 5U is of particular importance in the south part of the study area, which is adjacent to the Driver waterflood unit, where sandstone zone f (of unit 5U) is an oil reservoir (Guevara, in press). Similarly, unit 1L has been penetrated but may locally remain untapped in sand-rich areas of this operational unit (for example, in the vicinity of well E-4#1, fig. II-14), especially in the west part of the area (fig. II-31).

Continuations of sand-rich belts of the study area (fig. II-32) contain the sweet spots of the Preston/Shackelford (Tyler and Gholston, in press) and Driver (Guevara, in press) waterflood units. This relation between cumulative production and reservoir stratigraphy suggests that oil recovery in the sand-rich belts of the study area, especially in those of the east part, may be locally comparable to the relatively high recovery of sweet spots of the Driver unit (table II-1). Programs of infill drilling should aim at production from sparsely drilled areas having superior effective porosity (figs. II-24 through II-27) in sand-rich belts of the study area (figs. II-8 through II-11).

These programs should also take advantage of the local superposition of reservoir rocks (fig. II-12) for the selection of well locations penetrating multiple objectives.

Programs of water injection and enhanced oil recovery must be based both on fracture data and detailed reservoir stratigraphy. Locations of injection and production wells should be selected using isolith and porosity maps, in addition to data on fractures. The geographic and stratigraphic distribution of these wells should consider the occurrence of preferential flow paths along belts of isolith maxima (figs. II-8 to II-11) having the highest values of effective porosity (figs. II-24 through II-27). In particular, optimum flow paths will be contacted where sand-rich belts are oriented parallel to fracture trends.

Appendix II-A. Geostatistical analysis.

Manually contoured maps are often criticized as being biased by the geologist's preconceived concepts of the product being generated (net-sand map, net-pay map, etc.). To test our mapping, geostatistical methods were used to confirm the validity of the occurrence and direction of stratigraphic trends in the ununitized area. This methodology involves the comparison of hand-drawn and computer-generated contours. The hand-contoured isolith map of operational unit 1U of the upper Spraberry (fig. II-8) was selected for this test because this unit contains important oil reservoirs and because the map was prepared using the most complete set of data points available for the study area.

Geostatistics is a statistical approach to the estimation of spatial data values and averages over a region, given a set of measured values at various points in space. In geostatistics an estimation tool is used, the (semi-) variogram, constructed from the raw data set. The variogram is then used to determine optimal weighting factors to apply to sampled values, which are used in a subsequent step involving a moving average technique to arrive at interpolation estimates (Journel and Huijbreghts, 1978).

The map shows the locations of 214 well logs (data points), the values of total thickness of sandstone and siltstone determined using these logs, and a 1-mi^2 grid system overlaid onto the data points. For this study, a finer Cartesian coordinate grid was superimposed parallel to the existing grid. It divided the side of each large square (1 mi^2) on the map into 100 grid units. Using this coordinate system, the study area on the map was contained by a rectangular area approximately 800 units wide by 900 units long, corresponding to a scale of 75.5 grid units per map inch. This grid is not directly related to any standard global grid-referencing system; for convenience of description, the E-W direction across the map is referred to as the X-direction, and

the direction toward the top of the map the Y-direction, or N-S, although they are not truly north-south or east-west. The locations of the data points on this grid were digitized using a digitizing tablet. The precision of location of each point on the grid was estimated to be 1/50 inch (about 1.5 grid units). The thickness values were then added to the computerized file of locations.

Kriging

Data points are evenly distributed over the whole area with typically three or four samples in each 1-mi^2 grid cell. Basic statistical analysis of the thickness data involved breaking the area into four quadrants with common point (x,y) = (400,400). The mean (μ) and standard deviation (ρ) of the data were computed for each quadrant (table IIA-1). The individual data values for each quadrant were plotted as a histogram of thickness values on normal linear axes and as a cumulative histogram on normal probability paper axes. The statistical program Dataplot (Filliben, 1984) was used for these computations. The analyses indicate that, although differences in statistics do exist in the four quadrants, the normal distribution is well approximated throughout and the zonal trend is small. Consequently the area was treated as a whole and not zoned in subsequent computations. The histogram and the normal probability plot of the total data set are presented (figs. IIA-1 and IIA-2).

Table IIA-1. Means and standard deviations of values of total thickness of sandstone and siltstone by quadrant (in ft).

	NW	NE	SW	SE
μ	45.8	42.1	43.6	43.9
ρ	4.7	5.1	6.6	4.5

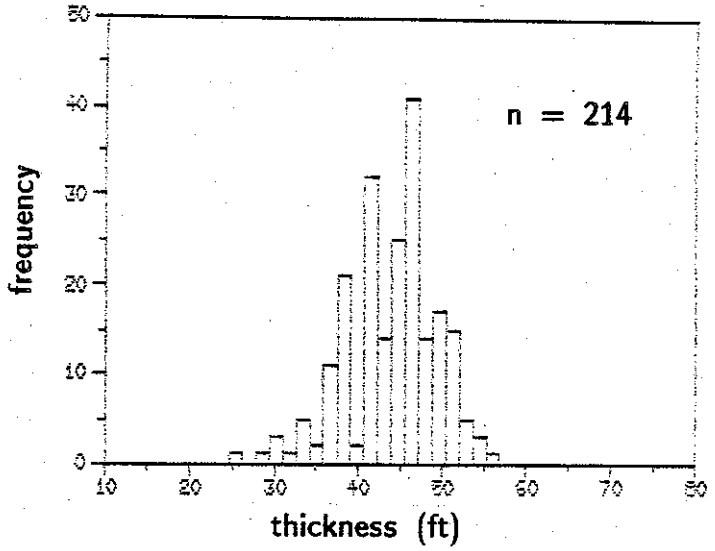

Figure IIA-1. Histogram of values of total thickness of sandstone and siltstone, operational unit 1U (upper Spraberry), ununitized area, Spraberry Trend.

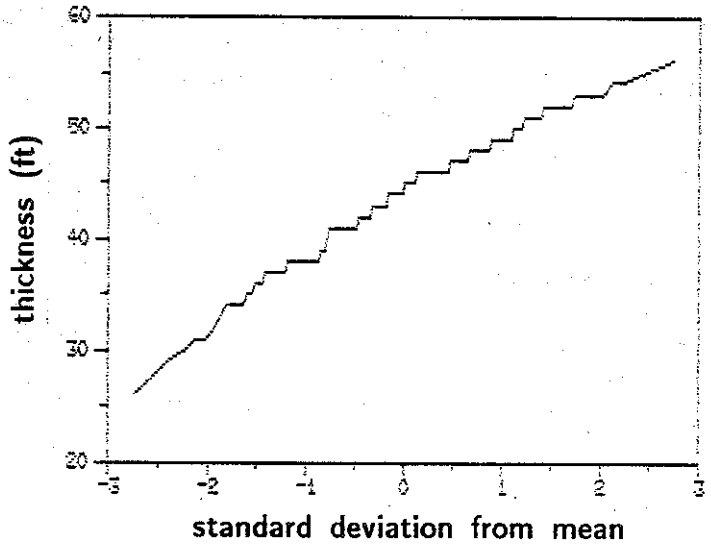

Figure IIA-2. Normal probability plot of values of total thickness of sandstone and siltstone, operational unit 1U (upper Spraberry), ununitized area, Spraberry Trend.

smooth curve) having the parameters nugget value (C0) 13.5 ft^2, sill (C) 10.5 ft^2, and range (a) 105 grid units. These values were used in the subsequent interpolation phase.

For the interpolation process, a second computer program from Knudson and Kim (1978) was used. This program was also modified for computers at The University of Texas at Austin. The program, originally called UKRIG, has been renamed NEWUK in Bureau of Economic Geology usage. It has the capability of performing simple (not universal) kriging estimation of the average value of square blocks, using spherical variogram models. In this application, the program was set up to estimate the average sand thickness value of square blocks of side 25 grid units (about 0.25 mi). For this purpose each large square of side 100 grid units was divided into 4 smaller squares. The program was instructed to perform kriging interpolation by confining its search for data points to a neighboring area bounded by a circle with radius equal to 200 grid units, and to use no more than the 10 closest points (if more were present). All blocks in the study area could be estimated under these conditions.

Contouring

After kriging, the contouring program CPS-1 (Radian Corporation, 1979) was used to contour the values of average total thickness of sandstone and siltstone. CPS-1 is a sophisticated package allowing many options for interpolation and contouring. In this case, the ZFIT verb of CPS-1 was used. ZFIT creates its own internal interpolation array for subsequent contouring, in this case on a spacing of 20 grid units between nodes. The contour threading was then done using ZFIT's interpolations and the CLV4 verb of CPS-1. ZFIT was chosen because it allows greater flexibility than other options while keeping extra computation to a minimum. ZFIT's own

interpolation methods did not introduce any significant distortion into the pattern of contours because the number and coverage of block values provided by the kriging step afforded very extensive and close control of the contours. To verify this, however, several contouring runs were done on the same data using other CPS-1 options (such as MGRD or DSPL), and no significant change in contour pattern was observed.

Results

The resulting map (fig. IIA-4) represents a contouring of average thickness values over square blocks of side 0.25 mi (25 grid units). Thus, isolated spots with extreme thickness values (high or low) will tend not to be reflected in the contours. However, sustained values across 1 or 2 mi will appear in the contours. The contours thus are well adapted to showing trends in the data without reference to geological hypotheses that have not been included in the computations.

The contours as shown depend on the variogram model that was chosen. In particular, the model used has a nugget value of 13.5 ft^2, which corresponds to a local uncertainty of reading thickness values from well logs equivalent to a standard deviation of 3.7 ft. This value is indicated by the variogram study. For comparison and to detect the sensitivity of the results to nugget value (which in some geostatistical studies can be significant) a second run was done in which the nugget value was set at 6.5 ft^2 (a value not justified by the data). Although, as expected, the resulting contours indicated some more internal structure in the contours, the overall trends on the map were identical to those obtained with the original variogram. It was concluded that the results of the study were not significantly sensitive to the precision of the nugget value used.

Because the computer-generated contour map of kriged average values (fig. IIA-4) shows trends that are similar to those of the corresponding hand-contoured isolith map (fig. II-8), geostatistical analyses provide confirmation of the occurrence and directions of two main dip elongate axes of sandstone and siltstone deposition in operational unit 1U in the ununitized area, one in the east-central part, and another in the west part.

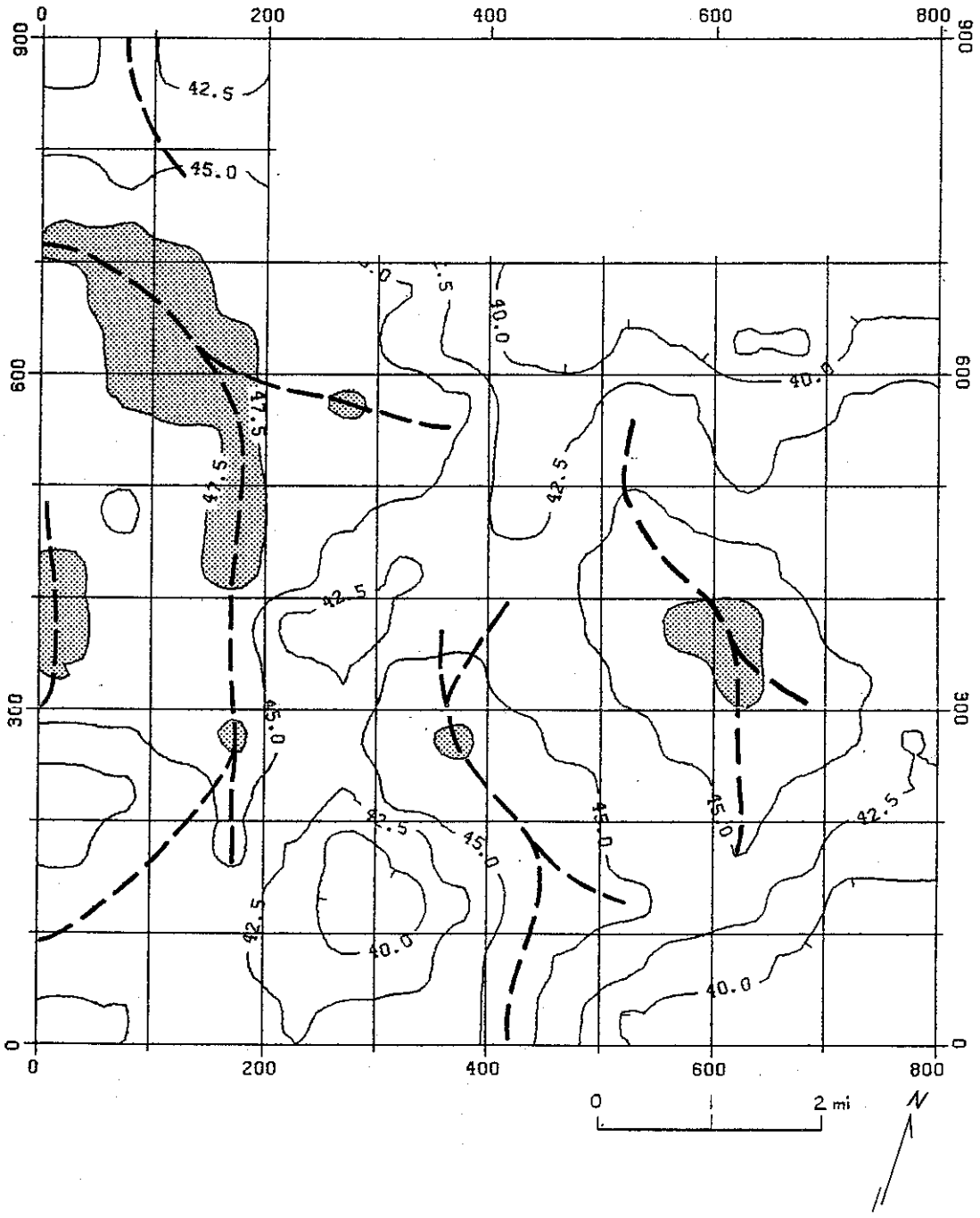

Figure IIA-4. Contour map of kriged average values of total thickness of sandstone and siltstone (ft), operational unit 1U (upper Spraberry), ununitized area, Spraberry Trend. Averages were taken over square blocks having 0.25-mi sides equivalent to 25 grid units. Dashed lines are axes of belts having greater kriged average values of total thickness of sandstone and siltstone. Patterned areas have values greater than 47.5 ft. Contour interval is 2.5 ft.

III. WELL STUDIES

A. Sources of Data

Detailed geological and petrophysical information on Spraberry oil reservoirs is scarce. Most wells were logged using only gamma-ray and neutron tools. Only occasionally are resistivity, density, or sonic logs available from wells in the Spraberry Trend. This is true even in wells that have been drilled in the 1980's. Consequently, completion intervals have commonly been selected only on the basis of gamma-ray correlation of nearby oil-producing intervals. Also, although cores were cut in the main oil reservoirs in several areas during initial development of the Spraberry Trend, only a small number of cores are currently available, and their state of preservation is generally poor, precluding detailed studies of external geometry, lithofacies architecture, and petrophysical properties of these reservoirs. Similarly, reservoir pressure data from specific reservoirs, such as those in operational units 1U and 5U of the upper Spraberry and 1L of the lower Spraberry, are scarce to unavailable. Furthermore, because most wells have been completed in more than one producing interval and production is commingled, the production characteristics of each of these reservoirs are generally not well known.

To obtain new reservoir data, the RCRL project contracted Schlumberger Well Services, Midland, to run a state-of-the-art suite of open-hole logs in a newly drilled well in the Spraberry Trend in cooperation with Mobil Producing Texas and New Mexico. With the additional economic support of several oil companies participating in the RCRL project, suites of open- and cased-hole logs were run in a second study well (fig. II-1). The results of only one of the open-hole log suites is presented in this report because logs and cores from the second study well were obtained in the last month of the project and have not been analyzed. The objective of the log suites was

the identification and evaluation of those logs that would permit (1) the determination of porous and permeable intervals and their corresponding fluid saturations in these low-porosity and low-permeability reservoirs as a means of detecting bypassed or unproduced oil-bearing reservoir compartments and (2) the identification of natural fractures.

Programs of coring and reservoir pressure measurements were implemented. Mobil Producing Texas and New Mexico provided drilled sidewall cores from the most important Spraberry oil reservoirs in the first well; whole cores were obtained in the second well. These cores were used to relate lithology to log response and reservoir quality. An important complementary objective was the measurement of formation pressures in the multilayered, multicompartment oil accumulations of the Spraberry Formation. These data would help evaluate the working hypothesis that these accumulations are indeed vertically stratified and laterally compartmentalized.

Open-Hole Log Suites

Open-hole logs were run in the Mobil Preston-37 and Mobil Judkins A No. 5 wells. The Preston-37 well was drilled in the south-central part of the Preston waterflood unit, which is operated by Mobil Producing Texas and New Mexico. The Judkins A No. 5 well was drilled less than 2 mi east of the Mobil-operated Shackelford waterflood unit in an ununitized area (fig. II-1). Objectives for oil production in these wells were prospective intervals in the Wolfcamp and in the Dean Sandstone, which are stratigraphic units underlying the Spraberry Formation. Oil production tests are planned in Spraberry reservoirs of the Judkins A No. 5 well, but these reservoirs were not tested in the Preston-37 well.

Open-hole logs were recorded in the Preston-37 well in September 1986, and in the Judkins A No. 5 well in June 1987 (table III-1). Schlumberger Well Services used data from the open-hole logs to produce computed formation-evaluation and fracture logs (table III-2).

Table III-1. Open-hole log suites recorded in study wells, Spraberry Trend.

Well log	Well	
	Preston	Judkins
Natural gamma-ray spectroscopy (NGT)/Caliper	yes	yes*
General spectrometry (capture tau) (GST)	no	yes
Geochemical evaluation (GET)	no	yes
Dual induction spherically focused (DIT/SFL)/SP	yes	no
Phasor induction/SFL/Gamma ray (GR)	no	yes
Dual laterolog (DLL)	no	yes
Electromagnetic propagation (EPT)/GR/Caliper	yes	no
Lithodensity/Compensated neutron (LDT/CNL)/GR/Caliper	yes	no
Lithodensity (LDT)/Dual neutron (CNTG)/GR/Caliper	no	yes
Long spacing sonic (LSS/WFM)/GR/Caliper	yes	no
Digital sonic (STC)/GR	no	yes
Formation microscanner (FMS)	yes	yes

*No caliper log.

Table III-2. Logs computed from log suites of study wells, Spraberry Trend.

Log	Well		Purpose of log
	Preston	Judkins	
VOLAN	yes	yes*	Formation evaluation, stratigraphic data
GLOBAL	yes	no	Formation evaluation, stratigraphic data
ELAN	no	yes*	Formation evaluation, stratigraphic data
CFIL	yes	no	Fracture identification
Filmap	no	yes	Fracture identification
Dual dip	yes	no	Fracture identification, stratigraphic data

*Currently being processed by Schlumberger Well Services.

The natural gamma-ray spectroscopy log (NGT) measures the total natural radioactivity of the formation and the radioactivities due to thorium, uranium, and potassium, which are the three main sources of natural radiation. NGT data were used in this study for stratigraphic correlation, clay typing, and attempting to identify fractures.

Thermal neutron logs provide measurements of the hydrogen content of the formation, which is scaled in porosity units. The determined hydrogen content and corresponding porosity values are based on the capture of attenuated neutrons that have been slowed mainly by hydrogen atoms. The neutrons are introduced into the formation by a radioactive source housed in the logging tool. The compensated neutron log (CNL) records measurements of slow (thermal) neutrons by two selective detectors. The dual porosity compensated neutron log (CNTG) presents data of both slow (thermal) and intermediate (epithermal) neutrons; each neutron type is measured by two detectors. Neutron logs were used as a porosity tool and, in combination with other logs, for lithological interpretation.

The lithodensity log (LDT) records the bulk density of the formation, which is a measure of porosity when lithology is known. A special measurement of the LDT log, the photoelectric effect (Pe), is used to determine porosity in complex formations. The sensors of the logging tool are housed in pads that are pressed against the borehole walls. Therefore, LDT data of the Preston-37 well are adversely affected in those intervals where the pads were not in contact with the formation (for example, in oversized hole intervals resulting from caving or wall spalling), even though the short-spacing detection system of the tool partly compensates for this effect.

Of particular importance in the evaluation of Spraberry oil reservoirs is the determination of true formation resistivity (Rt), representative of the connate water saturations. This is most difficult in stratigraphic intervals, such as the Spraberry Formation, having bed thicknesses thinner than 10 inches. Theoretically, the dual laterolog (DLL) would give the best vertical resolution for Rt. However, the depth of investigation of the DLL becomes shallow, and therefore this log does not simply determine Rt. This is controlled mainly by the ratio between the resistivity of the drilling mud filtrate (Rmf) and that of the formation water (Rw) (fig. III-1). An

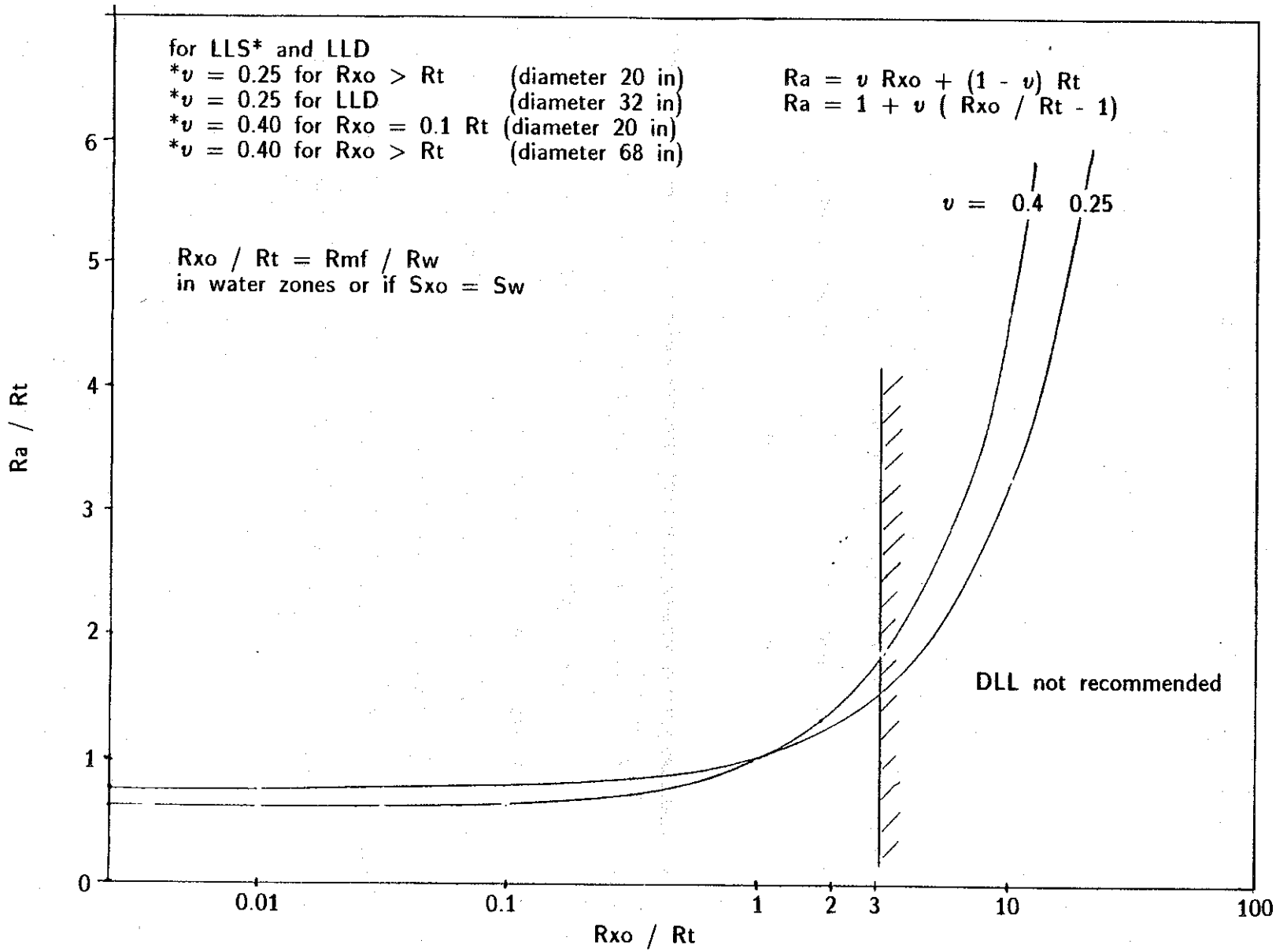

Figure III-1. DLL response to contrast between Rxo and Rt for various pseudo-geometrical factors.

additional objective of the DLL in this study was the detection of natural fractures, based on the difference between the resistivity of the deep and shallow laterolog and the resistivities in the areas closer to the borehole (using the MSFL or SFL from the DIL) log. The DLL was not run in the Preston-37 well.

The dual induction log (DIL) provides measurements of deep resistivities that can closely approximate the true formation resistivity if the beds are more than 5 ft thick. The DIL and a spherically focused laterolog (SFL), which measures the resistivity in the shallow formation or area immediately adjacent to the borehole, were recorded in the Preston-37 well. Phasor induction logs were recorded in the Judkins A No. 5 well, inducing electric currents having 10, 20, and 40 kHz to improve vertical resolution. Corresponding SFL logs are displayed alongside the induction phasor logs.

Mobility or producibility of the remaining oil in place may be determined using the relation between the saturations of the flushed zone near the borehole and the connate water saturation of deeper parts of the formation. The electromagnetic propagation log (EPT) reflects the saturation in the flushed zone in its display of the propagation time and the attenuation of an electromagnetic wave transmitted parallel to the borehole. These are mainly functions of the dielectric properties of the formation, which are mainly influenced by the water saturation. This is caused by the much larger value of the dielectric constant of water compared with that of rock matrix or hydrocarbons. Similarly to the LDT log, the EPT log records measurements made by a device in contact with the borehole walls, and thus it is adversely affected by oversized rugose borehole configurations.

Use of the EPT log in Spraberry reservoirs was advisable for several reasons. Oil mobility and residual oil saturations could be estimated from EPT data. Also,

because water salinity has low influence on this log, EPT data would permit estimations of residual oil saturations (ROS) in intervals having unknown water salinity such as in the potentially waterflooded sectors of the oil reservoirs of the Preston-37 well. Partly drained or undrained reservoir compartments could thus be detected. Similarly, the vertical resolution of this log, approximately 2 inches, is appropriate for evaluation of the highly stratified Spraberry oil accumulations.

In spite of these potential benefits, the EPT log was only of marginal benefit in the Preston-37 well. The lithologic characterization and the index of residual oil saturation (ROS) were highly questionable. The poor performance of the EPT log in this well is probably a result of the borehole ellipticity that is indicated by data from the calipers of the formation microscanner log (FMS). The EPT log was not recorded in the Judkins A No. 5 well.

The long-spacing sonic log (LSS) includes full sonic waveform recording (WFM). In addition to their use for porosity determinations and lithological assessment in the VOLAN and GLOBAL evaluations, data from the LSS log were used in fracture detection by calculating a secondary porosity index that was used both in the VOLAN evaluation and in conjunction with data from the NGT log. This index is defined as the difference between the porosity determined from the density-neutron log combination and that derived from the LSS log. Also, sonic waveform analysis provided data on amplitudes of compressional (P), shear (S), and Stoneley waves that were used in the composite fracture identification log (CFIL).

The formation microscanner log (FMS) displays continuous microresistivity images along two 2.8-inch-wide, orthogonal strips of the wellbore walls. Resistivity is recorded by 27 overlapping electrodes mounted on 2 orthogonal pads in a modified dipmeter tool. The FMS images depict bedding, fractures, and other formation features because

such anomalies reflect shales and drilling mud, which are less resistive than other parts of the formation to an electrical current induced by the logging tool. The features thus stand out as lineaments on the display of all 27 resistivity curves and as zones of varying shades of gray on the processed resistivity images (darker shadings indicate lower resistivities). The log also records the borehole size in two orthogonal directions corresponding to those of the pads on which the resistivity sensors are mounted. Because at least some of the recorded resistivity anomalies could have been induced when the borehole was being drilled, the differentiation between natural fractures that extend deep into the formation and borehole features restricted mainly to the immediate vicinity of the borehole (for example, wall cavings controlled by lithology, stress-related wellbore spalling, and bit scratches along borehole walls) is generally ambiguous on FMS images. Thus, adequate identification of natural fractures requires additional information to verify FMS data.

Cores from Spraberry Reservoirs

Cores were cut in the Preston-37 and Judkins A No. 5 wells at depths selected by geologists of the Bureau of Economic Geology and Mobil Producing Texas and New Mexico. Results of studies of cores from the Preston-37 well are included in this report. Cores from the Judkins A No. 5 well are still being processed at the facilities of Core Laboratories, Midland. They will be available for the second research year of the project.

Preston-37 cores: Mobil Producing Texas and New Mexico contracted Schlumberger Well Services, Midland, to drill sidewall cores in the most important oil reservoirs of the upper and lower Spraberry in the Preston-37 well. Conventional

bottom-hole cores could not be cut as originally planned, owing to loss of mud circulation in the borehole. Core depths were selected at the well site using a field print of the GR-LDT log.

Recovery of cores 1.5 inches long and 1 inch in diameter was attempted at 18 depth locations. Only 12 cores were retrieved, 7 from the upper Spraberry and 5 from the lower Spraberry (fig. III-2, table III-3). Macroscopic descriptions, photography under natural and ultraviolet light, and measurements of the length of the cores (table III-3) were completed before sampling for petrophysical and petrographic analyses. Eight cores (five in the upper Spraberry and three in the lower Spraberry) consist of very fine grained sandstone to coarse siltstone; the other four cores (two in the upper Spraberry and two in the lower Spraberry) are mainly shale. Including the laminae of the 7317-ft core, all sandstones (except the 8036-ft sample) showed bright, yellowish fluorescence under ultraviolet light. The sandstones at 7158 ft, 7160 ft, 7323 ft, 8028.1 ft, and 8052.9 ft (table III-3) bled oil that coated the transparent film in which each sample was wrapped, clearly indicating that the cored intervals are oil bearing.

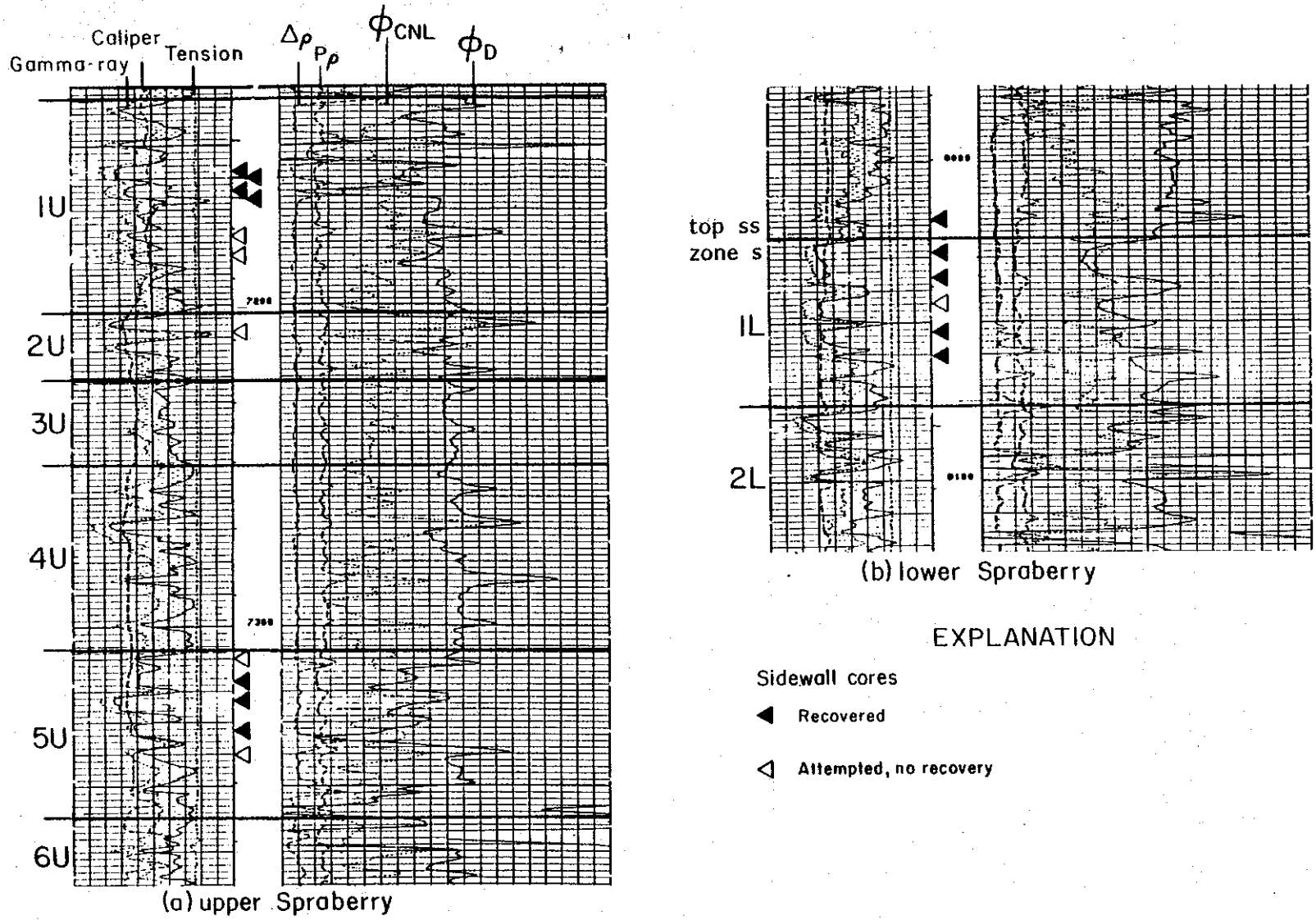

Figure III-2. Drilled sidewall cores, upper and lower Spraberry, Preston-37 well (locations shown on lithodensity-compensated neutron log).

Table III-3. Drilled sidewall cores, Preston-37 well.

Operational unit*	Depth (ft)	Length (inch)	Lithology**	Fluorescence	Comments
			upper Spraberry		
1U	7158	1 3/4	Sst	yellow	split core, bled oil
1U	7160	1 11/16	Sst	yellow	split core, bled oil
1U	7164	1	Sst	yellow	broken core
1U	7164.5	1	Sst	yellow	split core
1U	7178	--	--	--	no recovery
1U	7184	--	--	--	no recovery
2U	7208.1	--	--	--	no recovery
5U	7310	--	--	--	no recovery
5U	7317	1 5/8	Sst, lam	yellow	whole core
5U	7323	1 5/8	Sst	yellow	whole core, bled oil
5U	7332	1 3/4	Sh	no	whole core
5U	7340	--	--	--	no recovery
			lower Spraberry		
1L	8018	1	Sh	no	core chip, 1/4 inch diam.
1L	8028.1	1 3/4	Sst	yellow	whole core, bled oil
1L	8036.1	1 5/8	Sst	no	whole core
1L	8043.8	--	--	--	no recovery
1L	8052.9	1 5/8	Sst	yellow	whole core, bled oil
1L	8060	1 5/8	Sh	no	whole core

*See figure I-7 for details on stratigraphic location.
**Sst = sandstone; Sh = shale; lam = laminated.

The cores from the upper Spraberry are split and broken. Although some attempts were unsuccessful due to mechanical problems of the coring tool, relatively poor recovery in the Preston-37 well was at least partly due to borehole caving and well ellipticity (indicated by the caliper logs) that suggest fractures in these intervals.

Judkins A No. 5 cores: A total of 119.5 ft of bottom-hole cores were recovered from the Spraberry Formation in the Judkins A No. 5 well (table III-4) and preserved in dry ice. Core Laboratories recorded corresponding core gamma-ray logs, took photographs under natural and ultraviolet light, and cut plug samples for petrophysical and petrographic determinations. Core Laboratories will also slab the core and send it to the Bureau of Economic Geology for sedimentological description and, if necessary,

additional sampling. The thickest beds of sandstone and siltstone were bleeding oil at the time of coring and showed bright, yellowish fluorescence under ultraviolet light.

Table III-4. Judkins A No. 5 cores.

Operational unit		Cored interval (ft)
	upper Spraberry	
1U		7010.0 - 7070.0
5U		7180.5 - 7202.0
	lower Spraberry	
1L		7878.0 - 7908.0
1L		7930.0 - 7938.0

B. Reservoir Characterization

Reservoir Stratigraphy

Core and log data indicate that the upper and lower Spraberry consist of discrete operational units of interbedded very fine grained sandstone, siltstone, shale, and thin carbonate mudstones (fig. I-7). Thickest accumulations of the sandstones and siltstones occur in the upper part of operational units 1U and 5U (upper Spraberry) and in operational unit 1L (lower Spraberry), forming part of sandstone zones that cap upward-coarsening and upward-thickening sequences. The thickest beds of sandstone, which are the best oil reservoirs, occur in sandstone zones c and f of the upper Spraberry and s of the lower Spraberry (fig. I-7). Isolith maps indicate that sandstone and siltstone of the operational units occur mainly in belts approximately parallel to the basin axis (see Section I, this report). Stratigraphic subdivisions of

upper and lower Spraberry in the Preston-37 and Judkins A No. 5 wells are presented in table III-5.

Table III-5. Stratigraphic subdivisions of the upper and lower Spraberry, Preston-37 and Judkins A No. 5 wells.

Operational unit and sandstone zone*	PRESTON-37 WELL Top (log depth) (ft)	JUDKINS A No. 5 WELL Top (log depth) (ft)
	upper Spraberry	
1U	7137	7007
1Uc	7155	7025
2U	7205	7072
3U	7225	7094
4U	7250	7118
5U	7308	7180
6U	7361	7225
	lower Spraberry	
1L	8002	7847
1Ls	8024	7873
2L	3087	7924

*See figure I-7 for wireline log and details on stratigraphic locations.

Petrographic Parameters Influencing Reservoir Quality

Samples of very fine grained sandstones to coarse siltstones from the Preston-37 cores were examined using petrographic and scanning electron microscopy. Additionally, to identify the clay minerals, the Mineral Studies Laboratory of the Bureau of Economic Geology conducted qualitative X-ray diffraction analyses of whole rock and clay-size fractions of representative samples.

To enhance the visual identification of porosity, the cores were impregnated with a blue epoxy before cutting the thin sections. The petrographic slides were stained for mineral identification. Alizarin Red-S was used to differentiate between calcite (which is stained pink) and dolomite (which remains white), and potassium ferricyanide to distinguish dolomite (which remains white) from ferroan dolomite or ankerite (which turns blue). Potassium feldspars were stained (yellowish-green) using a sodium

cobaltinitrite solution after etching the thin section with fumes of hydrofluoric acid. Samples studied with the scanning electron microscope (SEM) consist of gold-coated rock chips that were cut from the core to expose fresh, clean surfaces.

No major compositional or textural differences were observed between the upper and lower Spraberry samples studied, which are silty, very fine grained sandstones and sandy, coarse-grained siltstones (referred to as sandstones in this report). Spraberry reservoir rocks consist mainly of quartz (70 to 90 percent). Orthoclase, plagioclase (up to 10 percent total feldspars), and clay minerals (less than 10 percent) also are present. Pyrite, generally associated with organic matter, and sericite or muscovite are minor mineral components. Zircon, rutile, and tourmaline are accessory minerals. Cement is mainly carbonate and some quartz overgrowths. Carbonate cement is distributed irregularly in patches; it consists predominantly of silt-sized, generally zoned, euhedral crystals of dolomite and ferroan dolomite or ankerite. Staining indicates that calcite occurs in only very small proportions or is not present in the samples studied.

Intergranular primary porosity is locally preserved but most was lost during early compactional diagenesis. Compactional lithification is suggested by mica flakes that are broken or bent around quartz grains (fig. III-3a) and by embayed grains and quartz overgrowths that resulted in tight fabrics. Secondary porosity due to dissolution of feldspars (fig. III-3b) and carbonates occurred after compactional diagenesis and was followed by carbonate cementation (fig. III-3c). Petrographic data suggest that secondary matrix porosity may be locally important in Spraberry reservoirs of the Preston-37 well. Secondary porosity was recognized on thin sections by the occurrence

a. Uneven packing at 7164 ft. Tight packing and bent mica flake suggest compactional diagenesis; localized more open fabric suggests secondary porosity (10 X 10 X 25; no nichols).

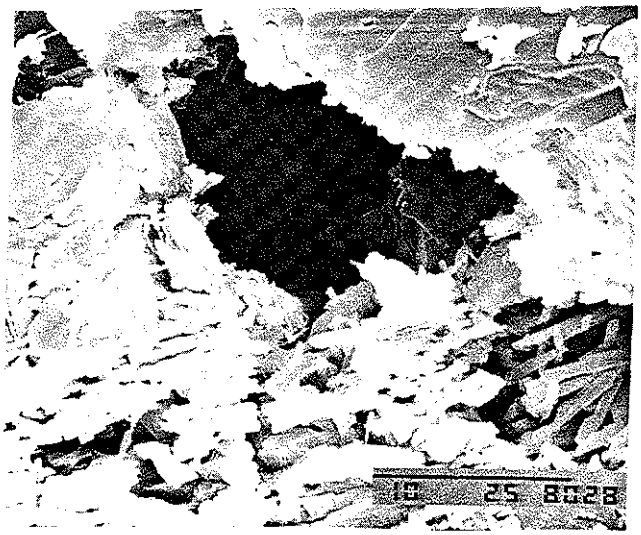

b. Secondary porosity at 8028 ft. Enlarged pore due to dissolution of orthoclase. Clay partly lining fracture is illite (SEM image; scale bar is ten microns long).

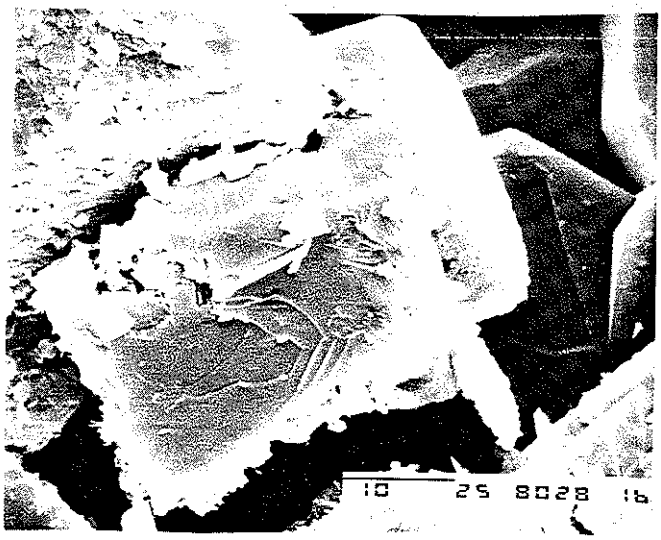

c. Porosity partly filled by quartz overgrowths and dolomite at 8028 ft (SEM image; scale bar is 10 microns long).

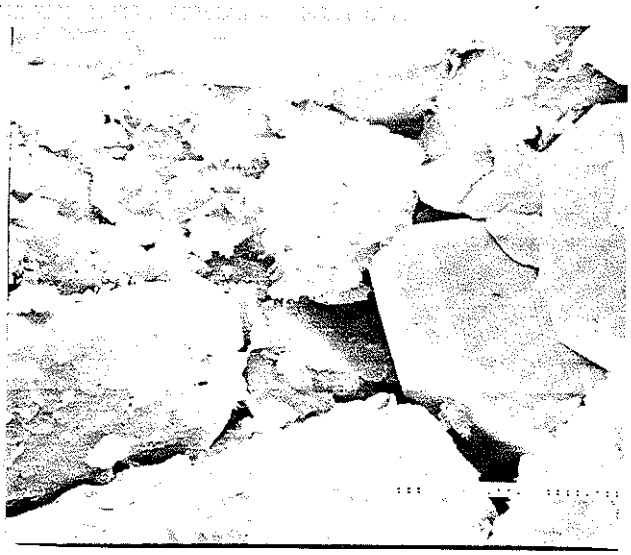

d. Porosity partly filled by quartz overgrowths and illite at 8028 ft (SEM image; scale bar is 10 microns long).

Figure III-3. Porosity of very fine grained sandstones to coarse grained siltstones. Preston-37 cores.

of oversized pores, grains that are almost floating, and adjacent tight and porous fabrics.

Clay minerals were identified using X-ray diffraction data. Samples were pulverized in a tungsten carbide shatterbox. Data were collected from 2 to 20 degrees two-theta. Whole-rock, X-ray diffraction data indicate that illite, kaolinite, and to a lesser extent chlorite are the main clay minerals in upper and lower Spraberry reservoirs and adjacent shales (table III-6). SEM images indicate that clays partly fill pores (fig. III-3d), locally lining grains and fractures (fig. III-3b).

Because well log analysis suggests the occurrence of mixed-layer clays (figs. III-4 and III-5), X-ray diffraction analysis was conducted on the clay-size fraction of two upper Spraberry samples (7160 ft, operational unit 1U; and 7317 ft, unit 5U) to further test the presence of the swelling clays smectite and illite. The presence of mixed-layer clays would cause problems in waterflooding by occluding porosity. These clays are identified by comparing the reflection at 9 degrees two-theta (10 angstroms) of an air-dried sample, which shifts to a lower angle when the same sample is exposed to ethylene glycol vapor (indicating the increase in distance between the planes responsible for this reflection). The samples studied did not show any change in reflection after the glycol treatment, and therefore the analyses conducted do not support the hypothesis of the occurrence of smectite. If indeed present, smectite probably occurs in the shales that separate the reservoir rocks, or it may be present in the reservoir rocks in such a low proportion that it could not be detected in analysis of the small volume of sample available.

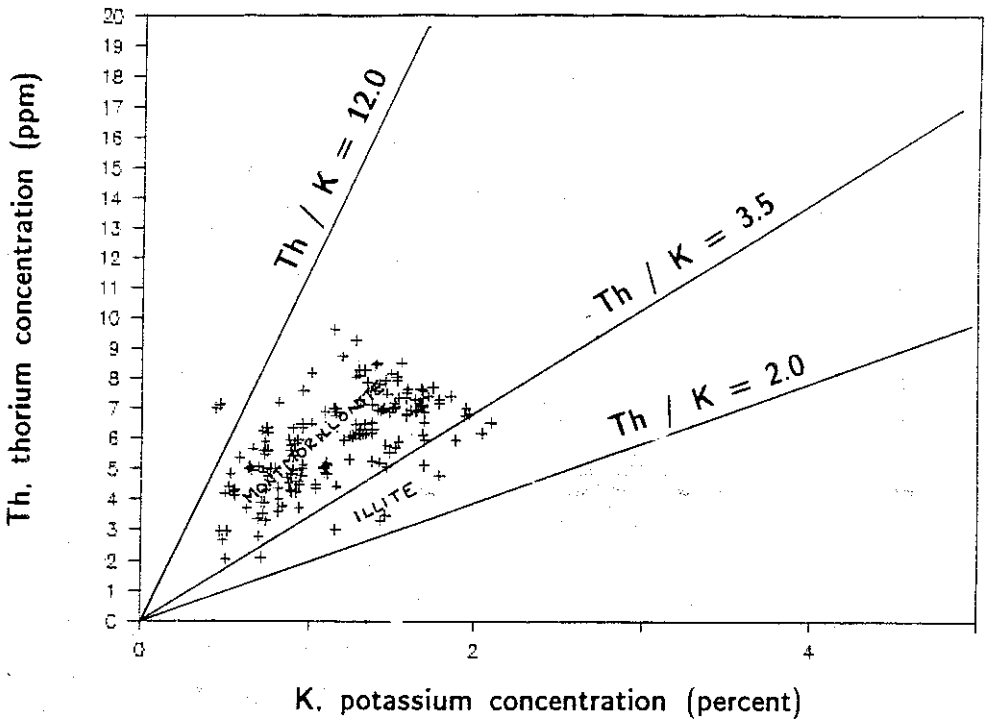

Figure III-4. Identification of clay minerals using NGT data, upper Spraberry, Preston-37 well.

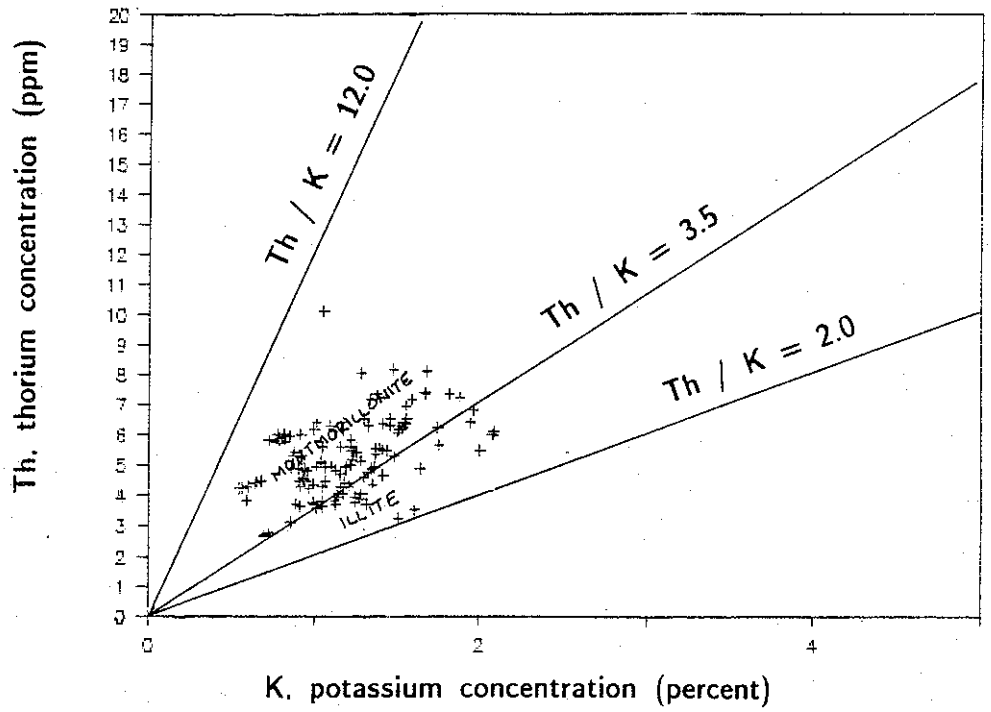

Figure III-5. Identification of clay minerals using NGT data, lower Spraberry, Preston-37 well.

Table III-6. Relative abundance of clay minerals in Preston-37 cores (determined using X-ray diffraction data).

Stratigraphic interval	Operational unit	Depth (ft)	Illite*	Kaolinite*
upper Spraberry	1U	7158	x	x
	1U	7160	x	x
	1U	7164	x	x
	1U	7164.5	x	x
	5U	7317	x	x
	5U	7323	x	x
	5U	7332	x	x
lower Spraberry	1L	8028.1	x	x
	1L	8036.1	x	x
	1L	8052.9	x	x
	1L	8060	x	x

*Relative abundance increases to the right. All samples show only slight peaks for chlorite.

Continuous cores would provide data to further evaluate the control of facies on the areal distribution of porosity and permeability and the relation between matrix porosity, especially secondary porosity, and areas of greater oil production or "sweet spots." Similarly, analysis of cores from other locations, such as those of the Judkins A No. 5 well, are needed to further determine the type, mode of occurrence, and distribution of clay minerals. This information is of special importance for the adequate evaluation of oil prospective intervals using well logs and for drilling and completion practices that should avoid the adverse effects of swelling clays or of plugged pore throats due to mobilization of fines in the reservoir.

Core Analysis, Preston-37 Well

Porosity, permeability, fluid saturation, and grain density (at standard conditions of pressure and temperature) were determined in samples of very fine grained

sandstone to coarse siltstone from the Preston-37 sidewall cores (table III-7). These analyses were undertaken by N. L. ERCO/N. L. Industries, Inc., Houston (now part of Core Laboratories). Data on fluids from the nearby Driver waterflood unit (table III-8) were used in the determination of core saturations. Results of core analysis indicate that matrix porosities range from 8.1 to 14.3 percent, and grain densities from 2.66 to 2.73 g/cc. Water saturations range from 27.6 to 80.6 percent (per volume) and oil saturations are less than 1 percent, except in one sample having 4.2 percent. Although permeability was determined on only three samples of the upper Spraberry and on three samples of the lower Spraberry (table III-7), the data suggest that porosity-permeability relations are different in upper and lower Spraberry reservoirs (fig. III-6).

Table III-7. Core analysis, Preston-37 well (Dean-Stark method).

Oper. unit	Depth (ft)	Por. (%)	Air perm. (md)	So (%)	Sw (%)	Sg (%)	Grain den. (g/cc)	Comments (lithology***)
				upper Spraberry				
1U	7158.0	11.5	0.27	0.3	27.6	72.0	2.69	Sst,f,slt,mic,(c)
1U	7160.0	14.3	0.39	0.5	46.7	52.8	2.67	Sst,f,slt,mic,(c)
1U	7164.0	13.3	*	0.5	47.5	51.9	2.26	Sst,f,slt,mic,c
1U	7164.5	13.8	**	0.7	62.4	36.8	2.67	Sst,f,slt,mic,(c)
5U	7323.0	8.1	0.07	0.5	42.9	56.6	2.72	Sst,f,slt,(mic,pyr,c)
				lower Spraberry				
1L	8028.1	13.9	0.91	4.2	67.1	28.7	2.67	Sst,f,slt,mic,(c)
1L	8036.1	10.6	0.07	0.9	80.6	18.5	2.73	Sst,f,slt,mic,(pyr,c)
1L	8052.9	11.3	0.15	0.6	48.6	50.8	2.67	Sst,f,slt,mic,(c)

* Multisided chip, not usable for the determination of permeability to air.
** Core sample too small for reliable determination of permeability to air.
*** Sst: sandstone; f: very fine grained; slt: silty; mic: micaceous; pyr: pyritic; c: carbonaceous; (c, pyr, mic): slightly carbonaceous, etc.

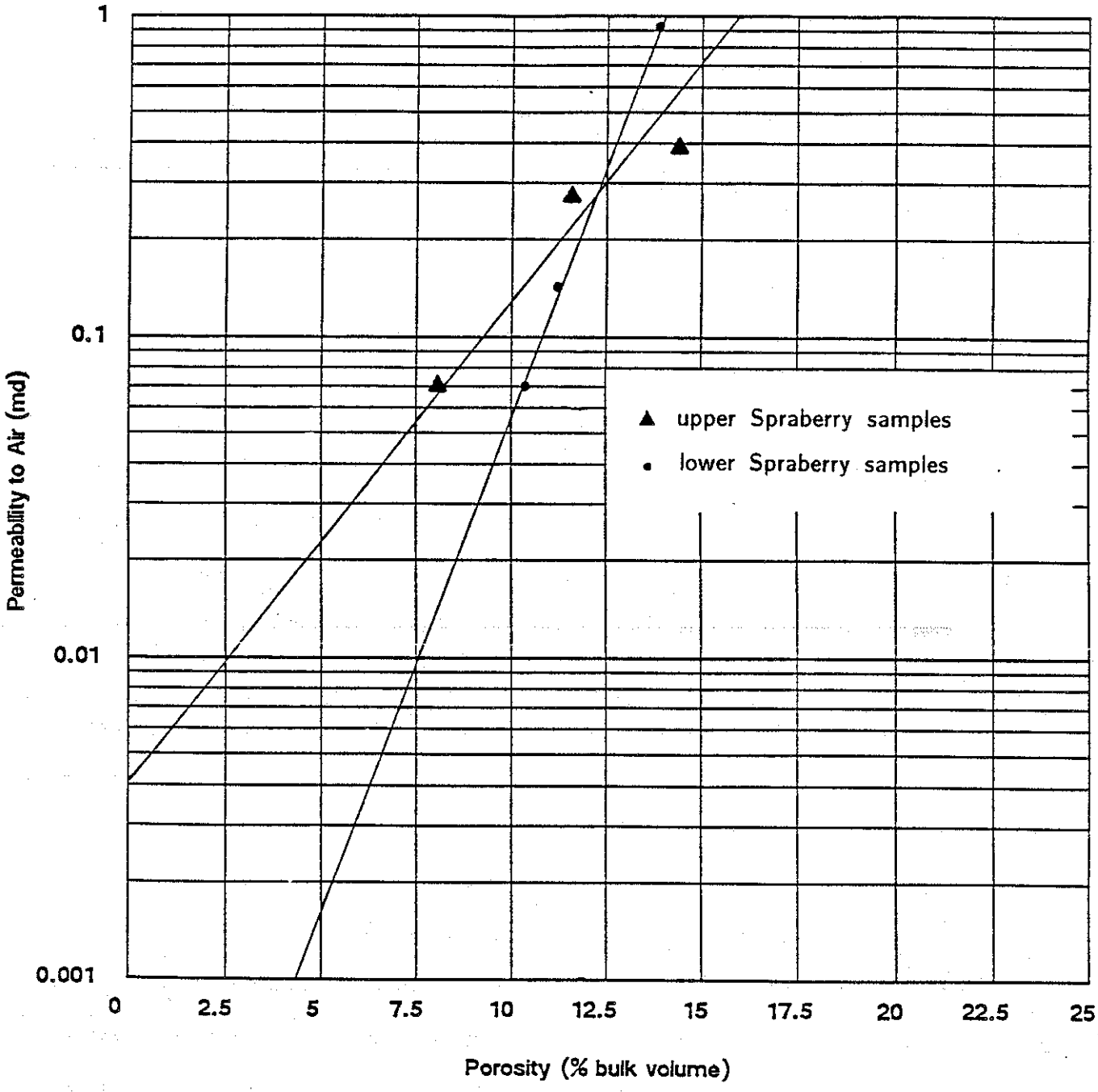

Figure III-6. Porosity-permeability relations in Spraberry reservoirs. Preston-37 cores.

Table III-8. Data on reservoir fluids* used in the determination of saturations of Preston-37 cores.

Producing interval	Water density (g/cc)	Oil gravity (degrees API)
upper Spraberry	1.08 to 1.1	38.6**
lower Spraberry	1.08 to 1.1	41.9***

* From the Spraberry Driver Unit (SDU), provided by T. Morrow, Standard Oil Production Company, Midland.
** From well SDU-883
*** From well SDU-580

Formation Evaluation Using Well Logs, Preston-37 Well

The suite of open-hole logs recorded in the Preston-37 well were used to compute two formation evaluation logs, VOLAN and GLOBAL. Data processing of the VOLAN log was done by Schlumberger in Midland. RCRL staff provided reservoir parameters and participated in the processing of the GLOBAL log at Schlumberger's facilities in Austin.

The VOLAN log is based on a volumetric analysis that uses a semirigid model of the predominant lithologies (for example, sandstone and shale; limestone and shale; limestone, dolomite, and shale). It provides assessments of porosity and saturations, volume of clay, and a profile of (matrix) permeability.

Data from the open-hole log suite were used to process the VOLAN log of the Preston-37 well. This log (figs. III-7 to III-9) indicates that (1) sandstone beds of the operational units, each bed ranging in thickness from approximately 5 ft (1.5 m) to about 9 ft (3 m), are separated vertically by shales and thin carbonates; and (2) the upper parts of the sandstone beds are cemented by carbonates. Although the VOLAN log indicates that both limestone and dolomite are present (figs. III-7 to III-9), only dolomite and ferroan dolomite or ankerite were observed in the petrographic thin sections examined. Another discrepancy between the VOLAN log and petrographic data is the percent of clay present in the thickest sandstone beds. Although the VOLAN log

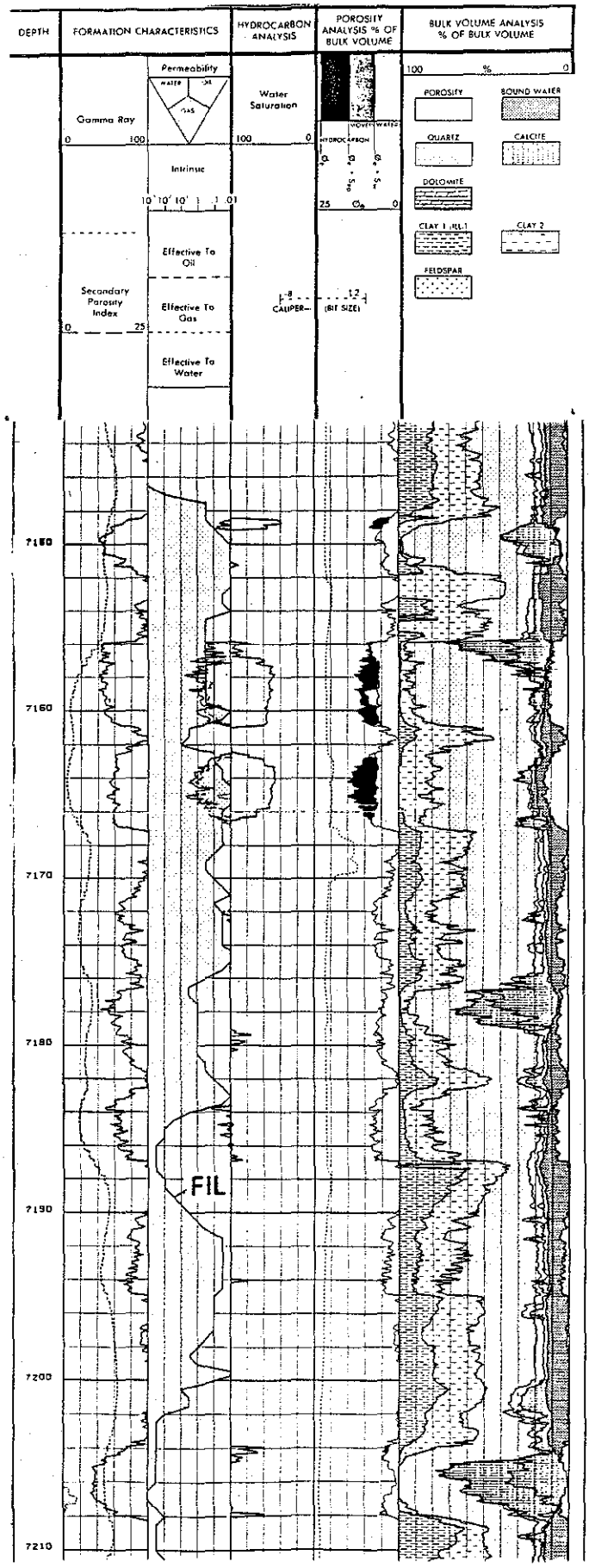

Figure III-7. VOLAN log, parts of operational units 1U and 2U, upper Spraberry, Preston-37 well. Tops (VOLAN depths): sandstone zone b = 7148 ft; sandstone zone c = 7156 ft; operational unit 2U = 7220 ft (see figure I-7 for stratigraphic subdivisions).

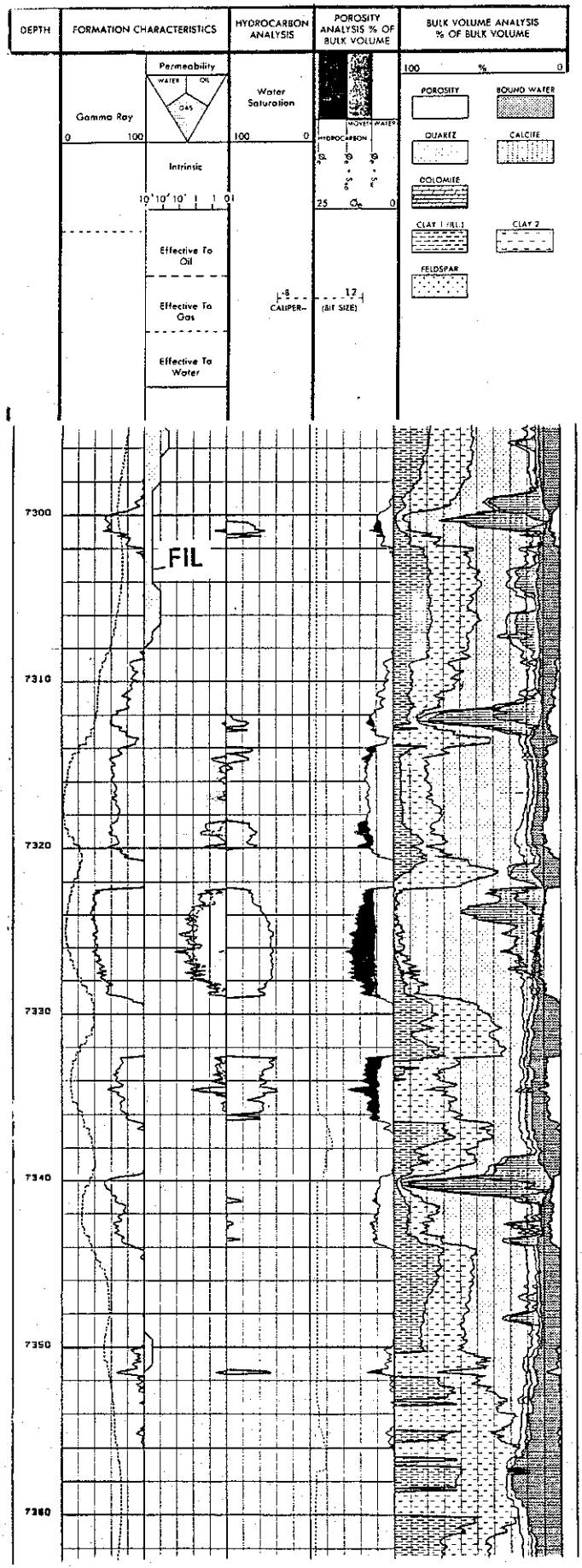

Figure III-8. VOLAN log, operational units 4U (base), 5U, and 6U (top), upper Spraberry, Preston-37 well. Tops (VOLAN depths): 5U = 7308 ft; 6U = 7361 ft (see figure I-7 for stratigraphic subdivisions).

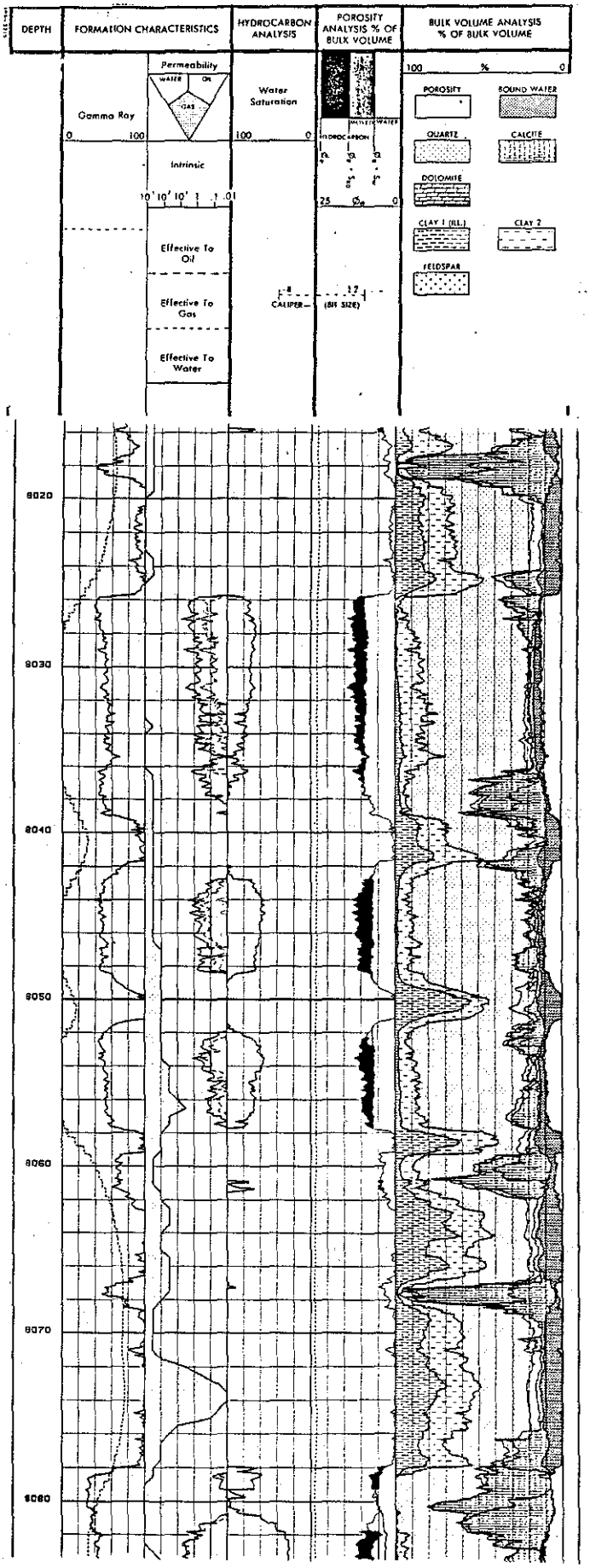

Figure III-9. VOLAN log, parts of operational units 1L and 2L, lower Spraberry, Preston-37 well. Tops (VOLAN depths): sandstone zone s = 8025 ft; 2L = 8078 ft (see figure I-7 for stratigraphic subdivisions).

locally shows the presence of more than 10 percent clay (locally more than 20 percent), petrographic data suggest less than 10 percent clay minerals present in the sandstones examined.

The VOLAN log of the Preston-37 well indicates that the best porosities in operational units 1U and 5U of the upper Spraberry and 1L and 2L of the lower Spraberry, ranging from approximately 6 to less than 15 percent, correspond to the sandstone zones (figs. III-7 to III-9). The Volan log also indicates the occurrence of hydrocarbons in the sandstone zones of the operational units and that water saturations in these oil-bearing intervals range from approximately 50 to about 70 percent. Porosities and saturations indicated by the VOLAN log are generally comparable to those determined from core analysis (table III-7).

Results obtained in the GLOBAL log (figs. III-10 and III-11) also are comparable to those of the VOLAN log. Petrographic data from cores were used to specify parameters for the GLOBAL interpretation of the Preston-37 well. The GLOBAL log uses a mathematical minimization of error to simultaneously solve the response equations of the various logging devices. Before they were interpreted, the edited logs from the Schlumberger computing center were environmentally corrected, including Kalman filtering of the NGT data. A resistivity program was run on the ILd, ILm, and SFLU curves of the DIL/SFL log to determine Rt, an approximate Rxo, and error bound on those computations. This processing is necessary to allow further interpretation with a minimization technique. The main interpretation program used is Schlumberger's Dual-Water Global, a minimization interpretation technique using dual-water theory. Total porosity, including the effect of bound water associated with clay minerals, is computed. Volume fractions of the various minerals (dolomite, orthoclase, illite) also are determined. The effective porosity is computed by subtracting the bound-water filled

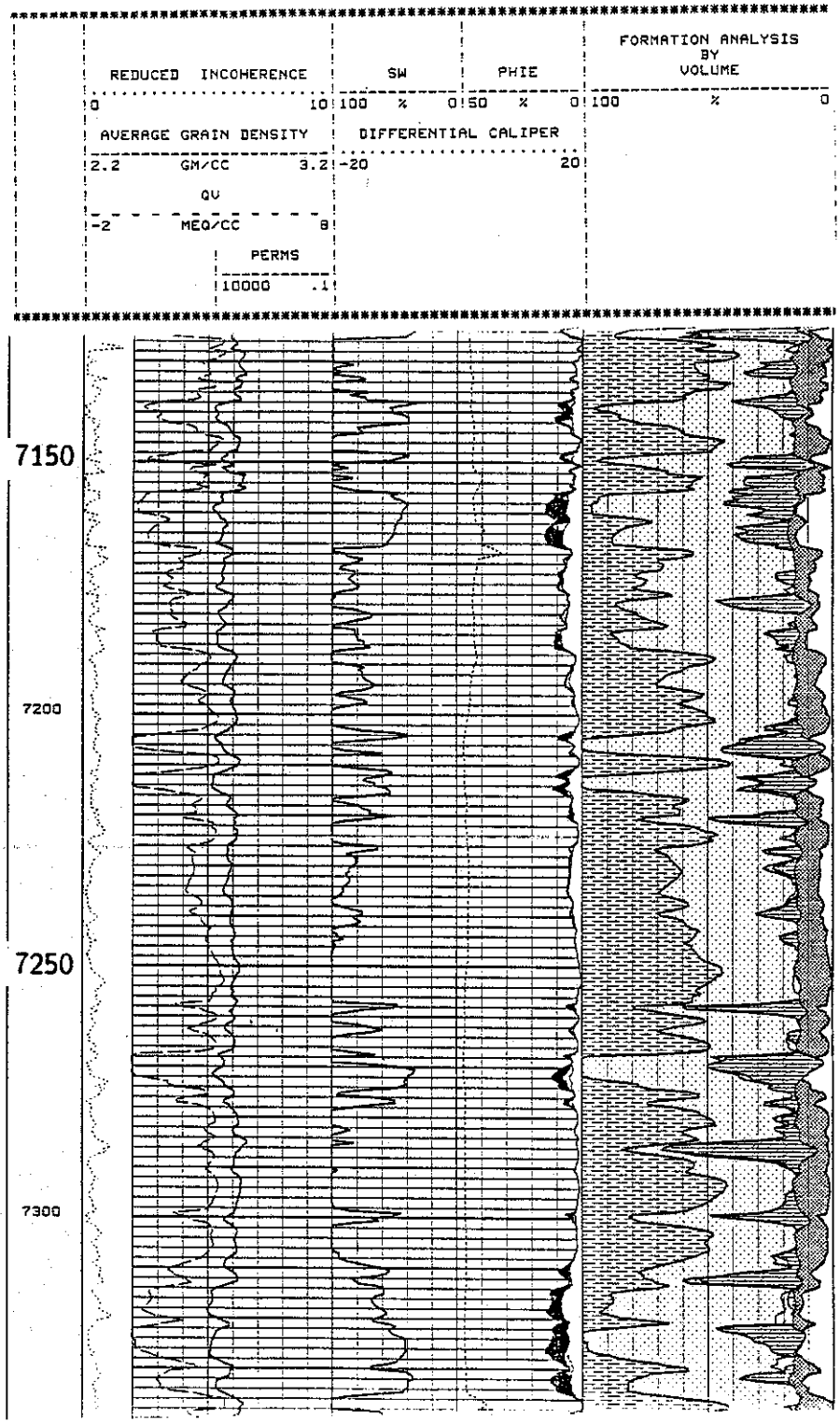

Figure III-10. GLOBAL log, part of the upper Spraberry, Preston-37 well. Tops (GLOBAL depths): operational unit 1U = 7137 ft; sandstone zone b = 7148 ft; sandstone zone c = 7156 ft; 2U = 7203 ft; 5U = 7309 ft (see figure I-7 for stratigraphic subdivisions).

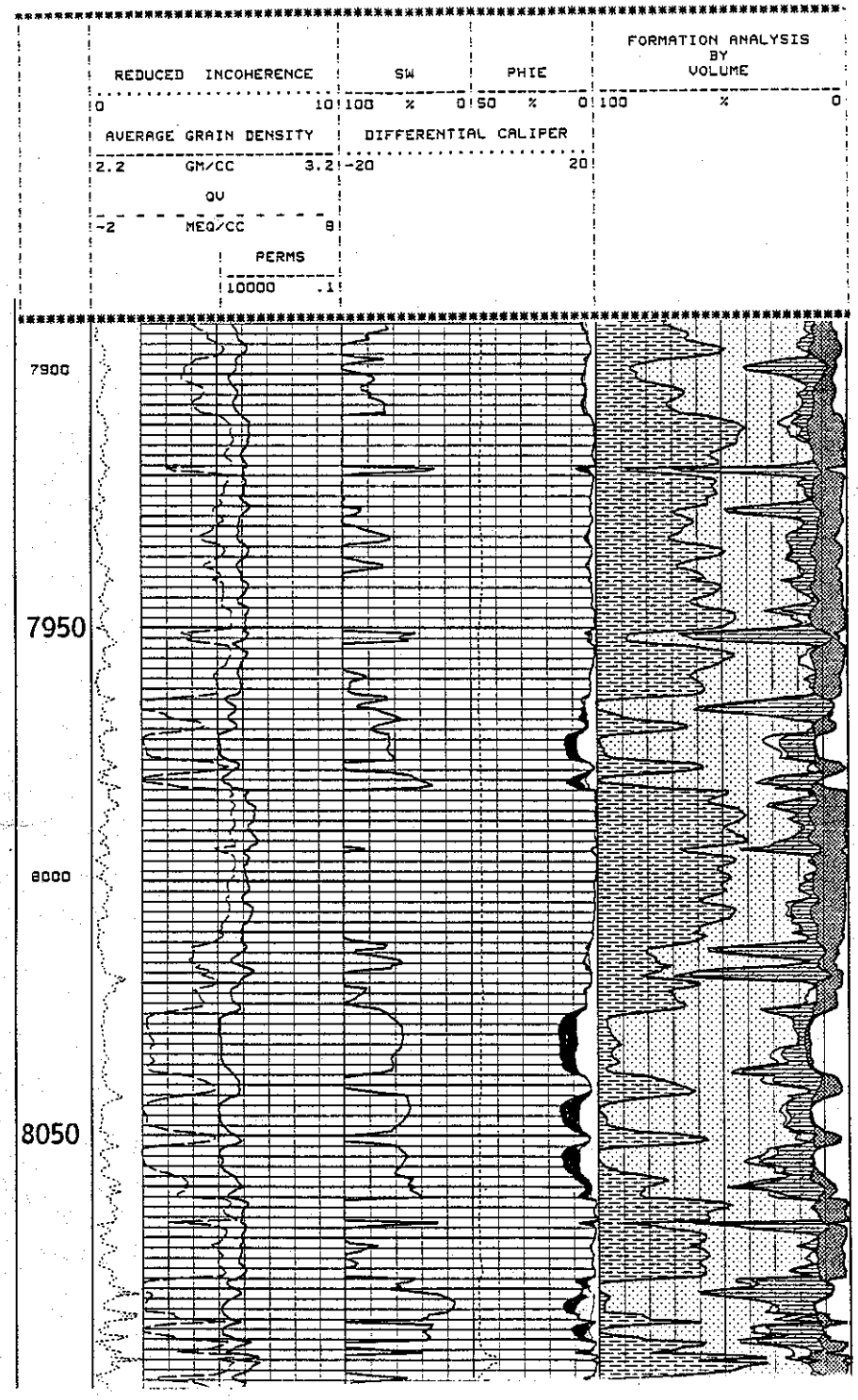

Figure III-11. GLOBAL log, base of the middle Spraberry and upper part of of the lower Spraberry, Preston-37 well. Tops (GLOBAL depths): operational unit 6M = 7963 ft; 1L = 8012 ft; sandstone zone s = 8025 ft; 2L = 8078 ft (see figure I-7 for stratigraphic subdivisions).

porosity from the total porosity, according to the bound-water saturation. This saturation, Swb, is related to the amount of water associated with a particular clay mineral. One basic model consisting of four components (table III-9) was used for the entire analyzed section of the Spraberry Formation, except for sections of bad hole, where a simplified model was used. The parameters used for the various minerals are shown in table III-10 (clay parameters are for dry clay). The Wyllie time-average equation is used with the sonic log for simplicity, and volumetric (not density dependent) equations are used for the GR, THOR, and POTA. Maximum feldspar volume is limited to 7 percent, based on core data, to improve program stability.

Table III-9. Lithologic components used in the GLOBAL model, Preston-37 well.

Component	Comments
Sandstone	A micaceous, pyritic, fine-grained quartz sandstone. Owing to the accessory minerals, this sandstone has interpretation parameters somewhat different from those of a pure quartz sand (it is heavier and more radioactive).
Dolomite	Ferroan dolomite or ankerite. The parameters used are intermediate between pure dolomite and pure ankerite to fit log responses in the dolomite streaks. The dolomite is significantly less radioactive than the sandstone but has a high U and RHOB.
Feldspar	Orthoclase parameters are used because no zones of sufficiently high feldspar concentration exist to determine the parameters from the logs. Orthoclase is characterized by high potassium content and therefore high net GR but otherwise looks similar to a very light sandstone on the logs.
Clay	Mainly illite and some montmorillonite (although no smectite was indicated by X-ray diffraction data, the actual parameters used in GLOBAL show a slightly higher apparent porosity than typical pure illite, thereby implying that some high-bound water mixed-layer clay is present).

Table III-10. Parameters used in the GLOBAL log, Preston-37 well.

Parameter	Unit	Value			
Rw	(ohmm)	0.0323 @ 8100 ft			
Rmf	(ohmm)	0.135 @ 8100 ft			
Cwb	(mh/m)	1.207 @ 8100 ft			
a		1.0			
m		2.0			
n		2.0			
Roh	(g/cc)	0.8 (hydrocarbon density)			
		Sandstone	Dolomite	Feldspar	Clay
RHOB	(g/cc)	2.69	2.86	2.52	2.90
NPHI	(percent)	--	--	3.00	17.50
DT	(μs/ft)	50.00	34.50	69.00	55.30
U	(barn/cc)	5.30	12.00	7.20	9.40
GR	(API units)	50.00	25.00	220.00	175.00
THOR	(ppm)	6.50	0.80	8.00	15.00
POTA	(percent)	0.80	0.20	10.50	4.125
TPL	(ns/m)	7.20	8.70	7.20	6.89
EATT	(db/m)	0.00	0.00	0.00	184.00
CEC	(meq/g)	0.00	0.00	0.00	0.322

Bad hole influences the GLOBAL log of the Preston-37 well at several depths. In some of these zones, the EPT curves (EATT, TPL) become unreliable and are disregarded. In other zones, the LDT curves (RHOB, U) are affected and are therefore severely downweighted. Because of the program construction the RHOB cannot be disregarded; therefore, in bad-hole zones the uncertainty attached to the RHOB is multiplied by 100. The Rt also is affected and downweighted owing to the typical spiky response of induction logs in sections with sharp hole variations. Because of loss of significant information in bad-hole sections, the model is simplified by disregarding feldspar whenever the LDT is unreliable. Even so, the model is marginally stable in zones of bad-hole conditions, and some additional tool weighting (reducing the GR uncertainty to drive the answer) and constraints (setting minimum clay volumes over certain unstable zones) are needed to achieve a reasonable answer.

The dolomite streaks typically have significant bed-boundary effects. The GLOBAL log of the Preston-37 well shows fictitious occurrences of hydrocarbons (purely because

of differing log vertical resolutions) above and below thin dolomite beds. Unfortunately, Schlumberger's environmental correction chain, which was used in this evaluation, no longer degrades the vertical resolution-matching through filtering. This would have helped eliminate such effects. Sandstone parameters were adjusted to achieve fairly clean sands having maximum clay levels of 10 percent in the thickest sandstone beds. Because effective porosity is quite sensitive to the clay content, setting the clay level tends to set the effective porosity. The computed volumes of feldspar are quite small and only rarely reach the 7 percent limit that was set on the basis of core data. It is important to note that computing small percentages of radioactive minerals, such as orthoclase, in the presence of other radioactive minerals, such as illite, is not a very reliable procedure. The log that influences this computation, the NGT, is significantly affected by statistical variations, even at typical reduced logging speeds. This implies that a single depth point value for feldspar content may not be significant. On the other hand, zone averages are more likely to be representative.

Use of the DLL/MSFL in the GLOBAL evaluation, in addition to or instead of the DIL log, will improve vertical resolution and would reduce Rt spikiness in bad-hole zones. The MSFL would provide a superior Rxo to the SFLU, which is too deep to be a true microresistivity tool. Also, DLL/MSFL data could be used as a fracture index. In the Preston-37 and Judkins A No. 5 wells, however, the Rxo/Rt ratio was quite high for the laterolog. This ratio should be lowered in other wells if the DLL is recorded using a saltier mud, down to ratios below 3 in the main sands (fig. III-1). The LDT log is quite valuable for identifying and quantifying dolomite content. The use of the NGT in the GLOBAL evaluation is not as clear, unless detailed core/interpretation comparisons show that the feldspar computation is consistent and useful. Use of the EPT log in the GLOBAL evaluation of the Preston-37 well was problematic. It tends to show more hydrocarbons than the resistivity tools do, owing

partly to the nonstandard nature of Spraberry sandstones. However, given that formation-water resistivities are not well known after a long history of waterflooding, a second independent computation of saturations would perhaps be useful.

Detection of Natural Fractures Using Well Logs

The NGT, LSS, and FMS logs were used to assess the occurrence of natural fractures in the Preston-37 well. Natural fractures have been regarded as the main factor controlling oil production from Spraberry reservoirs. The importance attributed to reservoir fractures is reflected in development practices in the Spraberry Trend, where well locations of most waterflood units were based on the orientation of the natural fractures.

There is no agreement on the occurrence of fractures among several fracture indicators that were determined using open-hole logs from the Preston-37 well. The VOLAN log, for example, includes two indices of reservoir fracturing. One is a secondary porosity index, shown in the first track from the left, which indicates that the well intersected natural fractures only in the vicinity of 7207 ft (fig. III-7). The other fracture indicator of the VOLAN log is based on the amplitudes of the compressional (P) and shear (S) waves from the LSS log. It is displayed in the second track from the left as a dotted area that extends further to the right at those depths where the probability of fracturing is greater. According to this index operational units 1U and 1L are fractured but 5U is not, and fracture probability is greater in operational unit 1L (figs. III-7 to III-9).

At the request of the RCRL project, the logging company produced a composite fracture identification log (CFIL) using data from the LSS log. In this technique, the amplitude of the Stoneley tube wave is compared with the amplitudes of the P and S

waves discriminating for shale effects. Although wave amplitude is somewhat affected by lithology, fracturing is suggested by low amplitudes of Stoneley and S waves and corresponding large amplitude of the P wave. The CFIL log indicates that the probability of fracturing is generally low to medium in the main oil reservoirs (figs. III-12 and III-13) and high to medium locally in the middle Spraberry (fig. III-14).

Fracture detection in the Preston-37 well using the NGT log was unsuccessful. The concept of gamma-ray spectroscopy as a fracture index is based on the propensity of natural fractures to develop some healing characteristics, often calcite cementation, that have an affinity for absorbing radioactive isotopes, usually uranium. This implies that the relative abundance of uranium compared with the relative change in all isotopes (thorium, uranium, potassium) would suggest fractures that are at least partly cemented. Because potassium is more than two orders of magnitude greater in abundance than thorium or uranium, it tends to obscure the changes in radiation levels. To help minimize this, uranium concentration (Iu) was compared with the sum of thorium and uranium concentrations (ppm):

$$Iu = Uppm \; / \; Tppm + Uppm$$

The relative concentration of uranium should be higher than the Iu average when an absorption anomaly occurs, such as calcite healing of fractures. However, the Iu index average will differ in the various lithologies; thus, a simple, overall average does not readily suffice. Consequently, a rather complex layering and averaging based on lithologies would be necessary to take this approach. Another approach is to compare this index of fracturing with some other fracture indicator, explained below, to see if they statistically agree. This method was chosen for this portion of the analysis.

The fracture index chosen to be contrasted with NGT data was the comparison of intergranular porosity from the sonic log to the total porosity given by the combination

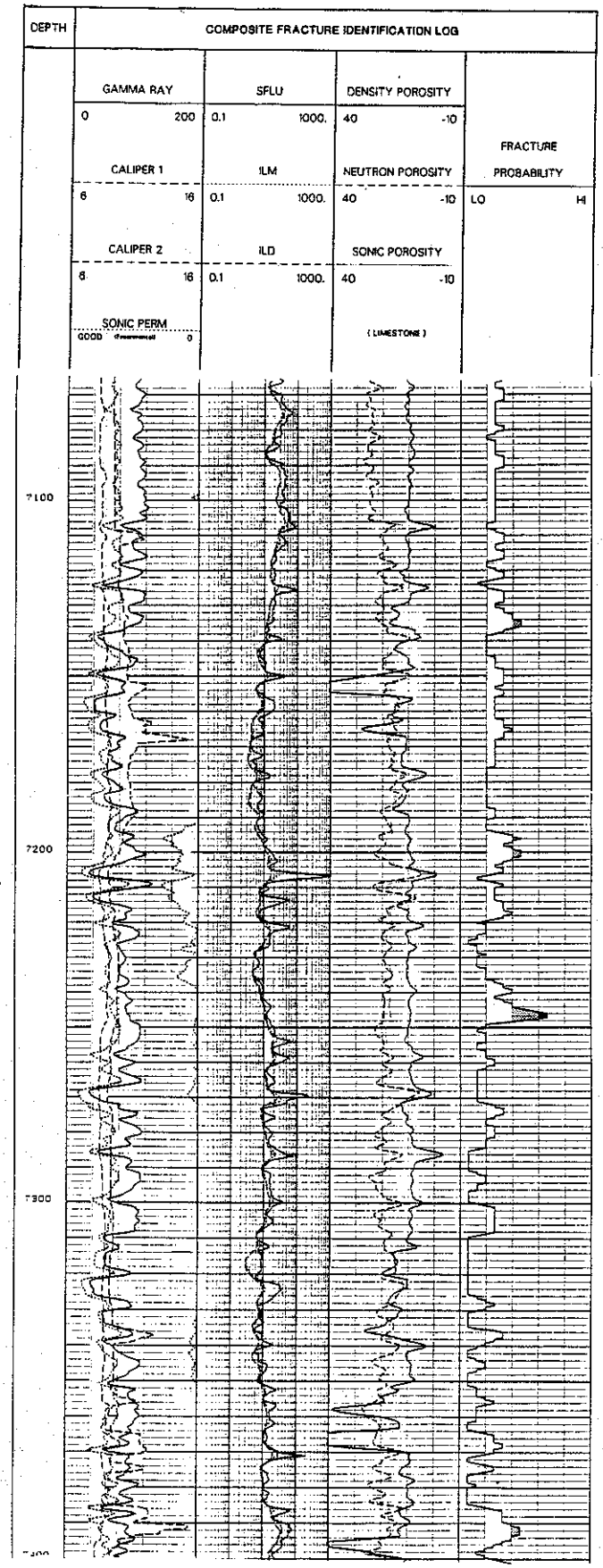

Figure III-12. Composite fracture identification log (CFIL) of the upper Spraberry, Preston-37 well. Tops (CFIL depths): operational unit 1U = 7137 ft; 2U = 7202 ft; 3U = 7224 ft; 4U = 7250 ft; 5U = 7308 ft; 6U = 7360 ft (see figure I-7 for details on stratigraphic subdivisions).

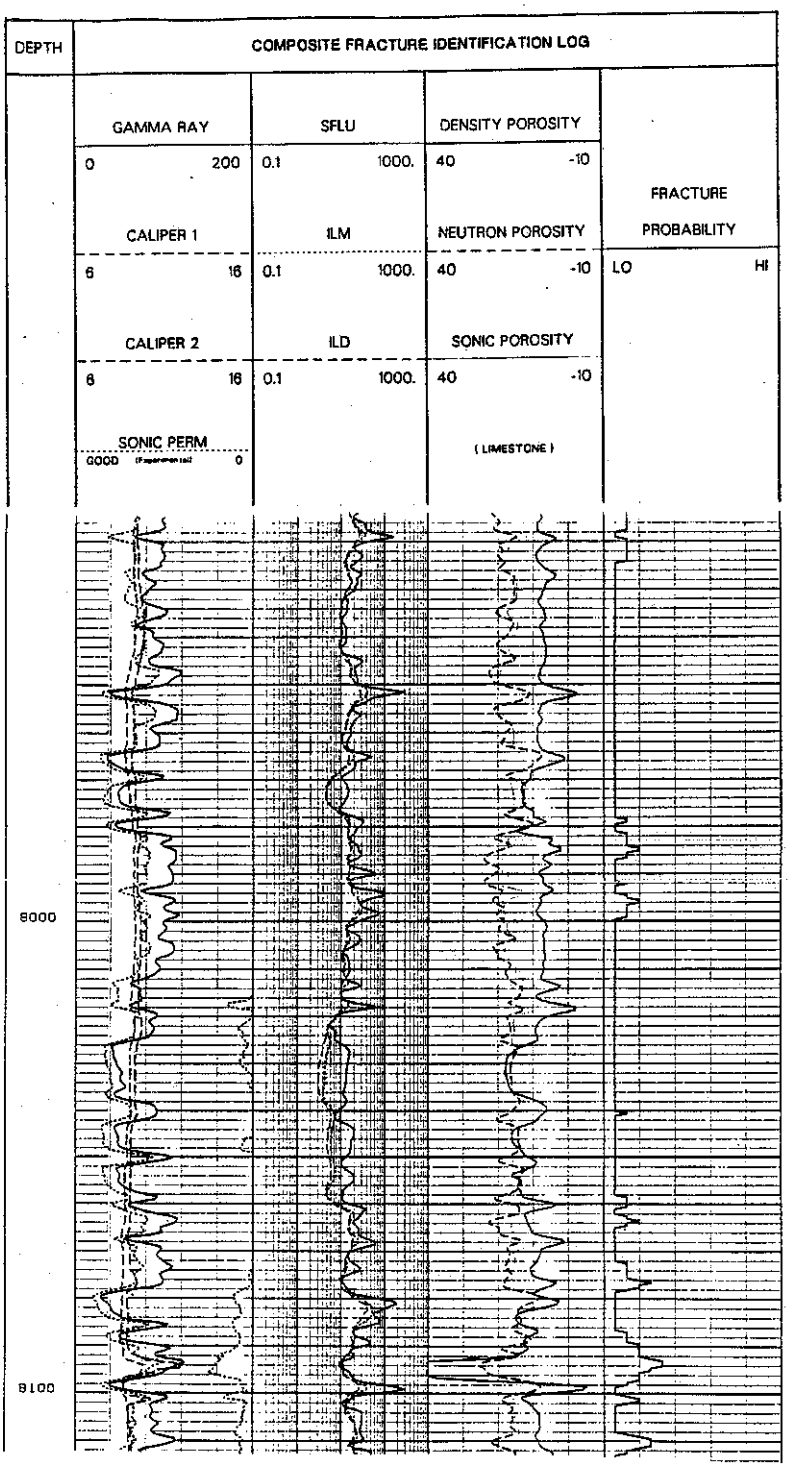

Figure III-13. Composite fracture identification log (CFIL) of the base of the middle Spraberry and the upper part of the lower Spraberry. Preston-37 well. Tops (CFIL depths): operational unit 5M = 7825 ft; 6M = 7863 ft; 1L = 8000 ft; sandstone zone s = 8024 ft; 2L = 8077 ft (see figure I-7 for stratigraphic subdivisions).

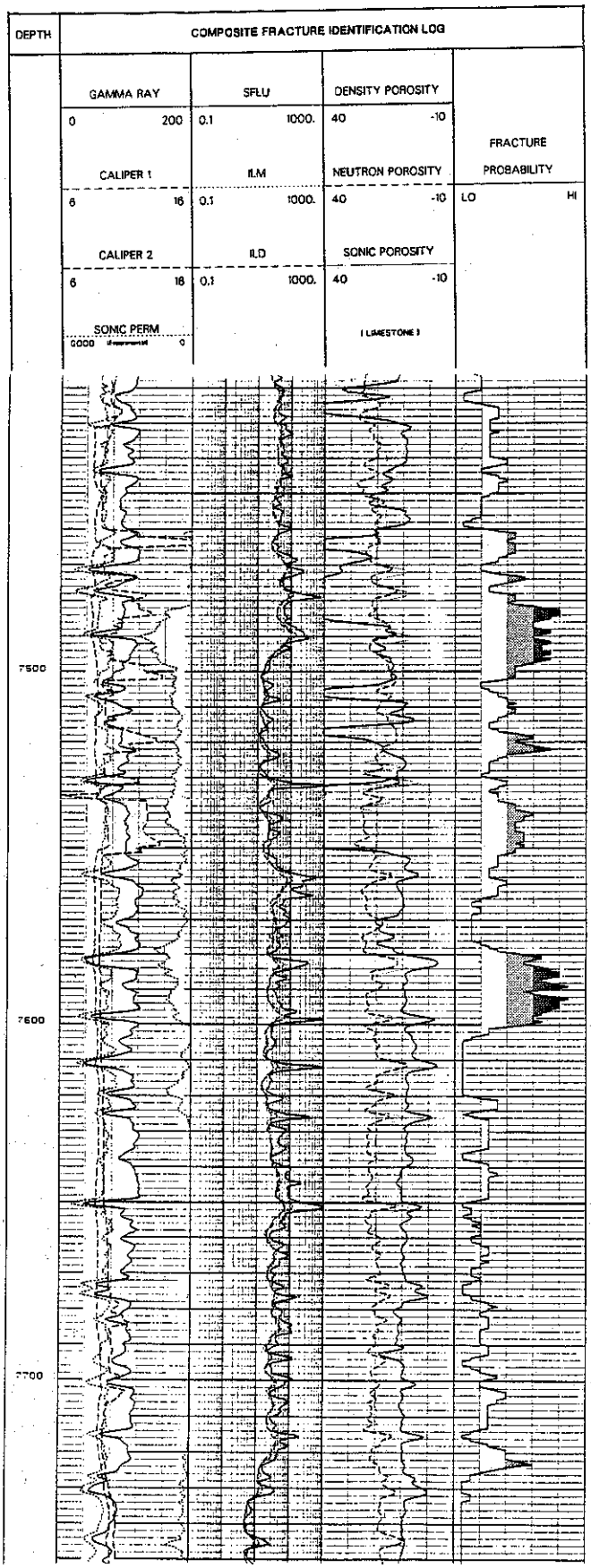

Figure III-14. Composite fracture identification log (CFIL) of part of the middle Spraberry, Preston-37 well. Tops (CFIL depths): operational unit 1M = 7497 ft; 2M = 7724 ft (see figure I-7 for stratigraphic subdivisions).

of neutron and density logs. This well-known "secondary porosity" method is quite reliable when a meaningful choice of matrix parameters is accomplished. To achieve this, the log data were carefully analyzed to identify the better reservoir rocks (least likely to contain major fractions of clay minerals). Optimum matrix velocities were then established to determine the sonic porosity. For this purpose, the density-neutron tools (LDT-CNL) were used through the U_{ma} - ρ_{ma} matrix identification (MID) technique (Schlumberger, 1987, p. 63-64). This method displayed a predominant quartz-dolomite trend (figs. III-15 and III-16). This permitted a simple transform of the indicated matrix density into the appropriate matrix travel-time based on the quartz-dolomite parameters, thus providing an effective way to normalize the two porosity methods. The results are shown in cross plots (figs. III-17 and III-18). The expected result, if the NGT were fracture-sensitive, would have been a strong correlation between the two indexes (Iu and secondary porostity), that is,

$$Iu \;|||\; (1 - \Phi_s / \Phi_t)$$

Instead, the Iu sensitivity is almost entirely independent of the sonic data. Thus no relation was found between NGT data and the occurrence of natural fractures in the Preston-37 well.

Of the logs recorded in the Preston-37 well, only the FMS logs permit the direct observation of fractures. FMS logs display resistivity anomalies that suggest the presence of fractures in the main oil reservoirs of the upper and lower Spraberry; successive passes of the FMS log (displaying orthogonal images along different strips of the borehole walls) (figs. III-19 to III-24) suggest that these resistivity anomalies (possible fractures) are oriented mainly in a NE-SW direction. Some of the anomalies are too long and centered on the FMS images or do not have well-defined, diffuse borders suggesting borehole break-outs, local bit or logging-tool tracks, or other features

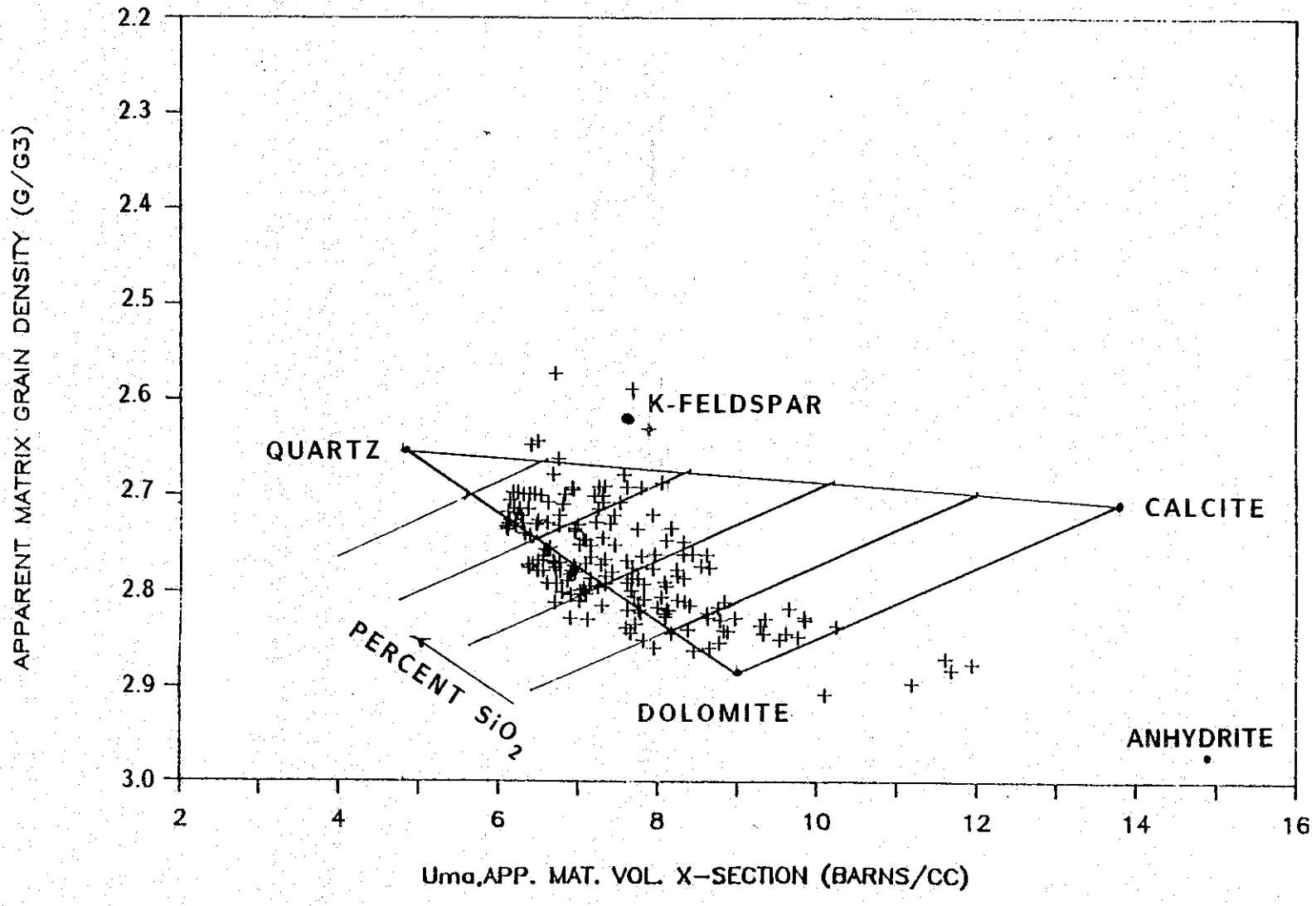

Figure III-15. Comparison of apparent matrix-density and apparent matrix-absorption characteristics, based on the use of the formation density, compensated neutron, and photoelectric absorption index logs. Upper Spraberry (7130 ft to 7370 ft). Preston-37 well.

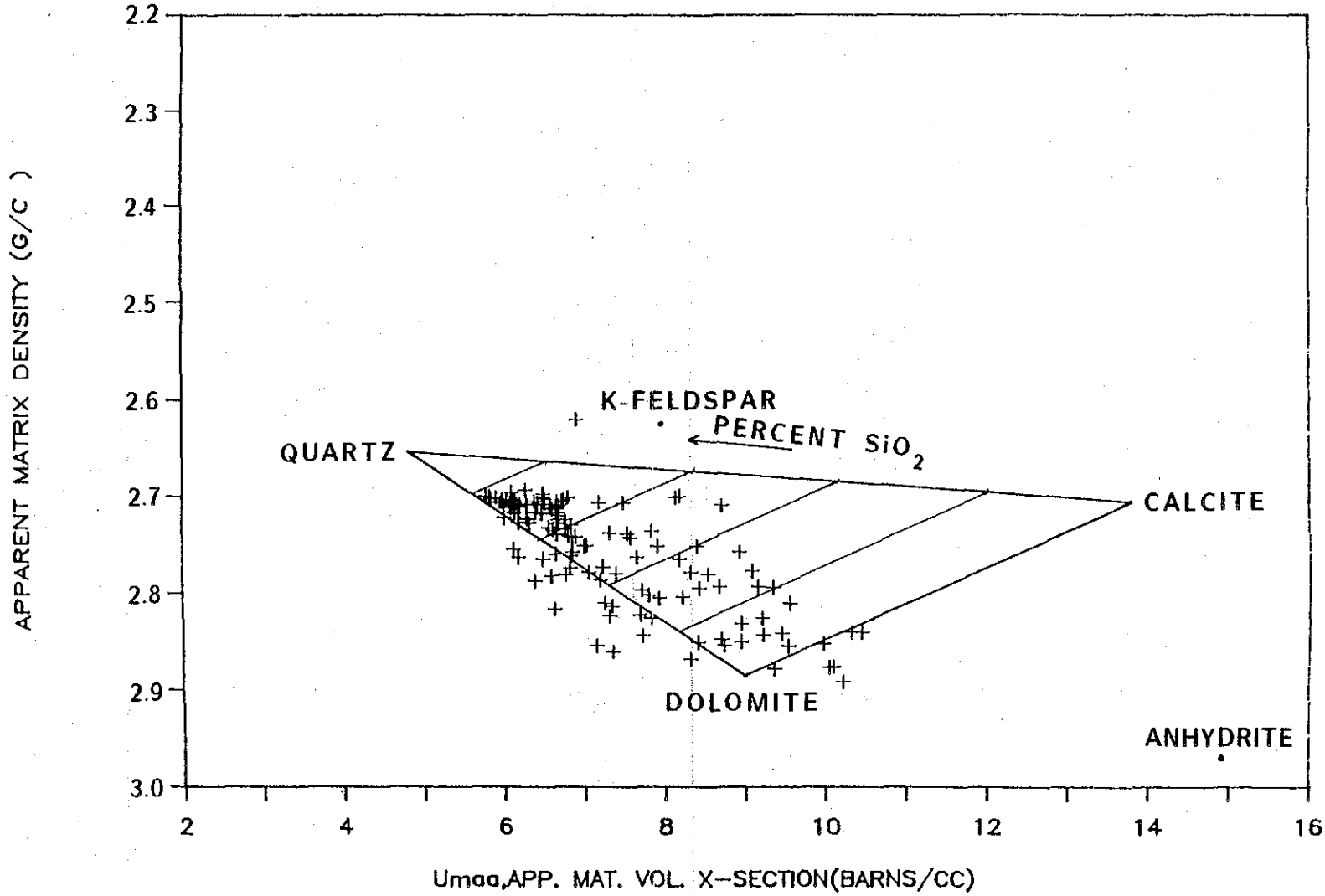

Figure III-16. Comparison of apparent matrix density and apparent matrix-absorption characteristics, based on the use of the formation density, compensated neutron, and photoelectric absorption index logs. Lower Spraberry (7960 ft to 8110 ft), Preston-37 well.

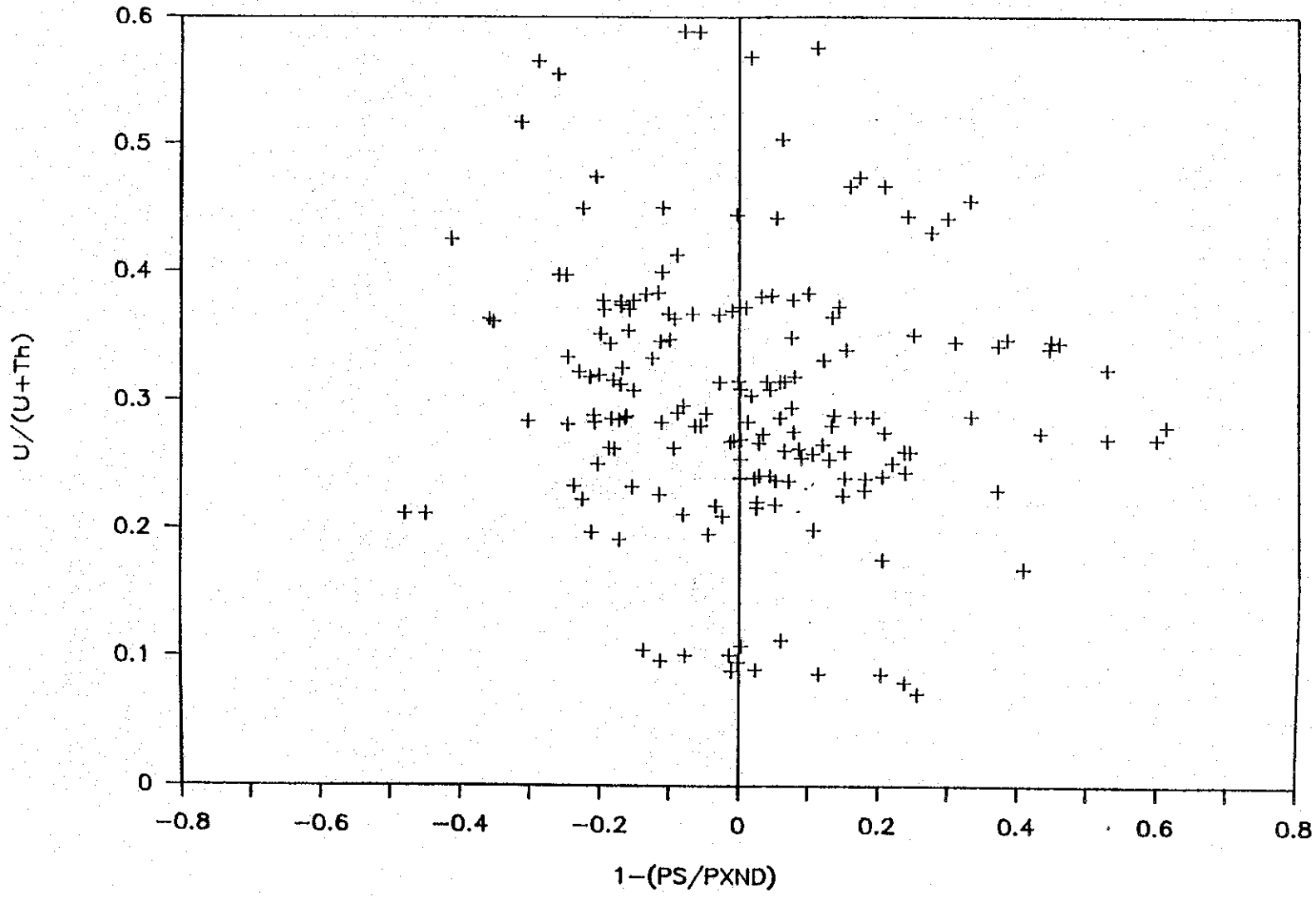

Figure III-17. Comparison of the fracture index Io (based on natural gamma-ray spectrometry data) to a secondary-porosity (fracture) index based on sonic porosity using a dual-mineral matrix-velocity determination. Upper Spraberry (7130 ft to 7370 ft), Preston-37 well.

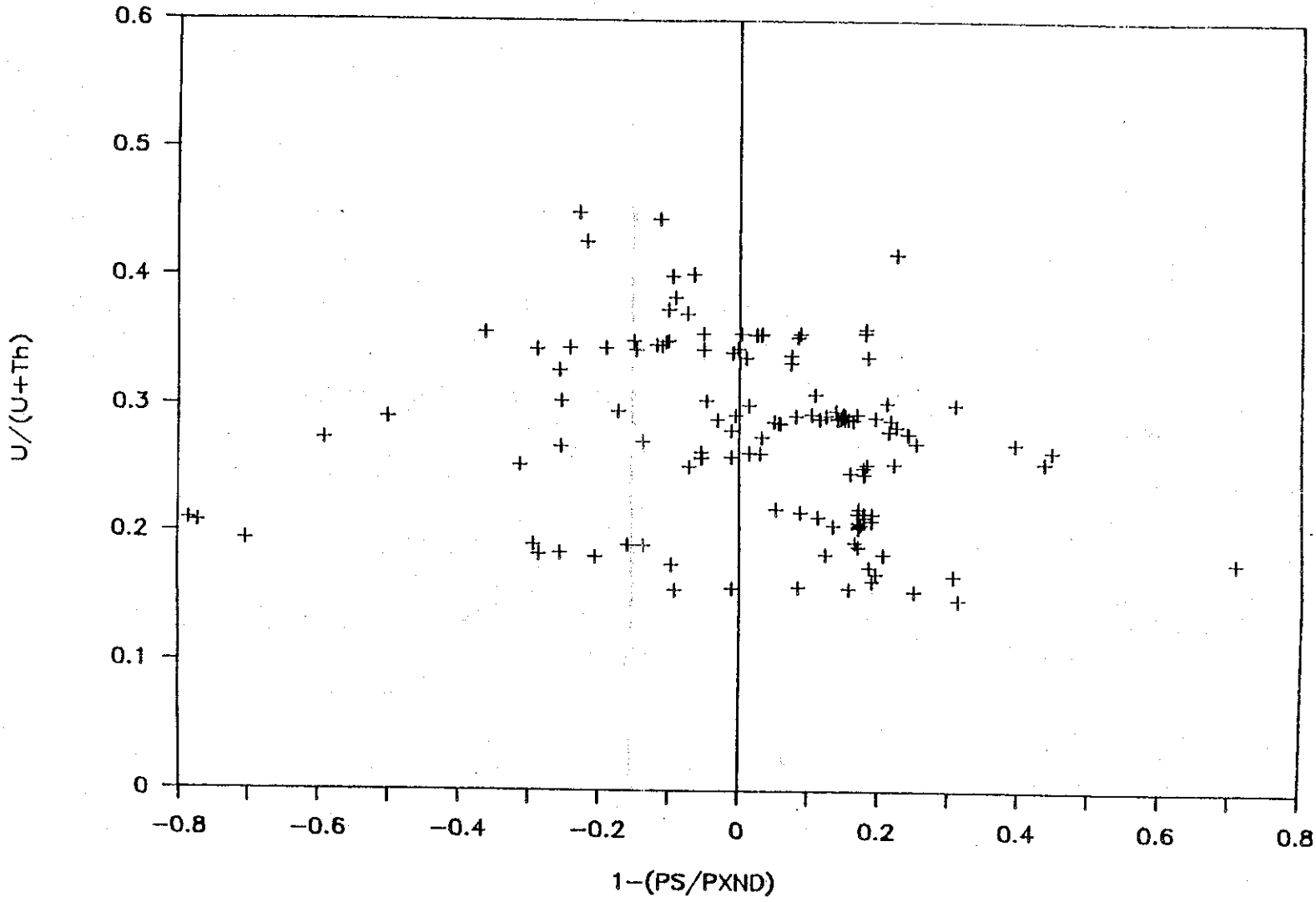

Figure III-18. Comparison of the fracture index Io (based on natural gamma-ray spectrometry data) to a secondary-porosity (fracture) index based on sonic porosity using a dual-mineral matrix-velocity determination. Lower Spraberry (7960 ft to 8110 ft), Preston-37 well.

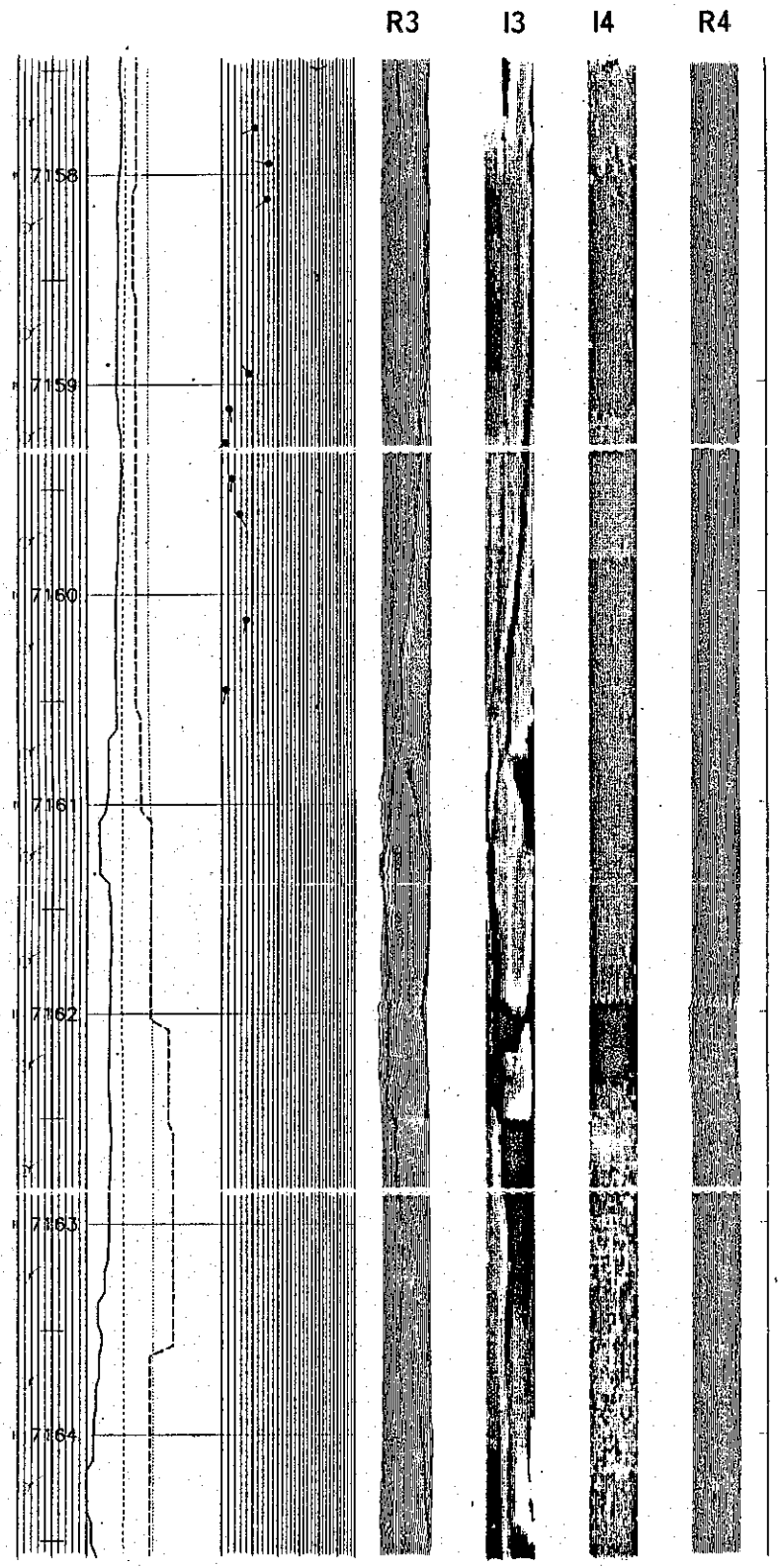

Figure III-19. FMS log (pass 1), sandstone zone c, unit 1U, upper Spraberry, Preston-37 well. Pad 3 data indicate fractures on SW borehole wall; no fractures are indicated by pad 4 data on the NW wall. (R = resistivity curves; I = processed images; 3 = pad 3 data; 4 = pad 4 data).

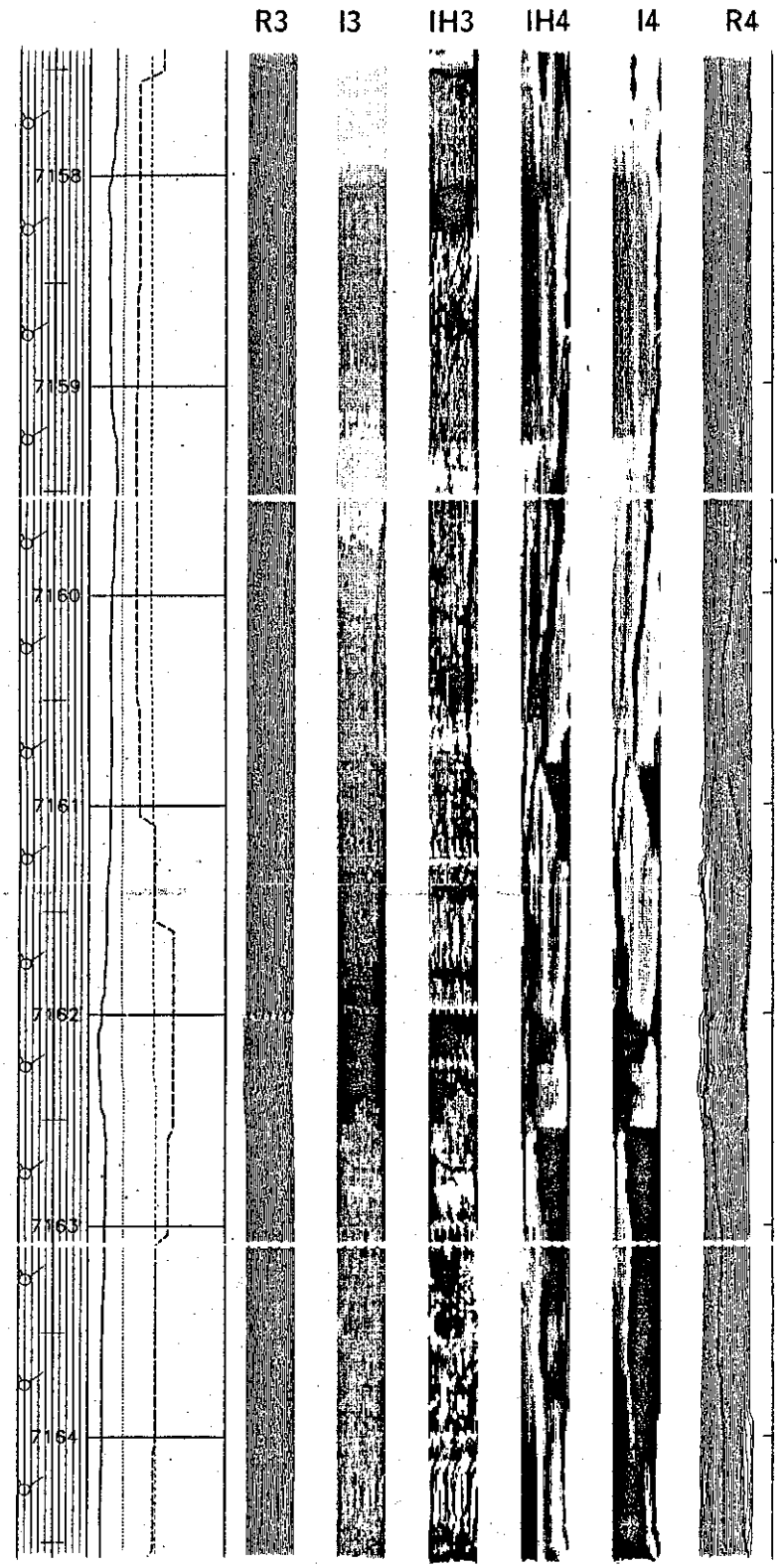

Figure III-20. FMS log (pass 2), sandstone zone c, unit 1U, upper Spraberry, Preston-37 well. Pad 4 data indicate fractures on SW borehole wall; pad 3 data suggest fractures on SE wall between 7159 ft and 7160 ft. (R = resistivity curves; I = processed images; IH = hilite reprocessed images; 3 = pad 3 data; 4 = pad 4 data).

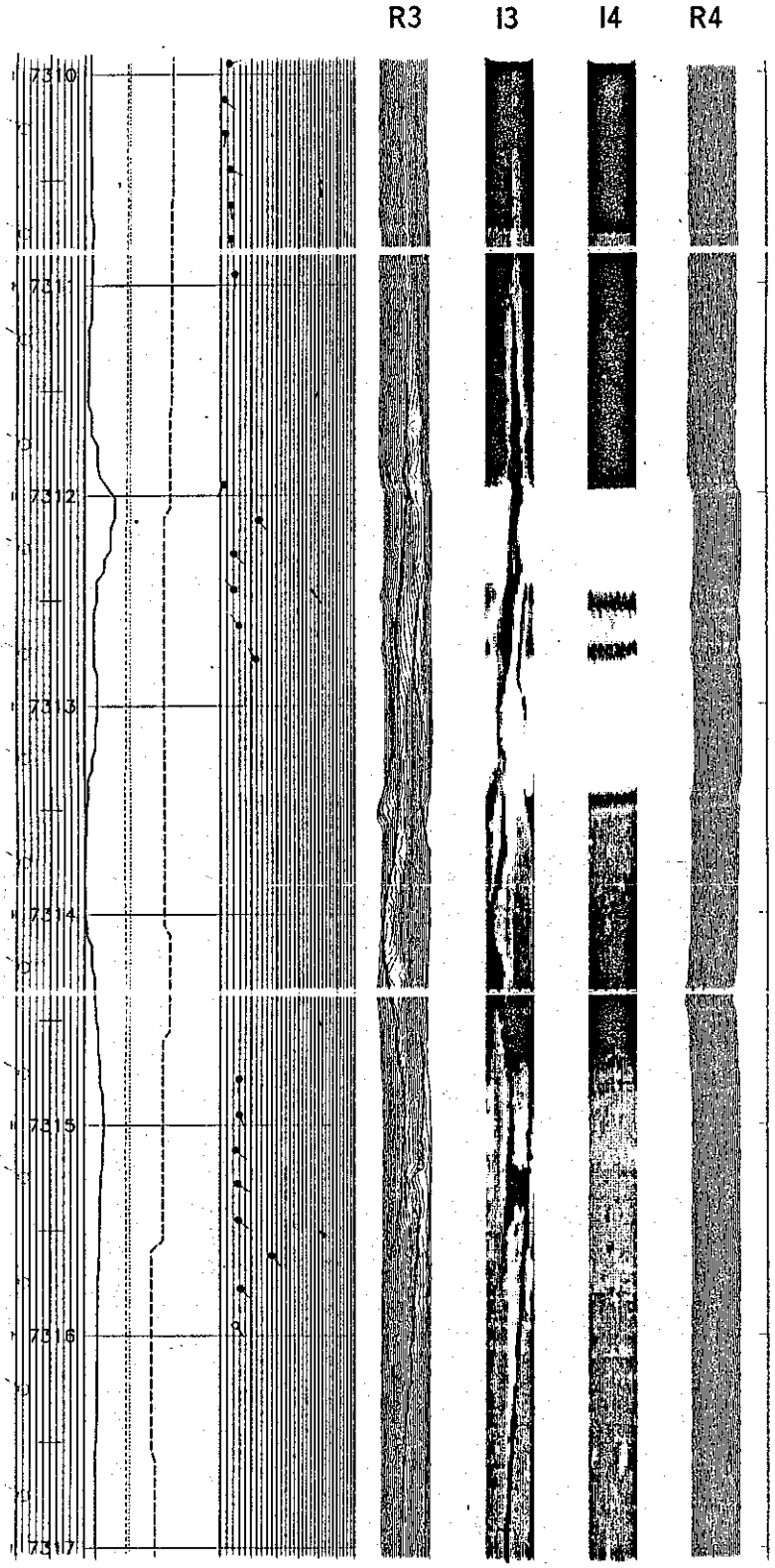

Figure III-21. FMS log (pass 1), upper part of sandstone zone f, unit 5U, upper Spraberry, Preston-37 well. Pad 3 data indicate fractures on SW borehole wall; no fractures are indicated by pad 4 data on the NW wall. (R = resistivity curves; I = processed images; 3 = pad 3 data; 4 = pad 4 data).

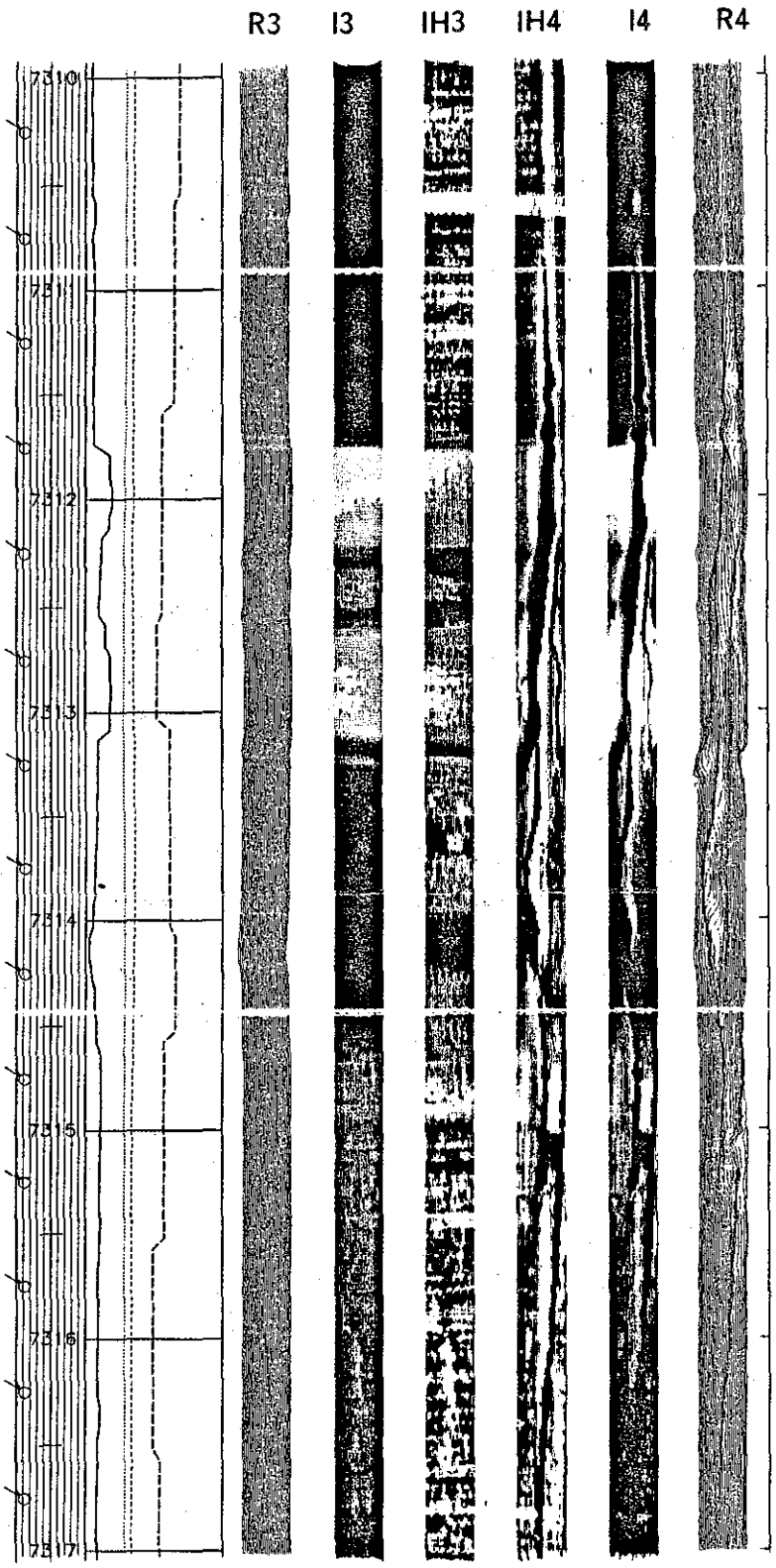

Figure III-22. FMS log (pass 2), sandstone zone f, unit 5U, upper Spraberry, Preston-37 well. Pad 4 data indicate fractures on SW borehole wall; no fractures are indicated by pad 3 data on the SE wall. (R = resistivity curves; I = processed images; IH = hilite reprocessed images; 3 = pad 3 data; 4 = pad 4 data).

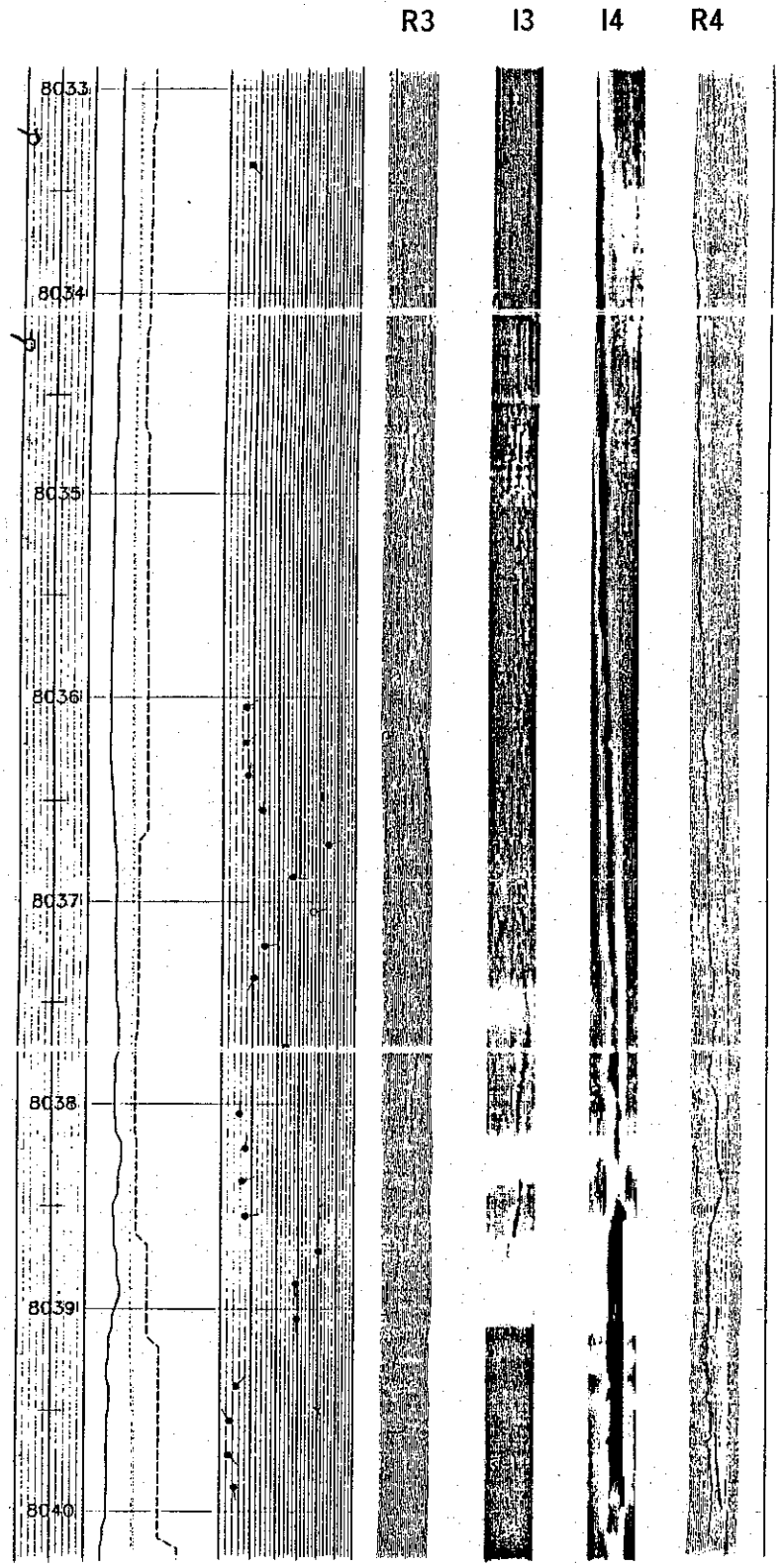

Figure III-23. FMS log (pass 1), sandstone zone s, unit 1L, lower Spraberry, Preston-37 well. Pad 4 data indicate fractures on NW borehole wall; pad 3 data indicate fractures between 8037 ft and 8039 ft on the SW wall. (R = resistivity curves; I = processed images; 3 = pad 3 data; 4 = pad 4 data).

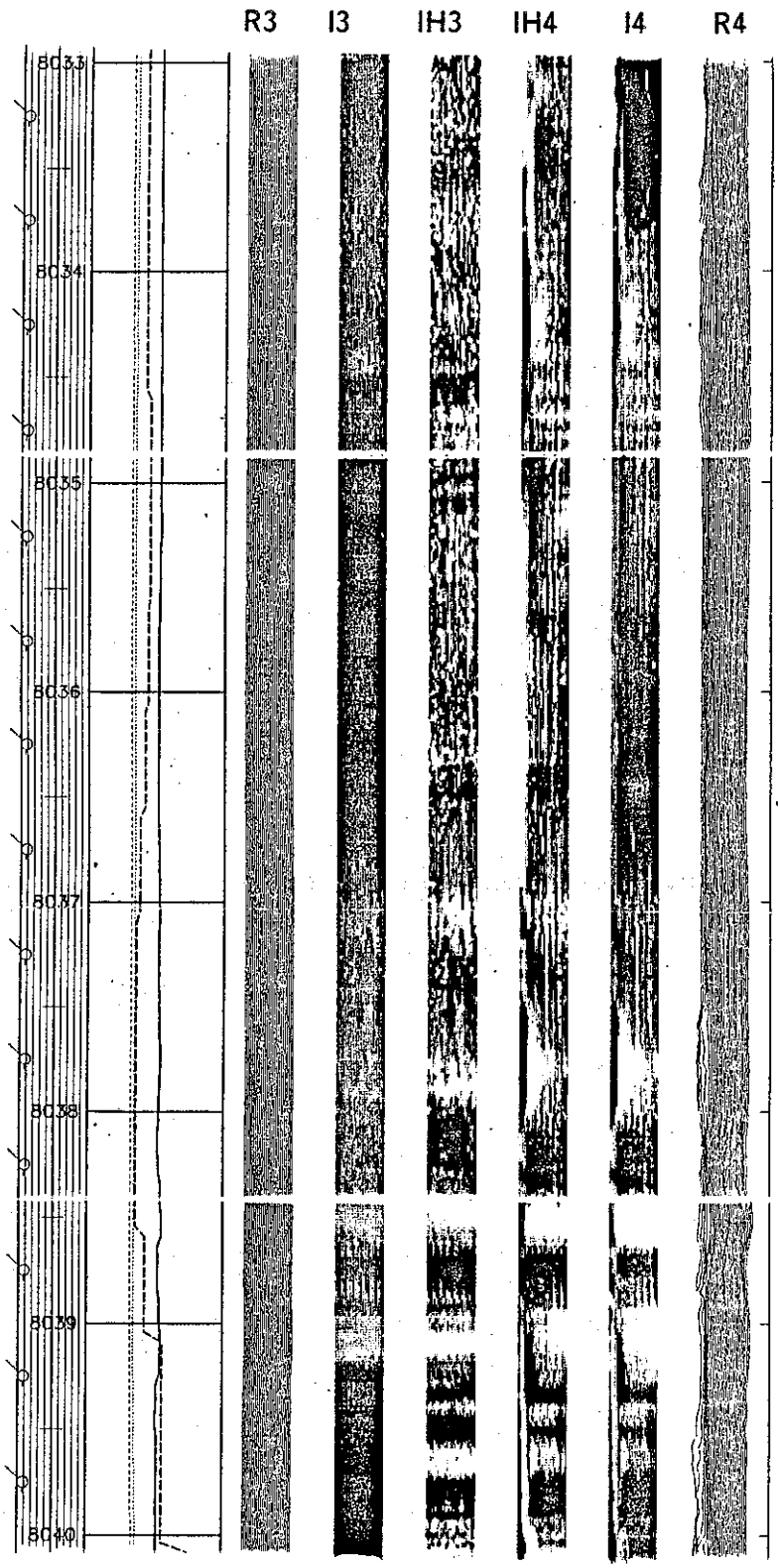

Figure III-24. FMS log (pass 2), sandstone zone s, unit 1L, lower Spraberry, Preston-37 well. Pad 4 data suggest fractures between 8033 ft and 8035 ft, and below 8037 ft, on ESE borehole wall; no fractures are indicated by pad 3 data on the NNE wall. (R = resistivity curves; I = processed images; IH = hilite reprocessed images; 3 = pad 3 data; 4 = pad 4 data).

that are not fractures. Therefore, the distinction between natural and drilling-induced fractures was not conclusive using FMS data from the Preston-37 well.

In addition to their interpretation as possible natural fractures, the FMS resistivity anomalies could represent drilling-induced fractures that do not extend deep into the formation and that are related to the local, current state of stress. A WNW-ESE principal horizontal stress would try to squeeze the borehole shut and would cause fractures, break-outs, and borehole elongation in the ENE-WSW direction (direction of minimum horizontal stress), as observed on FMS images and caliper data of the Preston-37 well. Similarly, the use of FMS data did not resolve the discrepancies existing among fracture indexes that were determined using other open-hole logs (figs. III-25 to III-29). Furthermore, caliper data indicate that oversized and elliptical boreholes interfere with the proper alignment of the FMS pads with respect to the borehole walls, and preclude adequate contact of the logging tool with the formation. Sensors in the two pads thus record data under different environmental conditions, generally resulting in poor quality images, especially in the direction of the long axis of the elliptical or oversized borehole.

Use of Log Suites in Formation Evaluation, Spraberry Reservoirs

Comparison of results of log and core analyses in the Preston-37 well indicates that the main petrophysical characteristics of Spraberry oil reservoirs can be adequately described using wireline logs. Such an evaluation requires analysis of data from natural gamma-ray, density, compensated neutron, and sonic logs to adequately describe the complex lithology and to determine realistic values of porosity. In addition to the

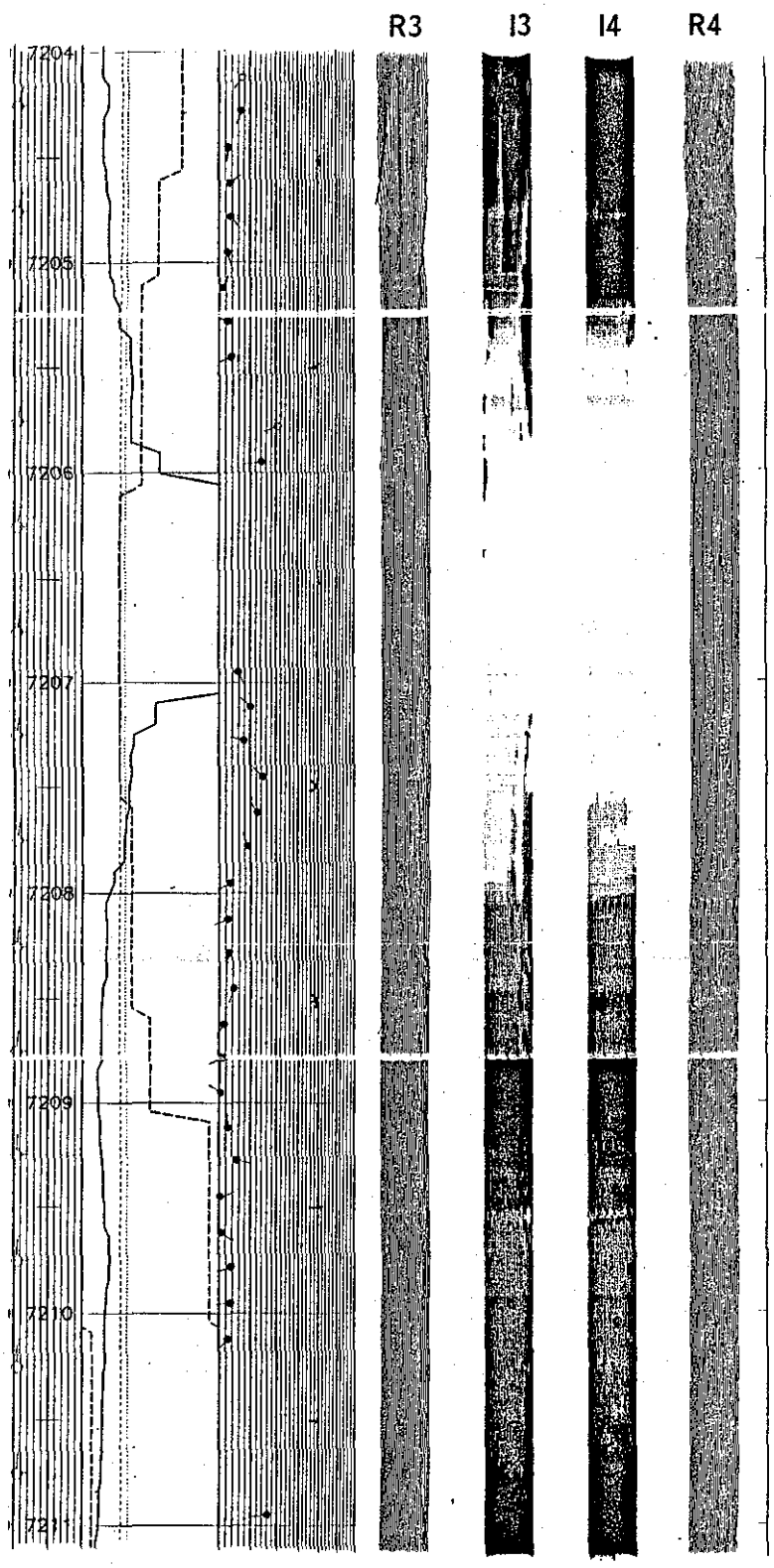

Figure III-25. FMS log (pass 1), unit 1U (lower part), upper Spraberry, Preston-37 well. Pad 3 data suggest fractures between 7204.5 ft and 7208.5 ft on W borehole wall; no fractures are indicated by pad 4 data on the N wall. The secondary porosity index of the VOLAN log indicates the only fractured interval in the vicinity of 7207 ft (fig. III-7). Note resistive bed (blank interval) between 7205.5 ft and 7208 ft (carbonate layer or carbonate-cemented sandstone). (R = resistivity curves; I = processed images; 3 = pad 3 data; 4 = pad 4 data).

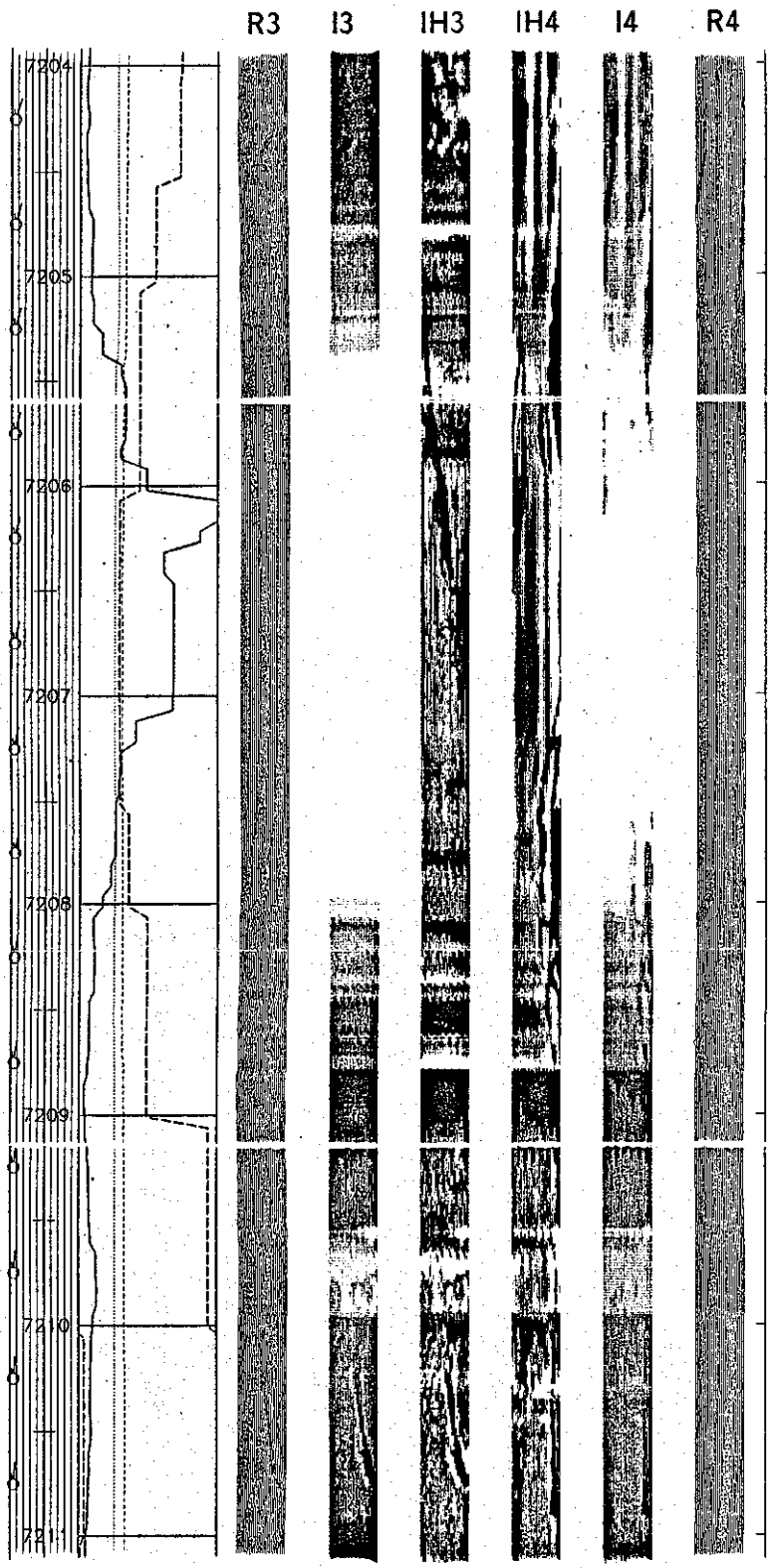

Figure III-26. FMS log (pass 2), unit 1U (lower part), upper Spraberry, Preston-37 well. Pad 4 data suggests fractures on ESE borehole wall; pad 3 data indicate fractures only at 7210 ft-7211 ft on WSW wall. The secondary porosity index of the VOLAN log indicates the only fractured interval in the vicinity of 7207 ft (fig. III-7). Note resistive bed (blank interval) between 7205.5 ft and 7208 ft (carbonate layer or carbonate-cemented sandstone). (R = resistivity curves; I = processed images; IH = hilite reprocessed images; 3 = pad 3 data; 4 = pad 4 data).

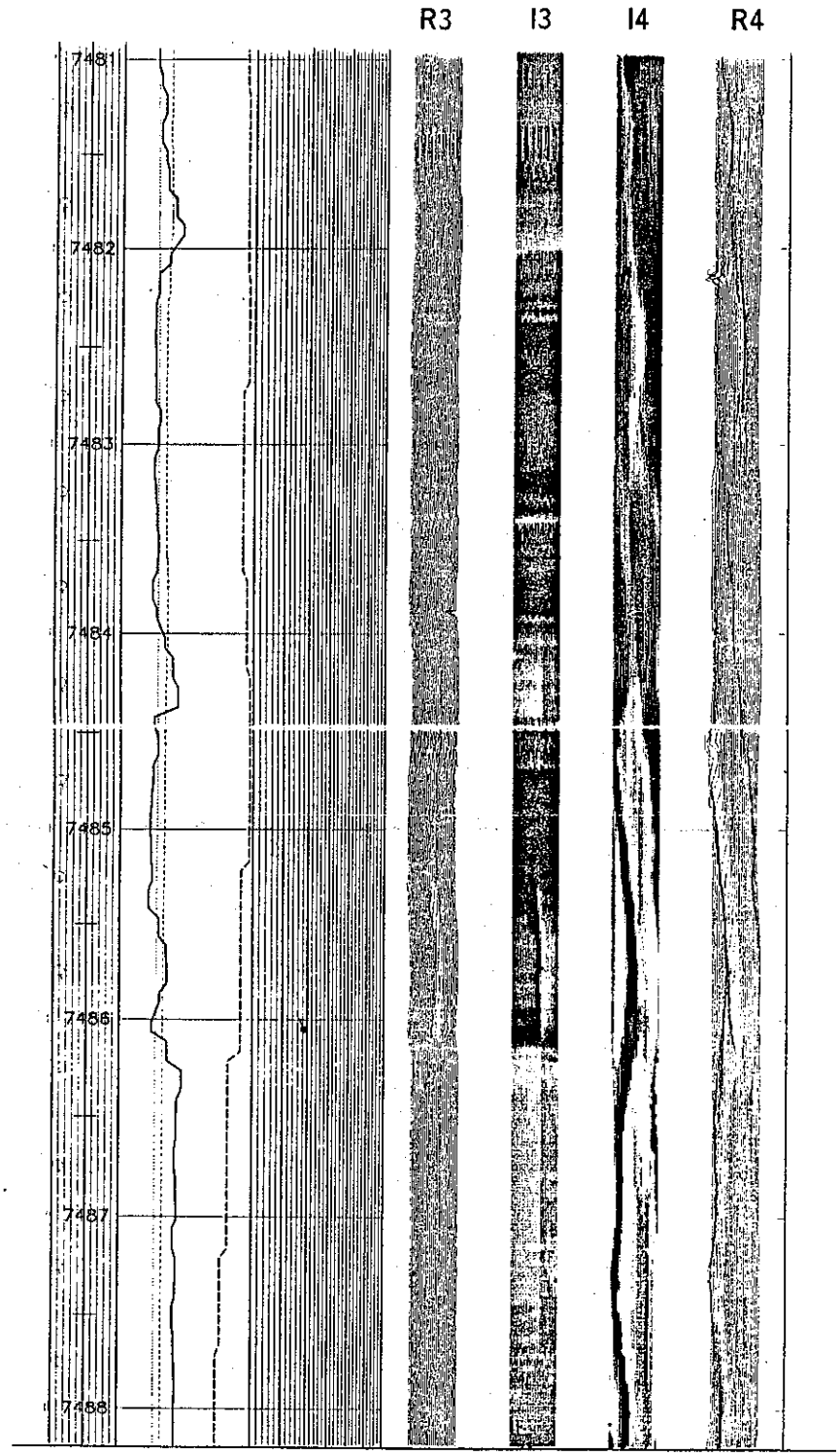

Figure III-27. FMS log (pass 1), middle Spraberry (part), Preston-37 well. Pad 4 data indicate fractures on ENE borehole wall; pad 3 data suggest fractures only between 7484 ft and 7486 ft on the WNW wall. The CFIL log indicates the highest probability of fracture occurrence between 7482 ft and 7498 ft (fig. III-14). (R = resistivity curves; I = processed images; 3 = pad 3 data; 4 = pad 4 data).

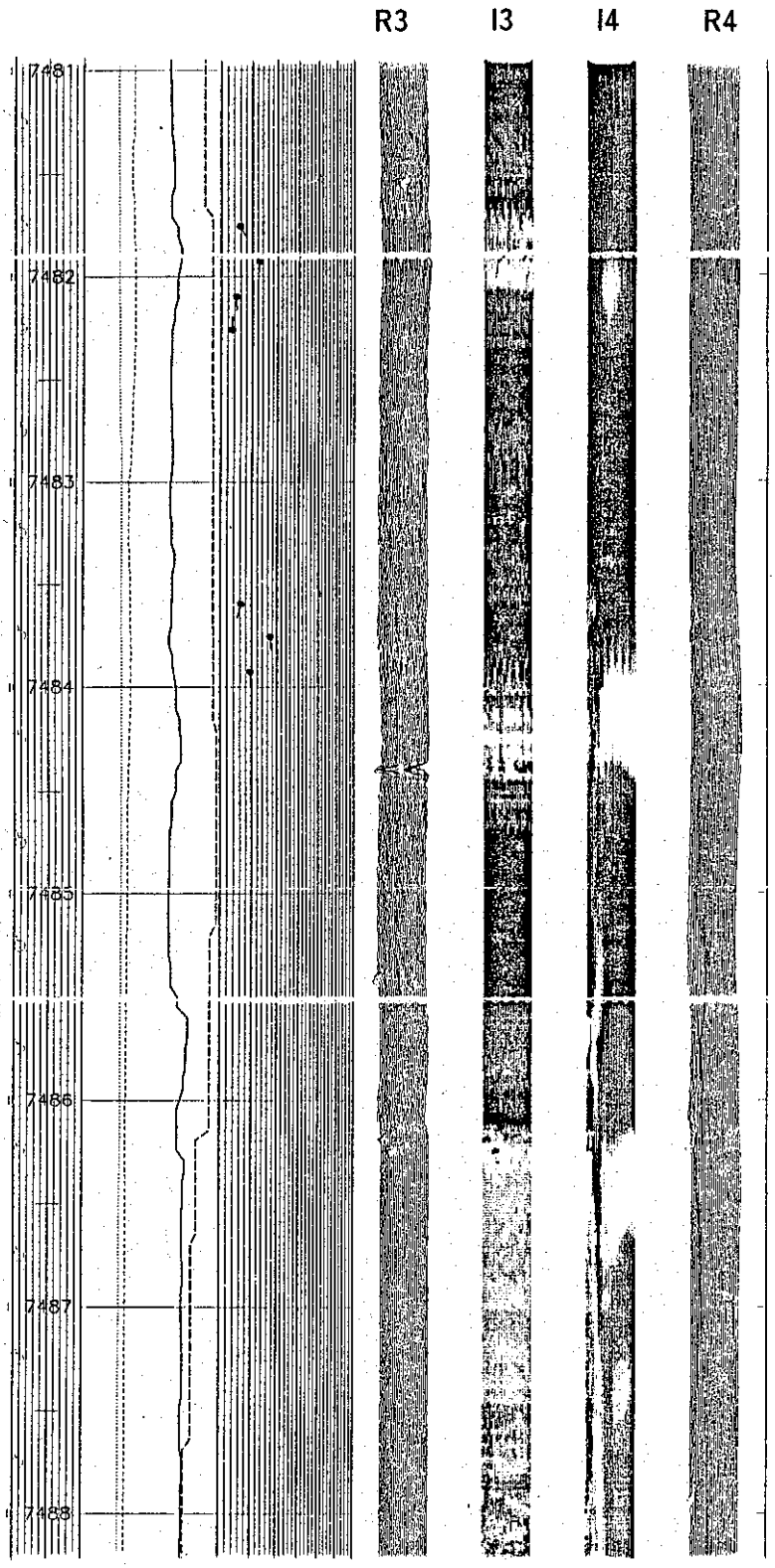

Figure III-28. FMS log (pass 2), middle Spraberry (part), Preston-37 well. Pad 4 data indicate fractures below 7485 ft on WSW borehole wall; no fractures are indicated by pad 3 data on the SSE wall. The CFIL log indicates the highest probability of fracture occurrence between 7482 ft and 7498 ft (fig. III-14). (R = resistivity curves; I = processed images; 3 = pad 3 data; 4 = pad 4 data).

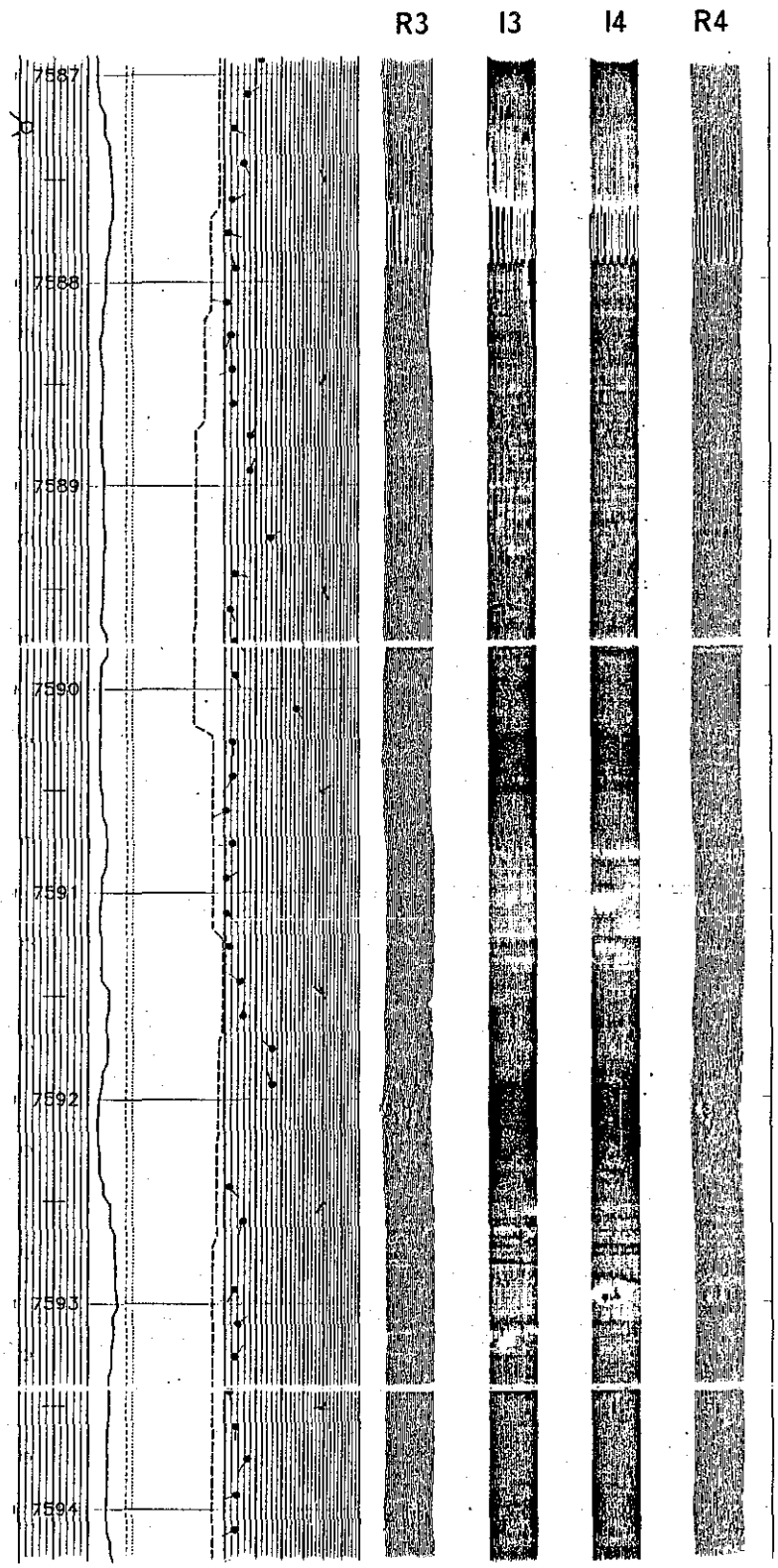

Figure III-29. FMS log (pass 2; no pass 1 images available), middle Spraberry (part). Preston-37 well. Pad 3 data suggest fractures only between 7588 ft and 7589 ft on NE borehole wall; no fractures are indicated by pad 4 data on the SE wall. The CFIL log indicates the highest probability of fracture occurrence between 7580 ft and 7600 ft (fig. III-14). Note concretion at 7593 ft and probably at 7591.5 ft. (R = resistivity curves; I = processed images; IH = hilite reprocessed images; 3 = pad 3 data; 4 = pad 4 data).

porosity logs, tools that record the deep resistivity (to determine Rt) are needed to assess fluid saturations.

Appropriate borehole conditions were critical with respect to the quality of the log data acquired in the Preston-37 well. Because oversized borehole sections adversely affected critical measurements of special logs using sensors in contact with the formation (for example, EPT and FMS logs), these contact logs should be recorded only if the borehole conditions are adequate. Similarly, FMS data should be used cautiously owing to the ambiguity of these images for the identification of natural fractures in Spraberry reservoirs. Other methods of fracture identification also should be evaluated. One alternate method is the borehole televiewer, which provides continuous images of the borehole walls using sonic data and which has also been used in stress analysis.

Reservoir Pressures

Previous studies of Spraberry reservoirs (Guevara and Tyler, 1986; Guevara, in press; Tyler and Gholston, in press) and mapping of sandstone and porosity distributions conducted by the RCRL project in an ununitized area of the Spraberry Trend (see Section II, this report), suggest that oil accumulations in Spraberry reservoirs are laterally discontinuous and stratified or multilayered. Because pressure data are essential to test the hypothesis of reservoir compartmentalization, measurements of reservoir pressures were programmed in the Preston-37 and Judkins A No. 5 wells and in operational units 1U and 5U of the upper Spraberry and 1L of the lower Spraberry. Separate, partly drained or untapped oil accumulations would be suggested by (1) formation pressures that are substantially higher than those expected

in almost depleted reservoirs and (2) different formation pressures in separate genetic reservoir intervals.

Determinations of formation pressures were attempted at 13 depth locations in the Preston-37 well (fig. III-30, table III-11) and at 14 locations in the Judkins A No. 5 well (table III-12), all using Schlumberger's Repeat Formation Tester (RFT). These tests provide information on the pressure of an individual matrix block in naturally fractured reservoirs (Stewart and others, 1981), such as the reservoirs of the study area. Retrieval of samples of reservoir fluids was not attempted in the Preston-37 well; fluid sampling was planned but failed in the Judkins A No. 5 well. Only two pressure tests were successful, both in lower Spraberry sandstones of the Preston-37 well (figs. III-31 and III-32). Several tests were unsuccessful (seal failures, tables III-11 and III-12) because the corresponding intervals could not be isolated (mainly as a result of an oversized borehole, as suggested by caliper data), and only the hydrostatic pressure of the drilling mud column could be measured. Other attempts failed (dry tests, tables III-11 and III-12) because, probably owing to an extremely tight rock, no significant amounts of formation fluids entered the sampling chambers of the tool during the test, and therefore no measurable pressure buildup took place.

The last read measurements (2532 psig and 2580 psig) in the two apparently successful RFT tests (fig. III-30, table III-11) represent reservoir pressures if the buildup pressures had reached equilibrium. However, there are two main possible explanations for the magnitudes of the pressures determined in these tests. One is that the intervals tested were not perfectly isolated, and drilling mud was leaking around the tool seal; therefore the pressure was increasing until eventually it would have reached the value of hydrostatic pressure had the test been long enough. The other explanation, which we consider the most likely, is that the final test readings indeed closely approach true

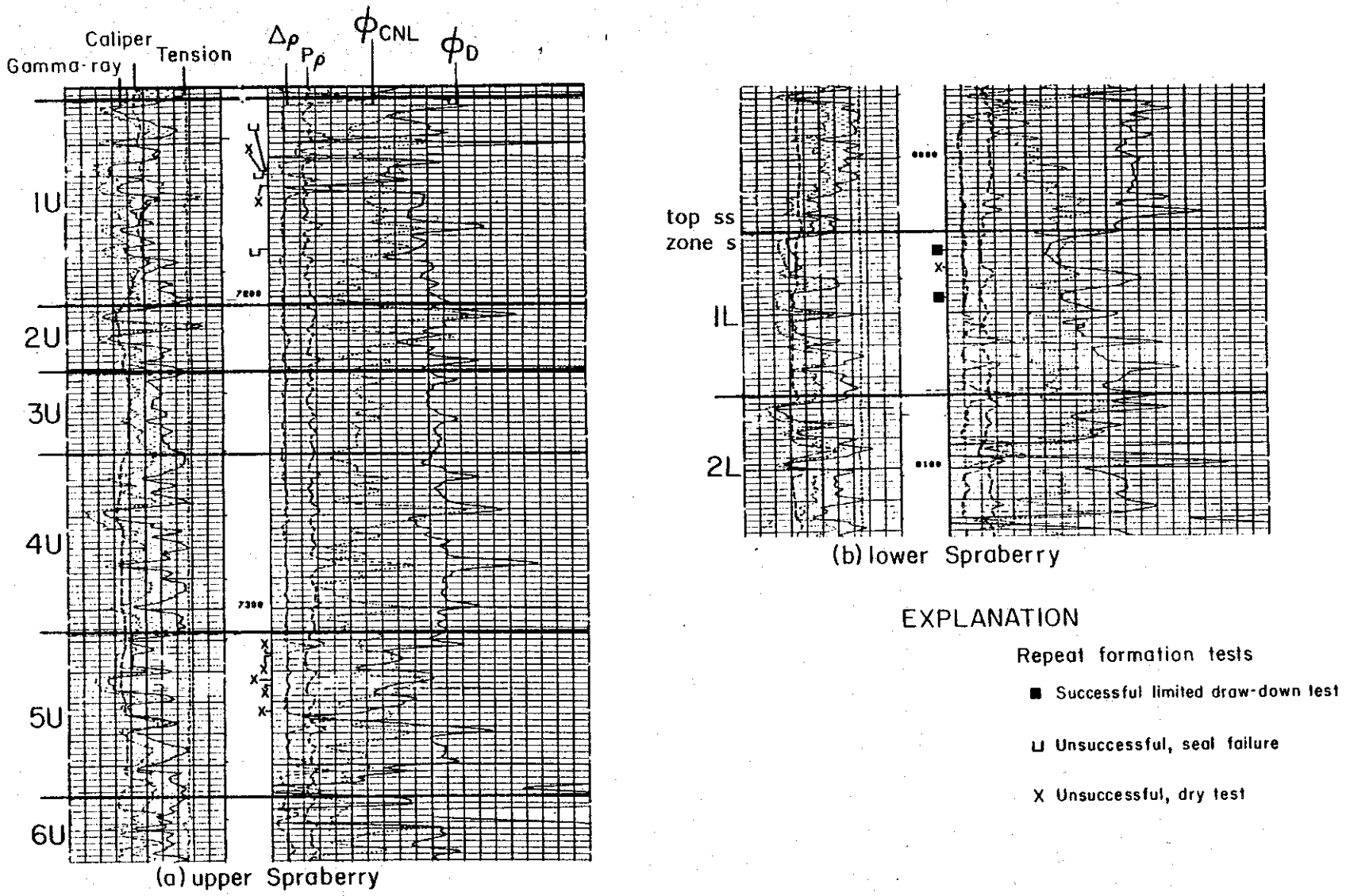

Figure III-30. Repeat formation tests, upper and lower Spraberry, Mobil Preston-37 well (locations shown on lithodensity-compensated neutron log).

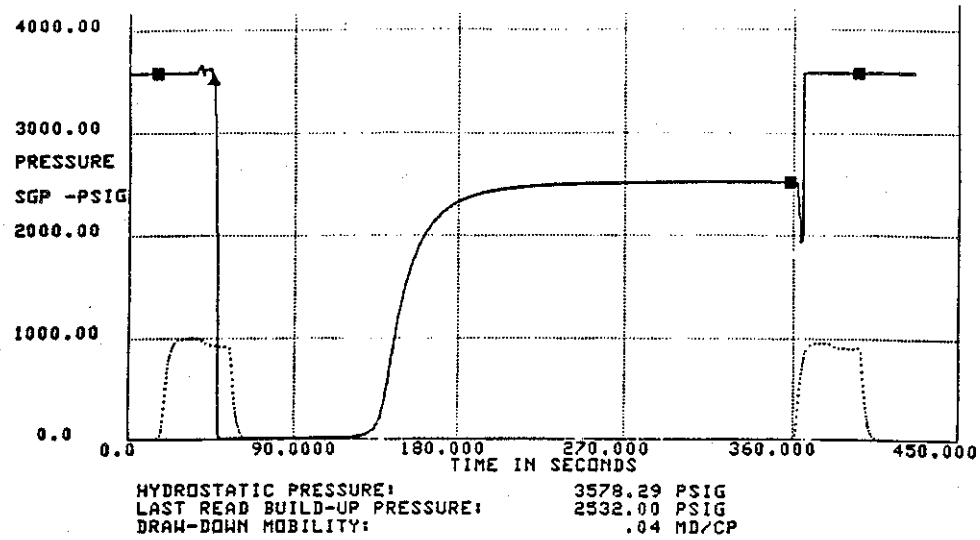

Figure III-31. Buildup pressure curve, repeat formation test at 8030 ft (lower Spraberry), Preston-37 well.

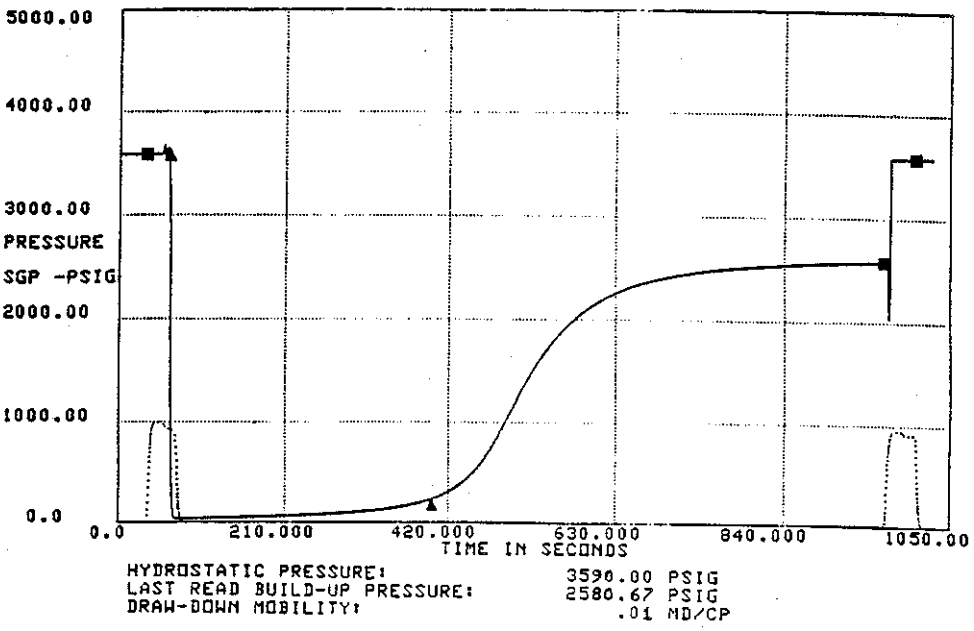

Figure III-32. Buildup pressure curve, repeat formation test at 8045 ft (lower Spraberry), Preston-37 well.

formation pressures. This interpretation is based on (1) the similarity between these final test readings and the original pressure (2500 psi according to Elkins and Skov, 1962) in lower Spraberry reservoirs of the nearby Driver waterflood unit; and (2) the relatively very slight variation in the last test measurements (table III-13), which suggests that buildup pressures were close to equilibrium (they were not increasing substantially), and that therefore tool seals were effective during these tests.

The actual values of the formation pressures may be lower than those determined in the Preston-37 well due to the effects of supercharging (Phelps and others, 1984) on RFT data. Supercharging is the additional pressure (superimposed on the true reservoir pressure) that results from the viscous flow of mud filtrate in low-permeability formations (such as the Spraberry reservoirs tested). Because results of only two closely vertically spaced tests are available, no vertical trends or anomalies of pressure distributions could be established. However, if the pressures determined in the Preston-37 well at 8030 ft and 8045 ft are indeed formation pressures, then the values measured represent pristine reservoir pressures that clearly indicate a partly drained or untapped Spraberry reservoir compartment.

Table III-11. Formation pressure tests, Preston-37 well.

Operat. unit	Depth (ft)	Test length (min)	Hydrostatic pressure (psig)	Last buildup pressure (psig)	Results
				upper Spraberry	
1U	7158	3	3193.53	(no buildup)	Unsuccessful; seal failure
1U	7159	4	3196.18	(no buildup)	Unsuccessful; dry test
1U	7160	3	3180.82	(no buildup)	Unsuccessful; seal failure
1U	7164	3	3187.94	(no buildup)	Unsuccessful; dry test
1U	7184	3	3188.65	(no buildup)	Unsuccessful; seal failure
5U	7316	2	3256.00	(no buildup)	Unsuccessful; dry test
5U	7317	4	3258.00	(no buildup)	Unsuccessful; dry test
5U	7323	6	3263.41	(no buildup)	Unsuccessful; dry test
5U	7325	4	3261.06	(no buildup)	Unsuccessful; dry test
5U	7333	3	3266.47	(no buildup)	Unsuccessful; dry test
				lower Spraberry	
2U	8030	8	3578.29	2532.00	Limited drawdown test; low permeability
2U	8036	9	3583.82	(no buildup)	Unsuccessful; dry test
2U	8045	18	3590.00	2580.67	Limited drawdown test; low permeability.

Table III-12. Formation pressure tests, Judkins A No. 5 well.

Operational unit	Depth (ft)	Test length (min)	Results
		upper Spraberry	
1U	7828.0	15	Unsuccessful; dry test
1U	7029.0	2	Unsuccessful; seal failure
1U	7042.9	3	Unsuccessful; seal failure
1U	7044.0	2	Unsuccessful; seal failure
1U	7044.0	4	Unsuccessful; dry test (repeated)
1U	7045.1	4	Unsuccessful; dry test
5U	7182.0	4	Unsuccessful; seal failure
5U	7183.9	4	Unsuccessful; seal failure
		lower Spraberry	
1L	7873.2	4	Unsuccessful; seal failure
1L	7874.1	2	Unsuccessful; seal failure
1L	7874.1	3	Unsuccessful; dry test
1L	7875.0	3	Unsuccessful; seal failure
1L	7876.1	1	Unsuccessful; seal failure
1L	7878.0	4	Unsuccessful; seal failure

Table III-13. Last read buildup pressures (in psig), RFT drawdown tests.

Test depth: 8030 ft	Test depth: 8045 ft
2512	2548
2516	2553
2520	2557
2523	2561
2526	2564
2527	2569
2529	2572
2530	2574
2531	2578
2532	2580

C. Source-Rock Potential and Organic Maturation of Spraberry Shales

Three black shale samples of the Spraberry Formation, from drilled sidewall cores of the Preston-37 well, were analyzed to assess their oil source-rock potential and maturation. These analyses are essential to determine (1) if potential source rocks of the Early Permian (Leonardian) Spraberry Formation are thermally immature, as postulated by Horak (1985a, 1985b) and Roach (1987) using theoretical models for which no supporting analytical data from rocks or crude oils were presented, or (2) if the Spraberry Formation generated hydrocarbons, as proposed by Houde (1979) using geochemical data from crude oils and by Wilkinson (1953) and Galloway and others (1983) without supporting analytical data. Initial results of these studies (Guevara and Mukhopadhyay, 1987) indicate that upper and middle Spraberry source rocks generated oils produced from upper Spraberry reservoirs and that lower Spraberry oils originated in both lower Spraberry and stratigraphically deeper, as yet unidentified source rocks.

Three samples from the Preston-37 well were studied, one from the upper Spraberry and two from the lower Spraberry (table III-14). Data were obtained using a

Leco carbon analyzer, a Rock-Eval II pyrolysis system, and through reflected-light microscropy of whole rock and pellets of kerogen concentrate. Determinations of total organic carbon (TOC) and pyrolysis data were contracted to D.G.S.I., The Woodlands, Texas.

All the samples contain more than 0.5 percent TOC (table III-15), which is the minimun organic carbon content in shales for the generation of appreciable amounts of liquid hydrocarbons. Maceral analysis revealed that upper and lower Spraberry shales contain more than 80 percent amorphous liptinite that displays yellowish-brown fluorescence in the upper Spraberry sample. Otherwise, the organic matter consists of a mixture of marine phytoplankton (acritarchs and possibly dinoflagellates) and terrestrial exinite (sporinite), less than 2 percent vitrinite, less than 2 percent inertinite, and abundant framboidal pyrite. The nature of the amorphous liptinite and fluorescence characteristics suggest that the organic matter is partly oxidized, having lost part of its hydrogen content before final deposition in an anoxic environment. Most of the nonfluorescent amorphous liptinites of the lower Spraberry contain abundant micrinite and metasapropelinite (a matured product of amorphous liptinite).

The nonamorphous portion of the organic matter in lower Spraberry samples contains metasporinite and minor metaalginite, suggesting a depleted and matured source rock that lost fluorescence due to organic maturation and hydrocarbon migration. Some relict structures of phytoplankton and spores within the amorphous liptinites suggest that the amorphous liptinite was formed by the biodegradation of phytoplankton and terrestrial exinites.

Vitrinites are scarce. Considering the abundance of organic matter, the mean vitrinite reflectances of the few data from the upper (0.65 percent Ro) and lower (0.78 percent Ro) Spraberry suggest that these rocks are mature. A graph of the hydrogen index (mg of hydrocarbons/g TOC) and the oxygen index (mg CO_2/g TOC) determined using Rock-Eval pyrolysis data (Espitalie and others, 1977) suggests that upper

Spraberry shales contain type IIB organic matter (intermediate between type II and type III kerogens, but closer to type II kerogen), and that lower Spraberry shales lie within the maturation path of type III kerogen (fig. III-33). Similarly, T_{max} data (table III-15) suggest that organic matter of upper and lower Spraberry shales is mature for hydrocarbon generation (the boundary between immaturity and maturity of organic matter is 430°C). High production index in all samples (table III-15) indicates that these rocks are within the principal phase of oil generation. Furthermore, low TOC and low hydrogen indices associated with high production indices suggest the occurrence of allochthonous bitumen in lower Spraberry shales.

TOC, Rock-Eval pyrolysis, and microscopic data indicate the occurrence of matured type IIB source rocks in the upper Spraberry and matured, depleted type IIB organic matter (transformed to type III kerogen due to maturity) in the lower Spraberry. Upper Spraberry source rocks are within the early phase of principal oil generation. Lower Spraberry source rocks are within the final phase of principal oil generation, considering the abundance of amorphous liptinite.

Indications of hydrocarbon migration through natural fractures were observed in the microscopy studies. One of the lower Spraberry samples (8060 ft) shows strong fluorescence in a partly cemented fracture. Fluorescence, which in the groundmass is restricted to the portion immediately adjacent to the fracture owing to droplets of flowing oil indicates that migration took place mainly along the fractures. Similarly, fluorescence in rhomb-shaped crystals partly healing the fracture indicates that oil migration took place after carbonate cementation.

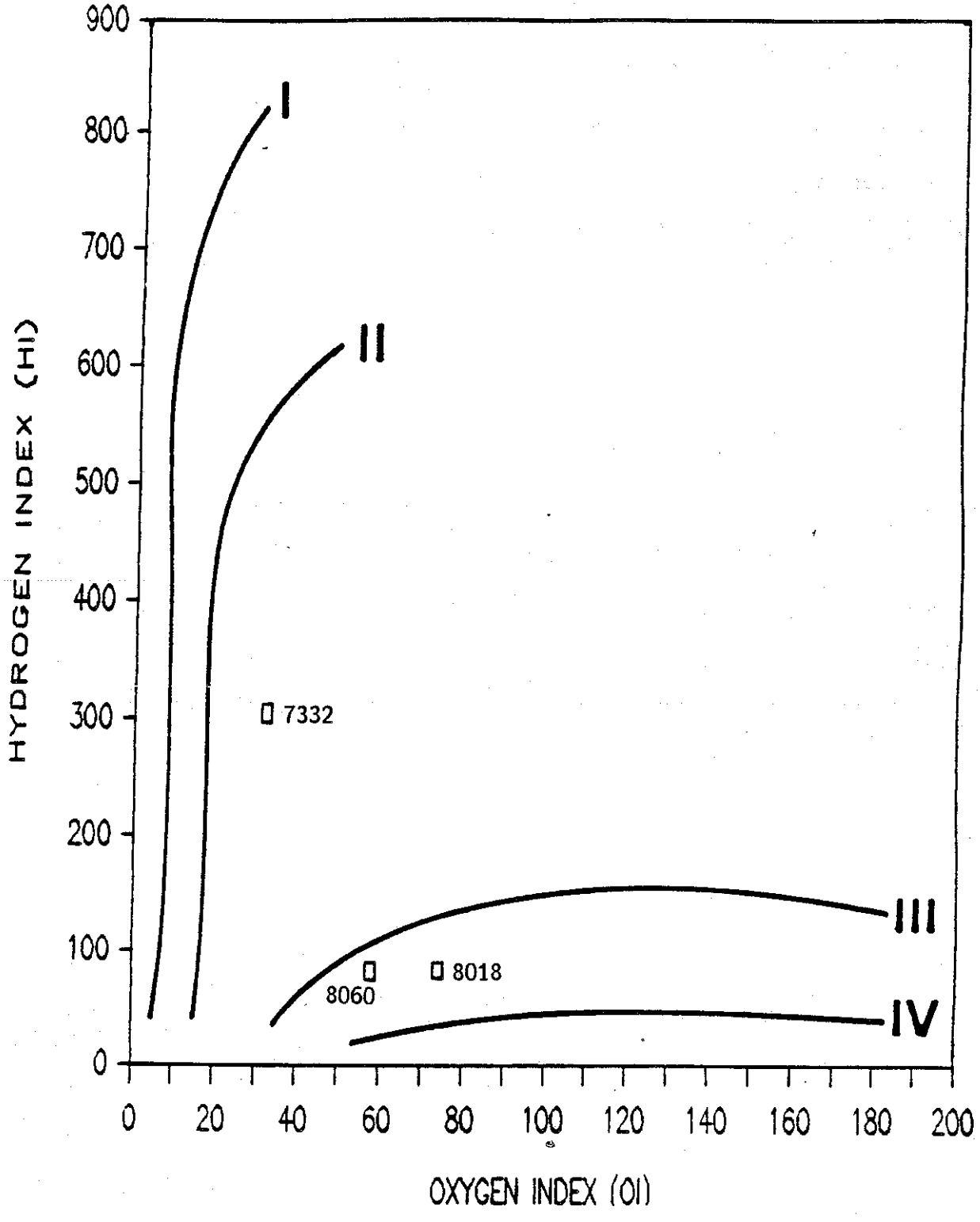

Figure III-33. Kerogen type determination using TOC and Rock-Eval pyrolysis data, Preston-37 well.

Table III-14. Shale samples analyzed, Preston-37 sidewall cores.

Stratigraphic unit	Operational* unit	Core depth in ft (ft below sea level)
upper Spraberry	5U	7332 (-4582)
lower Spraberry	1L	8018 (-5310)
lower Spraberry	1L	8060 (-5310)

*See figures II-1 and III-2 for sample locations.

Table III-15. Organic geochemistry data, Preston-37 cores.

Depth (ft)*	TOC (wt %)	T_{max} (°C)	Hydrogen index (HI)	Oxygen index (OI)	Production index (PI)
7332	1.68	438	304	320	0.22
8018	0.58	447	83	74	0.38
8060	0.57	446	82	58	0.52

*See figure III-2 for stratigraphic locations.

CONCLUSIONS

The complex lithofacies architecture of Spraberry reservoirs of the central Spraberry Trend results in highly heterogeneous, laterally discontinuous oil accumulations that are stratified, being vertically separated by shales and carbonates. Reservoirs occur in the upper parts of three submarine fan intervals recognized in the Spraberry Formation: the Jo Mill fan in the lower Spraberry and the Driver and the overlying Floyd fans in the upper Spraberry. Shales, carbonates, and locally interbedded sandstones and siltstones of the Midland basin plain (middle Spraberry) vertically separate the Jo Mill and Driver fans.

Regional mapping delineated a threefold subdivision of the Spraberry submarine fans. Sand-rich, mainly channelized, aggradational facies of the inner fan and mid-fan predominate in the north part of the basin, and laterally extensive, mud-rich, progradational facies of the outer fan occur in the south part of the basin, south of the Glasscock County narrows. Although the best-quality reservoir rocks are inner-fan and midfan sandstones and siltstones that occur in the shelf-proximal, north part of the basin, these sands contain only small and erratically distributed oil accumulations. The largest accumulations of oil are stratigraphically trapped in midfan to outer-fan sediments. Linear trends of high sand content provide belts of greater production generally parallel to the basin axis.

Probable pristine reservoir pressures measured in a well newly drilled in the Spraberry Trend confirm the local occurrence of untapped reservoir compartments in these stratigraphically complex reservoirs. These intrareservoir traps can be detected and the main petrophysical characteristics of Spraberry reservoirs appropriately described using an open-hole suite consisting of gamma-ray spectrometry, borehole-compensated density and neutron, full waveform sonic-acoustic, and enhanced-vertical-resolution resistivity logs. The differentiation between natural and induced fractures

remains problematic because no agreement was found between several commonly used log-derived fracture indices nor between these indices and continuous microresistivity images (FMS log) of the borehole walls.

Preliminary petrographic data indicate that matrix porosity and reservoir quality are locally influenced by mineral dissolution (resulting in secondary porosity) and cementation (which occludes primary and secondary porosity). Ankerite or ferroan dolomite is the predominant carbonate mineral, and calcite and swelling clays either occur in very low proportions or are absent. Organic geochemistry data show that Spraberry shales are mature oil source rocks. Upper Spraberry shales are within the early phase of principal oil generation, and lower Spraberry shales are within the final phase.

Current well spacing and completion practices result in untapped and partly drained reservoir compartments from which additional oil recovery can be obtained using the nontertiary techniques of well recompletions and geologically targeted infill drilling. The best prospects for conventional reserve growth are in areas having superior effective porosities in the belts defined by isolith maxima. In the ununitized area studied, these belts are continuations of sand-rich belts containing the sweet spots of the adjacent Preston/Shackelford and Driver waterflood units. Similarly, well locations for secondary or enhanced recovery programs must be based on the occurrence of stratigraphically controlled preferential flow paths. These areas of superior permeability correspond to sectors having the best effective porosities in sand-rich belts.

Using the strategies outlined above, aggressive exploration and extended development of Spraberry reservoirs that yields a 1- to 2-percent increase in recovery would add 40 to 80 million barrels of oil to the remaining reserve base. This effort would ensure sustained production at current levels into the next century.

ACKNOWLEDGMENTS

Funding for this study was provided by ARCO Oil and Gas Company, Exxon Company U.S.A., Mobil Producing Texas and New Mexico, Standard Oil Production Company, and Texaco Exploration and Production Technology Division. Collaboration by Mobil Producing Texas and New Mexico, which kindly provided cores and permitted extensive logging in two non-Spraberry wells, is gratefully acknowledged. We express our thanks to the staff of the companies supporting this project. In particular to Gordon Baker and Tim Roepke (Mobil), Mark F. Sheehan, Michael Haas, and Roger M. Slatt (ARCO), Sam D. Conner (Exxon), Elizabeth A. Bargar, Gordon Tinker, Sandra Waisley, Dave Bocaldo, Don Schmor, and Tom Morrow (Standard), and Michael Yusas and Emily Stoudt (Texaco). Our thanks also to Robert E. Barba, Schlumberger Well Services, West Texas Division, for his efforts to ensure high-quality data and rapid data turnaround.

Word processing was by Dottie Johnson and Kurt Johnson, under the supervision of Lucille C. Harrell. Drafting was by the Bureau cartography staff under the supervision of Richard L. Dillon. Mary Ellen Johansen edited the manuscript.

REFERENCES

Barfield, E. C., Jordan, J. K., and Moore, W. D., 1959, An analysis of large-scale flooding in the fractured Spraberry Trend area reservoir: Journal of Petroleum Technology, v. 11, p. 15-19.

Bartley, J. H., 1951, Stratigraphy and structure of the Spraberry Trend: The Oil and Gas Journal, v. 50, p. 101, 112.

Bouma, A. H., Normark, W. R., and Barnes, N. E., eds., 1985, Submarine fans and related turbidite systems: New York, Springer-Verlag, 351 p.

Bozanich, R. G., 1978, The Bell Canyon and Cherry Canyon Formations, southern Delaware Basin, Texas: The University of Texas at Austin, Master's thesis, 152 p.

Bristol, Brance, and Helm, Cy, 1951, Acid flushing fractures in Spraberry sand: The Oil and Gas Journal, v. 50, p. 94-97.

Elkins, L. F., 1953, Reservoir performance and well spacing, Spraberry trend area field of West Texas: American Institute of Mining, Metallurgical, and Petroleum Engineers Transactions, v. 198, p. 177-196.

Elkins, L. F., and Skov, A. M., 1960, Anisotropic spread of pressure transients delineates Spraberry fracture orientation: Society of Petroleum Engineers of the American Institute of Mining, Metallurgical, and Petroleum Engineers, 35th Annual Fall Meeting, Denver, Colorado, SPE Paper 1516-G, 8 p.

_____ 1962, Large scale waterflood performance, Spraberry field, West Texas: Society of Petroleum Engineers of the American Institute of Mining, Metallurgical, and Petroleum Engineers, 37th Annual Fall Conference and Exhibition, Los Angeles, California, SPE Paper 405.

Elkins, L. F., Skov., A. M., and Gould, R. C., 1968, Progress report on Spraberry waterflood-reservoir performance, well stimulation and water treatment handling: Journal of Petroleum Technology, v. 20, no. 9, p. 1039-1049.

Espitalie, J., Madec, M., Tissot, Bernard, Mennig, J. J., and Laplat, P., 1977, Source rock characterization method for petroleum exploration: Offshore Technology Conference Proceedings, v. 9, part 3, p. 439-444.

Ewing, T. E., and Reed, R. S., 1984, Depositional systems and structural controls of Hackberry Sandstone reservoirs in southeast Texas: The University of Texas at Austin, Bureau of Economic Geology Geological Circular 84-7, 48 p.

Filliben, J. J., 1984, DATAPLOT--introduction and overview: Washington, National Bureau of Standards Special Publication 667.

Galley, J. E., 1958, Oil and geology in the Permian Basin of Texas and New Mexico, in Habitat of oil: a symposium: American Association of Petroleum Geologists, p. 395-446.

Galloway, W. E., 1983, Depositional architecture and reservoir characterization of Late Paleozoic submarine slope and basin depositional systems--Midland and Delaware Basins, Texas (abs.): American Association of Petroleum Geologists Bulletin, v. 67, p. 466.

Galloway, W. E., and Cheng, E. S., 1985, Reservoir facies architecture in a microtidal barrier system--Frio Formation, Texas Gulf Coast: The University of Texas at Austin, Bureau of Economic Geology Report of Investigations No. 144, 36 p.

Galloway, W. E., Ewing, T. E., Garrett, C. M., Jr., Tyler, Noel, and Bebout, D. G., 1983, Atlas of major Texas oil reservoirs: The University of Texas at Austin, Bureau of Economic Geology Special Publication, 139 p.

Gibson, G. R., 1951, The relation of fractures to the accumulation of oil in the Spraberry Formation: The Oil and Gas Journal, v. 50, p. 107, 116-117.

Guevara, E. H., in press, Geological characterization of Permian submarine fan reservoirs of the Driver waterflood unit, Spraberry Trend, Midland Basin, Texas: The University of Texas at Austin, Bureau of Economic Geology Report of Investigations.

Guevara, E. H., and Mukhopadhyay, P. K., 1987, Source rock potential and oil source correlation, Permian (Leonardian) strata, central Spraberry Trend, Midland Basin, Texas--preliminary study (abs.): American Association of Petroleum Geologists Bulletin, v. 71, p. 561-562.

Guevara, E. H., and Tyler, Noel, 1986, Influence of facies architecture on hydrocarbon recovery from naturally-fractured submarine-fan reservoirs, central Spraberry Trend, Texas (abs.): American Association of Petroleum Geologists Bulletin, v. 70, p. 597.

Habitch, J. K. A., 1979, Paleoclimate, paleomagnetism, and continental drift: American Association of Petroleum Geologists Studies in Geology No. 9, 30 p.

Handford, C. R., 1981a, Deep-water facies of the Spraberry Formation (Permian), Reagan County, Texas, in Siemers, C. T., Tillman, R. W., and Williamson, C. R., eds., Deep-water clastic sediments--a core workshop: Society of Economic Paleontologists and Mineralogists Core Workshop No. 2, p. 372-395.

_____ 1981b, Sedimentology and genetic stratigraphy of Dean and Spraberry Formations (Permian), Midland Basin, Texas: American Association of Petroleum Geologists Bulletin, v. 65, p. 1602-1616.

Harms, J. C., 1974, Brushy Canyon Formation, Texas: a deep-water density current deposit: Geological Society of America Bulletin, v. 85, p. 1763-1784.

Horak, R. L., 1985a, Sequential tectonism and hydrocarbon distribution in the Permian Basin (abs.), in The geologic evolution of the Permian Basin--a symposium: Permian Basin Section, Society of Economic Paleontologists and Mineralogists, Program with Abstracts, p. 14-15.

_____ 1985b, Tectonic and hydrocarbon maturation history in the Permian Basin: The Oil and Gas Journal, v. 83, p. 124-129.

Houde, R. R., 1979, Sedimentology, diagenesis, and source bed geochemistry of the Spraberry Sandstone, subsurface Midland Basin, West Texas: The University of Texas at Dallas, Maters's thesis, 198 p.

Journel, A. G., and Huijbregts, C. J., 1978, Mining geostatistics: New York, Academic Press, 600 p.

Knudson, H. P., and Kim, Y. C., 1978, A short course on geostatistical ore reserve estimation: University of Arizona, Tucson, College of Mines, Department of Mining and Geological Engineering.

Mardock, E. S., and Meyers, J. P., 1951, Radioactivity logs define lithology in the Spraberry Formation: The Oil and Gas Journal, v. 50, p. 96-102.

Matchus, E. J., and Jones, T. S., 1984, East-west cross section through Permian Basin of West Texas: West Texas Geological Society Publication No. 84-79.

McLennan, Lamar, Jr., and Bradley, W. H., 1951, Spraberry and Dean sandstones of West Texas: American Association of Petroleum Geologists Bulletin, v. 35, p. 899-915.

Mutti, Emiliano, 1974, Examples of ancient deep-sea fan deposits from circum-Mediterranean geosynclines, in Dott, R. H., and Shaver, R. H., eds., Modern and ancient geosynclinal sedimentation: Society of Economic Paleontologists and Mineralogists Special Publication No. 19, p. 92-105.

_____ 1977, Thin bedded turbidite facies and related depositional environments in the Paleogene Hecho Group system (south-central Pyrenees, Spain): Sedimentology, v. 24, p. 107-131.

Mutti, Emiliano, Nilsen, T. H., and Ricci Lucchi, F., 1978, Outer fan depositional lobes of the Laga Formation (upper Miocene and Lower Pliocene), east central Italy, in Stanley, D. J., and Kelling, G., eds., Sedimentation in submarine canyons, fans, and trenches: Stroudsburg, Pennsylvania, Dowden, Hutchinson, and Ross, p. 210-233.

Mutti, Emiliano, and Ricci Lucchi, F., 1972, Le torbiditi dell'Appennine settentrionale: introducione all'analisi di facies: Memorie Societa Geologica Italiana, v. 11, p. 161-199. (English translation Nilsen, T. H., 1978, International Geology Review, v. 20, no. 2, p. 125-166).

_____ 1975, Turbidite facies and facies associations, in Mutti, Emiliano, and others, eds., Examples of turbidite facies and facies associations from selected formations of northern Apennines: Ninth International Congress of Sedimentology Field Trip, Nice, p. 21-36.

Mutti, Emiliano, and Sonnino, Maurizio, 1981, Compensation cycles: a diagnostic feature of turbidite sandstone lobes: Second European Regional Meeting of the International Association of Sedimentologists, Abstract Volume, p. 120-123.

Nelson, C. H., and Nilsen, T. H., 1984, Modern and ancient deep-sea fan sedimentation: Society of Economic Paleontologists and Mineralogists Short Course No. 14, Lecture Notes, 404 p.

Normark, W. R., 1970, Growth patterns of deep-sea fans: American Association of Petroleum Geologists Bulletin, v. 54, p. 2170-2195.

_____ 1978, Fan valleys, channels and depositional lobes on modern submarine fans: characters for recognition of sandy turbidite environments: American Association of Petroleum Geologists Bulletin, v. 62, p. 912-931.

Phelps, G. D., Stewart, G., and Peden, J. M., 1984, The effect of filtrate invasion and formation wettability on Repeat Formation Tester measurements: Society of Petroleum Engineers of the American Institute of Mining, Metallurgical, and Petroleum Engineers, 1984 European Petroleum Conference, London, England, SPE Paper 12962.

Radian Corporation, 1979, CPS-1 Contour Plotting System, user's manual: Austin, Texas.

Redin, T., 1984, Oil and gas production from submarine fans of Los Angeles Basin (abs.): American Association of Petroleum Geologists Bulletin, v. 68, no. 4, p. 520.

Ricci Lucchi, F., 1975, Depositional cycles in two turbidite formations of northern Apennines: Journal of Sedimentary Petrology, v. 45, p. 3-43.

_____ 1978, Turbidite dispersal in a Miocene deep-sea plain: the Marnoso-arenacea of the northern Apennines, in van Loon, A. J., ed., Keynotes of the MEGS-II (Amsterdam, 1978): Geologie en Mijnbouw, v. 57 p. 559-576.

Ricci Lucchi, F., and Valmori, E., 1980, Basin-wide turbidites in a Miocene, over-supplied deep-sea plain: a geometric analysis: Sedimentology, v. 27, p. 241-270.

Roach, J. W., 1987, Biogenically formed petroleum should be considered: World Oil, June, p. 84-86 and 88-91.

Sarg, J. F., in press, Middle-Late Permian depositional sequences, Permian Basin, West Texas-New Mexico, in American Association of Petroleum Geologists Memoir.

Schlumberger Educational Services, 1987, Log interpretation principles/applications: Houston, 198 p.

Senning, R. G., 1951, The Spraberry play in West Texas: World Oil, v. 133, p. 125-136.

Siemers, C. T., 1978, Submarine fan deposition in the Woodbine - Eagle Ford interval (Upper Cretaceous), Tyler County, Texas: Gulf Coast Association of Geological Societies Transactions, v. 28, p. 493-533.

Silver, B. A., and Todd, R. G., 1969, Permian cyclic strata, northern Midland and Delaware Basins, West Texas and Southeastern New Mexico: American Association of Petroleum Geologists Bulletin, v. 93, p. 2223-2251.

Stewart, George, Wittmann, Manfred, and van Golf-Racht, Theodor, 1981, The application of the Repeat Formation Tester to the analysis of naturally fractured

reservoirs: Society of Petroleum Engineers of the American Institute of Mining, Metallurgical, and Petroleum Engineers, 56th Annual Fall Conference and Exhibition, San Antonio, Texas, SPE Paper 10181.

Stow, D. A. V., Howell, D. G., and Nelson, C. H., 1985, Sedimentary, tectonic, and sea-level controls, in Bouma, A. H., Normark, W. R., and Barnes, N. E., Submarine fans and related turbidite systems: New York, Springer-Verlag, p. 15-22.

Tyler, Noel, and Ambrose, W. A., 1985, Facies architecture and production characteristics of strandplain reservoirs in the Frio Formation, Texas: The University of Texas at Austin, Bureau of Economic Geology Report of Investigations No. 146, 42 p.

_____ 1986, Depositional systems and oil and gas plays in the Cretaceous Olmos Formation, South Texas: The University of Texas at Austin, Bureau of Economic Geology Report of Investigations No. 152, 42 p.

Tyler, Noel, Galloway, W. E., Garrett, C. M., Jr., and Ewing, T. E., 1984, Oil accumulation, production characteristics, and targets for additional recovery in major oil reservoirs of Texas: The University of Texas at Austin, Bureau of Economic Geology Geological Circular 84-2, 31 p.

Tyler, Noel, and Gholston, J. C., in press, Heterogeneous deep-sea fan reservoirs, Shackelford and Preston waterflood units, Spraberry Trend, West Texas: The University of Texas at Austin, Bureau of Economic Geology Report of Investigations.

Tyler, Noel, Gholston, J. K., and Ambrose, W. A., 1986, Genetic stratigraphy and oil recovery in a late Cretaceous wave-dominated deltaic reservoir, Big Wells (San Miguel) field, South Texas: The University of Texas at Austin, Bureau of Economic Geology Report of Investigations No. 153, 38 p.

Tyler, Noel, and Guevara, E. H., 1987, Complex reservoir architecture of Leonardian (Spraberry) submarine fans, Midland Basin: implications for additional oil recovery (abs.), in The Leonardian facies in W. Texas and S. E. New Mexico and

Guidebook to the Glass Mountains, West Texas: Permian Basin Section, Society of Economic Paleontologists and Mineralogists Publication 87-27, p. xi.

van Hilten, D., 1962, Presentation of paleomagnetic data, polar wandering, and continental drift: American Journal of Science, v. 260, p. 401-426.

Vest, E. L., Jr., 1970, Oil fields of Pennsylvanian-Permian Horseshoe Atoll, West Texas, in Halbouty, M. T., ed., Geology of giant petroleum fields--symposium: American Association of Petroleum Geologists Memoir 14, p. 185-203.

Walker, R. G., 1978, Deep-water sandstone facies and ancient submarine fans: models for exploration for stratigraphic traps: American Association of Petroleum Geologists Bulletin, v. 62, no. 6, p. 932-966.

_____ 1984, Turbidites and associated coarse clastic deposits, in Walker, R. G., ed., Facies models: Geoscience Canada, Reprint Series 1 (2d ed.), p. 171-188.

Watson, M. P., 1984, Submarine fans in a developing extensional regime--their significance in the North Sea hydrocarbon province (abs.): American Association of Petroleum Geologists Bulletin, v. 68, no. 4, p. 538.

Wilde, P., Normark, W. R., and Chase, T. E., 1978, Channel sands and petroleum potential of Monterey deep-sea fan, California: American Association of Petroleum Geologists Bulletin, v. 62, p. 967-983.

Wilkinson, W. M., 1953, Fracturing in Spraberry reservoir, West Texas: American Association of Petroleum Geologists Bulletin, v. 37, no. 2, p. 250-265.

Williamson, C. R., 1978, Depositional processes, diagenesis, and reservoir properties of Permian deep-sea sandstones, Bell Canyon Formation, Texas--New Mexico: Texas Petroleum Research Committee, Report No. UT 78-2, 261 p.

World Oil, 1952, Will the Spraberry pay out?: v. 135, no. 1, p. 50-51.